MINERALOGY, GEOCHEMISTRY, PETROGENESIS AND STRUCTURAL RELATIONSHIPS OF THE AILLIK BAY ALKALINE INTRUSIVE SUITE, LABRADOR, CANADA

STEPHEN FRANCIS FOLEY

CANADIAN THESES ON MICROFICHE

I.S.B.N.

THESES CANADIENNES SUR MICROFICHE

National Library of Canada
Collections Development Branch

Canadian Theses on
Microfiche Service

Ottawa, Canada
K1A 0N4

Bibliothèque nationale du Canada
Direction du développement des collections

Service des thèses canadiennes
sur microfiche

NOTICE

The quality of this microfiche is heavily dependent upon the quality of the original thesis submitted for microfilming. Every effort has been made to ensure the highest quality of reproduction possible.

If pages are missing, contact the university which granted the degree.

Some pages may have indistinct print especially if the original pages were typed with a poor typewriter ribbon or if the university sent us a poor photocopy.

Previously copyrighted materials (journal articles, published tests, etc.) are not filmed.

Reproduction in full or in part of this film is governed by the Canadian Copyright Act, R.S.C. 1970, c. C-30. Please read the authorization forms which accompany this thesis.

THIS DISSERTATION
HAS BEEN MICROFILMED
EXACTLY AS RECEIVED

AVIS

La qualité de cette microfiche dépend grandement de la qualité de la thèse soumise au microfilmage. Nous avons tout fait pour assurer une qualité supérieure de reproduction.

S'il manque des pages, veuillez communiquer avec l'université qui a conféré le grade.

La qualité d'impression de certaines pages peut laisser à désirer, surtout si les pages originales ont été dactylographiées à l'aide d'un ruban usé ou si l'université nous a fait parvenir une photocopie de mauvaise qualité.

Les documents qui font déjà l'objet d'un droit d'auteur (articles de revue, examens publiés, etc.) ne sont pas microfilmés.

La reproduction, même partielle, de ce microfilm est soumise à la Loi canadienne sur le droit d'auteur, SRC 1970, c. C-30. Veuillez prendre connaissance des formules d'autorisation qui accompagnent cette thèse.

LA THÈSE A ÉTÉ
MICROFILMÉE TELLE QUE
NOUS L'AVONS REÇUE

NL-339 (r. 82/08)

Canada

MINERALOGY, GEOCHEMISTRY, PETROGENESIS AND STRUCTURAL RELATIONSHIPS OF THE AILLIK BAY ALKALINE INTRUSIVE SUITE, LABRADOR, CANADA

by

© Stephen Francis Foley, B.Sc.

A thesis submitted in partial fulfillment
of the requirements for the degree of
Master of Science

Department of Geology
Memorial University of Newfoundland
January,, 1982

St.John's Newfoundland

ABSTRACT

The Aillik Bay alkaline intrusive suite comprises dykes of alkaline lamprophyre (sannaite and olivine sannaite), kimberlite and carbonatite. Structural and mineralogical criteria indicate that the dykes are related to an intrusive centre of nephelinite-carbonatite type situated beneath the Labrador Sea to the northeast of the study area.

Dykes were emplaced in three structural episodes; two concentric sets are separated in time by a dominant radial set. Sannaites make up the first set and the bulk of the second whereas kimberlites and carbonatites exclusively occupy the third dyke set. Formation of segmented dykes is attributed to flow instabilities enhanced by a volatile-rich fluid moving ahead of the magma. This fluid was presumably exsolved from the magma as a result of pressure reduction during emplacement, and also assisted in the formation of parallel fracture zones adjacent to kimberlites and carbonatites.

Sannaites are characterised by leucocratic ocelli which are frequently zoned: a central zone dominated by carbonate and analcite gives way to an outer zone of Fe-mica, pyroxene, nepheline, K-feldspar and analcite. The outer zones were formed by segregation of late-stage melt. One sample bears globules which are clearly the result of liquid immiscibility. Immiscibilty and segregation are accompanied by concentration of incompatible elements. Groundmass mineralogy shows chemical evolution similar to nepheline syenites.

Minerals in kimberlite delineate a more complex history,

beginning at depth in a low oxygen fugacity environment. Kimberlites lack high pressure equilibrated diamond 'marker' minerals, and thus diamond potential is low. Carbonatites typically exhibit relict kimberlitic textures.

Sannaite and olivine sannaite were derived by flow differentiation from a parental magma, the composition of which is defined. All rock types were derived by partial melting of an incompatible element enriched mantle source. Structural inheritance permitted successive emplacement of rocks representing progressively smaller and deeper derived melt fractions via the intrusive centre.

ACKNOWLEDGEMENTS

Financial support or this study was provided by a Memorial University graduate fellowship and an N.S.E.R.C. grant to J.Malpas. Logistic and financial assistance was supplied by J.G.Burns of Placer Development Ltd. from the Placer Devt./BRINEX joint project.

I wish to express my thanks to the following people:

(1) My supervisor John Malpas for his guidance and editorial assistance during this study.

(2) Many members of the faculty and graduate students of the Geology Department of Memorial University for discussions and advice during laboratory work and thesis preparation.

(3) J.G.Burns, R.P.Watts (BRINEX, Northwest River) and H.A.Williamson (Labrador Institute of Northern Studies) for advice and assistance during fieldwork, and W.Ryder (Newfoundland Dept. Mines and Energy) for equipment loan.

(4) A.F.King, R.A.Doherty, A.B.Ryan, C.F.Gower, M.J.Flanagan and J.G.Burns for discussions on the geology of the Alllik Bay area.

(5) Ivan Dalton for able and cheerful assistance in fieldwork.

(6) D.Press, H.Longerich, G.Andrews and W.Marsh for assistance and instruction in producing various analyses and photographs.

(7) Memorial University Computing Services staff, and in particular Randy Dodge, for assistance in thesis production.

TABLE OF CONTENTS

TABLE OF CONTENTS (continued)

LIST OF TABLES

LIST OF FIGURES

LIST OF FIGURES (continued)

LIST OF FIGURES (continued)

CHAPTER 1 : INTRODUCTION

LOCATION AND ACCESS

The area of study is situated on the east coast of Labrador between 59°08' and 59°23'W and between 55°09' and 55°19'N (fig. 1-1). Access is by float plane or coastal boat, the latter of which operates in the summer months and stops at Makkovik. Many large lakes or sheltered inlets can be used by float planes serviced from Goose Bay or Northwest River, 200-220 km to the southwest.

PREVIOUS WORK

The first geological reports on the Aillik Bay area were parts of reconnaissance surveys (Daly,1902; Kranck,1937, 1947, 1953; Douglas, 1953; Christie et al.,1953). Kranck (1953) described the numerous intrusive episodes and noted the presence of ultramafic lamprophyres which he termed aillikites. Unpublished theses by Moore (1951), Cooper (1951) and Riley (1951) cover aspects of Kranck's surveys in more detail, with Moore (1951) including petrographic descriptions of the lamprophyres.

British Newfoundland Exploration Ltd.(BRINEX) started exploration on their large concession area in 1953. This has resulted in many unpublished reports on molybdenum and especially uranium showings, summarised by Gandhi (1976). Several university theses are studies of geology and mineralisation of the Aillik Group (Barua, 1969; Gill, 1966;

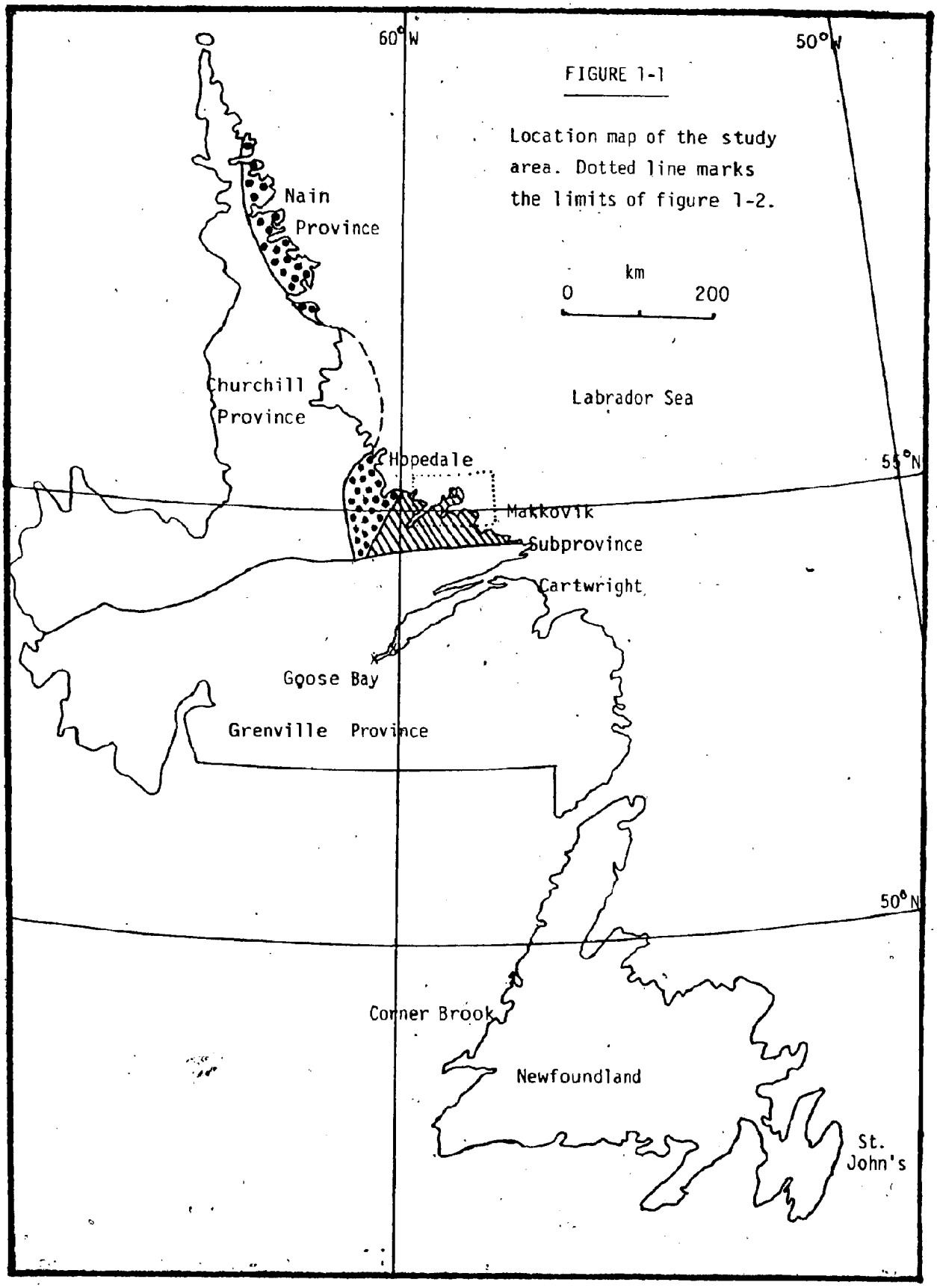

FIGURE 1-1

Location map of the study area. Dotted line marks the limits of figure 1-2.

King, 1963). White (1973) and Minatidis (1976) concentrated on uranium mineralisation, which occurs over a wide area along strike from acidic volcanic beds at Cape Makkovik in the study area.

The Geological Survey of Canada (GSC) undertook radiometric dating in the area (mostly K-Ar whole-rock and mineral ages) as part of a project to define provinces within the Canadian Shield (Leech et al., 1963; Stockwell,1964; Wanless et al., 1970, 1972, 1974). Taylor (1971, 1972) defined a Makkovik sub-province of the Nain province (fig. 1-1), in which structural trends are northeasterly as compared with north to northwesterly in the Archean Nain province to the north. The Makkovik sub-province in the study area includes the Aphebian Aillik Group as well as the southern extremities of the Archean Hopedale Complex.

The Newfoundland Government started mapping the Labrador Central Mineral Belt (Smyth et al., 1975) in 1974. The Aillik Group is included in accounts by Bailey (1978), Bailey et al. (1979), Doherty (1980), Gower (1981) and briefly by Ryan (1979). The first 1/100,000 map was recently published (Bailey et al.,1981).

The most detailed accounts of the Aillik Group in the Makkovik area are by Gandhi et al. (1969) and Clark (1971, 1974). These authors recognised that felsic tuffs and lavas, previously mapped as metasediments, form a large part of the Aillik Group, with Makkovik as the volcanic centre (Clark, 1979). King's (1963) thesis is the most detailed account dealing specifically with the succession on the Cape Makkovik peninsula.

The GSC radiometric dates, coupled with further data by Gandhi et al. (1969) and Grasty et al.(1969), have assisted in distinguishing between many post-deformational igneous intrusions. The emplacement of felsic stocks ceased before 1400 Ma, whereas diabasic dykes are dated at around 1400 Ma and in the range 700 - 1000 Ma. Diabase dykes were earlier studied by Wheeler (1933). A lamprophyric intrusion close to Makkovik village is dated at 1550 Ma (Wanless et al., 1970). Lamprophyres east of Cape Harrison, 80km to the southeast of Makkovik were discussed by Elders and Rucklidge (1969). These are believed to be part of the 1550 Ma event since they are cut by diabase (Gower, 1980) related to the Michael Gabbro (Fahrig and Larochelle, 1972; Gower 1981). The Adlavik Intrusive Suite, an earlier post-Hudsonian mafic igneous complex, is described by Stevenson (1970), Clark (1974, 1979) and Gower (1981). Gandhi et al. (1969) suggested that one of these gabbroic bodies was the source to the abundant dioritic dykes of Cape Makkovik.

The dykes of the Aillik Bay intrusive suite are briefly described by Kranck (1953), Moore (1951, p.39-47) and King (1963). King and McMillan (1975) suggest a Mesozoic age for carbonatitic lamprophyre based on identification of microfauna in a breccia cut by lamprophyric dykelets at Ford's Bight (fig. 1-2). This raises the possibility of two distinct phases of activity because Leech et al. (1963, p.116-117) dated a lamprophyre at 535-570 Ma (K-Ar on biotite). However, Hawkins (1977) suggested the latter date may be innaccurate due to excess argon in micas.

Hawkins (1977) examined the petrography and petrology of the Aillik Bay suite, concluding that kimberlites (the aillikites of Kranck, 1953) are genetically related to carbonatites and monchiquitic lamprophyres. He catalogued ultramafic nodules occurring within the dykes, which he interpreted to be of cognate origin. He also suggested forceful injection of dykes from an igneous centre located to the northeast of Aillik Bay, and that their emplacement was associated with rifting in the Labrador Sea (Currie, 1970, 1975; King and McMillan, 1975).

PURPOSE OF THIS STUDY

Recent studies in the geology of kimberlites have shown that true kimberlites with minerals equilibrated at high pressures, and thus with potential diamond content, are not normally associated with lamprophyre and carbonatite activity. The main purpose of this study is to present microprobe analyses of minerals from the Aillik Bay dykes in order to clarify the affinities of the suite.

Mineral chemistry is also used, in conjunction with whole-rock data, to more closely investigate petrogenesis of the suite. A reclassification of the lamprophyres differing from that of Hawkins (1977), shows that they can all be related to a parental magma, the composition of which is defined. The processes by which the individual rock types are believed to have been derived from that parental magma are discussed. These include flow differentiation, liquid immiscibility, crystal

accumulation and carbonatisation.

Structural and other evidence is accumulated to verify the suggestion of Hawkins (1977) that the suite is part of a central complex related to rifting of the Labrador Sea.

TERMINOLOGY OF MAFIC DYKE ROCKS

Kimberlite:

The term kimberlite is generally used for a potassium-rich, inequigranular ultramafic rock which may contain ultramafic xenoliths of mantle origin and diamond. Olivine is an essential constituent and occurs as phenocrysts, normally of two generations, with any of the following minerals: calcite, serpentine, garnet, phlogopite, diopside, perovskite, ilmenite, spinel and monticellite. The term is thus generally considered to include diamondiferous rocks such as those in southern Africa (Dawson,1971) and Siberia (Lebedev,1964), as well as diamond-free varieties occurring as part of alkaline central complexes such as Fen, Norway (Griffin and Taylor,1975).

Mitchell (1979) criticised the all-inclusive use of the term, and suggested that it should be restricted by mineralogy and field associations. Kimberlites would then be rocks with magnesian ilmenites, and in which garnets are pyrope- rich and clinopyroxenes are Al-poor diopsides. They would not be associated with alkaline central complexes, carbonatites, or structurally associated with rift zones. A number of economically-based classifications agree with these

mineralogical considerations (e.g. Snyman, 1974), but are intended to serve restricted areas and so cannot be applied generally.

The 'central-complex kimberlites' (Dawson, 1967) are characterised by titaniferous magnetites, Ti-Al salite-augites, manganoan ilmenites, and garnet, which if present, may be andradite-grossular or melanite. They are intimately associated with a wide variety of alkaline rocks and carbonatite.

The world's two largest kimberlite provinces, southern Africa and Yakutia, USSR, have a zonation of kimberlite type away from the craton centre (Dawson, 1980, p.16-20). Diamondiferous kimberlites occur on the cratons, and are usually unaccompanied by other intrusions, whereas the outer zones have various olivine-rich rocks with leucite, nepheline, melilite and monticellite. A middle zone is garnetiferous but diamond-free. This configuration implies a gradation between high- and low-pressure kimberlites rather than a simple division. In order to investigate this possibility, more probe data is needed on occurrences such as Bargydamalakh (Soviet Union), where kimberlite is said to form a composite intrusion with olivine melilitite (Ukhanov, 1965).

In this thesis, reference to kimberlites as defined by Mitchell (1979) will be to 'true kimberlites'. 'Kimberlite' is used for rocks of the central- complex type, since these occur abundantly in the Aillik Bay suite. Mitchell (1979) suggested they should be called lamprophyres, but they do not fit any of the recognised lamprophyre names, and so perhaps a new name is required to solve the kimberlite dilemma. It may be in order to

resurrect the name aillikite (Kranck,1939,1953) except for the fact that the Aillik Bay dykes are apparently part of an alkaline complex of uncertain type (see chapter 3). If a new name is to be chosen, the type rock should have known associations.

Lamprophyres:

Lamprophyres are generally considered to be porphyritic melanocratic dyke- rocks in which all phenocrysts are mafic minerals. Olivine, if present, occurs only as phenocrysts, and felsic minerals are restricted to the groundmass which is usually altered. Panidiomorphic texture and hydrous mineralogy (essential mica and/or amphibole) are characteristic.

There is a great variety of possible minerals, especially in the alkaline and ultrabasic lamprophyres. This results in a large number of names, many of which are so closely defined as to be useless outside the type area.

The commoner names are listed in table 1-1 as they appear in most petrology texts (Hatch et al.,1972,p.419; Williams et al.,1936,p.85; Chatterjee,1974, p.392; Huang,1962,p.161).

A division is commonly made between 'syenitic' lamprophyres in which orthoclase is the principal felsic phase, and dioritic where plagioclase predominates. Rock (1977) reclassified lamprophyres into shoshonitic, alkaline, ultrabasic, and leucite lamproite types, of which only the first two are common. Under shoshonitic he included minette, vogesite, spessartite and kersantite on the grounds that all are mildly potassic, of

TABLE I-1: Commonly used classification of lamprophyres as it appears in many petrology texts. Sannaite would fall into the Orthoclase x Ti-amphibole/biotite square.

DOMINANT MAFIC MINERALS	DOMINANT FELSIC MINERALS		
	ORTHOCLASE	PLAGIOCLASE	NO FELDSPAR
BIOTITE	MINETTE	KERSANTITE	
HORNBLENDE	VOGESITE	SPESSARTITE	
Ti-BIOTITE or Ti-AMPHIBOLE		CAMPTONITE	ALNOITE

intermediate SiO2, and are commonly associated with granites or mildly potassic alkaline rocks. The IUGS subcommission on nomenclature (Streckeisen,1979) recommended that Rock's shoshonitic group be termed the calc-alkaline group. The alkaline lamprophyres are characterised by phenocrysts of olivine (Fo 80-85), kaersutite/ barkevikite, titanpyroxene and titanbiotite in a matrix of pyroxene, amphibole and/or biotite with feldspars and/or feldspathoids. They are associated with nepheline syenite, gabbro or alkaline basalt. The ultrabasic lamprophyres are associated with carbonatites and are characterised by melilite, calcite and perovskite. Rock (1977,p.162) states that lamprophyre dyke swarms generally consist of only one of these sub-groups.

Rock's classification is preferable in that it places more emphasis on the composition of the mafic minerals present. Alkaline lamprophyres may contain the same felsic phases as shoshonitic types and thus be confused with them unless the Ti-rich nature of biotite or amphibole is recognised. Alkaline lamprophyres are commonly misidentified, and given the names of shoshonitic types, so that the correct alkaline names are unfamiliar to most petrologists. An example is the 'minette' of the Najavo volcanic field in Arizona which contains minerals characterising sannaite (Roden,1981).

The Aillik Bay dykes fall into the alkaline and ultrabasic classes of Rock (1977). Rock (1977,p.137) cites Aillik Bay as a possible example where two coexisting sub-groups can be explained by association with two unrelated intrusive episodes.

His conclusion is correct, because he uses the descriptions of Kranck (1953), who identified the dioritic (H2) dykes (see chapter 2) at Aillik Bay as lamprophyres, but made no distinction between dykes of the alkaline complex. The association of alkaline and ultrabasic types poses no petrological problems since nephelinitic and carbonatitic rocks commonly occur together (e.g.Ferguson and Currie,1971; LeBas,1980; Currie,1975a; Melcher,1966; Garson,1966; Gold,1970).

Hawkins (1977) used the terms minette and monchiquite to describe the Aillik Bay dykes. The use of minette is wrong, since it implies association with granitic rocks, and fails to account for the Ti-rich biotites.

Monchiquite is variously described as feldspar-free, analcite-bearing, or as having an isotropic or glass base possibly altered to zeolites. After an extensive literature survey, Rock (1977,p.161) concludes that monchiquite should refer to 'any feldspar-free alkaline lamprophyre with a fine grained, practically amorphous base which now comprises a range of feldspathoids and zeolites, though it may originally have been glassy'. The presence of analcime and absence of feldspars cannot be used to define monchiquite, since they are not mutually exclusive (e.g.Gallagher,1963).

Monchiquite is inappropriate for Aillik Bay dykes even though they contain feldspathoids and zeolites, since feldspars are predominant.

The minettes and monchiquites of Hawkins (1977) are described in this study as varieties of sannaite. The term

sannaite was coined by Brogger (1921), and is defined as a 'lamprophyre containing phenocrysts of augite with aegerine rims, barkevikite rimmed by biotite, and biotite in a base of alkali feldspars (orthoclase and albite), augite, aegerine, nepheline, etc.'(Sorensen,1974,p.573). It clearly describes alkaline lamprophyres with essential alkali feldspar, and it's use will avoid confusion with minettes. Sannaite is one of the lamprophyre names recommended by the IUGS subcommission (Streckeisen,1979). The Aillik sannaites differ from the above definition in that many contain olivine, and have SiO2 contents below the 40-46 wt% typical of alkaline lamprophyres (Rock,1977, p.132). Both these features are explained by the association with kimberlites and carbonatites.

GEOLOGY OF THE AILLIK BAY AREA

GENERAL GEOLOGY

Aillik Bay lies in the northwest part of the Makkovik sub-province, as defined structurally by Taylor (1971, 1972). This sub-province is an Aphebian- Paleohelikian 'window' preserved between the Archean Nain province to the north and the Grenville province to the south.

The rocks to the northwest of Kaipokok Bay, including Turnavik Island, are Kenoran-deformed gneisses and migmatites of the Hopedale Complex (fig. 1-2). It now appears that these were reworked in Hudsonian times, although absolute ages of metamorphism are as yet uncertain (Ryan and Kay, in press). The

term 'Makkovik gneiss' has been suggested for the gneisses of Sutton's(1972) Hopedale Complex in the area close to Kaipokok Bay, following more extensive regional surveys of the Archean to the north. The gneisses and migmatites of Turnavik have a dominantly north to northwestward structural trend, although this is modified to northeastward close to the contact with the Aillik Group, hence the inclusion of part of the Hopedale Complex in the Makkovik sub-province.

The coast from Kaipokok Bay to Big Bight, including the Cape Makkovik peninsula, is made up of Aphebian Aillik Group. The Aillik Group comprises Hudsonian-deformed felsic (with minor mafic) tuffs and lavas, plus quartzites and arkoses believed to be their epiclastic derivatives (Clark, 1974; Gandhi et al., 1969).

The main penetrative deformation in the Aillik Group resulted in a planar fabric folded about north to northeast trending axes. Shearing parallel to the main foliation obscures contact relationships and fold axes, such that the thickness of the Aillik Group is difficult to estimate (Bailey et al., 1979), although estimates of 7620m (Gandhi et al., 1969) and 8500m (Clark, 1974) have been made. Clark (1974, 1979) describes several stratabound tectonic slides and envisages a large zone of simple shear as the cause of the Makkovik sub-province structural trend. Clark (1974) introduced the first stratigraphic subdivision of the Aillik Group, which is reproduced here as table 1-2.

Both the Hopedale Complex and Aillik Group are intruded by

DOTER COVE FORMATION	RANGER BIGHT COMPLEX (1497± 22 Ma)	POMIADLUK FORMATION : MANAK BAY FORMATION
		PERRET'S POINT FORMATION (1545± 14 Ma)
		NESBIT HARBOUR FORMATION

TABLE 1-2: Schematic representation of the relationships between formations of the Aillik Group in the Makkovik area (after Clark, 1979).

numerous granitic to dioritic stocks, and rarer mafic to ultramafic rocks. Many granitic stocks and mafic dykes were intruded pre- or syn-Hudsonian, and so are now strongly foliated. There were at least six episodes of mafic to ultramafic dyke intrusion, at least three of which post-date all other igneous activity. The Aillik Bay intrusive suite is the latest igneous event.

In the present study, mapping was generally restricted to the good coastal outcrops, and some changes to the maps of King (1963) and Hawkins (1977) have been made (figs. 1-3 and 1-4). The geology of Turnavik Island is further subdivided, and more structural information is given. Hawkins (1977) identified an anticlinal closure on the Cape Aillik peninsula approximately 4km to the west of Cape Makkovik. He used this to suggest that the Cape Makkovik succession is right way up and on the eastern limb of the anticline. Several small folds not mapped by Hawkins (1977) show that in detail the structure is more complex.

TURNAVIK ISLAND

Migmatites of the Archean Hopedale Complex (Sutton,1972) are preserved on the western part of the south coast of Turnavik. The paleosome consists of multideformed granitic gneiss, amphibolite, quartz-veined plagioclase-hornblende-biotite semipelite, tonalitic gneiss and massive, fine grained quartzofeldspathic psammite. These are cut by quartz, epidote and chlorite dykes and veins later folded about axes now trending 340-350 .

The neosome is orthoclase-rich granite in composition, and irregularly cross-cuts the paleosome, in places brecciating it to form an agmatite (fig. 1-5). These migmatites are equivalent to the 'younger migmatites' of the Makkovik Gneiss (Ryan and Kay, in press), which crop out west of Kaipokok Bay.

Two major generations of deformed granitic rocks intrude the migmatites and form the greater part of Turnavik. The first, and volumetrically lesser, is a medium grained granitic gneiss in which biotite and hornblende define a strong foliation trending consistently just east of north. It contains several thin (10m wide maximum) melanocratic amphibolite bands in which occassional tight fold closures predating the main foliation can be found plunging at a moderate angle (mostly 40-45°) due west (fig. 1-6).

Later intrusions of hornblende-bearing K-feldspar megacrystic granites are foliated parallel to the earlier gneissic granite, or else cut it at an acute angle to the north. K-feldspar megacrysts commonly measure 2-5cm, and are elongated parallel to the foliation.

The contact between the two granite types is in places clearly intrusive, with stoped blocks of gneiss and amphibolite up to 2 metres across within the megacrystic granite. More commonly, however, the contact is the site of later intense shearing which causes a reduction in grain size and an increase in flattening up to half a metre from the contact. Length to width ratios of megacrysts are commonly doubled in these zones. A discontinuous mid-grey ultramylonite up to 5cm wide occupies

Figure 1-5: Migmatite (unit 1) on the south shore of Turnavik Island. Paleosome is tonalitic with disrupted rafts of amphibolite. The neosome is granitic to syenitic.

Figure 1-6: Quartz-rich pegmatite developed in f1 fold closure within melanocratic part of the foliated granite unit on Turnavik Island.

the contact zone in places. Similar megacrystic granites and migmatites occur to the west of Kaipokok Bay, about 18 km to the southwest of Turnavik Island, where Ryan and Kay (in press) consider the granites to be emplaced synkinematically with a 'straightening event' affecting the Archean.

Sinuous thin syenite, and later, thicker (up to 50cm) granite pegmatite dykelets cut the megacrystic granites (fig. 1-7). These dykelets cut the foliation at high angles and occasionally follow granite contacts, and many show evidence of multiple intrusion.

The pegmatites also cut elongate pods up to 110 x 20m of quartz-veined semipelitic leuco-amphibolite schists similar to those seen in the migmatite paleosome (fig. 1-8). The margins of these tectonically emplaced blocks are later sheared, causing tight folding in the pegmatite.

The ptygmatic nature of the pegmatites within the megacrystic granite suggests that the host rock's foliation may belie a complex structural history.

A melanocratic diorite to hornblende-gabbro forms the southwestern headland of Turnavik. It is compositionally homogeneous, and possesses a weak foliation trending approximately 340 . It postdates the migmatites, but its age relative to the gneissic granites is uncertain. It is possibly equivalent to the hornblendite-hornblende gabbro noted by Hawkins (1977, p.24) on West Turnavik (incorrectly marked as East Turnavik by him) and Graplin islands. These hornblende-rich rocks may be related to the Adlavik intrusive suite

Figure 1-7: Granite pegmatite dyke occupying a shear zone which crosses the contact between the two major types of foliated granite on Turnavik Island. The contact between the two gneissic sub-units is frequently sheared.

Figure 1-8: Semipelitic leuco-amphibolite occurring as a fault-bounded pod within megacrystic granite, south shore of Turnavik Island. Similar material occurs in the migmatite paleosome.

(Clark,1979).

CAPE MAKKOVIK PENINSULA

The rocks of the Cape Makkovik peninsula are the northern equivalents of the Big Island (units 2-6) and Makkovik Formations (units 8-9) of Clark (1974).

Gneiss with tectonic breccia (unit 2)

This unit comprises fine grained gneiss , originally quartzofeldspathic sediments and/or acid volcanics, and a carbonate-rich tectonic breccia (fig.1-9). The gneisses are banded parallel to strong foliation on the scale of 0.5 to 4cm. 60% of the bands are quartzofeldspathic and weather white to yellow, whereas the rest are light green to grey due to a higher content of epidotised mafic minerals.

The breccia consists of blocks of this gneiss plus rarer metamorphosed mafics (epidote- actinolite- chlorite- calcite), in a carbonate matrix. Blocks vary in size from less than 1cm to 1m x 35cm, and form 50-80cm thick bands within the unit. Fragments are more rounded, smaller, sparser and more elongate in matrix dominated zones. Blocks are mostly subangular due to abrasion by movement, including rotation within the matrix.

A similar, but thinner breccia within unit 9 entrains part of a mafic dyke for 50m along strike, suggesting that the breccia may be the locus for considerable strike-slip movement.

Many blocks are cut perpendicular to the foliation by quartz veins up to 6cm wide which predate brecciation. These

Figure 1-9: Tectonic breccia (unit 2). Psammite blocks of variable size in a dark matrix dominated by carbonate. Imbrication of blocks suggests movement toward the northeast.

Figure 1-10: Feldspathic psammite displaying platy jointing due to differential weathering of foliation planes. A lens of bright orange calcite is in the centre of the photograph.

veins are rare in the gneisses outside the brecciated horizon, and so they may have caused the localisation of brecciation. They probably fill tension cracks perpendicular to the principal axis of least stress during the flattening event.

In restricted areas this unit is gradational into unit 3.

Gneisses with calcite lenses (unit 3)

The western edge of this unit comprises a finely banded and folded feldspathic gneiss with rounded quartz and pink, secondarily feldspathised clasts. It originates, at least in part, as a conglomerate or breccia. The feldspathised clasts diminish in number eastwards.

The thicker eastern part of the unit is composed of similar gneisses impersistently folded on a small scale. These are postdated by thin breccia units similar to those of unit 2 but with smaller and sparser blocks. Anastomosing networks of carbonate-rich fine grained material define platy blocks approximately 6 x 2m. Carbonate thus forms no more than 10% of the rock.

Unit 3 also includes pods up to 30cm x 3cm of bright orange calcite frequently rimmed by amphiboles (fig.1-10). This calcite is apparently unrelated to the breccia matrix, but is represented in mafic pods included in the breccia.

Feldspathic gneiss (unit 4)

Unit 4 is a sequence of fine grained quartzofeldspathic gneisses with alkali feldspar-rich patches 5-10cm across. Small

scale, inhomogeneous low amplitude/long wavelength folding of the foliation can be seen as a result of colour variation. Unit 4 also contains mafic pods, elongated along the foliation, which exhibit well formed crystals of epidote, quartz, actinolite and subordinate potassic feldspar (fig.1-11). These originated as mafic dykes or lavas.

Feldspathised Gneisses (unit 5)

This unit is approximately 250m thick at Buttress Point, but tapers out completely to the south. The dominant rock is a hornblende-bearing plagioclase- rich psammitic augen schist (fig.1-12). Mafic minerals make up 10% of the rock, and are concentrated in wisps up to 80cm long and 1/2cm wide.

Quartz-feldspar-mica schists occur in two 8-9m thick zones; one central, and one at the western edge of the unit where it was mapped as a separate unit by King (1963) and Hawkins (1977). Red-stained quartz veins are common in the central schist sub-unit.

The expression of feldspathisation varies from 1-2mm irregular red crystals in the matrix, to replacement of augen and overgrowth of the foliation (fig.1-13). The large K-feldspar neoblasts are concentrated in various parts of the unit to form up to 60% of the rock.

Variable schists and leucogneisses (unit 6)

This unit is best exposed near Low Point where it varies from yellow and white quartzofeldspathic gneisses to

Figure 1-11: Mafic pod (epidote-quartz-actinolite-K-feldspar) within the feldspathic psammite unit 4.

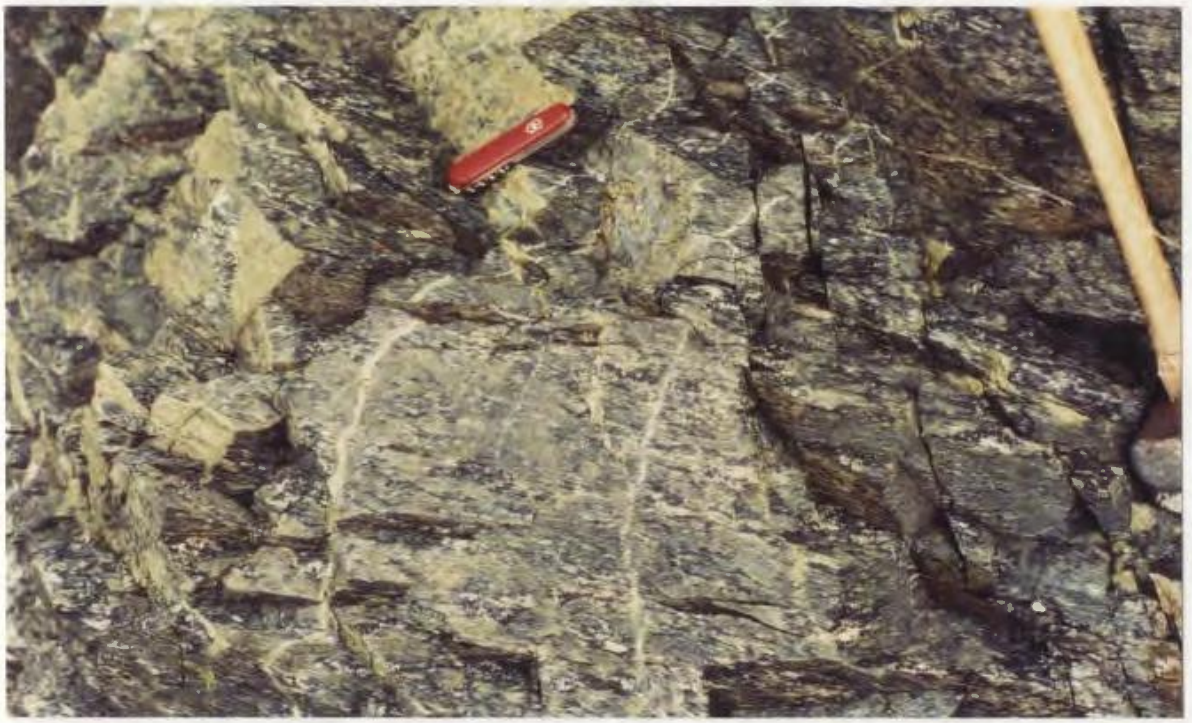

Figure 1-12: Plagioclase-rich psammitic schist with mafic wisps; unit 5. Cape Makkovik peninsula west shore.

Figure 1-13: Secondarily feldspathised part of unit 5. A later minor foliation dips at a moderate angle to the southeast. The principal foliation is parallel to bedding. Secondary red K-feldspar is here replacing augen. Picture taken facing south-southeast.

quartz-plagioclase-epidote-amphibole rocks with minor red garnet. The easternmost part is white, K-feldspar porphyroclastic, leucogneisses with mafic wisps which increase in abundance eastwards to form greenschist horizons making up 20% of the rock. Rarely, quartz-chlorite segregations occur within the mafic schists. To the south, these mafic schists anastomose around 10-20m pods of quartzose rocks.

Relationships with adjacent units are mostly obscured by later intrusions. The contact with amphibolite of unit 7 at Low Point is gradational although shearing close to the contact is considerable, evidenced by disruption of post-schistosity quartz veins in the amphibolite.

Amphibolite (unit 7)

The amphibolite has two major variants: a biotite-rich schist and a dominant hornblende-plagioclase rock with minor quartz, chlorite and small garnet-pyrite pods. The latter type is patchy on the scale of a few centimetres, and varies from planar foliated to an augen schist.

Pillow structures were found just to the southwest of this area by Clark (1971) in a unit correlated with unit 7 here by Gandhi (1976). No such evidence for origin could be found in this area.

Quartzofeldspathic protomylonite (unit 8)

Most of this unit consists of white elongated quartz and feldspar 1mm or less in length forming augen in an extremely

fine grained foliated matrix of similar composition (fig.1-14).

Inhomogeneous deformation allows recognition of earlier features in some parts. Just east of Low Point the rocks resemble banded tuffs, varying from dark grey to light green eastwards. Pyrite is abundant, especially in the lighter coloured rocks. In the central part of the unit, 10-30m thick layers rich in both mafic and felsic minerals suggest development by deformation of ash-flow tuffs.

Development of later cleavage trending approximately north-northeastwards has remobilised material from mafic wisps, resulting in en echelon patterns between the two cleavages.

The easternmost rocks of unit 8 are thinly banded white and light green with sporadic gneissic layering in coarser parts which grades in and out from the mylonite. The contact between this and unit 9 is gradational with increasing abundance of porphyroclasts (fig.1-15).

This unit is the site of numerous molybdenum and uranium showings, currently under investigation by Placer Development Ltd. The protomylonite is evidently the northward equivalent of the Makkovik Formation tuff member on Big Island, 10km to the south of Cape Makkovik (Clark, 1974, p.39-40).

Porphyroblastic gneiss (unit 9)

More than 80% of the rocks of this unit consist of quartz and feldspar porphyroblasts (2-5mm) in a very fine grained matrix containing less than 20% mafics. Deformation is variable, with little elongation of porphyroblasts in some places, and

Figure 1-14: Protomylonite unit (8). Rocks probably originated as bedded tuffs.

Figure 1-15: Eastern part of the protomylonite unit, including incompletely disrupted gneissic layering.

length:width ratios of 4:1 defining severe flattening and moderate constriction in others.

The rocks are generally yellow in colour, or light to mid grey in areas of higher modal plagioclase or mafics. Mafic minerals are dominated by biotite, and generally occur in 5-10cm x 5mm wisps. They vary in abundance throughout the succession and also along the foliation.

Late shearing occurs in restricted zones oriented SW-NE, cutting quartz veins which cross the earlier foliation. This results in a reduction in grain size and weathering to a white friable rock. The edges of these sheared zones grade rapidly into the normal rock type.

On the east coast, several variants of unit 9 bear a marked resemblance to rocks seen on the west coast. These include secondary K-feldspar replacing augen, thin elongate lenses of plagioclase-white mica rich rock, and tectonic breccia with a carbonate matrix. These occurrences suggest genetic links between rocks on either side of the mylonite zone, as suggested earlier by Clark (1974, p.103-105) for the south side of Makkovik Bay.

The Ranger Bight slide on Big Island occurs in a mafic unit, probably equivalent to the amphibolites of unit 7. The gradational contact between units 6 and 7 here suggests that the Ranger Bight Complex of Clark (1974, p.105-106) should be part of the Big Island Formation. The Ranger Bight slide may therefore be a much smaller feature than implied by Clark (1974).

The contact between the amphibolites and protomylonite at Cape Makkovik is obscured by shearing and later intrusions. The relationship between the Big Island and Makkovik Formations thus remains uncertain.

INTRUSIVE ROCKS

Small stocks, mostly less than 80m across, occur in great abundance on Cape Makkovik peninsula. Cross-cutting relationships and xenolith content permit the delineation of two major generations: (i) diorites and quartz diorites and (ii) monzonite, monzosyenite and quartz syenite. Many contacts are confused by igneous brecciation and associated leucocratic dykelet and vein injection. Epidiorites, characterised by green pseudomorphic amphibole, presumably after pyroxene, are commonly found cutting the porphyroblastic psammites of unit 9. King (1963) identified scapolite in some of these epidiorites.

The earliest intrusions are pre- or syn-deformational, but exhibit a weaker fabric than their country rocks. Later stocks postdate the main deformation, but are affected by weak shearing parallel to it.

A small monzogabbro on the east coast, and a hornblende peridotite near Low Point are the youngest stocks, since they show no sign of deformation.

Relationships between the many small stocks here and the numerous intrusive events within the Aillik Group as a whole (Gandhi et al., 1969; Clark, 1979) are uncertain.

Dykes are divided here into five major groups, which are

listed below in approximate chronological order:

(H1) Premetamorphic mafic dykes, now amphibolite schists.

(H2) Blue weathering diorite dykes with low angle dips.

(H3) Pink felsite dykes.

(H4) Diabase dykes, frequently porphyritic.

(H5) Lamprophyres and carbonatites of the Aillik Bay intrusive suite.

The first four are described briefly here, and the fifth is covered in detail in the next chapter.

AMPHIBOLITE DYKES (H1)

At least two periods of amphibolite dykes are seen on Cape Makkovik; the dykes are mostly less than two metres thick (fig.1-16). Variable features include plagioclase porphyroblasts, some replaced by granular feldspars, and calcite-biotite, amphibole-chlorite and epidote-quartz-chlorite mineralisation. Some mafic pods described as part of the country rocks may also have originated as mafic dykes.

DIORITE (H2)

This is the most voluminous dyke set in the area, forming mostly low angle dykes (fig.1-17), dipping generally southeastwards (see next chapter, fig.2-4). The dykes are 1.5 to 3.5m thick and form up to 15% of some outcrops.

The rock is generally fine-medium grained, homogeneous, and essentially bimineralic hornblende and plagioclase, with minor sphene, quartz, and opaque oxides. Amphibole crystals 0.2 to

Figure 1-16: H1 amphibolite dyke cutting psammites of unit 9.

Figure 1-17: H2 diorite dykes froming typical flat-lying sheets.

2.0cm, mostly with red oxide rims, occur sparsely, as well as rarer irregularly shaped feldspathic patches which may be partly digested xenolithic material.

These dykes have been variously described as diorite (Gandhi et al.,1969), quartz-diorite (Sutton,1972), and kersantitic lamprophyre (Kranck,1953; Moore, 1951). However, the interstitial plagioclase is only slightly altered to clay minerals and is of medium grain size, and amphibole dominates the mafic phases. Spessartite would therefore be the correct term were criteria sufficient to warrant a lamprophyre name.

FELSITE (H3)

Homogeneous pink to white aphanitic felsite dykes are the least abundant of any dyke-type. They are 80cm to 2m thick and frequently have poorly defined chilled margins.

Both H2 and H3 dykes are unmetamorphosed but show signs of minor shearing, and are frequently internally fractured along their margins. A few H2 dykes exhibit unusual sigmoidal joints (Kranck,1961; King,1963) apparently due to late shearing parallel to the country rock foliation.

DIABASE (H4)

Several near-vertical dykes 8 to 24m wide strike approximately 080 across the Cape Makkovik peninsula. They commonly have 30 - 50% large (22cm max, 3-8cm average) plagioclase phenocrysts which do not normally show any preferred orientation. Mats of smaller crystals also occur (fig.1-18). The

Figure 1-18: Porphyritic example of H4 diabase. Phenocrysts are up to 22cm across. Note the mat of smaller crystals at the left of the picture.

Figure 1-19: H4 diabase with few plagioclase megacrysts. Note the concentration of phenocrysts at the dyke margin at the top of the picture.

widest dykes often have 2-5m wide phenocryst-free borders. In dykes with fewer phenocrysts (e.g.fig.1-19), phenocrysts may be aligned parallel to dyke margins. Concentration of phenocrysts at dyke margins occurs in a dyke on the east coast of Cape Makkovik peninsula. This contradicts normal flow laws (Bhattacharji, 1967) and is probably due to multiple intrusion or varying speed of intrusion.

Many thinner (10cm to 2m) fine grained basaltic dykes follow a similar strike. They weather a similar mid-brown colour and are almost certainly related to the porphyritic dykes. Porphyritic dykes are not seen on Turnavik, but continue west of Kaipokok Bay (Sutton, 1972).

CHAPTER 2 : STRUCTURE AND FIELD CHARACTERISTICS OF AILLIK BAY DYKES

A. REGIONAL DISTRIBUTION

The alkaline lamprophyres and carbonatites of the Aillik Bay alkaline intrusive suite are concentrated in the northern parts of the Cape Makkovik and Cape Aillik peninsulas, and on the Turnavik Islands (fig.2-1). They rapidly diminish in number southwards and are rare south of the north end of Banana Lake on the Cape Makkovik peninsula. Lamprophyres occur sparsely on Dunn and Strawberry Islands (J.G.Burns, pers.comm.), but do not persist further along the coast to the southeast (C.F.Gower, pers.comm.).

On Turnavik Island, the vast majority of dykes are steeply dipping and strike between 040 and 060 (fig.2-1), and so cross-cutting relationships to distinguish between periods of dyke emplacement are not available.

Three principal sets are present on Cape Makkovik (fig.2-2), and are listed below in approximate chronological order (oldest to youngest) as defined by cross-cutting relationships:

(i) Vertical or steeply dipping, east-west striking dykes. These are carbonate- poor sannaites and olivine sannaites.

(ii) North to northwest striking, steeply dipping dykes including ocellar sannaites with variable amounts of carbonate, and kimberlites.

(iii) Low angle sheet intrusions with variable strike, mostly roughly east-west. These include kimberlites, and carbonatised

Figure 2-2: Contoured stereogram of poles to alkaline complex dykes on the Cape Makkovik peninsula. Contours at 1%, 3%, 7% and 11% per 1% area. 96 readings.

Figure 2-3: Contoured stereogram of poles to foliation planes for the Aillik Group on the Cape Makkovik peninsula. Contours at 1%, 3% and 10% per 1% area. 129 readings.

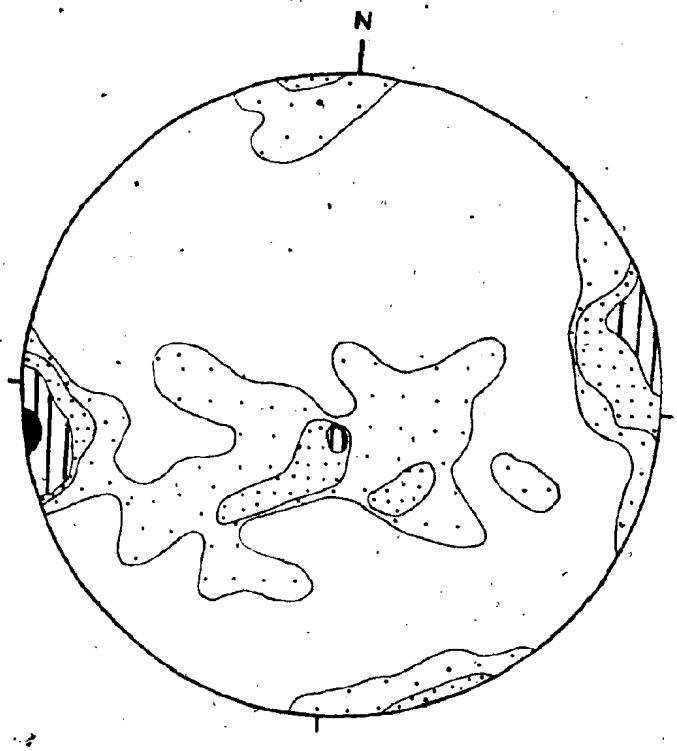
N

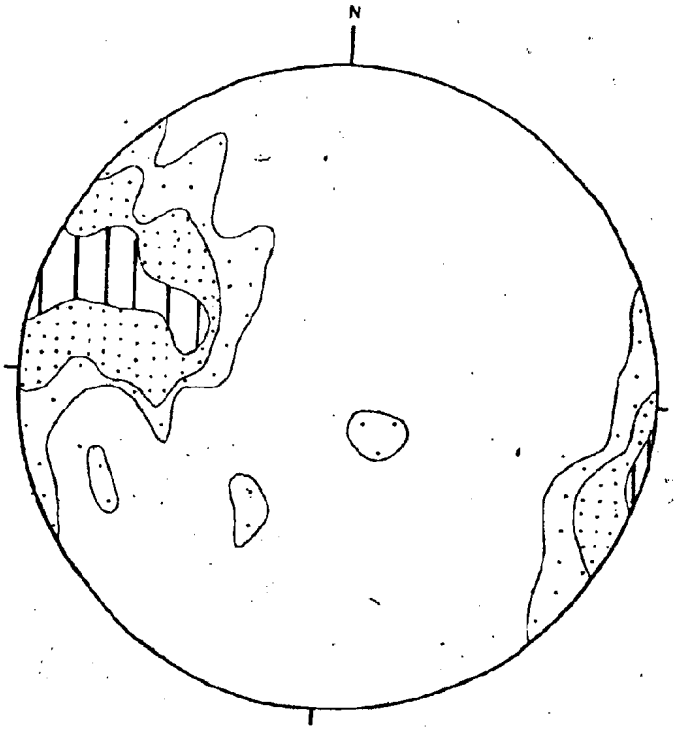
N

kimberlites and sannaites.

Rarely, dykes of the second set are seen to cut those of the first set, suggesting a small degree of contemporaneity. The low angle sheets are always youngest.

Figures 2-3 to 2-5 summarise structural trends existing prior to emplacement of the alkaline dykes. The main foliation of the Aillik Group (fig.2-3: the D2 deformation of Clark, 1974,1979) defines a structural trend not followed by any of the alkaline dykes. The abundant Helikian diorites (H2 - see chapter 2) form flat-lying sheets (fig.2-4), and the H4 diabase dykes have a consistent strike of approximately 080 degrees (fig.2-5). The latter trend has clearly influenced emplacement of the first alkaline dykes, and the diorite sheets may have influenced dips in the carbonate-rich lamprophyre sheets.

The north to northwest striking second set of alkaline dykes on the Cape Makkovik peninsula is not related to pre-existing structures. Together with the dominant strike of Turnavik Island dykes, it appears to form a radial dyke system defining an intrusive centre to the northeast (fig.2-1). Data for the smaller islands of the Turnavik group are taken from Hawkins (1977). The bulk of these data are from Cape Aillik so that the apparent disagreement with the proposed site for the intrusive centre is exaggerated. The low angle sheets could be cone sheets of the central complex, as will be discussed later.

The regional joint patterns (fig.2-6) correspond to dyke trends, including the pre-akaline complex dykes, and ignore earlier structures such as folds and foliations.

Figure 2-4: Stereogram of poles to H2 diorite dykes. Squares = Turnavik Island, triangles = Cape Makkovik peninsula.

Figure 2-5: Rose diagram showing orientation of H4 diabase dykes. 31 readings.

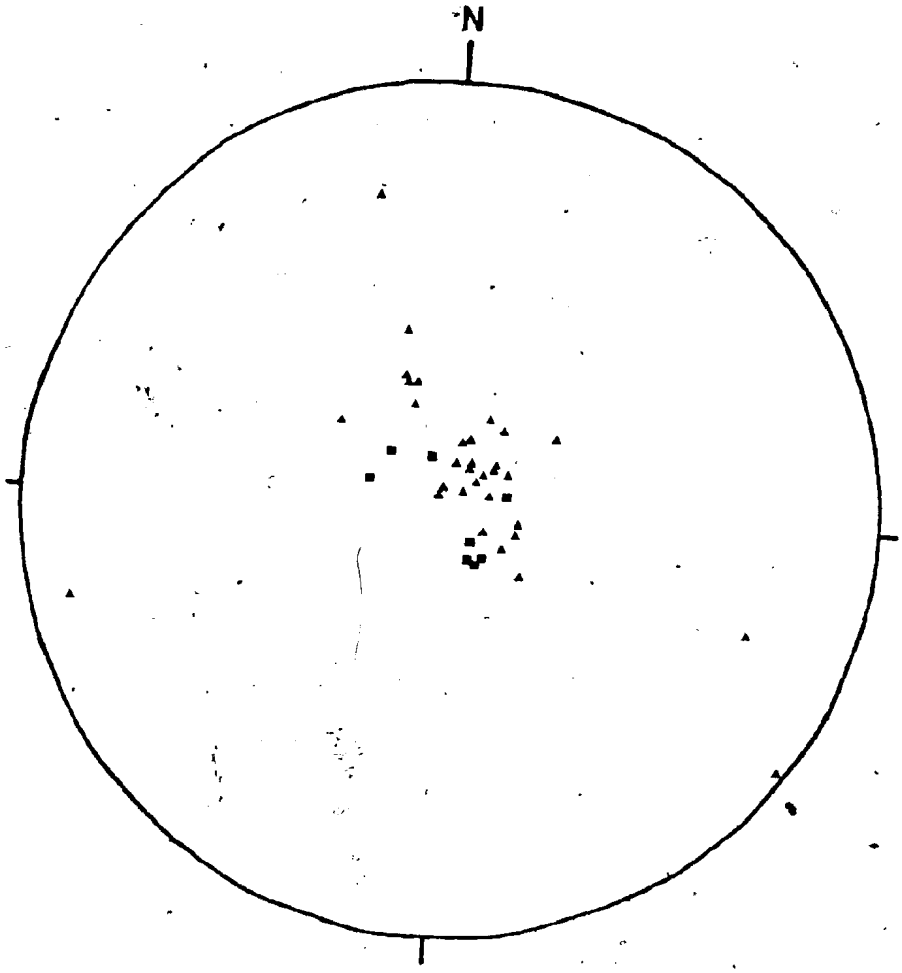
N

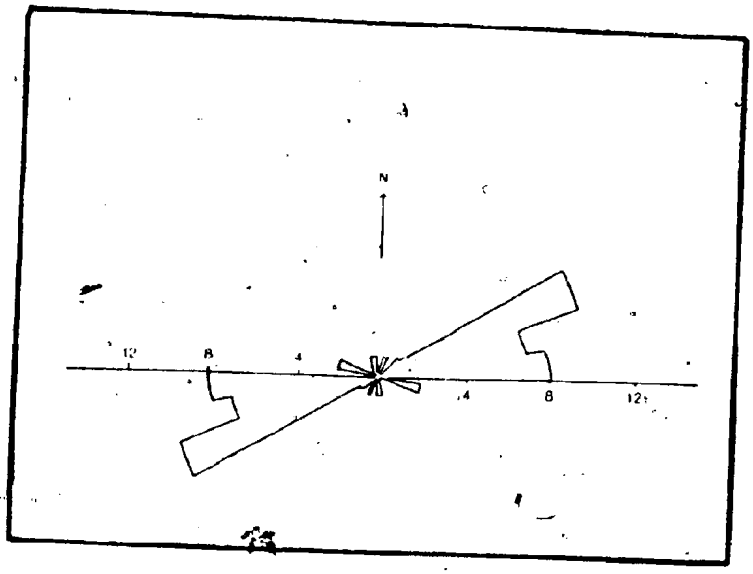
N
12
8
4
4
8
12

Figure 2-6: Contoured stereogram of poles to joint planes on the Cape Makkovik peninsula. Contours at 1%, 3%, 5%, 8% and 12% per 1% area. 160 readings.

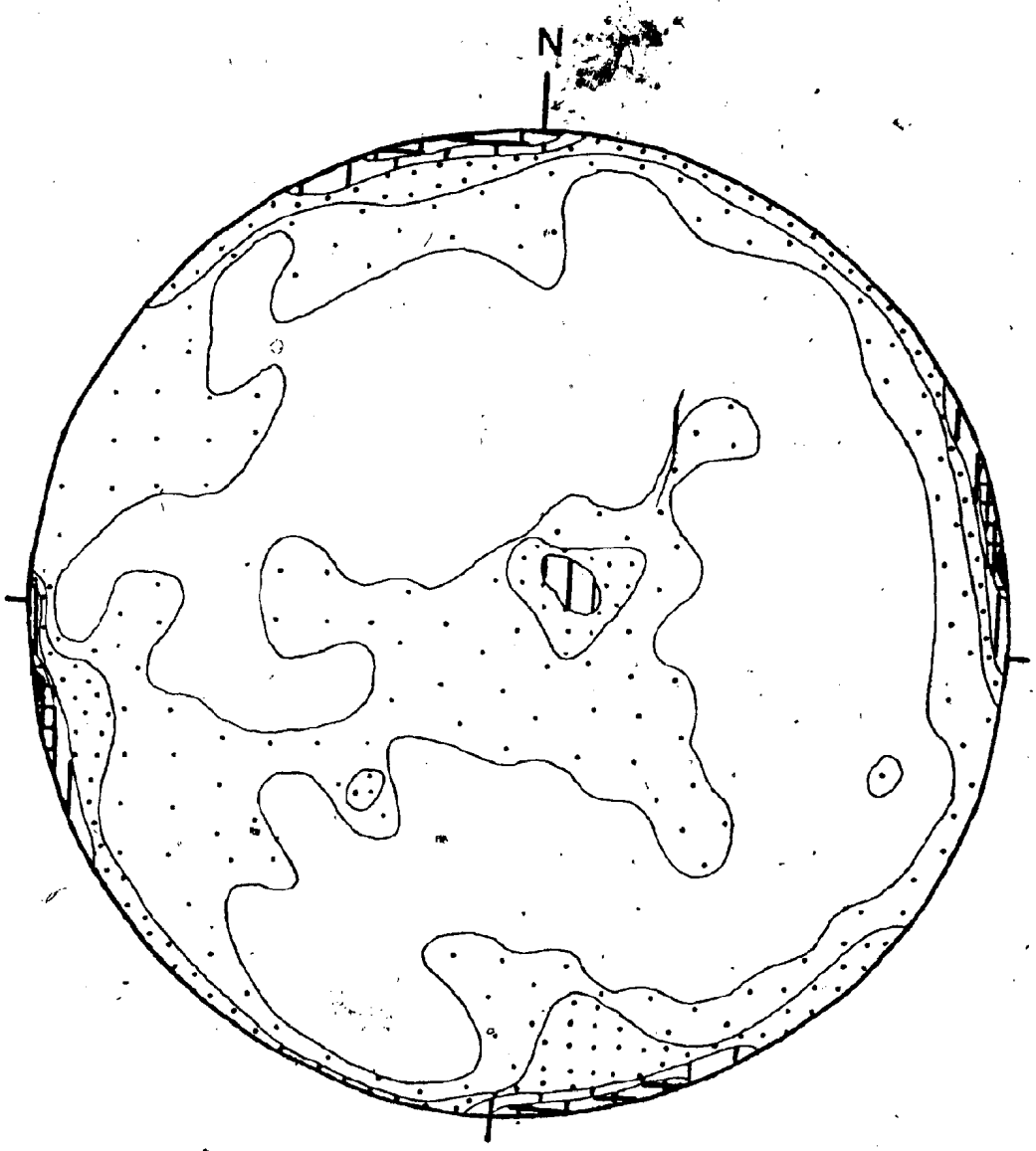

B. FIELD CHARCTERISTICS OF ALKALINE-COMPLEX DYKES

(i) Sannaites

Sannaites are mid-brown weathering dykes 6–60cm wide with a mid grey-blue fresh surface. Small phenocrysts of biotite with variable amounts of pyroxene and olivine are set in a grey matrix with variable carbonate. Pyroxene-rich dykes with relatively little carbonate form massive dark brown dykes (fig.2-7), whereas more carbonate-rich dykes are lighter coloured and frequently have calcitic veins or segregations.

The sannaites commonly have a coarsely porphyritic appearance due to carbonate and felsic globules up to 2cm across. The globules are irregular in shape but always have rounded edges. They may be rimmed by a thin film of fine grained green or red material, and the carbonate within them may be stained red.

Many dykes are banded parallel to dyke margins due to multiple intrusion. Multiple intrusion is demonstrated in fig.2-8, where a later dyke separates from an earlier dyke and then intrudes it. Globules are generally larger toward the centre of each intrusive phase, and coarser in later magma pulses. Contacts between bands may be sharp or gradational. Sharp contacts are most likely due to flow differentiation causing concentration of larger phenocrysts toward centre of intrusive phases (Bhattacharji, 1967; Barriere, 1976). Groundmass minerals frequently show little grain size contrast across sharp boundaries.

Different patterns of banding are described in detail by

Figure 2-7: Carbonate-poor sannaite dyke. Chilled margins are only very poorly developed.

Figure 2-8: Multiple intrusion in sannaites demonstrated by separation of bands. The later ocellar band reintrudes the earlier dykes. Host rock is hornblende-bearing megacrystic granite of Turnavik Island.

Hawkins (1977, p.46-57). Ultramafic xenoliths are rare in the sannaites, but do occur in thicker, more carbonate-rich dykes.

(ii) Kimberlites

Kimberlites are easily distinguishable in the field by their yellow-orange weathering surface and numerous megacrysts of bronze mica up to 3cm across. The fresh surface is light blue to grey with variable amounts of carbonate veining. Kimberlites generally form much thinner dykes than sannaites. They rarely exceed 30cm in width, and also occur as thin dykelets only 1-2cm wide, frequently parallel to a larger dyke. Mica and olivine phenocrysts are ubiquitous.

Many dykes contain elongate rounded to sub-spherical nodules as well as country rock slivers of variable size (up to 45 x 20cm). Nodules are normally difficult to identify due to fine grained red-brown alteration rims. Glimmerites (biotite dominated rocks) are the most common ultramafic type, and usually measure 2-5mm, although some are up to 3cm across. Hawkins (1977,p.97) catalogued nodule types, and suggested they belong to the MARID suite as defined by Dawson and Smith (1975). Titanomagnetite megacrysts occur in a kimberlite at the northwestern part of Turnavik Island (sample locality 378).

Well defined carbonate globules are rarer in kimberlites. They are much more irregularly shaped and do not occur in bands, and so are probably late stage segregations.

Multiple intrusion is common in kimberlites, frequently resulting in adjacent discrete dykes where later magma pulses

intrude the margins of pre-existing dykes. Multiple intrusion is commonest in the low angle sheets (recall fig.2-2), where the majority of intrusive phases are carbonate-rich kimberlite (fig.2-9).

(iii) Carbonatites and carbonatised lamprophyres.

Discrete carbonatites occur very rarely, but carbonatisation of other dykes is common. Alvikites (hypabyssal calcite-carbonatites: von Eckermann,1948,1966; Heinrich, 1966,p.12) are patchy red to grey weathering dykes, and include a large number of xenolithic slivers. Thin alvikitic dykelets occasionally occupy cross-fractures in sannaite dykes which were presumably caused by contraction during cooling. A beforsite (dolomitic equivalent of alvikite) occurs close to Aillik village (Hawkins,1977).

Carbonatisation is dominant in kimberlites, where carbonate forms the major part of the groundmass, and in thin section is seen to pseudomorph olivine. In sannaites the effects are less marked: some carbonate is present in the groundmass, but most is restricted to late veins or dyke selvages. Carbonate rich precursors to later pulses of sannaite can result in carbonate-rich bands within sannaite dykes (fig.2-10).

Bands in kimberlites are often poorly defined, apparently due to modification of contacts between bands by late movement of carbonate-rich fluids. Movement of these fluids can result in carbonate 'fronts' across which unaffected rock becomes becomes strongly carbonatised in the space of 50-70cm (fig.2-11).

Figure 2-9: Banded carbonate-rich kimberlite dyke. Bands are due to multiple intrusion and flow differentiation of late-stage carbonate segregations.

Figure 2-10: Multiple intrusion in kimberlitic dyke. The carbonate-rich selvage to the later intrusion is taken to be evidence for a volatile-rich precursory fluid. Mica is concentrated in the latest intrusion head, showing it to be volatile enriched.

(iv) Related ultramafic dykes

Unusual medium-coarse grained ultramafic dykes occur at 3 localities; one on Turnavik Island (sample localities 369-370), and two on the west coast of the Cape Makkovik peninsula (386 and 429). The Turnavik dyke is a 60cm wide green- grey weathering phlogopite-clinopyroxene-peridotite. The Cape Makkovik dykes are a green weathering mica-pyroxenite and a bronze-black pyroxene-carbonate-glimmerite. The mafic mineralogy is alkaline, and all the dykes have groundmass carbonate. They are interpreted to be related to the lamprophyre suite, and not to earlier hornblende peridotites described by Hawkins (1977). The glimmerite exhibits limited autobrecciation.

C. STRUCTURAL FEATURES OF INDIVIDUAL DYKES

(i) Description of features

Many dykes are accompanied by 1-6m wide zones of closely spaced parallel jointing of the adjacent country rock. The joints are mostly several metres long and may be spaced as closely as 5-10cm, particularly adjacent to nearly vertical dykes. Fracture zones are restricted or absent around sannaites, but always accompany kimberlites and carbonatised rocks (fig.2-12).

Many dykes are not continuous along their length, but occur in segments normally a few tens of metres long which have horned or tapered termination structures (fig.2-15). Dyke segments may

Figure 2-11: Carbonatisation front in a kimberlite sheet intrusion. Carbonate- rich yellow weathering kimberlite gives way to carbonate-poor kimberlite in the space of 50cm.

Figure 2-12: Carbonate-rich kimberlite sheet intrusion forming part of the youngest dyke set. Note development of the fracture zone parallel to the dyke, and also local variation in dip. The dyke is cutting psammites of unit 9 and a small felsite stock.

be connected by thin dykelets (fig. 2-15a), or may have horns curved to face each other (fig.2-15b). Tapered terminations are commonest in dykes with a poorly developed fracture zone. Complex structures (figs 2-15 e-g) only occur in dykes 15cm or less in width.

Dyke segments within parallel fracture zones occur in an apparently random fashion, and are not arranged en echelon across the fracture zone. This situation also occurs in Greenland kimberlites (Andrews and Emeleus,1975).

Fractures adjacent to dykes are frequently filled by yellow weathering carbonate-rich kimberlitic material (fig.2-13). These dykelets are commonly found as anastomosing networks between dyke segments within a fracture zone (fig.2-14), and appear to be continuations of the selvages of the dykes. The dykelets may therefore be formed by a volatile-rich precursor to dyke emplacement as described by Currie and Ferguson (1970). Rarely, zones of parallel fractures occupied by thin dykelets but with no main intrusive body occur. Anderson (1979) explained how a lower viscosity fluid will assist rapid crack growth by stress corrosion cracking. The more viscous magma body will be unable to proceed to the end of the previously formed crack (Pollard, 1973), and so the extremities of a dyke will remain as thin cracks filled only by the volatile-rich precursory fluid. Intrusion of the main magma body will reheat the dyke selvages which will have chilled due to rapid expansion in the rapidly growing crack (Currie and Ferguson,1970). This leads to remobilised dyke selvages which may re-intrude the main dyke

Figure 2-13: Development of thin yellow-weathering carbonate-rich kimberlite dykelets in a parallel fracture zone adjacent to a kimberlite dyke. Host rocks are foliated granite (unit 10; bottom) and D2 diorite.

Figure 2-14: Carbonate-rich kimberlite forming a vertical dyke on Turnavik Island. Dyke segments are interconnected by an anastomosing dykelet system which occupies cracks within the fracture zone.

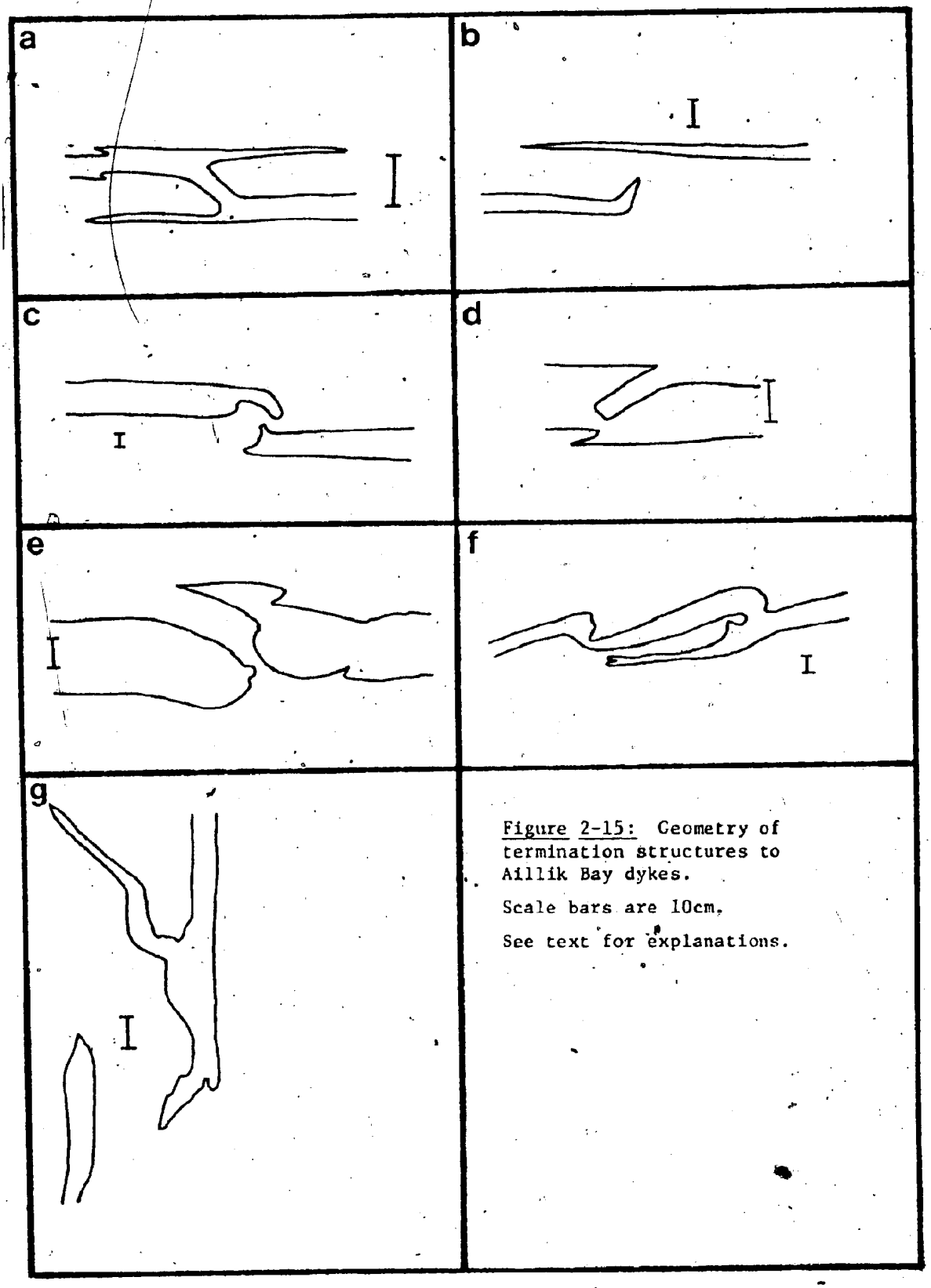

Figure 2-15: Geometry of termination structures to Aillik Bay dykes.

Scale bars are 10cm.

See text for explanations.

body, thus confusing age relationships.

(ii) Formation of fracture zones and segmented dykes

McHone (1978) suggested that closely spaced joints adjacent to lamprophyres in New England could be cooling fractures. Later minor tectonic movements could cause localisation of deformation at dyke margins due to contrasts in mechanical properties between dyke and host rock. Neither of these mechanisms explains the lack of such fractures adjacent to the earlier diabase dykes, many of which follow the same strike as alkaline complex dykes. The occurrence of fracture zones with only thin dykelets interpreted to be precursory to dyke emplacement suggests that fracture formation is an inherent part of carbonate-rich dyke emplacement and immediately precedes it.

Segmented dykes with or without termination structures have been described from dykes of differing composition (Kaitaro,1953; Barriere,1976b; Pollard et al., 1975).

Disconnected parallel fractures associated with dyke intrusion have often been assumed to be related to shearing (Hill,1977; Kaitaro,1952). Kaitaro (1952) suggests that shearing simultaneous with dyke intrusion is hard to disprove where a cross-connecting dyke exists (e.g.fig.2-15a). However, in cases where the cross-connection is not present (e.g.fig.2-15b) there is no evidence of shearing.

Segmented dykes are easiest to explain if they are assumed to split into fingers as they are intruded, rather than being later disconnected by structural deformation. The surfaces seen

in fig.2-15 can be treated as being perpendicular to the maximum principal axis of the stress field ($\sigma 1$) into which the magma was intruded. The dyke segments would therefore be simultaneously intruded, and then progressively enlarged.

Rotation of principal axes of stress within the $\sigma 2$-$\sigma 3$ plane would cause a sheet to become unstable, and breakup into segments would result. The rotation of components would presumably be due to very local inhomogeneities. This process would ideally lead to an en echelon pattern (fig.2-16), but the Aillik Bay segmented dykes are apparently random. The dyke segments would exploit the weakened planes of a parallel fracture zone, and movement of magma within the fracture zone may mask the en echelon pattern. The fracture zone may even create the inhomogeneity required to initiate breakup of the sheet.

Whilst the above process may explain segmented dykes within parallel fracture zones, the occurrence of some segmented dykes without fracture zones shows that other mechanisms must be considered.

Pollard et al.(1975) described a possible mechanism for breakup of sills into fingers with no change in location of principal stress axes. This was invoked to explain the numerous fingers at the periphery of a sill at Shonkin Sag, Montana (Hurlbut and Griggs,1939; Pollard et.al.,1975). Intrusion of magma as a sheet requires much less energy expenditure than intrusion as fingers, because fingers must overcome greater viscous drag due to a increased surface area.

Figure 2-16: Diagram showing breakup of a dyke into en echelon fingers by rotation of the intermediate and minimum principal axes of stress. Intrusion direction is indicated by the arrows. Local wall-rock inhomogeneities are considered to be the cause of rotation of axes.

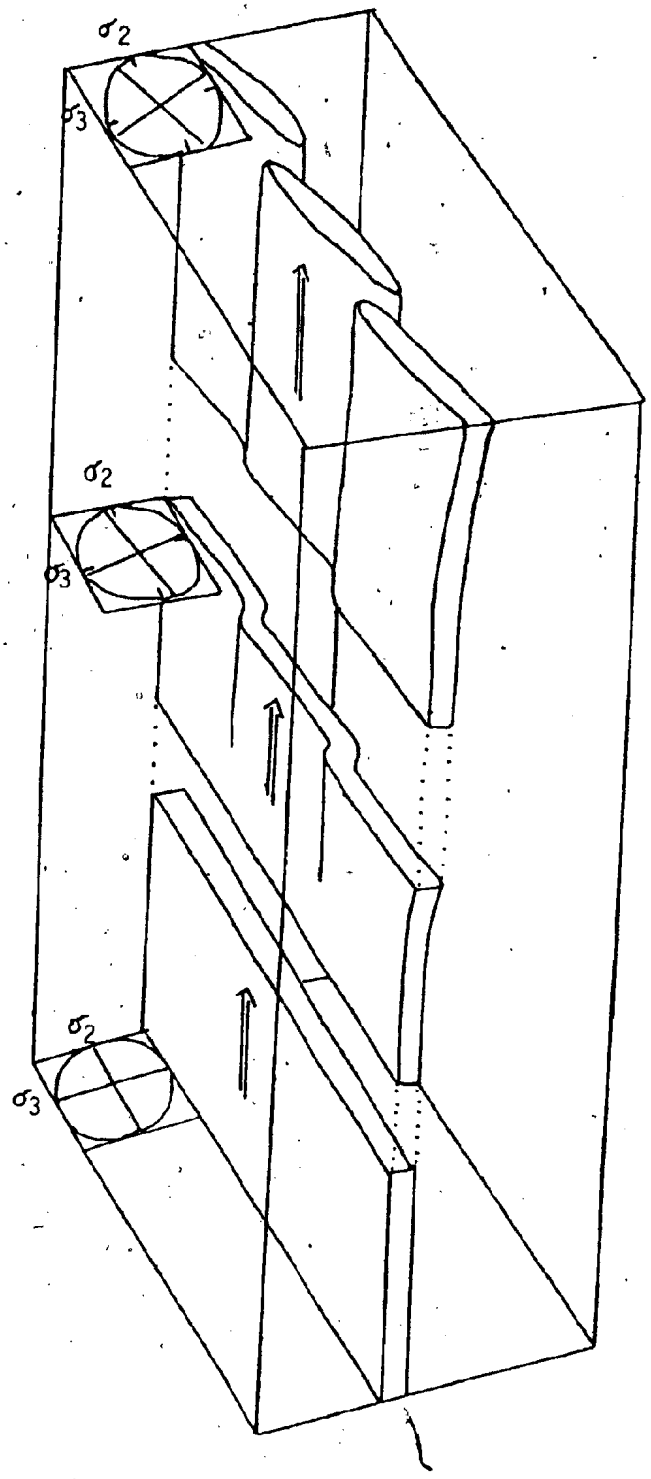
σ_2
σ_3
σ_2
σ_3
σ_2
σ_3

Pollard et al.(1975) cited the fluid flow experiments of Saffman and Taylor (1958), and proposed that flow instability could lead to initiation of fingers. By this mechanism, several points on the leading edge of a magma sheet would move faster due to very local variations in effective shear strength of the wall rock, thus creating lobes in the advancing interface. Pollard et al.(1975) state that the magnitude of the instability will be approximately proportional to the viscosity contrast at the interface. Volatile- rich magmas have low viscosities and would therefore be more likely to break up. Also, the growth of fingers will be limited by cooling and crystallisation: rapid solidification would occur unless volatiles remain trapped within the dyke, so that this process could be important in volatile-rich dykes without fracture zones.

Horned termination structures will occur where dyke segments grow laterally past one another in the direction of σ_2 (fig.2-17). Enlargement of the segments will be dominated by lateral extension as intrusion proceeds from 2-17a to 2-17b, since deformation will concentrate at dyke edges (Pollard and Johnson,1973; Pollard,1973). Stress concentration will occur in the region of overlap, and mutual attraction toward the region of overlapping yield zones will occur (fig. 2-17b: Frank,1965). Union of two segments may be realised where a cross-fracture occurs (as in fig.2-15a). The lateral movement of magma explains rotation of blocks of country rock between dyke segments (fig.2-15c).

Relict horns as in fig.2-15a will have grown before the

Figure 2-17: Diagram to explain cross-connections and horned termination structures. All diagrams are cross sections perpendicular to the principal direction of intrusion. Dyke segments (a) expand in the direction of sigma 2. When adjacent segments overlap (b) stress concentration occurs at x and causes mutual attraction. Horned termination structures (as fig.2-15a) are caused by segments propagating past each other at a distance too great to result in stress concentration (c). After extension in the direction of sigma 2 occurs, thickening of the segments is possible, such that the critical distance y' becomes small enough for mutual attraction to occur. This process leaves relict horns.

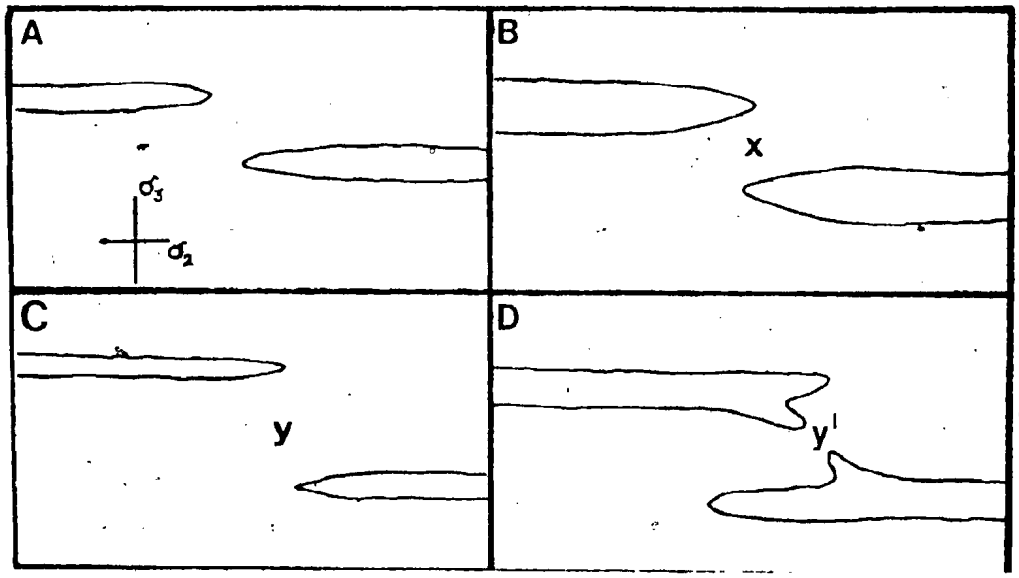

stress concentration was great enough to cause attraction (fig.2-17c). Continued intrusion causes thickening as well as extension of dyke segments, until overlapping of yield zones causes formation of the connection (fig.2-17d). The horn would be abandoned as soon as mutual attraction occurs.

Irregular and lobate terminations (fig.2-15 e-g) may be due to the combined effect of pre-existing fractures and volatile action. The alkaline nature of volatiles trapped at the sides of a propagating dyke will assist corrosion of wall rock (Martin,1980; Paterson,1978,p.78). Rapid accumulation of volatiles will facilitate rapid crack growth and opening of pre-existing fractures by stress corrosion (Anderson,1979; Martin and Durham,1975).

D. THE AILLIK BAY INTRUSIVE SUITE AS A CENTRAL COMPLEX

(a) Structural features of central complexes

As noted earlier, the orientations of dykes on Turnavik Island and the Cape Makkovik peninsula suggest that they radiate about a centre to the northeast (fig.2-1). The east-west striking dykes on Cape Makkovik and their rare counterparts on Turnavik could be cone sheets. Fig.2-1 includes data from Cape Aillik and other islands of the Turnavik group from Hawkins (1977).

A vertical dyke on Strawberry Island has a southeasterly strike (R.A.Doherty, pers.comm.), supporting the radial swarm hypothesis. Dykes occur sparsely on the mainland to the west of

Turnavik Island, where they are of northeasterly or easterly strike. However, the bulk of measurements are from only 65 degrees of arc, and such a sample is, on its own, perhaps too small to justify the supposition of a central complex. It is therefore pertinent to consider the evidence of other features at Aillik Bay.

The following features support the idea of a central complex:

(i) Radial dyke systems are often centred around a visible stock, as at Rhum, northwestern Britain (Dunham and Emeleus,1967) and Spanish Peaks, Colorado (Ode,1957; Johnson,1970).

(ii) Kimberlitic lamprophyres are so commonly associated with central complexes, as at Alno, Sweden (von Eckermann,1966) and Fen, Norway (Griffin and Taylor, 1975), that Dawson (1967) proposed the name 'central complex kimberlite'. Also, Rock (1977,p.140) remarked '(dyke) swarms unconnected with central plutons seem to carry proportionately fewer lamprophyres than those radiating from plutons'.

(iii) The presence of low angle sheets in the intrusive suite is only easily explained by a nearby magma chamber (Phillips,1974; Faller and Soper,1978).

The last of these requires further explanation. The presence of carbonatite in the low angle sheets cannot be used to infer a separate structural event because carbonatisation commonly occurs along pre-existing dykes. Kimberlite occurs both in radial dykes and low angle sheets.

The variance in dip of the sheets is probably of only local

significance. Ramsay and Sturt (1970) introduced a cutoff of 30cm in their study of dyke emplacement in northwestern Norway, below which thickness they considered sheet dips could be entirely a facet of very localised stress fields.

The 3 dyke sets at Aillik Bay can be explained by a simple model with a gradually rising magma diapir. This is summarised in Fig.2-18d.

As the diapir rises due to density contrast between its magma and the surrounding rocks, $\sigma 1$ is vertical or near-vertical, and $\sigma 3$ is radial (fig.2-18a). The relative magnitude of $\sigma 1$ will gradually increase due to lessening of overburden as the diapir nears the land surface, until failure occurs in a plane perpendicular to $\sigma 3$ (Anderson,1951). Intrusion of magma into fractures formed in this way will result in conic dykes. The east-west early set of dykes at Aillik Bay are interpreted to have formed in this manner.

The formation of radial dykes requires doming of the surface around the upwelling magma. On a well-developed dome, the weight of the rocks will tend to slide off the magma dome, so that the magnitude of $\sigma 3$ increases away from the centre of the dome. Thus, a central zone of lateral tension gives way to a zone of compression (fig.2-18b) in which fractures will be radial.

The low angle sheets could be caused by a build up of pressure in the magma chamber (Phillips,1974: fig.2-18c). Under these conditions, $\sigma 1$ would be perpendicular to the magma-rock interface, which is simplified as hemispherical (dome-shaped in

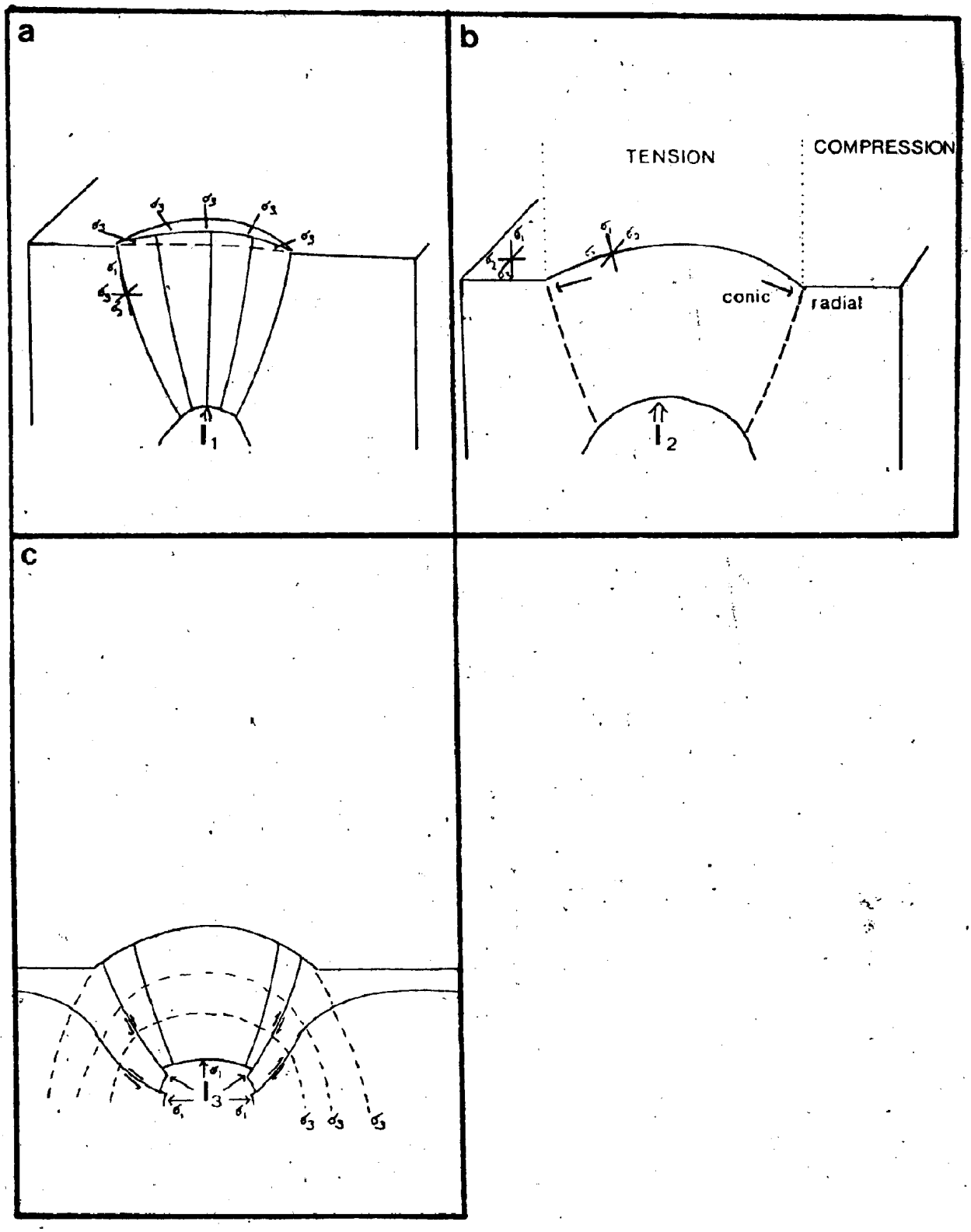
a
b
TENSION
COMPRESSION
conic
radial
c

Figure 2-18: Development of dykes sets seen at Aillik Bay in relation to a central complex. (a) Vertically directed stresses due to emplacement of a magma chamber cause ring dykes in the region of incipient uplift. (b) Doming of rocks with continued upward movement causes the minimum principal axis of stress to change from radial to concentric away from the centre due to the weight of uplifted rocks tending to slide from the dome. Resultant fractures are therefore radial at a distance from the centre. (c) Expansion of a high level magma chamber by retrograde boiling or introduction of volatiles from below causes tangential sigma 3. The surface is the only direction in which material can move in order to alleviate pressure buildup. Shear fractures develop as shown, and will extend to surface if shear stresses are maintained, or else will flatten out to form sheet fractures as seen on Cape Makkovik. (d) Emplacement model for Aillik Bay dykes using a combination of a, b and c. An upward moving magma chamber (I1-I2-I3) could cause ring dykes (d1) followed by radial dykes (d2) and low-angle sheet intrusions (d3).

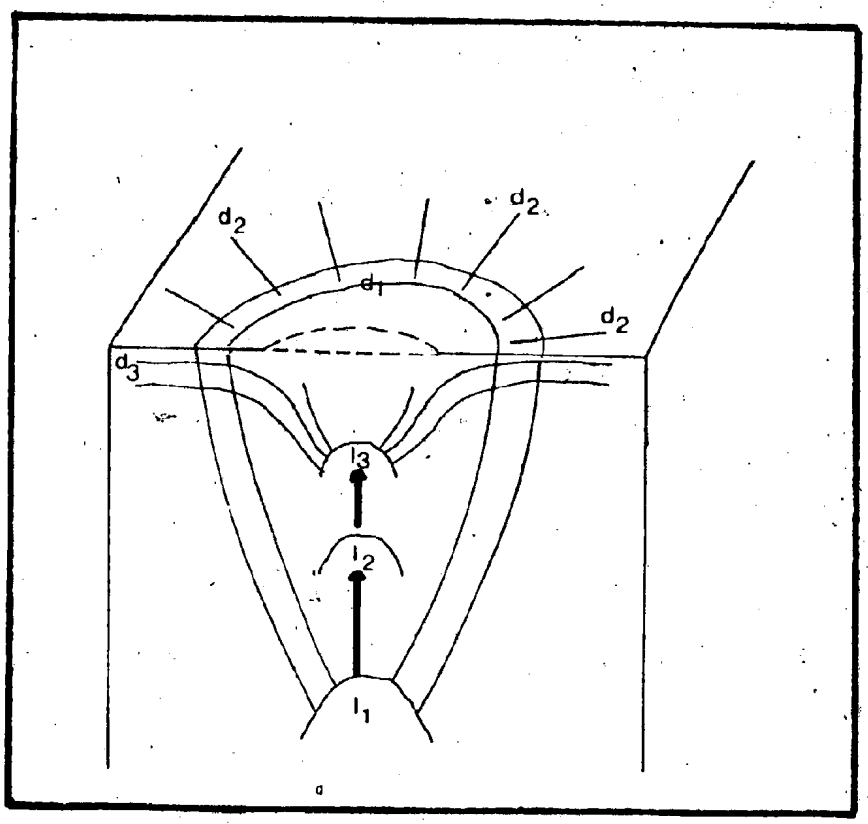

3 dimensions) in fig.2-18c), and σ_3 is tangential to the magma chamber. The roof of the magma chamber would be the only part able to move to compensate the compression, and so shear fractures would develop as shown. The fractures would either steepen to the surface if shear stresses were maintained (Phillips,1974), or flatten out to lie in the σ_3-σ_2 plane (Piper and Gibson,1972). The increasing importance of volatiles in the later stages of intrusion at Aillik Bay supports this idea.

This process is clearly more applicable at shallow depths because of the relatively limited rise in magma pressure needed to overcome the overburden. The increased aspect ratio of the intrusion (diameter of magma chamber/ depth below surface) at shallow depths would assist formation of cone sheets with low angle dips (Phillips,1974).

Bahat (1979,1980) has recently suggested formation of cone sheet fractures by a Hertzian fracture process as the first stage in the structural evolution of an igneous centre. This theory is developed from experiments where brittle solid is loaded with a spherical indenter (Bahat,1980,p.463-464) producing a cone shaped fracture which is initially steep but becomes progressively flatter away from the source (fig.2-19).

This process could apply to the two 'ring dyke' episodes at Aillik Bay. Dykes of the earliest set may appear artificially steep due to the influence of the earlier H4 diabase, and so the applicability of a Hertzian fracture model is difficult to assess. Hertzian fracture may be preferable for explaining this early dyke set, because crack propagation could occur at

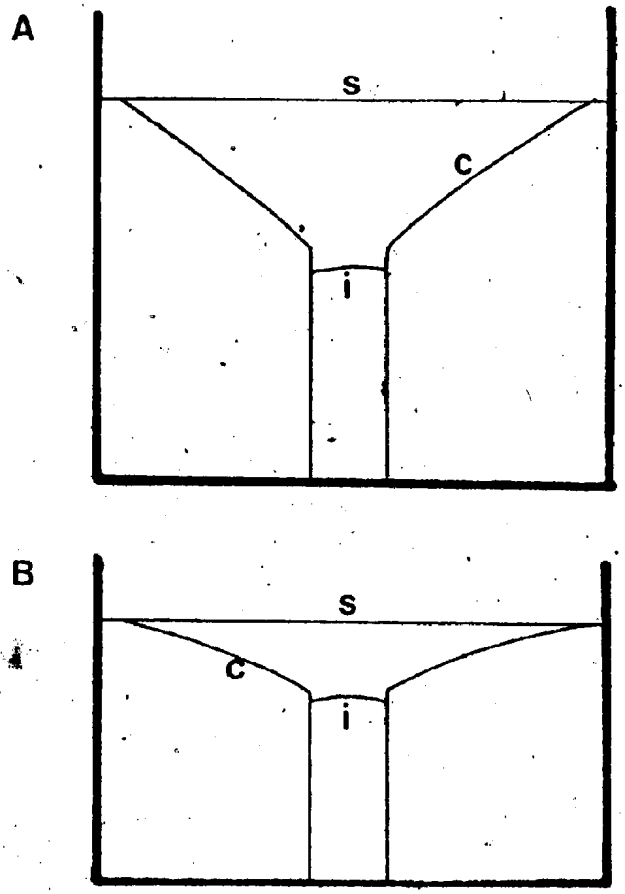

Figure 2-19: Typical shape of Hertzian conic fractures (c) produced experimentally by injection of a dense liquid into a cylindrical hole (i). Initially steep fractures (A) flatten out to intermediate dip. A thinner plate (or shallower intrusive centre) causes low-angle sheets (B) which flatten out distally. S represents ground surface.

relatively low magma pressures (Bahat,1980,p.466).

Conic fractures developed later from higher igneous centre (I3 in fig.2-18d) would have a proportionately lower angle of dip (fig.2-19b). Dykes utilising such fractures may be less prone to follow earlier vertical structures.

Any preference for either process of fracturing does not affect the proposed sequence of events.

(b) The Size of the Aillik Bay central complex

Extrapolation of dyke trends can only give an approximation of the location of the centre of the complex, and so other factors must be used to gain an idea of the size of the complex.

On the Cape Makkovik peninsula dykes diminish rapidly in number to the south, and are rare south of the north end of Banana Lake (fig.2-1). Radial dyke swarms characteristically show concentration of dykes within a few degrees of arc in several directions (Kaitaro,1953; Agard,1960; Johnson,1970,p.403 and 416). A relatively small scatter of dyke orientations such as exists on Turnavik and Cape Makkovik (fig.2-1) would be expected in dyke-rich zones. Aillik Bay dykes do not occur on the mainland coast other than at Cape Aillik and Cape Makkovik.

Extensions from radial dyke systems are most likely where radial fractures can exploit a set of pre-existing parallel fractures. The alternative view of a local increase in the deviatoric stress field reducing scatter in dyke orientation (Davidson and Park,1978) is not in keeping with formation of radial dykes by hydraulic tension fracture, which requires low

deviatoric stress. There apparently is no dyke-rich zone parallel to the regional foliation, since Clark (1971) did not see abundant lamprophyres on the shores of Kaipokok Bay.

The area covered by radial dyke systems from central complexes is extremely variable. Dykes extend up to 25km from the 4km diameter Alno complex in Sweden (von Eckermann,1966; Kresten,1980), 9km from the 3km diameter Tundulu complex in Malawi (Garson,1966; Gittins,1966,p.431), more than 20km at McClure Mt., Colorado (Gittins, 1966,p.531), 5km at Chisangaya, Zimbabwe (Heinrich,1966,p.29) and 30km at Swartbooisdorf, Namibia (Gittins,1966,p.463).

More extensive swarms are commonly associated with a number of centres, as at the 40km long Callander Bay-Manitou Islands-Burrit Island-Iron Island group in Ontario (Currie, 1975,p.72-83), or with a number of satellitic stocks around a large intrusion. Examples of the latter type are the 90km swarm at Gross Brukkaros, Namibia (Janse,1969), 25km at Jombo, Kenya (Gittins,1966,p.422), 100 square miles at Shawa, Zimbabwe (Johnson,1966,p.211) and the extremely large Pilanesberg centre in South Africa (Ferguson,1973).

A 100km lamprophyre swarm in New Zealand is related to a large intrusion below the present ground surface (Cooper, 1971,1979).

The Aillik Bay swarm could thus be considered quite extensive, assuming that it is related to a single stock at the position shown in fig.2-1.

The persistence of concentric dykes to almost 20km is

unusual, but Walker (1975) notes that flat lying sheets with locally variable dip are characteristic of distal cone sheets. Secher and Larsen (1978) describe tangential dykes 20km from the centre of the Sarfartoq carbonatite in western Greenland.

(c) Regional Considerations : The Labrador Sea rift

The Aillik Bay intrusive suite is one of a series of alkaline rock occurrences on the borders of the Labrador Sea. There were at least three major periods of activity, namely 1300–1000 Ma, 600–570 Ma and Mesozoic.

Lamprophyres, carbonatites and kimberlites occur along an 1100km stretch of the coastline of West Greenland from Ivigtut in the south to Umanak in the north.

Gardar age (1300–1000 Ma) rocks comprise numerous alkalic igneous complexes, mostly foyaite, nordmarkite and granite, of which Ilimaussaq and Igdlerfigssalik are the best known. The Gardar intrusions include late-stage alkalic lamprophyres (Upton,1970,1974; MacDonald,1966; Emeleus and Upton,1976).

Kimberlites and lamprophyres of late Precambrian and Mesozoic age are concentrated in the Ivigtut-Frederikshaab Isblink area (Andrews,1969; Andrews and Emeleus,1975,1976; Hansen,1980) at around 62°N and south of Holsteinsborg at 66–67° N (Bridgwater et al.,1973; Escher and Watterson,1973; Brooks et al., 1978; Scott,1979).

Kimberlites of the Frederikshaab area have been dated isotopically at 609–584 Ma (K-Ar: Bridgwater,1970,1971) and 225–202 Ma (Rb-Sr: Andrews and Emeleus,1971; 40Ar/39Ar:

Bridgwater,1970). Alkaline lamprophyres and carbonatites in this area are Mesozoic (168-162 Ma by K-Ar: Walton,1966; Larsen, 1966; Bridgwater,1970; Larsen and Moller,1968a).

The Holsteinsborg dykes include late Precambrian (Andrews and Emeleus,1976) kimberlites and lamprophyres which are believed to be related (Scott,1979). The Sarfartoq carbonatite complex in the eastern part of the Holsteinsborg area has a well developed dyke system (Secher and Larsen,1978,1980; Larsen,1980).

Lamprophyres occur in the Umanak area at 71°N and appear to be of two ages: 600 Ma (K-Ar: Larsen and Moller,1968b) and Tertiary (30-40 Ma: Clarke and Pedersen, 1976). The Tertiary lamprophyres are said to include kersantite, camptonite and monchiquite, and cut Tertiary basaltic lavas which are believed to be related to the rifting of Baffin Bay (Clarke and Upton,1971).

The history of extensional tectonics in the Labrador Sea is thought to cover almost 600 Ma. Doig (1970) suggested that the 600-570 Ma alkaline rocks are associated with a widespread rifting episode including the St.Lawrence rift (Kumarapeli, 1978). Disturbance at this time is supported by the palaeomagnetic work of Fahrig et al.(1971), but no major continental separation occurred until after the Mesozoic emplacement of the coast-parallel dyke swarm of West Greenland (Watt,1969; Fahrig and Freda,1975). This swarm is cut by lamprophyres dated at 162 Ma by Larsen and Moller (1968a).

The Mesozoic dykes are probably related to Mesozoic rifting

of the southern Labrador Sea (Andrews and Emeleus,1975). The later Umanak lamprophyres are probably related to late Cretaceous-Tertiary continuation of the rift into Baffin Bay.

As noted earlier, the age of the Aillik Bay rocks is uncertain: an age of 570 Ma was obtained radiometrically (K-Ar: Leech et al.,1963), and a Mesozoic age was obtained by King and McMillan (1975) on the basis of Mesozoic nannofossils found in a breccia which is cut by carbonatitic dykelets. Both ages fit in with known periods of alkaline activity in the Labrador Sea area, but Hawkins (1977) considered that the 570 Ma date was influenced by excess argon in micas (Evans and Tarney,1964). Dates of around 600 Ma in Greenland have been similarly questioned. It is possible that the bulk of the Aillik Bay dyke swarm was emplaced 570 Ma ago, and that it was affected by carbonatite activity in Mesozoic times.

Later magmas commonly focus on earlier intrusive centres. McHone (1978) describes lamprophyres in New England which are concentrated around centres which they clearly postdate in all cases. The link between coexisting alkaline rocks may be structural rather than genetic. A number of intrusions, either discrete or cupolas of a much larger intrusion at depth, will greatly complicate stress patterns. Later intrusions are likely to be influenced by fracture systems formed by earlier stocks (Moore,1975).

Alkaline central complexes are very commonly associated with major geological lineaments, which may be major geological boundaries or inferred deep crustal faults (Arsenyev,1963;

Stracke et al.,1979). The Aillik Bay complex sits astride the Archean-Aphebian boundary (fig.2-1). This boundary was the site of considerable movement during the Hudsonian orogeny (Marten,1977), and may have controlled the siting of alkaline magmatism.

Igneous centres on the margins of rift zones are said in many cases to be focused on lineaments transverse to the rift (Mohr and Potter,1976). These may be landward extensions of oceanic fracture zones (Stracke et al.,1979; McHone, 1978). Mathias (1974) suggested that the Walvis Ridge fracture zone in the southern Atlantic may have influenced parallel zones of alkaline rocks of the Lucapa graben, Angola (Rodrigues,1970) and the Damaraland region, Namibia (Martin et al.,1960).

Increasing alkalinity away from rifts is a common feature of rift-related igneous activity (Neumann and Ramberg,1978). This relationship holds for transverse lineaments in southeastern Australia (Stracke et al.,1979; Ferguson, 1980) where kimberlites are the furthest inland expression of the lineaments. Alkaline magmatism migrates toward cratonic areas hence the occurrence of carbonatite as the latest phase of activity at Aillik Bay. The position of the Sarfartoq carbonatite complex at the eastern end of the Holsteinsborg alkaline intrusive region is noteworthy.

Many of the above points can be amalgamated to suggest that a distal position on a simple rift and transverse lineament system best suits the evidence at Aillik Bay. This analogy drawn from other areas also fits the limited geophysical data for

Aillik Bay. Detailed gravity and magnetic surveys are not available nearshore, but the regional gravity survey defines an east- west anomaly aligned with the proposed central complex (Van der Linden and Srivastava,1975). The anomaly is approximately parallel with the Grenville front, which occurs 50-80km to the south (Gower et al.,1980). Van der Linden and Srivastava (1975) state that left-lateral offset, which occurred in the southern Labrador Sea during rifting, was on strike from the Grenville Front, so that deep structural control associated with this feature is very likely.

Geophysical surveys led Van der Linden (1975) to propose a model of extension by crustal attenuation for the Labrador Sea, although he notes that preference for this or for more conventional sea-floor spreading models is largely a matter of choice (Van der Linden,1977,p.210). Black et al.(1976) note that modification of a continental margin by such a process could lead to considerable changes in stress fields which may in turn affect intrusive patterns.

CHAPTER 3 : PETROGRAPHY and MINERAL CHEMISTRY

SANNAITES

Sannaites are alkaline lamprophyres characterised by titanium-rich biotite or kaersutite set in a felsic groundmass dominated by K-feldspar. The sannaites can be divided into olivine-rich and olivine-poor varieties. The amount of olivine may vary considerably within banded dykes suggesting separation of olivine-rich and olivine-poor types from a similar source. Mineralogical differences are more extreme in discrete dykes of each type.

Phenocrysts in the sannaites are olivine and salitic pyroxene plus later mica and titanomagnetite. These form a seriate panidiomorphic texture with groundmass minerals which may include pyroxene, titanomagnetite, biotite, apatite, K-feldspar, rutile, nepheline, carbonate and analcite.

Olivine is the earliest formed phase and now occurs as rounded phenocrysts between 0.5mm and 1.5mm in size. Olivine has most of the chemical features described later for the olivine-rich sannaites, but is usually totally pseudomorphed by submicrocrystalline carbonate.

Clinopyroxene phenocrysts are common only in olivine-poor sannaites, which are also characterised by more abundant felsic minerals (K-feldspar and nepheline) in the groundmass. The pyroxene forms colourless to pale grey euhedral phenocrysts or rarer glomeroporphyritic aggregates. Phenocrysts are strongly zoned optically, and have rims marginally richer in Mg and Ti,

and poorer in Si (table 3-1,analyses 1-5).

Small cores of green sodic pyroxene occur rarely in large phenocrysts. It is not known whether these are xenocrysts or early phenocrysts.

Clinopyroxene also forms the bulk of the groundmass in the form of pale green 0.01mm to 0.05mm long tabular to acicular pyroxene crystals.

Groundmass pyroxenes are variable in composition. In the $MgSiO_3$-$CaSiO_3$-$FeSiO_3$ system most plot in the wollastonite-rich region beyond the diopside-hedenbergite join (fig.3-1). They are rich in TiO_2, Al_2O_3 and CaO in common with those in many silica undersaturated alkalic rocks (Mitchell,1980; Akasaka and Onuma,1980; Curtis and Gittins,1979). Thin deep green rims to groundmass pyroxene crystals are found in the more evolved feldspar or nepheline ocellic sannaites (fig.3-2). The rims are too thin for reliable probe data to be obtained, but Cooper (1979) described acmitic rims in very similar rocks from New Zealand. A late acmitic trend is common in pyroxenes of nephelinitic rocks (Mitchell,1980; Gomes et al., 1970).

Oxide and opaque phases are extremely varied in the sannaites. Most are euhedral groundmass crystals and crystal aggregates 0.01mm to 0.2mm across. Early-formed crystals may be up to 0.7 x 0.3mm, and are mostly relatively pure titanomagnetites. Groundmass titanomagnetites contain appreciable Mg and Al, and have lower Ti contents (table 3-2). The low Ti contents may be due to contamporaneous rutile crystallisation. Rutile occasionally occurs as intergrowths with

TABLE 3-1: Representative analyses of pyroxenes from sannaite.

Sample no.	325-71	325-72	325-76	325-79	325-82	3332a-54
SiO2	45.62	46.28	43.90	44.89	45.13	47.91
Al2O2	7.63	8.72	9.84	8.50	6.65	4.45
TiO2	2.64	2.18	3.00	2.37	2.77	2.76
FeOt	6.75	8.76	6.75	6.25	7.62	6.38
CaO	23.33	21.26	22.88	22.88	23.39	23.51
MgO	12.45	11.06	11.61	12.35	12.53	13.24
MnO	0.09	0.16	0.07	0.08	0.11	0.10
Na2O	0.58	1.18	0.55	0.62	0.34	0.55
K2O	0.02	0.01	0.02	0.01	0.00	0.01
Total	99.11	99.61	98.62	97.95	98.54	98.91
End members (by the method of Cawthorn and Collerson,1974)						
Jadeite	3.88	7.67	3.67	4.03	2.26	3.95
Acmite	0.00	0.00	0.00	0.00	0.00	0.00
CaTiTsch.	6.68	5.46	7.58	5.91	7.17	7.61
CaTsch.	13.04	15.65	16.96	17.38	10.36	0.05
Wollas.	35.50	31.31	33.14	33.36	36.94	42.32
Enstat.	31.26	28.88	29.07	30.53	32.13	36.15
Ferros.	9.64	8.84	9.58	8.78	11.13	9.93

Sample no.	3332a-2a	L519-33	L519-36	408-67	408-68	408-70
SiO2	45.86	50.59	50.73	46.83	46.85	45.96
Al2O3	4.30	1.99	1.60	3.30	4.13	4.28
TiO2	2.34	3.35	1.34	3.42	3.42	4.20
FeOt	5.87	9.23	5.52	6.69	6.45	7.29
CaO	24.05	19.62	21.50	24.76	23.07	25.45
MgO	15.38	14.54	16.02	14.34	13.38	13.22
MnO	0.14	0.11	0.04	0.07	0.10	0.07
Na2O	0.45	0.64	0.66	0.30	0.77	0.29
K2O	0.02	0.08	0.02	0.00	0.02	0.01
Total	98.41	100.15	97.43	99.71	98.19	100.80
End members (by the method of Cawthorn and Collerson, 1974)						
Jadeite	3.08	5.41	4.92	2.13	5.72	2.10
Acmite	0.00	0.00	0.00	0.00	0.00	0.00
CaTiTsch.	6.04	10.14	3.80	9.43	9.70	11.55
CaTsch.	2.25	-16.24	-5.40	-6.73	-6.77	-6.75
Wollas.	40.65	41.32	42.89	45.61	43.43	45.77
Enstat.	39.95	43.64	45.03	39.19	37.59	36.03
Ferros.	8.63	15.73	8.77	10.36	10.33	11.30

Figure 3-1: Pyroxene compositions plotted in the system $MgSiO_3$-$CaSiO_3$-$FeSiO_3$

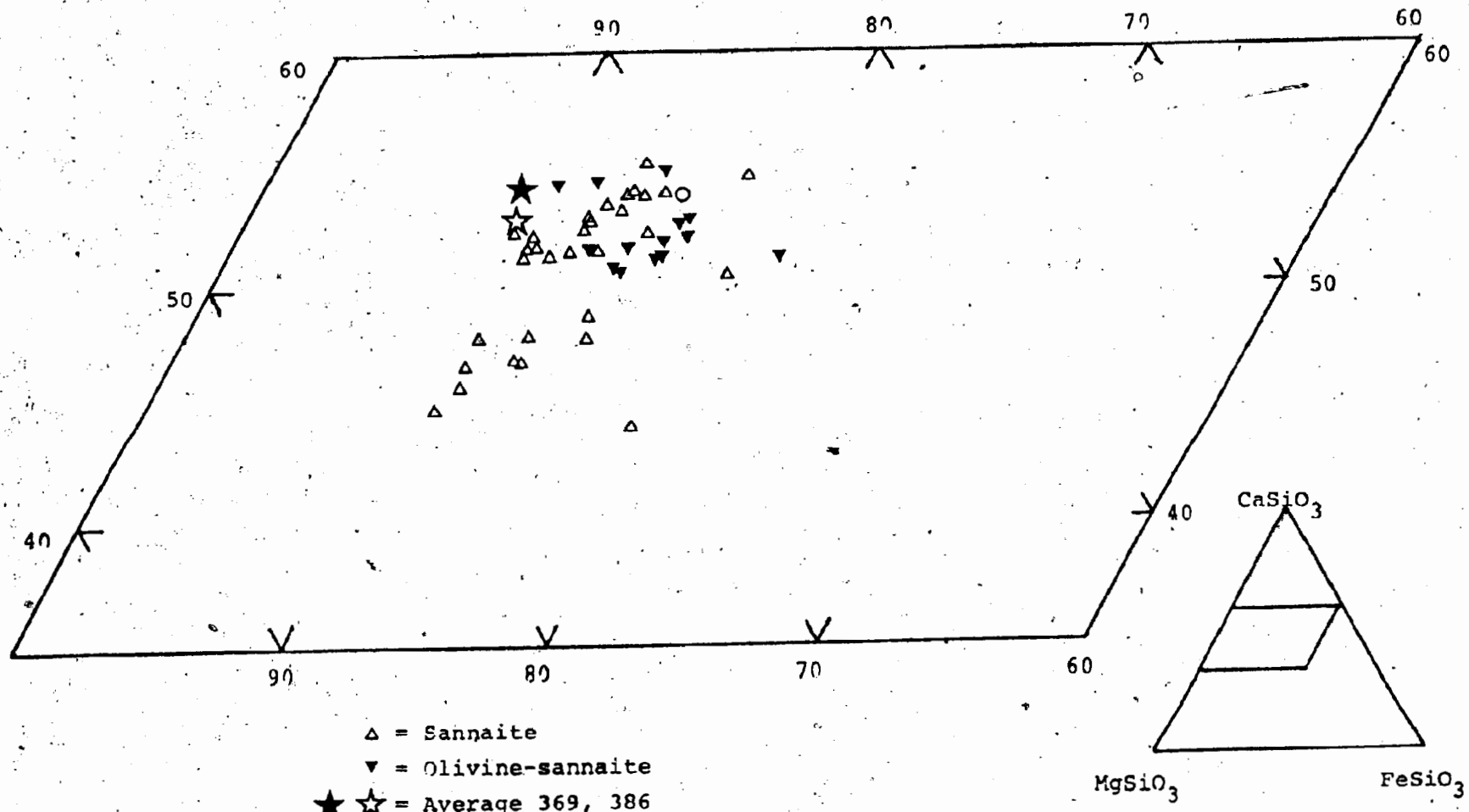

Figure 3-2: Development of green pyroxene adjacent to felsic groundmass in sannaite. Groundmass here is carbonate, analcite and apatite.
Magnification x 200

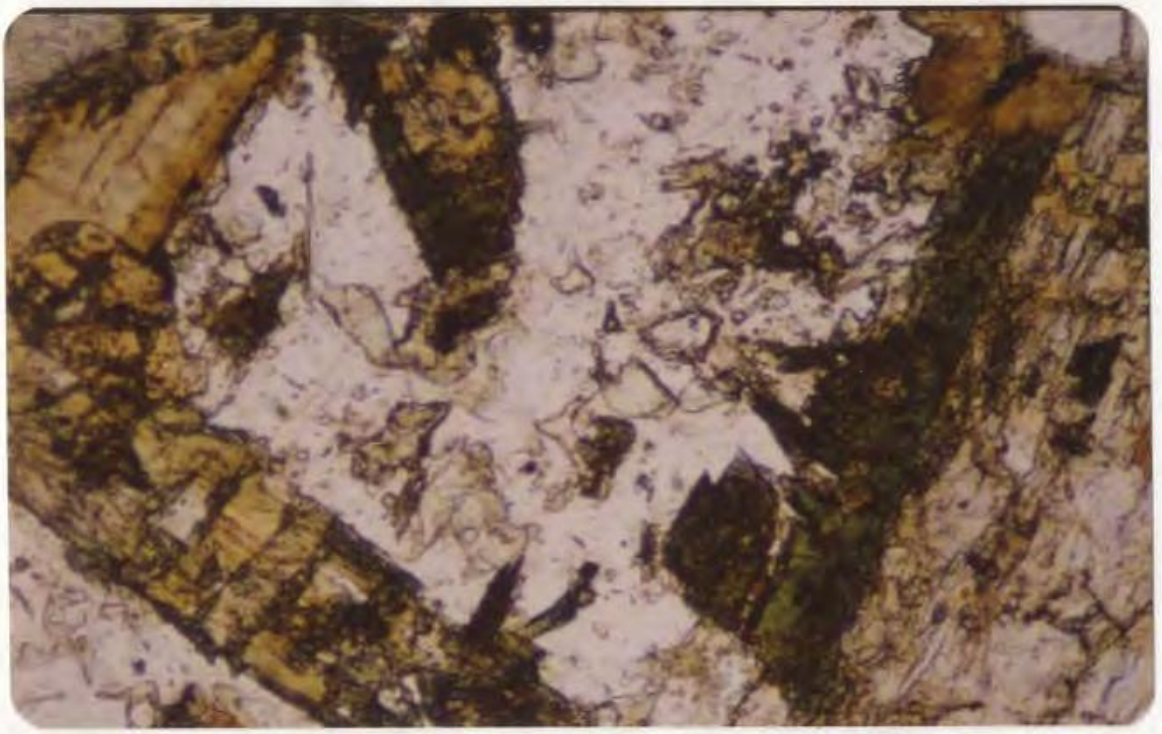

Figure 3-3: Sannaite: acicular pyroxene and apatite plus granular opaque phases in a felsic groundmass. Poikilitic inclusion of these minerals in mica (centre) demonstrates late formation of mica.
Magnification x 60

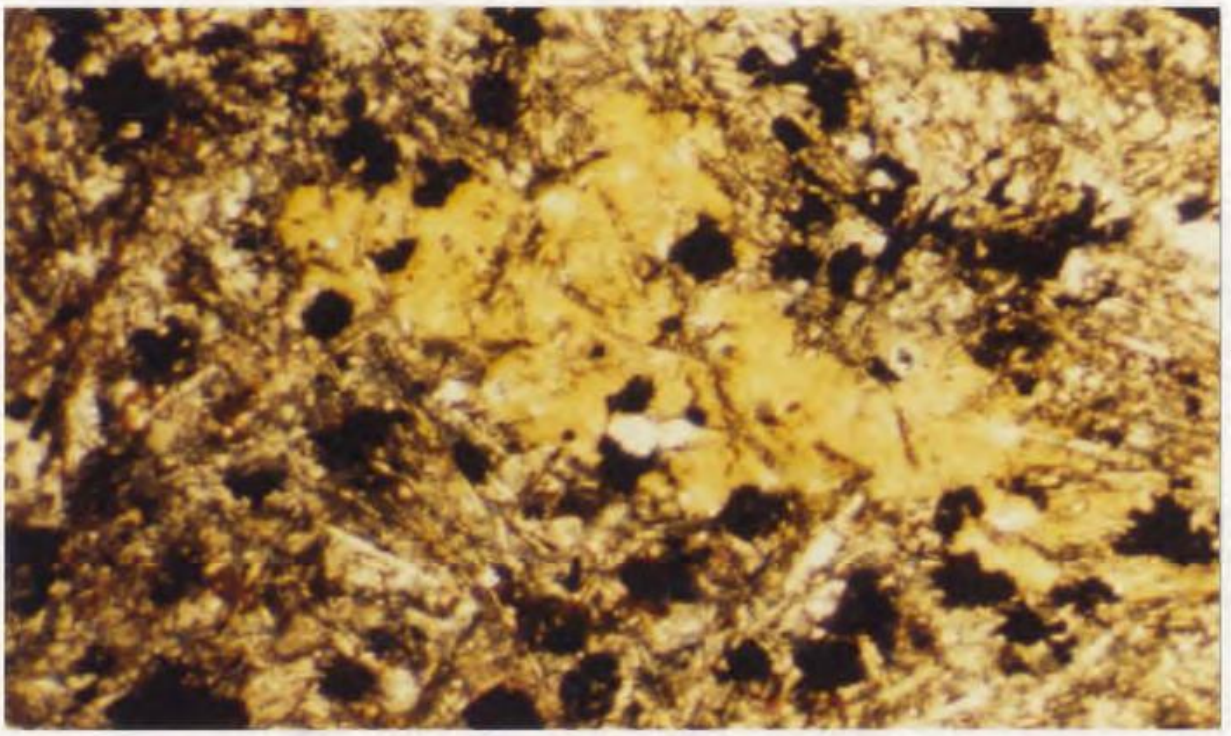

TABLE 3-2: Representative analyses of oxide minerals from sannaite

Sample no.	333-03	333-04	333-06	333-05	333-07
Cr2O3	0.00	0.00	0.00	0.00	0.00
Al2O3	0.96	2.87	0.96	0.05	0.55
TiO2	7.00	11.93	24.89	95.35	93.92
FeOt	84.76	76.41	71.29	0.49	0.63
MgO	0.18	3.56	0.02	0.00	0.00
MnO	0.13	0.77	0.15	0.00	0.01
Total	93.03	95.54	97.31	95.89	95.11
Structural formula on the basis of 4 oxygens;					
Cr	0.000	0.000	0.000	0.000	0.000
Al	0.054	0.146	0.046	0.002	0.018
Fe	3.396	2.752	2.411	0.011	0.015
Ti	0.252	0.386	0.757	1.993	1.979
Mn	0.005	0.028	0.005	0.000	0.000
Mg	0.013	0.229	0.001	0.000	0.000

groundmass pyroxenes. The oxides lack twinning and exsolution features. The most evolved sannaites contain subordinate amounts of pyrite as the latest opaque phase. Pyrite forms rims on rutile crystals.

Mica occurs as relatively large (up to 3mm) but late crystals which poikilitically enclose acicular salite and granular titanomagnetite (fig.3-3). The crystals are strongly zoned from pleochroic cores (α=pale to mid green-brown; β,γ= neutral to mid green-brown) to deep red-brown rims (α= neutral to pale olive green; β,γ= reverse pleochroic olive green to deep red-brown) (fig.3-4).

Chemical compositions of the micas are listed in table 3-3. Reverse pleochroic red-brown rims have been observed in true kimberlites (Emeleus and Andrews,1975) and in carbonatite-related rocks (Heinrich,1966,p.198; Mitchell,1980). The red rims at Aillik Bay have very high FeO/(FeO+MgO) and low Al2O3 relative to the cores. Chemical trends at Fen (Mitchell,1980) and Pyramidefjeld (Emeleus and Andrews,1975) are similar but Al2O3 loss is more extreme. Red reverse pleochroism is attributed to ferric iron occupying tetrahedral sites in place of Al (Faye and Hogarth,1968).

Micas are commonly corroded by the action of volatiles concentrated in late stage fluids, and in many cases the red rims are removed. The late red- brown Fe-rich mica is dominant in sannaites with highest modal mica, where it forms small euhedral crystals and is the latest crystallising mafic phase.

Apatite is always present, but in widely varying amounts.

TABLE 3-3: Representative analyses of micas from sannaite

Sample no.	3332b-31	3332b-32	333-50	333-51	333-53	333-54
SiO2	37.46	37.50	37.75	37.02	37.71	37.28
Al2O3	15.16	15.54	15.25	15.52	15.02	15.29
TiO2	3.17	2.50	2.73	3.23	3.25	3.16
FeOt	10.55	9.55	9.82	9.88	9.74	9.93
CaO	0.08	0.08	0.03	0.06	0.04	0.04
MgO	18.93	19.55	19.22	19.27	19.39	19.21
MnO	0.11	0.19	0.14	0.14	0.14	0.14
Na2O	0.36	0.31	0.37	0.32	0.37	0.37
K2O	8.51	8.70	8.77	9.00	9.21	8.91
Total	94.33	93.92	94.08	94.44	94.87	94.33

Structural formula on the basis of 22 oxygens;

Si	5.513	5.520	5.554	5.446	5.519	5.486
Al	2.630	2.696	2.645	2.691	2.591	2.652
Fe	1.299	1.176	1.208	1.215	1.192	1.222
Ti	0.351	0.277	0.302	0.357	0.358	0.350
Mn	0.014	0.024	0.017	0.017	0.017	0.018
Mg	4.153	4.290	4.215	4.226	4.231	4.214
K	1.598	1.634	1.646	1.689	1.720	1.673
Na	0.103	0.089	0.106	0.091	0.105	0.106
Ca	0.013	0.013	0.005	0.010	0.006	0.006

Sample no.	333-55	333-56	333-59	333-60	333-61	333-63
SiO2	36.52	36.45	36.07	35.15	36.76	37.13
Al2O3	15.09	15.11	8.92	8.35	9.01	14.97
TiO2	2.47	2.64	2.43	2.38	2.19	2.78
FeOt	12.34	12.69	29.38	32.01	28.31	9.80
CaO	0.01	0.04	0.12	0.11	0.21	0.21
MgO	17.50	17.95	8.63	7.43	9.18	19.11
MnO	0.19	0.27	0.58	0.72	0.60	0.16
Na2O	0.36	0.34	0.23	0.11	0.09	0.14
K2O	8.82	9.33	8.68	8.59	8.60	8.98
Total	93.30	94.82	95.04	94.85	94.95	93.28

Structural formula on the basis of 22 oxygens;

Si	5.503	5.436	5.862	5.823	5.929	5.526
Al	2.681	2.656	1.709	1.631	1.713	2.626
Fe	1.555	1.583	3.993	4.435	3.818	1.220
Ti	0.280	0.296	0.297	0.297	0.266	0.311
Mn	0.024	0.034	0.080	0.101	0.082	0.020
Mg	3.931	3.991	2.091	1.835	2.207	4.240
K	1.696	1.775	1.800	1.816	1.770	1.705
Na	0.105	0.098	0.073	0.035	0.028	0.040
Ca	0.002	0.006	0.021	0.020	0.036	0.034

Figure 3-4: Deep red-brown reverse pleochroic rims on mica. Mica has overgrown pyroxene, apatite and titanomagnetite. The K-feldspar bearing groundmass is typically altered in this example.
Magnification x 120

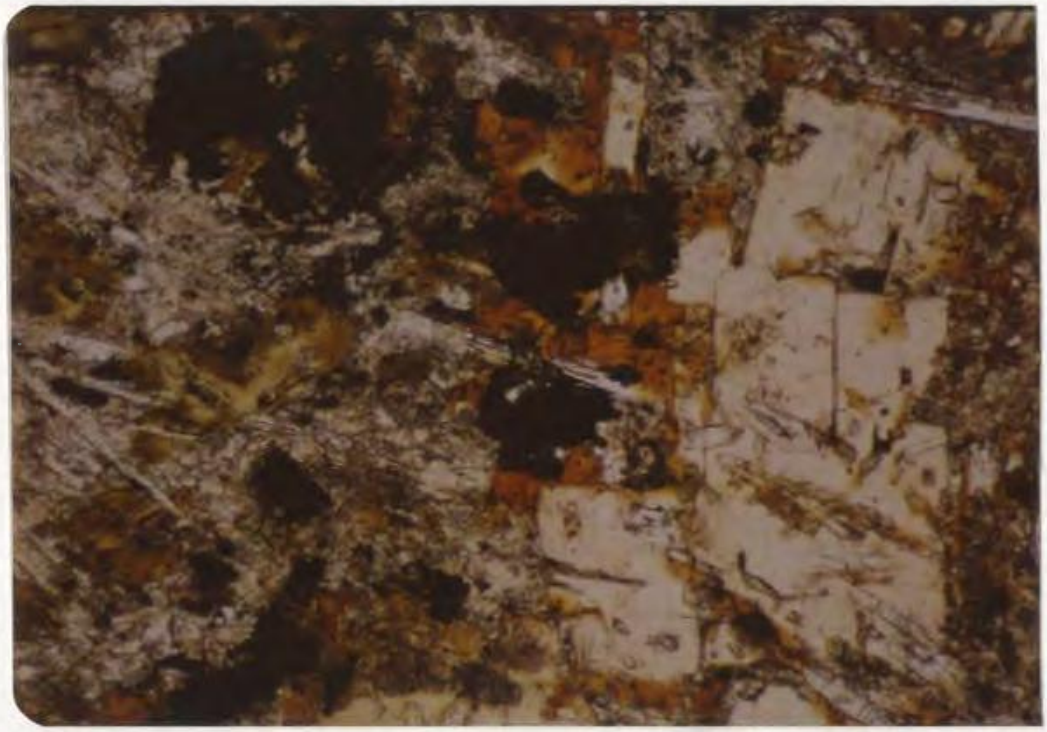

Figure 3-5: Olivine sannaite. Altered and rounded olivine phenocrysts in a groundmass of acicular pyroxene, apatite, titanomagnetite, mica and carbonate.
Magnification x 60

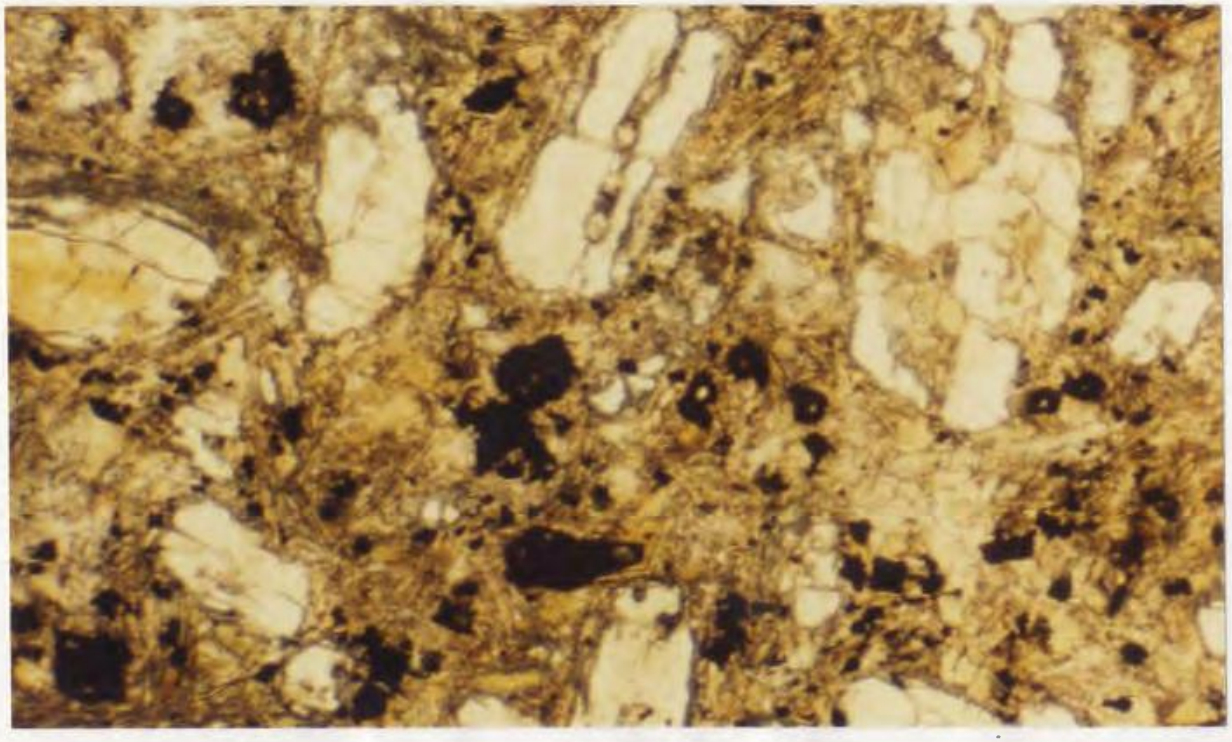

It occurs mostly as tabular to acicular prismatic crystals in the groundmass. Where most abundant, it also occurs as phenocrysts up to 1.5mm long which predate early titanomagnetites.

The felsic groundmass is normally orthoclase, but nepheline may be abundant in rocks with large amounts of clinopyroxene phenocrysts. Representative analyses are given in table 3-4. Carbonate and analcite are minor groundmass phases.

Most sannaites contain leucocratic 'globular structures' rich in felsic minerals which vary in size from 0.5mm to in excess of 6mm. Many are bordered by tangentially arranged pyroxene or mica and so can be termed ocelli (Phillips, 1973). The ocelli are described in detail in a later section where their origin is discussed.

Carbonate forms up to 10% of sannaites, mostly as very fine-grained deuteric or later alteration of groundmass minerals. Carbonate is preserved as well- formed interstitial crystals in rocks with restricted growth of submicrocrystalline deuteric carbonate. It also occurs as earlier pseudomorphs of olivine, and thus is clearly coeval with the sannaites. Carbonate and clay mineral alteration of the groundmass is always present, but olivine-free sannaites are the least altered of all the alkaline complex rocks.

Flow structure is frequently well defined, particularly in banded dykes, by parallelism of acicular pyroxene and to a lesser extent by mica. Randomly oriented inclusions of pyroxene in micas show the flow structure to be a late feature. It is

TABLE 3-4: Representative analyses of K-feldspar and nepheline from sannaite

Sample no.	333-20	333-21	333-25	333-11	333-18
SiO2	64.91	63.88	64.14	63.77	64.47
Al2O3	18.55	18.63	18.92	18.34	18.54
TiO2	0.00	0.00	0.00	0.00	0.00
FeOt	0.11	0.14	0.06	0.19	0.06
CaO	0.01	0.02	0.00	0.00	0.00
Na2O	0.12	0.32	0.16	0.16	0.13
K2O	16.19	15.48	15.84	15.96	15.83
Total	99.89	98.47	99.12	98.42	99.03
End members;					
Or	98.84	96.85	98.49	98.50	98.77
Ab	1.11	3.04	1.51	1.50	1.23
An	0.05	0.10	0.00	0.00	0.00

Sample no.	325-83	325-84	325-93
SiO2	44.57	43.56	45.76
Al2O3	32.95	33.04	33.58
TiO2	0.00	0.00	0.00
FeOt	0.66	0.65	0.70
CaO	0.80	0.80	0.84
Na2O	15.16	14.41	14.95
K2O	5.92	5.71	5.48
Total	100.06	98.17	101.31
End members;			
Ne	79.56	79.32	80.57
Ks	20.44	20.68	19.43

post-dated only by crystallisation of felsic groundmass minerals, red mica, and some opaque phases.

Banded dykes are commonly made up of olivine-poor bands with numerous ocelli, and olivine-rich bands. Ocellar bands are coarser grained and have a relatively high content of felsic minerals. Olivine-rich bands tend to be finer grained, more melanocratic, and have a better developed flow texture defined by preferred orientation of pyroxene, mica and apatite. This flow texture is commonly accentuated at band margins, where olivines are scarce due to flow differentiation (Komar,1976; Barriere,1976).

OLIVINE-RICH SANNAITES

Olivine accounts, on average, for 30% of olivine sannaites. It occurs as rounded phenocrysts up to 4mm across, but mostly 0.1mm to 0.25mm (fig.3-5). Olivines are commonly altered to extremely fine grained carbonate, and less commonly to serpentine and iddingsite. Rare examples of all 3 types coexisting show a progression from iddingsite, through serpentine to carbonate toward grain margins.

Olivine compositions are listed in table 3-5. Phenocryst cores range from Fo77 to Fo85. Rims are mostly around Fo81, and show much less variation in Mg and Fe content than the cores. The lowest forsterite values are restricted to the cores of large phenocrysts, whereas smaller crystals have relatively Mg-rich cores.

The range in composition is similar to that of carbonate-

TABLE 3-5: Representative analyses of olivines from olivine sannaite.

Sample no.	L514-21	L514-22	L514-23	L514-24	L514-25	L514-26
SiO2	39.49	38.78	39.14	39.97	39.10	40.36
Al2O3	0.00	0.04	0.05	0.03	0.05	0.04
TiO2	0.04	0.04	0.05	0.03	0.05	0.02
FeOt	18.23	17.66	15.89	16.03	16.90	14.75
CaO	0.28	0.25	0.18	0.21	0.20	0.20
MgO	42.93	43.50	44.19	44.16	42.97	45.62
MnO	0.20	0.19	0.19	0.13	0.18	0.16
Na2O	0.01	0.00	0.09	0.04	0.01	0.05
Total	101.18	100.47	99.78	100.61	99.42	101.20
Fo	77.54	78.10	80.11	79.95	78.64	81.75

Sample no.	306-50	306-52	306-53	306-55	306-57	408-01
SiO2	39.90	40.05	40.07	39.66	38.84	39.13
Al2O3	0.02	0.02	0.04	0.00	0.00	0.02
TiO2	0.00	0.05	0.05	0.00	0.04	0.01
FeOt	15.06	15.38	15.29	15.15	16.14	16.23
CaO	0.21	0.68	0.73	0.63	0.48	0.23
MgO	44.90	44.72	43.78	43.77	43.77	44.24
MnO	0.09	0.18	0.14	0.13	0.14	0.15
Na2O	0.05	0.04	0.03	0.01	0.00	0.04
Total	100.23	101.12	100.13	99.35	99.41	100.05
Fo	81.19	80.81	80.57	80.68	79.68	79.78

Sample no.	408-02	408-03	408-04	408-05	408-06	408-07
SiO2	38.92	38.46	38.84	39.60	39.34	39.23
Al2O3	0.00	0.02	0.02	0.05	0.06	0.04
TiO2	0.00	0.00	0.00	0.00	0.00	0.00
FeOt	16.11	16.21	16.18	12.31	12.17	13.46
CaO	0.23	0.20	0.21	0.20	0.17	0.20
MgO	43.46	43.49	43.72	47.97	47.93	46.36
MnO	0.18	0.17	0.16	0.11	0.09	0.12
Na2O	0.07	0.00	0.03	0.02	0.02	0.02
Total	98.97	98.55	99.16	100.26	99.78	99.43
Fo	79.62	79.53	79.64	84.94	85.08	83.30

rich lamprophyres in northwestern Ontario (Platt and Mitchell,1979), and in nepheline-bearing lamprophyres in West Greenland (Hansen,1980). Olivines in all three areas contain appreciable Ca (>0.15 wt%), which is also noted in melilitic rocks (Nixon et al, 1980).

In some rare rocks, euhedral olivines occur with inclusions of perovskite. These rocks have a hiatal texture (Moorhouse, 1959,p.160) but similar groundmass mineralogy to the usual sannaite: acicular pyroxene, and titanomagnetite, which forms borders around discrete perovskite crystals.

The matrix is formed of acicular pyroxene (36% average), mica (10%), carbonate (9%), opaques (8%) and minor phases including K-feldspar, perovskite, apatite and brown amphibole. Clinopyroxene phenocrysts are rare.

Pyroxene and mica analyses are listed in tables 3-6 and 3-7 respectively. Pyroxenes are similar to the more calcic sannaitic pyroxenes (fig.3-1), except that many are richer in Ti (up to 5 wt%). The most Ti-rich pyroxenes are pale orange but do not show pleochroism. Ti-pyroxenes are also rich in Al, and poor in Si, suggesting dominance of the Ti-Al couple in substitutions. Al would replace Si in tetrahedral co-ordination, and Ti^{4+} would go into octahedral sites. Ti exceeds Al in some sannaite pyroxenes with low contents of Ti and Al (fig. 3-1). This leads to negative Tschermak's molecule in the calculated end-members in the tables, because Ti is assumed to form only Ti-tschermak's molecule by the method used (Cawthorn and Collerson,1974). The view of Kuznetsova et al. (1980) that Ti could enter tetrahedral

TABLE 3-6: Representative analyses of pyroxenes from olivine sannaite

Sample no.	379-10	379-21	379-22	379-23	379-24
SiO2	43.54	43.97	45.47	44.29	43.25
Al2O3	6.50	6.55	5.65	5.96	6.50
TiO2	4.91	4.95	5.65	5.96	5.01
FeOt	7.88	8.15	8.03	8.23	9.82
CaO	22.80	23.24	22.65	23.18	21.66
MgO	11.76	11.70	12.49	12.02	10.42
MnO	0.11	0.03	0.03	0.10	0.14
Na2O	0.63	0.54	0.45	0.47	1.50
K2O	0.01	0.04	0.03	0.01	0.04
Total	98.14	99.17	100.45	100.22	98.34
End members (by the method of Cawthorn and Collerson,1974)					
Jadeite	4.62	4.08	3.53	3.57	11.28
Acmite	0.00	0.00	0.00	0.00	0.00
CaTiTsch.	13.83	13.82	16.47	17.32	14.35
CaTsch.	-3.58	-3.05	-10.65	-11.06	-10.79
Wollas.	39.75	40.08	41.48	42.09	39.72
Enstat.	32.84	32.37	36.10	34.62	29.58
Ferros.	12.52	12.70	13.07	13.46	15.86

Sample no.	379-31	379-32	379-1a	379-2a	306-33
SiO2	46.72	47.49	47.88	44.32	46.68
Al2O3	4.96	3.85	2.82	5.88	3.80
TiO2	3.49	2.86	2.83	4.40	3.36
FeOt	7.45	7.11	6.70	7.93	8.07
CaO	23.27	22.76	23.24	22.83	22.95
MgO	13.17	13.82	13.74	12.05	12.20
MnO	0.11	0.04	0.14	0.06	0.10
Na2O	0.37	0.33	0.40	0.46	0.38
K2O	0.03	0.01	0.01	0.02	0.27
Total	99.57	98.27	97.76	97.95	97.81
End members (by the method of Cawthorn and Collerson,1974)					
Jadeite	2.75	2.43	3.02	3.44	4.18
Acmite	0.00	0.00	0.00	0.00	0.00
CaTiTsch.	9.58	8.00	8.15	12.40	9.75
CaTsch.	-0.57	-1.55	-6.59	-2.27	-6.38
Wollas.	40.86	41.72	45.26	40.22	44.18
Enstat.	35.83	38.29	39.22	33.67	35.09
Ferros.	11.54	11.12	10.95	12.53	13.19

TABLE 3-7: Compositions of oxide minerals in olivine sannaite

Sample no.	379-12	379-13	379-15	379-16	379-01
TiO2	7.51	9.43	12.15	16.19	10.66
Al2O3	1.71	1.75	2.75	1.97	3.72
FeOt	82.57	78.87	73.75	71.07	75.29
MnO	0.18	0.21	0.36	0.24	0.80
MgO	0.37	0.89	1.20	0.92	6.31
Cr2O3	0.00	0.02	0.02	0.03	0.00
Total	92.35	91.18	90.23	90.41	96.79
Structural formula on the basis of 4 Oxygens;					
Cr	0.000	0.001	0.001	0.001	0.001
Al	0.096	0.097	0.149	0.105	0.183
Fe	3.285	3.113	2.838	2.675	2.633
Ti	0.269	0.335	0.420	0.548	0.335
Mn	0.007	0.008	0.014	0.009	0.028
Mg	0.026	0.063	0.082	0.062	0.393

Sample no.	379-02	379-03
TiO2	14.65	14.21
Al2O3	2.61	2.75
FeOt	74.82	74.36
MnO	0.79	0.86
MgO	6.21	5.93
Cr2O3	0.02	0.00
Total	99.11	98.10
Structural formula on the basis of 4 oxygens;		
Cr	0.001	0.000
Al	0.124	0.132
Fe	2.524	2.539
Ti	0.444	0.436
Mn	0.027	0.030
Mg	0.373	0.361

sites is considered unlikely by most authors (eg. Hartman,1969; Huggins et al.,1977). Ti must therefore be included in the pyroxene by substitution with cations other than Al, or else form submicroscopic exsolution lamellae. The Ti-Al substitution couple is the most important couple in most pyroxenes (Cameron and Papike,1981). The higher Ti content in pyroxenes is probably due to the paucity of oxide phases, since Ti cannot be accomodated in sulphides.

Mica occurs as euhedral groundmass laths which exhibit normal pleochroism (α = pale brown to red-brown; β, γ = very pale brown to dark red-brown). Reverse pleochroism and extreme absorption in rims does not occur.

Micas are compositionally zoned to more Fe-rich rims, but this trend is much less extreme than in some olivine-free sannaites (FeOt max.21 wt% vs. 32 wt%). Micas are Ti-rich (7-9 wt%), and Si-poor.

Groundmass opaques in olivine sannaites are normally pyrite. These are mostly pure, but may have Mg and Ti contamination, probably due to inclusions of other phases.

The major difference between these rocks and olivine-poor sannaites is the abundance of olivine and rarity of leucocratic ocelli. Although the olivine-rich sannaites are distinctly more melanocratic, if the felsic ocelli of the olivine- poor sannaites are discounted, there is only a 3-4% difference in colour index.

Considering the concentration of olivine crystals toward the centre of individual bands, and the occurrence of

olivine-rich and ocellar bands in the same dyke (fig.3-6), it is not unreasonable to suppose that the two types of sannaite originated from a common parent by flow differentiation.

Phases of magma emplacement may be recognised easily in banded rocks with poor flow texture by variation in mineralogy of olivine pseudomorphs. Carbonate is generally more abundant than in olivine-poor sannaites, in the same modes of occurrence. The relative amounts of carbonate types vary between intrusive phases within banded dykes. Staining of carbonate with Alizarin Red and Potassium Ferricyanide reveals that many ocelli are calcitic, but are often overgrown at the edges by dolomite which dominates deuteric alteration of the groundmass.

In the most carbonate- rich examples, groundmass pyroxene laths are pseudomorphed by multidomainal granular aggregates of carbonate.

One olivine sannaite contains rounded to subangular inclusions of titanomagnetite up to 1cm across. These are chemically similar to titanomagnetites in olivine-free sannaites (table 3-8). They have serrated rims caused by reaction with groundmass fluids (fig.3-7).

KIMBERLITE and CARBONATISED KIMBERLITE

Kimberlites consist of varying sizes of olivine and mica phenocrysts in a matrix of mica, carbonate, apatite, titanomagnetite and/or perovskite. Nodules and megacrysts are abundant in some kimberlites, but are absent in others.

Nodules are varieties of glimmerite, mostly more than 80%

Figure 3-6: Poorly defined boundary between olivine-rich (left side) and ocellar (right side) bands in a sannaite dyke. Note brown mica and slender greenish pyroxene associated with the ocellus.

Magnification x 35

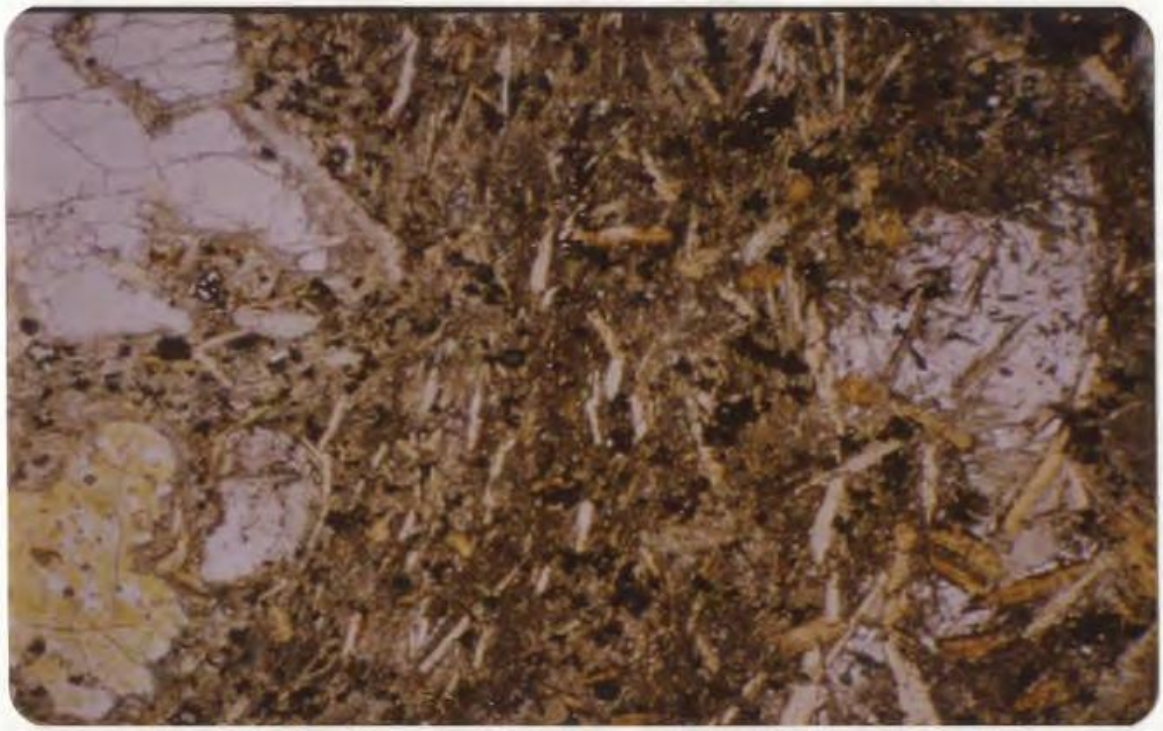

Figure 3-7: Olivine sannaite. Titanomagnetite megacryst has serrated edges due to reaction with groundmass fluids. Note orange tinge to pyroxenes with extreme Ti content, and very limited development of felsic minerals.

Magnification x 120

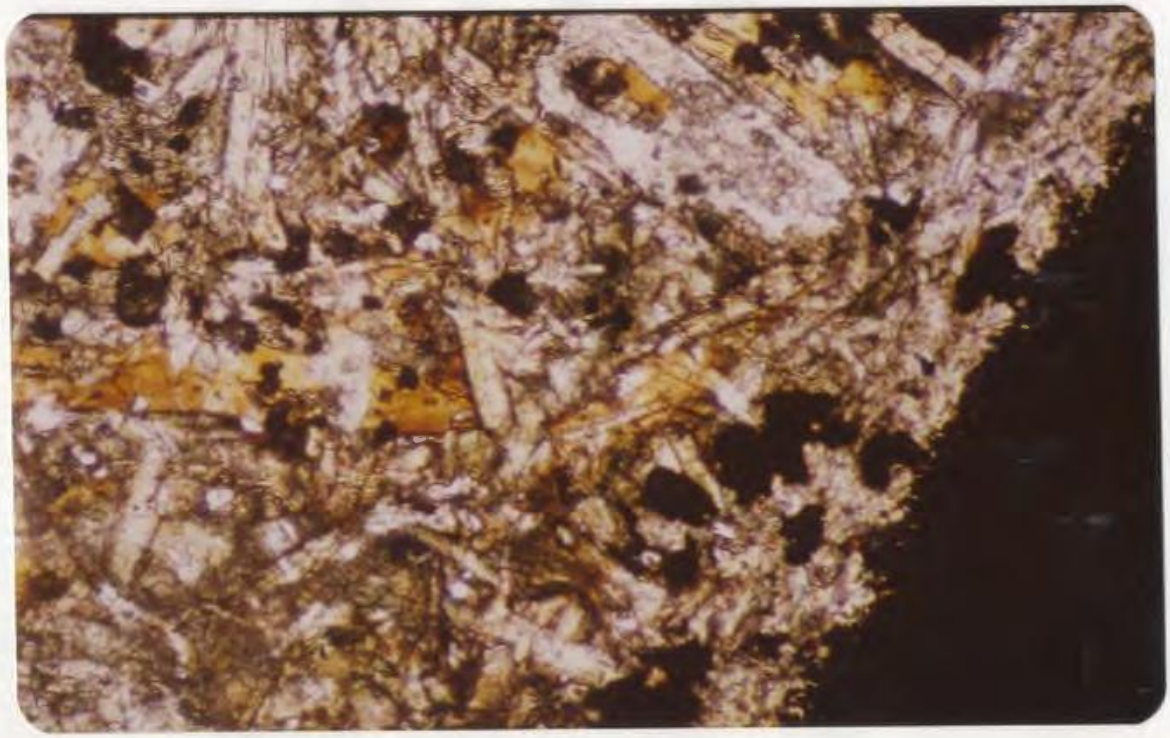

TABLE 3-8: Representative analyses of micas from olivine sannaites

Sample no.	L514-90	L514-91	L514-92	L514-93	L514-94
SiO2	34.77	36.44	35.54	36.63	36.20
Al2O3	15.02	14.00	14.75	14.25	14.33
TiO2	9.54	9.30	8.42	8.83	8.85
FeOt	11.00	10.32	12.68	12.27	11.76
CaO	0.05	0.02	0.04	0.00	0.02
MgO	15.75	16.14	14.54	15.31	15.34
MnO	0.07	0.05	0.15	0.06	0.08
Na2O	0.43	0.37	0.48	0.45	0.43
K2O	8.54	8.96	8.21	8.48	8.55
Total	95.17	95.60	94.81	96.28	95.56
Structural formula on the basis of 22 oxygens;					
Si	5.130	5.329	5.284	5.347	5.320
Al	2.612	2.413	2.585	2.452	2.482
Fe	1.357	1.262	1.577	1.498	1.445
Ti	1.059	1.023	0.942	0.969	0.978
Mn	0.009	0.006	0.019	0.007	0.010
Mg	3.464	3.518	3.223	3.332	3.360
K	1.608	1.672	1.557	1.579	1.603
Na	0.123	0.105	0.138	0.127	0.123
Ca	0.008	0.003	0.006	0.000	0.003

Sample no.	L5T4-95	L514-96	L514-97	379-50	379-51
SiO2	35.10	35.84	35.27	34.07	35.11
Al2O3	14.74	13.98	13.58	12.80	14.91
TiO2	8.57	8.89	9.01	8.73	7.58
FeOt	11.21	12.76	13.16	21.13	10.69
CaO	0.04	0.00	0.26	0.01	0.07
MgO	15.75	14.41	14.89	9.14	16.55
MnO	0.14	0.10	0.11	0.28	0.09
Na2O	0.37	0.39	0.43	0.26	0.34
K2O	8.83	8.49	8.41	8.57	8.61
Total	94.75	94.86	95.12	94.99	93.95
Structural formula on the basis of 22 oxygens;					
Si	5.212	5.335	5.262	5.310	5.234
Al	2.580	2.453	2.388	2.351	2.620
Fe	1.392	1.589	1.642	2.754	1.333
Ti	0.957	0.995	1.011	1.023	0.850
Mn	0.018	0.013	0.014	0.037	0.012
Mg	3.486	3.197	3.312	2.123	3.678
K	1.673	1.612	1.601	1.704	1.638
Na	0.107	0.113	0.124	0.079	0.098
Ca	0.006	0.000	0.042	0.002	0.012

mica with minor amounts of the following phases; pyroxene, apatite, carbonate and olivine.

The coarsest mica grains within glimmerites are frequently deformed (fig.3-8). Glimmerites commonly exhibit decussate or idiotopic granular textures (Spry,1969, p.187) in areas of finer grain size. These areas are interpreted to be recrystallised in response to thermal metamorphism within the magma. A summary of nodule types is given by Hawkins (1977,p.97).

Rounded megacrysts of mica, titanomagnetite and olivine up to 1cm across are thought to originate within the kimberlite magma or its parental fluids.

Olivine ranges in size from 5mm cryptically zoned phenocrysts to second generation crystals less than a tenth that size. Chlorite and serpentine alteration is commoner than in the sannaites, but olivines are generally better preserved in all but the most carbonate- rich kimberlites (fig.3-9).

Microprobe analyses of olivines are given in table 3-9. Phenocryst cores show more extreme variation in forsterite content (Fo71-Fo87) than in olivine sannaites. Rims are more forsteritic than in sannaites, ranging from Fo81-Fo86. The maximum variation for rims in one rock is 3 mol% Fo. The variation in chemistry of the rims is possibly due to removal of an outer equilibrated rim, evidenced by rounding of phenocrysts. The most magnesian cores frequently have more magnesian rims (eg. table 3-9; anal.350-17,18 to 350-21,23; and 350-43 to 350-47). Alternatively, mixing of olivines from areas of slightly different equilibration conditions may have occurred.

Figure 3-8: Glimmerite nodule in kimberlite. Large deformed micas partially recrystallised to small polygonal grains. Interstitial material is mostly carbonate.
Magnification x 120

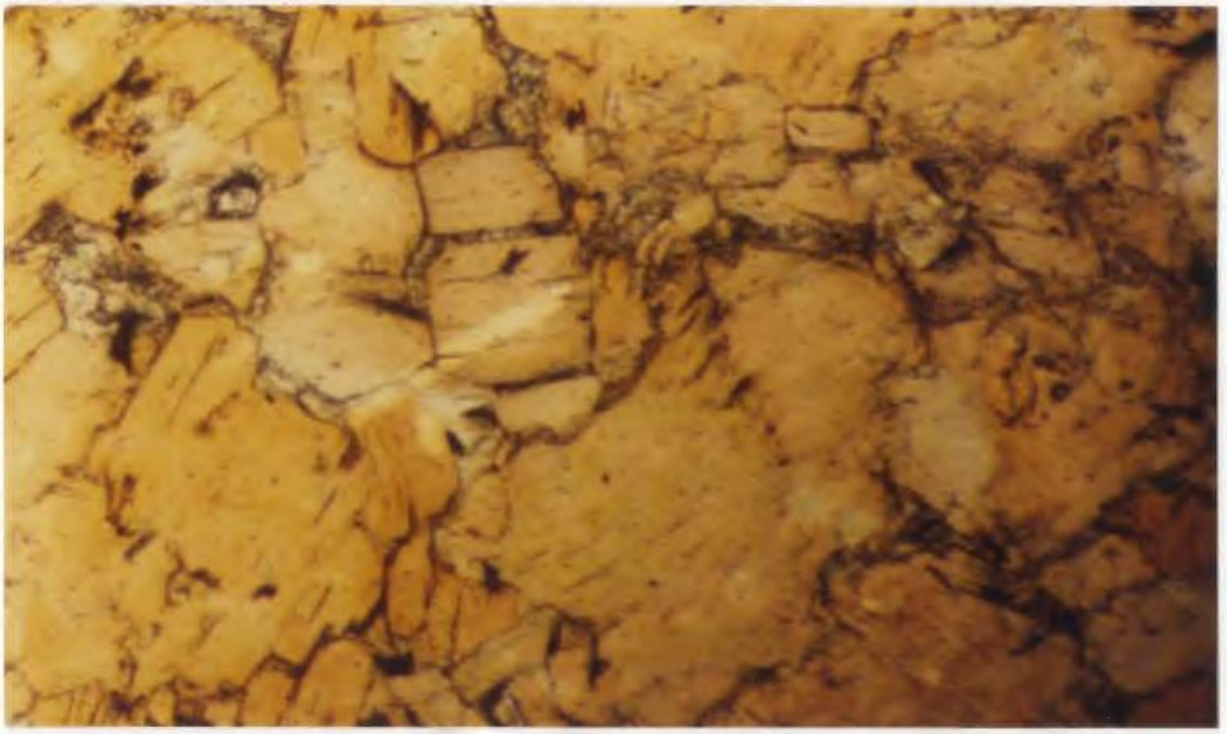

Figure 3-9: Kimberlite. Fresh rounded olivine and mica (upper centre) in a groundmass dominated by carbonate (high order white), mica and titanomagnetite. Crossed polars.
Magnification x 35

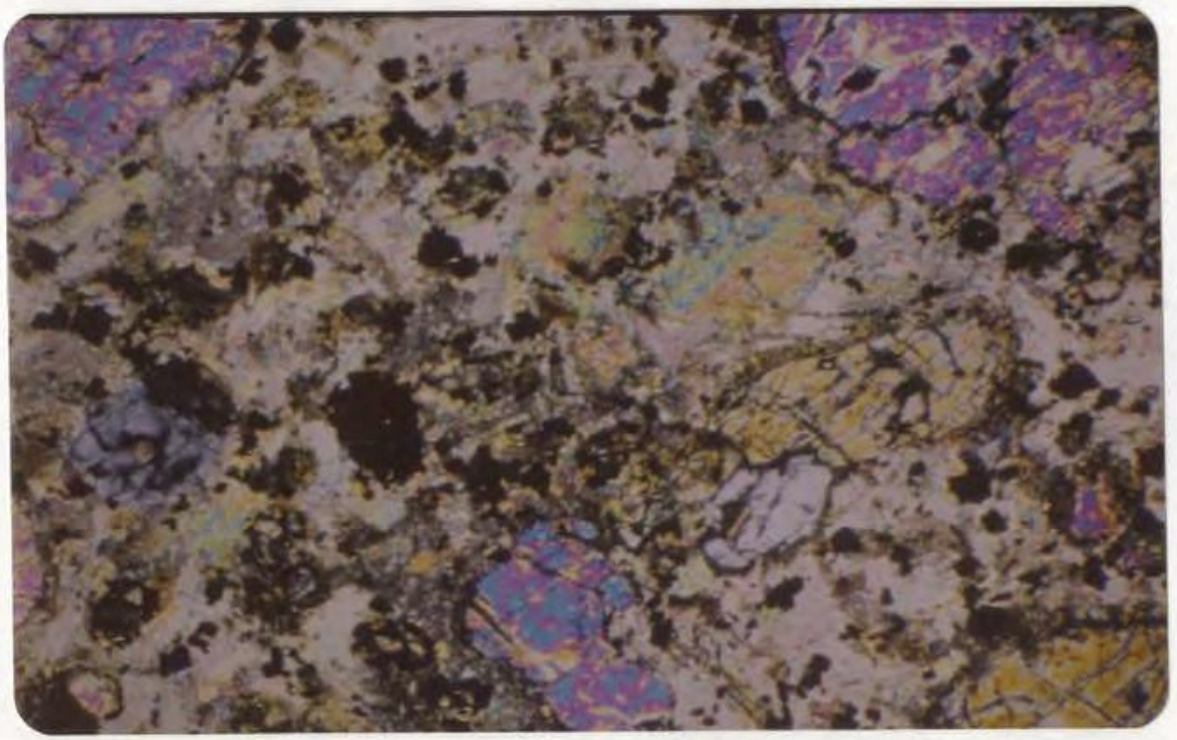

TABLE 3-9? Representative analyses of olivines from kimberlite

Sample no.	321-04	321-30	321-40	321-42	321-43	350-03
SiO2	39.53	40.38	39.67	38.59	39.79	39.62
Al2O3	0.02	0.00	0.04	0.00	0.02	0.02
TiO2	0.01	0.01	0.04	0.02	0.05	0.05
FeOt	14.32	10.47	13.26	22.25	16.00	12.40
CaO	0.00	0.02	0.11	0.04	0.16	0.17
MgO	45.03	48.95	46.13	39.27	44.64	46.25
MnO	0.25	0.05	0.07	0.19	0.25	0.13
Na2O	0.09	0.01	0.08	0.00	0.01	0.05
NiO	0.05	0.24	0.38	0.14	0.01	0.38
Total	99.30	100.13	99.78	100.50	100.93	99.07
Fo	81.99	87.13	83.44	71.87	80.16	84.38

Sample no.	350-04	350-06	350-09	350-13	350-16	350-17
SiO2	40.60	39.89	40.38	40.42	39.33	39.59
Al2O3	0.05	0.05	0.05	0.04	0.02	0.46
TiO2	0.00	0.01	0.00	0.00	0.03	0.01
FeOt	12.41	12.50	12.45	12.47	18.07	15.21
CaO	0.15	0.15	0.16	0.20	0.21	0.20
MgO	47.16	47.08	47.71	46.58	42.57	45.11
MnO	0.04	0.10	0.10	0.18	0.11	0.13
Na2O	0.07	0.00	0.01	0.04	0.01	0.01
NiO	0.26	0.21	0.24	0.27	0.08	0.09
Total	100.74	99.99	101.10	100.20	100.43	100.81
Fo	84.62	84.50	84.73	84.40	77.33	81.11

Sample no.	350-18	350-21	350-23	350-24	350-25	350-26
SiO2	39.08	39.01	39.23	39.32	39.18	38.36
Al2O3	0.06	0.04	0.04	0.02	0.04	0.09
TiO2	0.01	0.05	0.00	0.04	0.02	0.00
FeOt	15.54	13.88	14.34	15.05	14.42	21.21
CaO	0.21	0.24	0.21	0.20	0.21	0.02
MgO	44.63	45.79	44.13	44.67	44.86	40.20
MnO	0.22	0.25	0.18	0.16	0.19	0.20
Na2O	0.01	0.02	0.04	0.01	0.02	0.02
NiO	0.08	0.15	0.07	0.14	0.12	0.08
Total	99.84	99.43	98.24	99.61	99.06	100.18
Fo	80.61	82.69	81.67	81.12	81.83	73.29

TABLE 3-9 (continued)

Sample no.	350-31	350-32	350-24	350-38	350-40	350-42
SiO2	39.26	39.77	39.84	38.17	39.57	39.75
Al2O3	0.04	0.04	0.04	0.04	0.05	0.06
TiO2	0.04	0.00	0.02	0.00	0.02	0.00
FeOt	12.91	12.88	13.09	16.34	10.32	10.35
CaO	0.19	0.17	0.18	0.16	0.06	0.09
MgO	46.70	46.46	46.60	43.61	48.41	48.52
MnO	0.13	0.14	0.14	0.13	0.07	0.10
Na2O	0.01	0.02	0.02	0.01	0.02	0.01
NiO	0.21	0.19	0.17	0.15	0.36	0.33
Total	99.49	99.67	100.10	98.61	98.88	99.21
Fo	83.97	83.93	83.75	79.44	87.17	87.16

Sample no.	350-43	350-47	406-08	406-10	406-18	406-22
SiO2	39.61	39.56	39.21	38.89	39.85	39.68
Al2O3	0.07	0.05	0.04	0.06	0.04	0.04
TiO2	0.00	0.00	0.02	0.02	0.00	0.01
FeOt	10.40	12.19	15.09	14.72	11.36	11.45
CaO	0.09	0.14	0.18	0.14	0.13	0.11
MgO	48.46	46.20	44.44	44.04	47.32	47.14
MnO	0.08	0.15	0.23	0.16	0.10	0.11
Na2O	0.03	0.02	0.01	0.02	0.02	0.02
NiO	0.35	0.25	0.14	0.12	0.29	0.31
Total	99.09	98.56	99.36	98.17	99.11	98.87
Fo	87.09	84.59	81.00	81.24	85.78	85.63

Sample no.	406-24	406-47	406-48	406-50	406-51	406-57
SiO2	39.68	39.15	38.73	39.14	38.75	39.67
Al2O3	0.04	0.02	0.00	0.00	0.00	0.04
TiO2	0.00	0.00	0.00	0.00	0.00	0.00
FeOt	11.42	13.99	13.93	15.45	15.42	10.73
CaO	0.10	0.23	0.23	0.17	0.18	0.08
MgO	46.84	45.05	45.09	45.07	44.62	49.00
MnO	0.14	0.43	0.41	0.16	0.16	0.10
Na2O	0.01	0.02	0.01	0.03	0.16	0.02
NiO	0.27	0.00	0.00	0.14	0.18	0.23
Total	98.50	98.89	98.40	100.16	99.47	99.87
Fo	85.59	82.34	82.42	80.86	80.73	86.86

Minor element contents vary sympathetically with Fo (fig.3-10). Ni shows a positive correlation, whereas Ca and Mn correlate negatively. This is clearest in the latest crystallising olivines.

The phenocryst cores with Fo < 75 are clearly different from the trends of most olivines. The low Ca content is noteworthy, since Simkin and Smith (1970) and Mitchell (1973) have suggested it is indicative of 'deep seated' origin. A xenocrystal origin for these grains can not be ruled out.

Micas range in size from around 1cm to groundmass laths only 0.01mm long. Most micas are strongly zoned, and seven pleochroic schemes, each with distinct chemical characteristics, can be recognised within one rock (table 3-10a). Analyses are given in table 3-10b, and representative analyses from other kimberlite samples are listed in appendix 1. It is extremely rare for a single crystal to have more than 3 zones. The outermost zones on some crystals are a very thin pale coloured rim to a strongly normal pleochroic pale brown to deep red-brown zone (fig.3-11). The outer zones of phenocrysts may be partially removed by later corrosion or abrasion. The deep red-brown zone occurs on almost all crystals in contact with the matrix, and also forms discrete laths within the matrix. All mica generations may be deformed, and age relationships between them are uncertain. Thus, there appears to be mica of several starting compositions introduced into a kimberlitic fluid from which common rims and the matrix phases precipitated.

The matrix generation (type 6 of table 3-10b) is enriched

Figure 3-10: Compositional variation in olivine from Aillik Bay kimberlites. Open symbols = phenocryst cores, solid symbols = phenocryst rims.

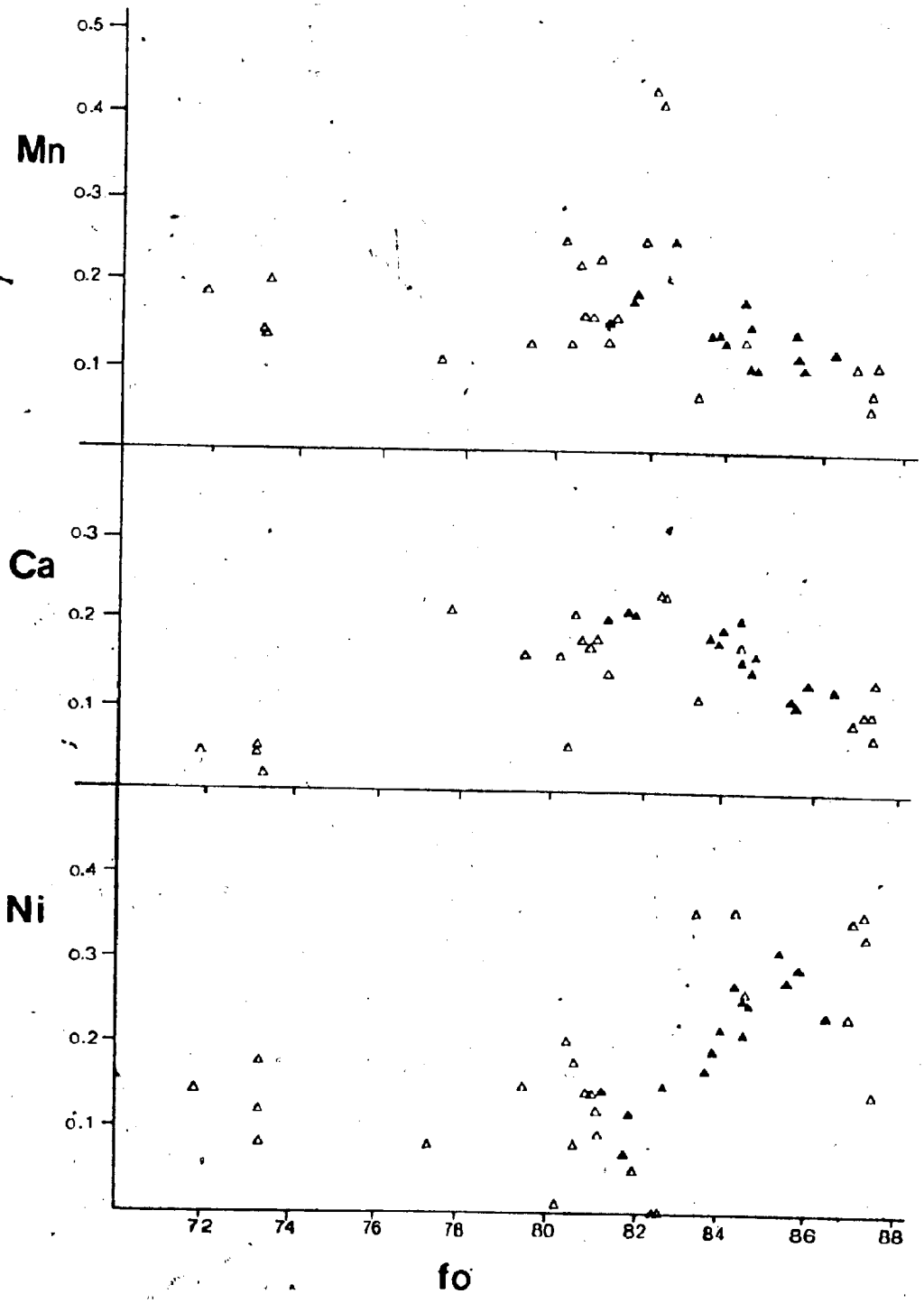

TABLE 3-10a : Pleochroic schemes of micas from kimberlite - sample 383

Type; used in Table 3-10b	α	β, γ	Mode of occurrence
1	mid orange-brown	very pale green to green brown	Glimmerite
2	bright red-brown	pale brown, green-brown, green	Phenocryst cores
3	non-pleochroic	very pale brown	Phenocryst cores
4	pale green	bright green to green-brown or brown	Phenocryst cores
5	pale brown	dark brown	Unzoned, assoc. altered mafics
6	neutral or very pale brown	orange-brown, brown, green-brown	Phenocryst rims & groundmass
7	neutral to pale orange	neutral or vary pale brown	Outer rims of phenocrysts

TABLE 3-10b: Analyses of micas from kimberlite sample 383
Type refers to Table 3-10a.

Sample no.	383-50	383-51	383-52	383-55	383-56	383-63
Type	1	1	1	2	2	2
SiO2	41.84	42.36	41.86	41.60	41.45	41.36
Al2O3	9.85	10.15	10.25	8.09	8.07	10.44
TiO2	0.86	0.72	0.81	0.44	0.45	1.15
FeOt	9.58	9.18	9.59	11.80	11.64	13.30
CaO	0.00	0.00	0.00	0.00	0.00	0.00
MgO	22.97	22.82	22.83	22.77	22.91	20.59
MnO	0.08	0.14	0.08	0.05	0.04	0.08
Na2O	0.21	0.16	0.08	0.13	0.13	0.28
K2O	8.58	8.52	9.25	8.86	8.54	8.74
Total	93.96	94.05	94.75	93.74	93.23	95.94
Structural formula on the basis of 22 oxygens;						
Si	6.121	6.165	6.092	6.197	6.189	6.040
Al	1.699	1.741	1.759	1.421	1.420	1.797
Fe	1.172	1.117	1.167	1.470	1.454	1.625
Ti	0.095	0.079	0.089	0.049	0.051	0.126
Mn	0.010	0.017	0.010	0.006	0.005	0.010
Mg	5.009	4.951	4.953	5.041	5.058	4.483
K	1.601	1.582	1.718	1.684	1.670	1.629
Na	0.060	0.045	0.023	0.038	0.029	0.079

Sample no.	383-64	383-69	383-70	383-71	383-92	383-93
Type	2	3	3	3	4	4
SiO2	41.70	42.27	42.19	42.64	39.27	39.16
Al2O3	10.32	12.15	11.52	12.23	11.01	11.23
TiO2	1.28	1.48	1.34	1.38	1.09	1.10
FeOt	13.38	7.07	6.91	7.27	17.88	17.78
CaO	0.00	0.00	0.00	0.00	0.00	0.00
MgO	20.67	22.93	23.54	23.39	15.41	14.95
MnO	0.10	0.04	0.02	0.07	0.25	0.16
Na2O	0.28	0.24	0.28	0.21	0.24	0.36
K2O	9.33	8.53	8.71	7.69	7.96	7.85
Total	97.06	94.71	94.51	94.88	93.11	92.59
Structural formula on the basis of 22 oxygens;						
Si	6.040	6.037	6.048	6.048	6.038	6.047
Al	1.762	2.045	1.947	2.045	1.995	2.044
Fe	1.621	0.844	0.828	0.863	2.296	2.287
Ti	0.139	0.159	0.145	0.147	0.126	0.128
Mn	0.012	0.005	0.002	0.008	0.033	0.021
Mg	4.463	4.882	5.030	4.946	3.532	3.441
K	1.724	1.554	1.593	1.392	1.561	1.546
Na	0.079	0.067	0.079	0.058	0.108	0.086

Table 3-10b (continued)

Sample no.	383-81	383-82	383-83	383-84	383-59	383-67
type	5	5	5	5	6	6
SiO2	36.49	36.83	37.00	36.96	38.53	37.78
Al2O3	15.34	15.48	14.99	14.93	15.79	15.45
TiO2	3.18	3.24	3.01	3.09	4.57	4.35
FeOt	20.14	20.09	19.94	19.75	7.28	7.32
CaO	0.00	0.00	0.00	0.00	0.05	0.03
MgO	10.25	10.29	11.25	11.24	20.48	20.21
MnO	0.19	0.17	0.11	0.13	0.02	0.02
Na2O	0.21	0.21	0.18	0.10	0.29	0.34
K2O	8.58	8.46	9.36	8.91	7.99	8.38
Total	94.38	94.77	95.84	95.11	95.00	93.88
Structural formula on the basis of 22 oxygens;						
Si	5.620	5.635	5.625	5.642	5.507	5.490
Al	2.785	2.792	2.686	2.686	2.660	2.647
Fe	2.594	2.571	2.535	2.521	0.870	0.890
Ti	0.368	0.373	0.344	0.355	0.491	0.475
Mn	0.025	0.022	0.014	0.017	4.364	4.378
Mg	2.353	2.347	2.550	2.558	1.457	1.554
K	1.686	1.651	1.815	1.735	0.080	0.096
Na	0.063	0.062	0.053	0.030	0.008	0.005
Ca	0.000	0.000	0.000	0.000	0.000	0.000

Sample no.	383-78	383-88	383-95	383-99	383-98	383-49
type	6	6	6	6	7	7
SiO2	37.79	36.21	37.64	37.39	41.58	42.56
Al2O3	15.69	15.82	16.12	16.13	10.27	8.02
TiO2	4.92	4.55	4.85	4.14	1.03	0.81
FeOt	6.75	6.87	7.33	6.42	8.06	8.00
CaO	0.03	0.02	0.02	0.02	0.11	0.10
MgO	20.29	20.18	19.64	19.80	23.89	23.68
MnO	0.01	0.04	0.06	0.04	0.07	0.14
Na2O	0.38	0.27	0.31	0.30	0.18	0.13
K2O	8.61	8.23	7.75	8.47	9.45	7.86
Total	94.47	92.19	93.72	92.71	94.64	91.30
Structural formula on the basis of 22 oxygens;						
Si	5.451	5.360	5.455	5.478	6.034	6.332
Al	2.668	2.760	2.754	2.786	1.757	1.407
Fe	0.814	0.851	0.888	0.787	0.978	0.995
Ti	0.538	0.507	0.529	0.456	0.112	0.091
Mn	0.001	0.005	0.007	0.005	0.009	0.018
Mg	4.363	4.453	4.243	4.324	5.168	5.252
K	1.585	1.554	1.433	1.583	1.750	1.492
Na	0.106	0.078	0.087	0.085	0.051	0.038
Ca	0.005	0.003	0.003	0.003	0.017	0.016

Figure 3-11: Zoning in kimberlite micas. Megacryst is reverse pleochroic (type 2; table 3-10a) with a normal pleochroic rim (type 6). The small crystal (far right) has a thin orange reverse pleochroic rim (type 7).
Magnification x 60

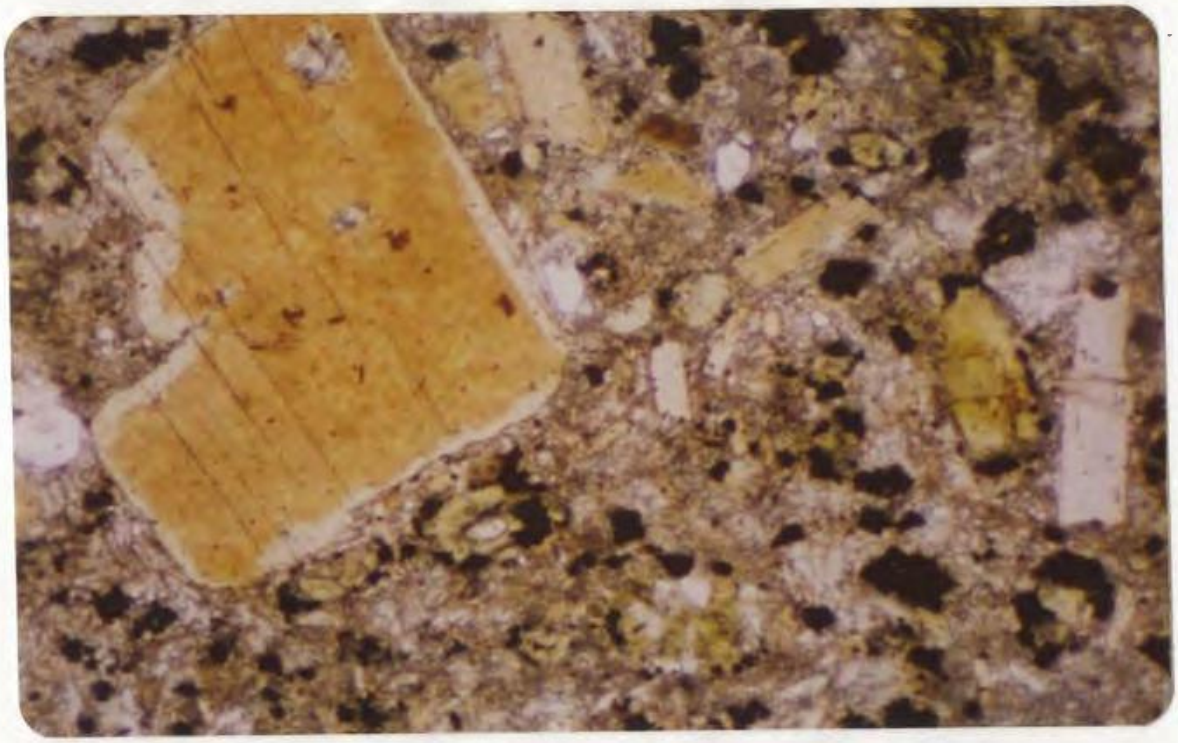

Figure 3-13: Carbonate-rich kimberlite with atolled titanomagnetites. The median zone is mostly carbonate. Note stronger development of the outer carbonate-associated reverse pleochroic mica zone. Late movement within the rock is evidenced by deformed type 6 mica.
Magnification x 35

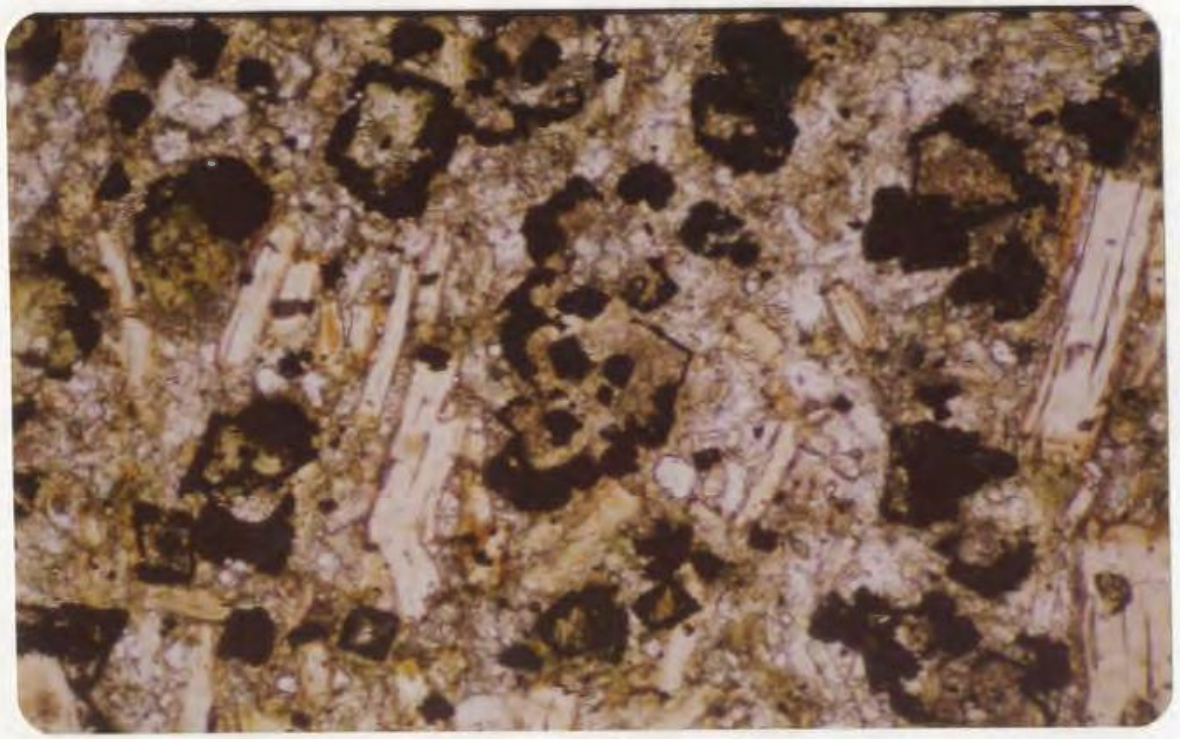

in Ti, and to a lesser extent Al relative to all previous mica generations. Various plots of wt % oxides (fig.3-12) suggest an iron depletion trend within the core micas with respect to Si and Mg. The position of the glimmerite nodule micas within this trend may imply a cognate origin.

The latest pale coloured rims directly reverse this trend; Ti and Al are depleted and Si, Fe and Mg are enriched (table 3-10b, anal. 383-49,98). This type is not well developed, but is best developed near carbonate- rich veins or patches. A depletion of Ti and Al is seen in sovites relative to damkjernites in the Fen Complex (Mitchell, 1980).

Micas from 'basaltic' kimberlites (Dawson,1967) usually have higher Mg/(Mg +Fe) (Smith et al.,1978; Delaney et al.,1980; Dawson and Smith,1975). Only the rare non-pleochroic micas at Aillik Bay are at all similar.

Micas similar to Aillik Bay kimberlite micas are found in micaceous kimberlites at Kirkland Lake, Ontario (Rimsaite,1971), West Greenland (Emeleus and Andrews, 1975) and Saglek, Labrador (Collerson and Malpas, unpubl.data).

Lamprophyric micas may have similar Mg/(Mg+Fe) and Al contents, but normally have higher Ti (up to 11 wt% in potassic lamproites in Montana (Velde,1975)), and higher Na (0.5 to >1.0 wt%; Cooper,1979; Roden and Smith,1979; Hansen,1980).

Total Na+K is considerably less than required to fill 2 sites for Aillik Bay kimberlitic micas. This may be partly due to loss of alkalies (? by volatilisation) during analysis, but could also be caused by charge balancing in response to large

Figure 3-12: Compositional variation in mica from kimberlite sample 383.

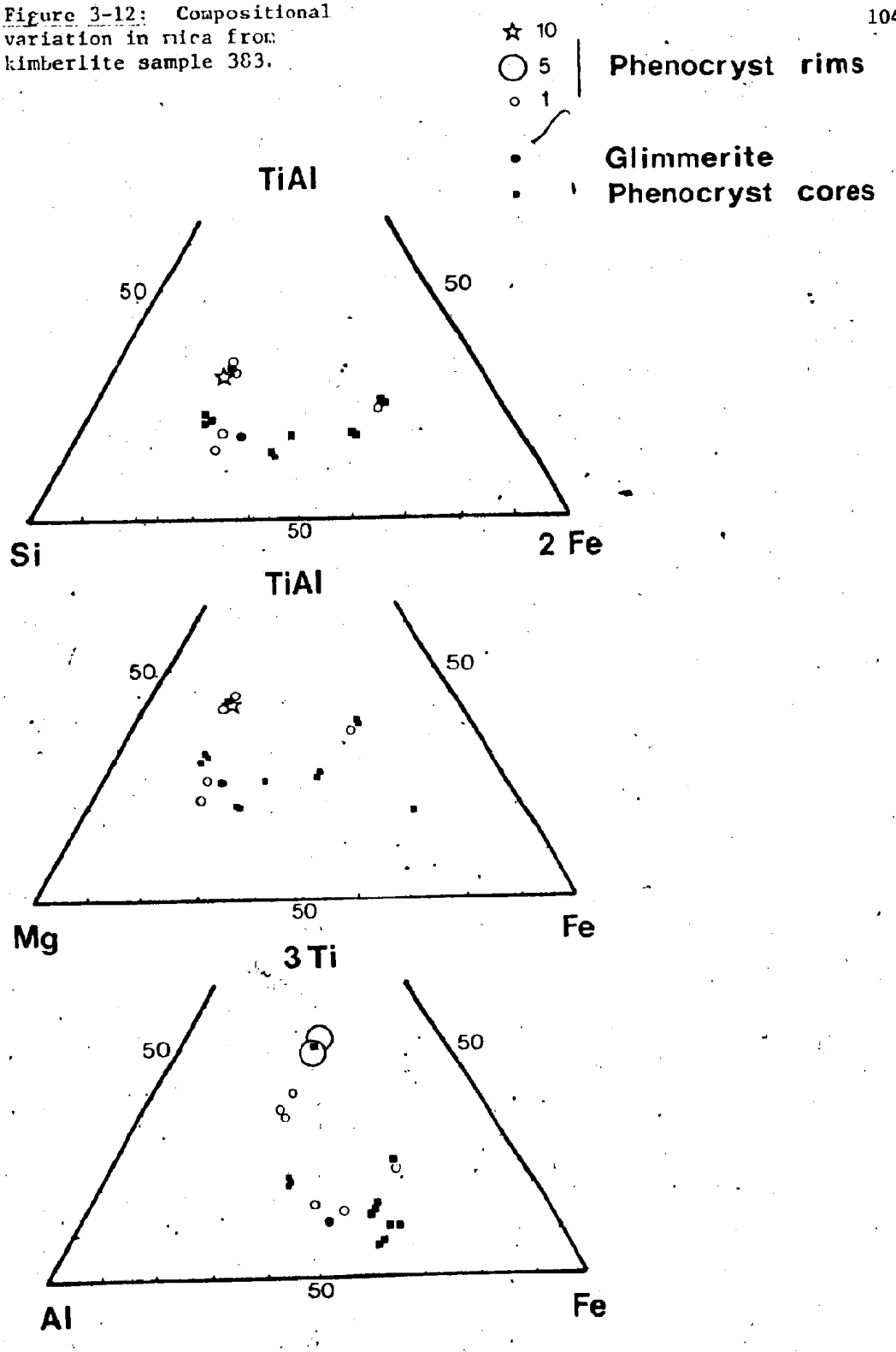

substitutions of Ti^{4+}, which will occupy octahedral sites (Robert,1976). Zussman (1979) notes that interlayer substitution of Ca or Na will facilitate larger amounts of Al substitution into tetrahedral sites, because their smaller ionic radii permit tetrahedral rotations. Ca and Na are very limited in the kimberlitic micas, but vacancy of interlayer sites would presumably have a similar effect.

Oxide phases make up 7% of kimberlites on average, but up to 22% in some cases. Oxide megacrysts are all titanomagnetite, some with inclusions of carbonate. Matrix oxides comprise titanomagnetite with rarer rutile, chrome-rich spinels and Mg-Al-titanomagnetites (table 3-11). Rutile occurs as corroded grains rimmed by titanomagnetites.

Mg-Al-titanomagnetites are the latest oxide phase, frequently forming 'atolls' described by Hawkins (1977). Atolls are growths of Mg-Al-titanomagnetite around earlier oxides with a median zone of carbonate which had nucleated on the oxide crystal (fig.3-13). Olivines may have incomplete rims of Mg-Al-titanomagnetite. A rarer type of atoll rim is apparently magnesioferritic ($Mg = 3[Ti+Al]$) titanomagnetite, but no satisfactory probe analysis could be obtained because of the small size of the rims.

Magnesian ilmenite, and spinels with high Mg and Ti contents are two of the most fundamental marker minerals in recognising true kimberlites (Haggerty, 1975; Mitchell,1978a,1979a). Ilmenites from alkaline central complexes have lower Mg and higher Mn (eg.Vartiainen et al.,1978).The

TABLE 3-11: Representative analyses of oxide minerals from kimberlite

Sample no.	406-10	406-11	383-01	406-01	406-05
TiO2	12.47	14.24	8.29	6.52	11.57
Al2O3	3.04	2.40	9.93	8.94	2.27
FeOt	75.32	78.81	40.73	35.37	77.03
MnO	0.56	0.28	0.12	0.38	0.69
MgO	5.56	0.09	10.87	10.54	4.82
Cr2O3	0.00	0.04	26.78	33.34	0.00
Total	96.95	95.85	96.73	95.09	96.38
Structural formula on the basis of 4 oxygens;					
Cr	0.000	0.002	0.775	0.952	0.000
Al	0.149	0.123	0.417	0.381	0.114
Fe	2.628	2.867	1.215	1.068	2.753
Ti	0.391	0.466	0.222	0.177	0.372
Mn	0.020	0.010	0.004	0.012	0.025
Mg	0.346	0.006	0.578	0.567	0.307

Sample no.	406-06	383-05	383-07	406-07	383-03
TiO2	11.75	8.55	11.38	12.97	15.95
Al2O3	2.33	0.24	6.96	7.69	5.51
FeOt	77.23	83.54	67.79	65.38	67.05
MnO	0.48	0.23	0.72	0.39	0.34
MgO	5.39	2.80	8.58	7.62	1.04
Cr2O3	0.00	0.02	0.00	0.05	4.47
Total	97.18	95.37	95.43	94.11	94.36
Structural formula on the basis of 4 oxygens;					
Cr	0.000	0.001	0.000	0.002	0.146
Al	0.116	0.013	0.330	0.364	0.268
Fe	2.725	3.192	2.279	2.197	2.314
Ti	0.373	0.294	0.344	0.392	0.495
Mn	0.017	0.009	0.025	0.013	0.012
Mg	0.339	0.191	0.514	0.456	0.064

presence of ilmenite in Aillik Bay 'kimberlites', reported by Hawkins (1977,p.169), could not be confirmed.

The spinels have MgO contents below 8 wt% except in Cr-rich varieties. MgO contents in spinels of true kimberlites are commonly 10-17 wt% (Haggerty,1975; Mitchell,1979b), and may exceed 20 wt% (Haggerty,1973). Ti rarely exceeds 5 wt% (Haggerty,1975).

The Cr-rich spinels (anal.3 and 4 of table 3-11) are similar to Cr-spinels in true kimberlites at Kirkland Lake (Mitchell, 1978a) and Premier Mine, South Africa (Elthon and Ridley,1979) except for lower Ti/Al ratios.

Spinels in carbonatite-alkaline complex rocks are characterised by increasing Mn contents and Fe3+/Fe2+ ratios, culminating in carbonatites with Mn-magnetites poor in Ti (McMahon and Haggerty,1979; Boctor and Svisero,1978; Mitchell,1978b). Mn contents in Aillik Bay kimberlite spinels do not exceed 0,7 wt% and contain considerable Ti, and thus cannot be considered typical of carbonatite-associated rocks.

Similar minerals occur in other lamprophyre and carbonate-rich lamprophyre occurences (Cooper,1979; Platt and Mitchell,1979). Titanomagnetites from Mesozoic lamprophyres in West Greenland are similar except for higher Mn (Hansen, 1980).

Oxide evolution toward that of typical carbonatites was presumably halted by the development of sulphides in carbonate-rich kimberlites.

Carbonates are abundant in all kimberlites, ranging from 25% to more than 90% of the rock in rare cases. The variation

enables steps in the proceeding carbonatisation to be outlined.

In the least carbonatised examples, carbonate forms a crystalline matrix with mica and apatite, and varies greatly in grain size (fig.3-9). More carbonatised rocks are characterised by submicrogranular alteration of olivine and accentuated atolled opaque development (fig.3-11). Coarse grained carbonate may form irregular rounded patches which are apparently late segregations of carbonate free from mica, apatite and titanomagnetite, which coexist with carbonate in the matrix. One sample has radiating magnesioriebeckite crystals grown within late carbonate segregations (table 3-12; fig.3-14). Riebeckite has previously been described in carbonatites of the Samalpatti Complex in southern India (Subramaniam et al.,1978), where it was considered to be caused by fenitisation. At Aillik Bay it is apparently due to late concentration of Na and volatiles in the kimberlite matrix. The surrounding carbonate is not sodic.

The most carbonate-rich kimberlites, more correctly termed metasomatic carbonatites, are almost entirely carbonate. Olivines are entirely pseudomorphed and only occasional phenocrysts of phlogopite, plus matrix apatite and Mg-titanomagnetite survive (fig.3-15). Matrix phlogopite is resorbed, and may appear as brown stains in carbonate. Veins and elongated patches made up of coarsely crystalline (upto 4mm) carbonate become more common, in which carbonate frequently takes the form of radiating laths. Amalgamation of these patches gives rise, at least in part, to the banded appearance of many carbonatised kimberlite dykes. Veins occasionally contain

TABLE 3-12: Composition of magnesioriebeckite from kimberlite

Sample no.	373-10	373-17	373-12	373-15	373-14
SiO2	52.38	53.98	54.25	53.77	53.84
Al2O3	0.11	0.99	0.10	0.11	3.11
TiO2	0.09	0.74	0.14	0.00	0.71
FeOt	28.86	24.40	24.05	24.38	19.39
CaO	1.09	1.04	1.06	0.05	0.31
MgO	2.10	5.54	6.46	9.50	10.91
MnO	0.01	0.04	0.01	0.06	0.04
Na2O	13.23	10.53	10.35	7.89	8.67
K2O	0.09	0.25	0.68	1.53	1.21
Total	97.96	97.51	97.10	97.29	98.19
Structural formula on the basis of 23 oxygens;					
Si	8.228	8.222	8.305	8.189	7.924
Al	0.020	0.178	0.018	0.020	0.540
Fe	3.792	3.108	3.079	3.105	2.387
Ti	0.011	0.085	0.016	0.000	0.079
Mn	0.001	0.005	0.001	0.008	0.005
Mg	0.492	1.258	1.474	2.157	2.394
K	0.018	0.049	0.133	0.297	0.227
Na	4.030	3.110	3.072	2.330	2.474
Ca	0.184	0.170	0.174	0.008	0.049

Figure 3-14: Radiating magnesioriebeckite bundles in a late-stage carbonate segregation in kimberlite.
Magnification x 60

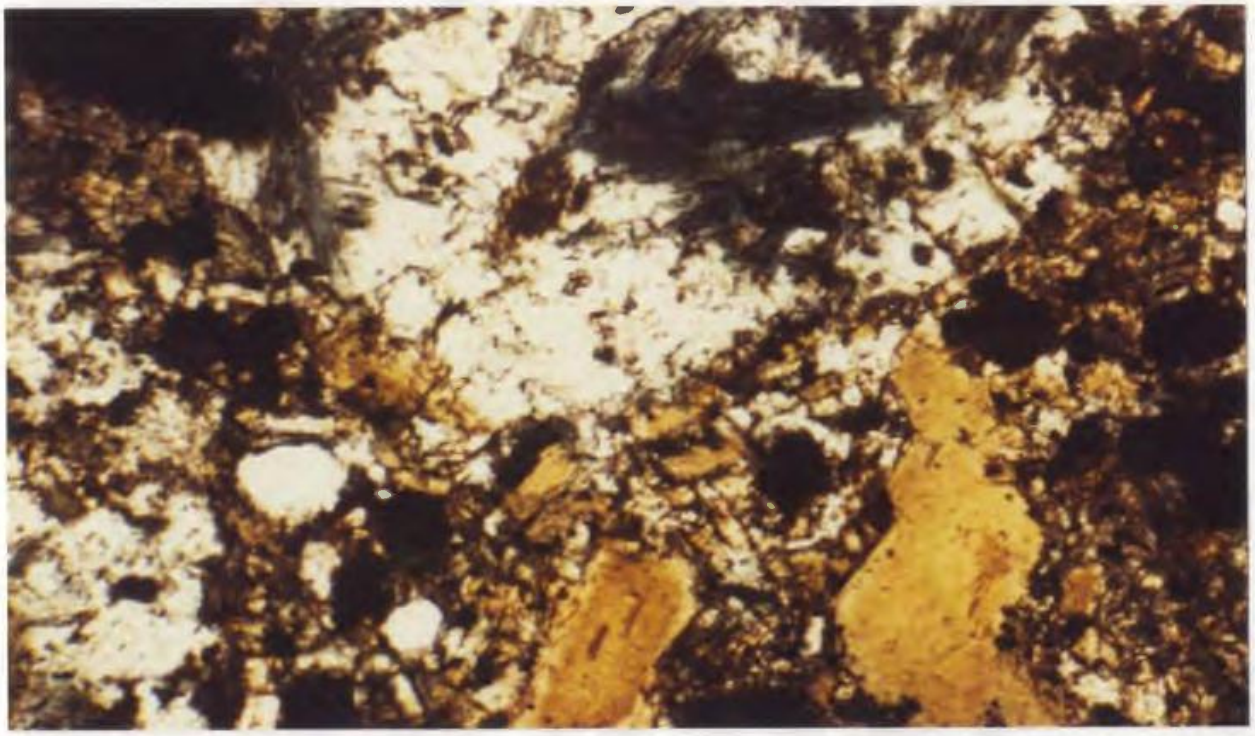

Figure 3-15: Intensely carbonatised kimberlite. Olivine is entirely pseudomorphed by submicrocrystalline carbonate. Coarsely crystalline carbonate is common in the groundmass.
Magnification x 40

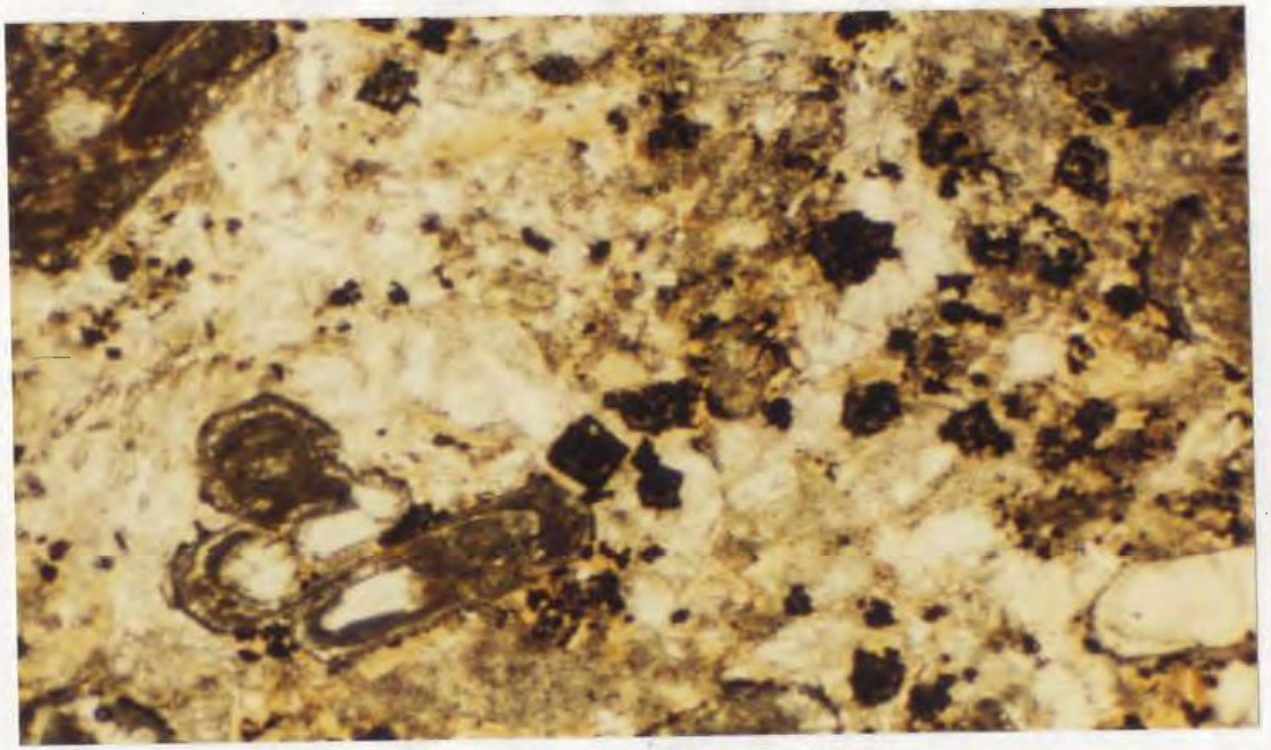

orthoclase.

Staining of carbonate shows more complex relationships than in olivine sannaites, but dolomite again generally postdates calcite.

CARBONATITES

Most carbonatites are metasomatic carbonatites (Frantsesson,1970) which have retained relict textures from kimberlite as described above. No discrete carbonatite dykes devoid of earlier textures occur on Cape Makkovik or on Turnavik Island, but an alvikite on Graplin Island, and a beforsite on Cape Aillik were described by Hawkins (1977). The alvikite comprises fine to medium grained xenomorphic calcite with minor dolomite. The beforsite has a similar texture but the carbonate is virtually all dolomite. Minor phases include apatite, K-feldspar, pyroxene and pyrite. The pyroxene in beforsite is a titanaegerine, which would be expected in the final stages of evolution of an alkaline-carbonatite complex (Mitchell,1980). K-feldspar occurs as rounded inclusions which are clouded by hematite dust. Heinrich and Moore (1970) describe similar features in carbonatites as being due to potash metasomatism.

CARBONATE COMPOSITIONS

Table 3-13 contains analyses of carbonates from sannaites, olivine sannaites, kimberlites and carbonatites. Carbonate occurs in 5 modes; as groundmass crystals, in ocelli, pseudomorphing olivine and other minerals, in late veins, and in

TABLE 3-13: Partial analyses of carbonate minerals from Aillik Bay dykes.

Abbreviations: SNT=Sannaite, OSNT=Olivine sannaite, KLP=kimberlite, CBT= carbonatite, GD=groundmass, OC=ocellus, PS=pseudomorph of olivine, VN=cross-cutting vein, IG= glimmerite nodule.

Sample no.	325-3b	3332b-4a	325-1a	325-2b	325-5a	L55-5a
type	SNT-PS	SNT-GD	SNT-OC	SNT-OC	SNT-OC	OSNT-PS
CaO	29.15	55.10	31.63	29.86	29.00	52.12
MgO	22.14	0.02	20.54	21.95	21.81	2.83
FeOt	5.17	0.36	5.02	4.36	4.99	1.10
MnO	0.16	0.08	0.27	0.20	0.24	0.21
SrO	0.29	2.36	0.45	0.59	1.14	1.31
Na2O	0.25	0.04	0.03	0.01	0.07	0.00
BaO	0.02	0.14	0.00	0.06	0.00	0.96
Total	58.20	58.20	58.05	57.15	57.37	58.56

Sample no.	L55-6a	367-3a	367-1a	L55-2a	L55-3a	L55-1a
type	OSNT-PS	OSNT-PS	OSNT-OC	OSNT-VN1	OSNT-VN1	OSNT-VN2
CaO	55.46	28.26	31.50	58.30	58.99	33.04
MgO	0.11	20.83	20.68	0.00	0.03	15.55
FeOt	0.39	5.69	6.84	0.05	0.07	5.77
MnO	0.08	0.26	0.16	0.00	0.03	1.24
SrO	0.51	0.33	0.33	1.03	1.78	0.14
Na2O	0.02	0.17	0.14	0.00	0.00	0.00
BaO	0.23	0.04	0.04	0.10	0.04	0.00
Total	56.84	55.72	59.84	60.54	60.98	55.80

Sample no.	L55-4a	383-3a	383-4b	321-2a	373-1a	373-2a
type	OSNT-VN2	KLP-PS	KLP-GD	KLP-GD	KLP-GD	KLP-GD
CaO	37.59	30.07	30.58	32.84	56.19	33.36
MgO	19.30	22.04	20.47	14.15	0.09	14.62
FeOt	2.53	3.07	3.86	7.72	0.28	7.84
MnO	0.35	0.32	0.16	0.32	0.46	1.37
SrO	0.33	0.11	0.05	0.36	0.35	0.30
Na2O	0.07	0.01	0.01	0.04	0.00	0.02
BaO	0.00	0.00	0.09	0.02	0.01	0.01
Total	60.27	55.66	55.28	55.46	57.46	57.54

Table 3-13 (continued)

Sample no.	383-1a	383-1b	383-2a	L512-2a	L512-3a	L512-4a
type	KLP-VN	KLP-VN	KLP-IG	CBT-GD	CBT-GD	CBT-GD
CaO	56.41	57.55	55.57	54.18	56.40	53.64
MgO	0.06	0.14	0.35	0.93	0.55	2.50
FeOt	0.08	0.16	0.32	0.73	0.25	0.79
MnO	0.16	0.11	0.14	0.96	1.03	0.39
SrO	0.81	0.14	0.27	0.06	0.18	0.13
Na2O	0.18	0.02	0.04	0.03	0.01	0.00
BaO	0.25	0.04	0.00	0.00	0.00	0.00
Total	57.98	58.19	57.11	58.81	58.45	58.70

Sample no.	L512-1a	L513-2a	L513-3a
type	CBT-GD	CBT-GD	CBT-GD
CaO	30.52	43.64	29.54
MgO	18.38	8.02	18.12
FeOt	5.76	3.36	6.05
MnO	1.11	0.16	0.86
SrO	0.01	0.38	0.15
Na2O	0.02	0.04	0.05
BaO	0.05	0.09	0.00
Total	55.88	55.70	54.78

glimmerite inclusions.

Compositions concentrate around almost pure calcite and ferroan dolomite (fig.3-16), both of which occur in all rock groups. Fe-magnesite and a Sr-rich phase are rarer types restricted to carbonate-rich kimberlites.

Interstitial carbonate in glimmerite nodules is calcite, and veins are normally dominated by one or other carbonate, suggesting discrete generations of Ca-rich and Mg-rich carbonates. The other 3 modes show no consistency in composition, but staining shows that dolomite generally postdates calcite. One olivine sannaite is cut by two generations of veins; the first calcite and the second dolomite. This rock contains earlier dolomite and calcite.

RELATED ULTRAMAFIC DYKES

The Turnavik Island phlogopite-clinopyroxene-peridotite has a striking texture defined by coarsely dendritic acicular to bladed olivine crystals (fig.3-17) 0.2-0.3mm wide and often in excess of 3cm long. Olivine has frequently recrystallised to shorter sub-grains. Olivine forms 60-65% of the rock, with the rest comprising pyroxene and coarse grained (2-4mm) interstitial mica, which is optically continuous for 1cm or more. Minor phases include 0.05mm to 0.4mm subhedral slightly spineliferous titanomagnetite, rutile, apatite and carbonate.

Titanomagnetite and rutile are included in olivine and frequently are concentrated close to olivine-olivine boundaries, with some overgrowth of the oxide phases (fig.3-18). Oxide

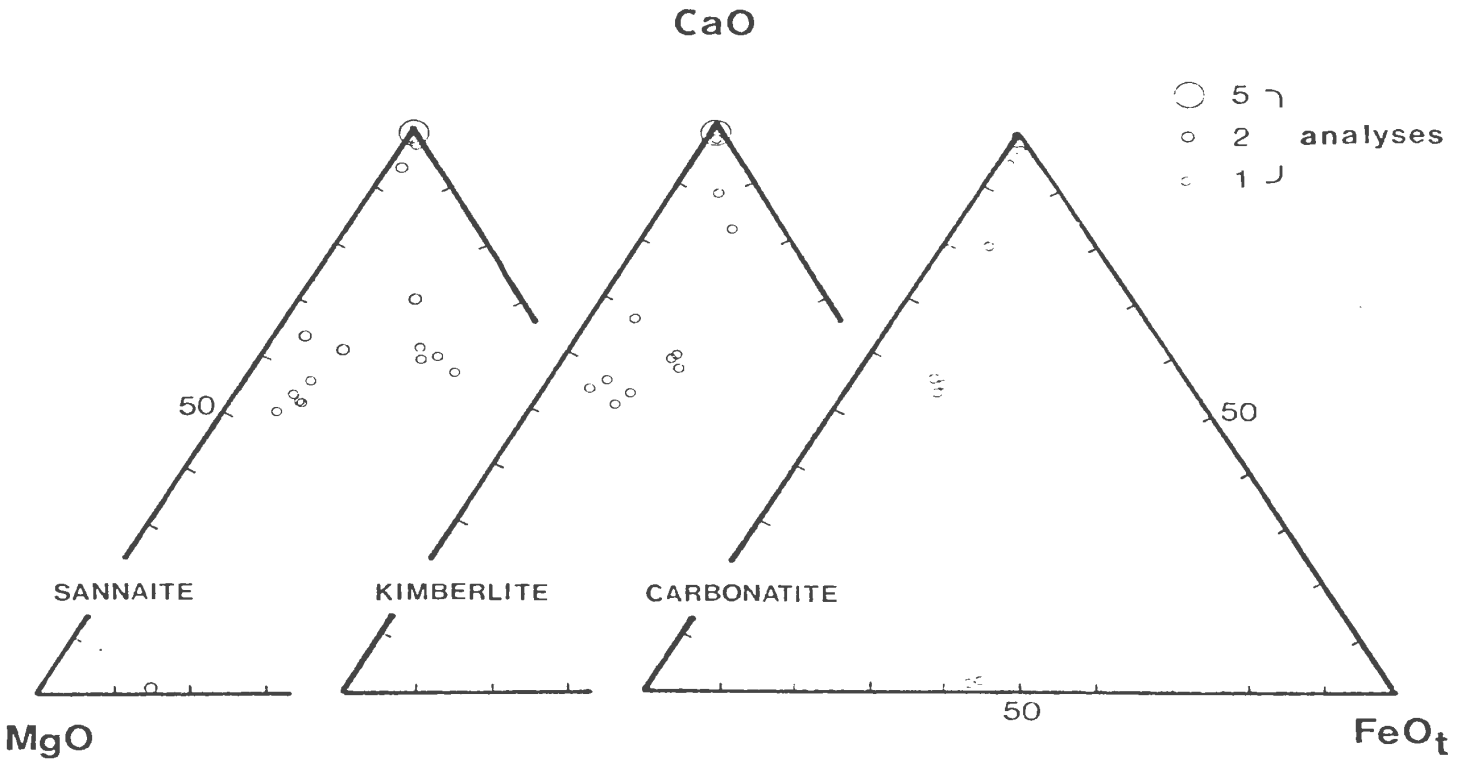
CaO
5
2 analyses
1
50
50
50
SANNAITE
KIMBERLITE
CARBONATITE
MgO
FeOt

B

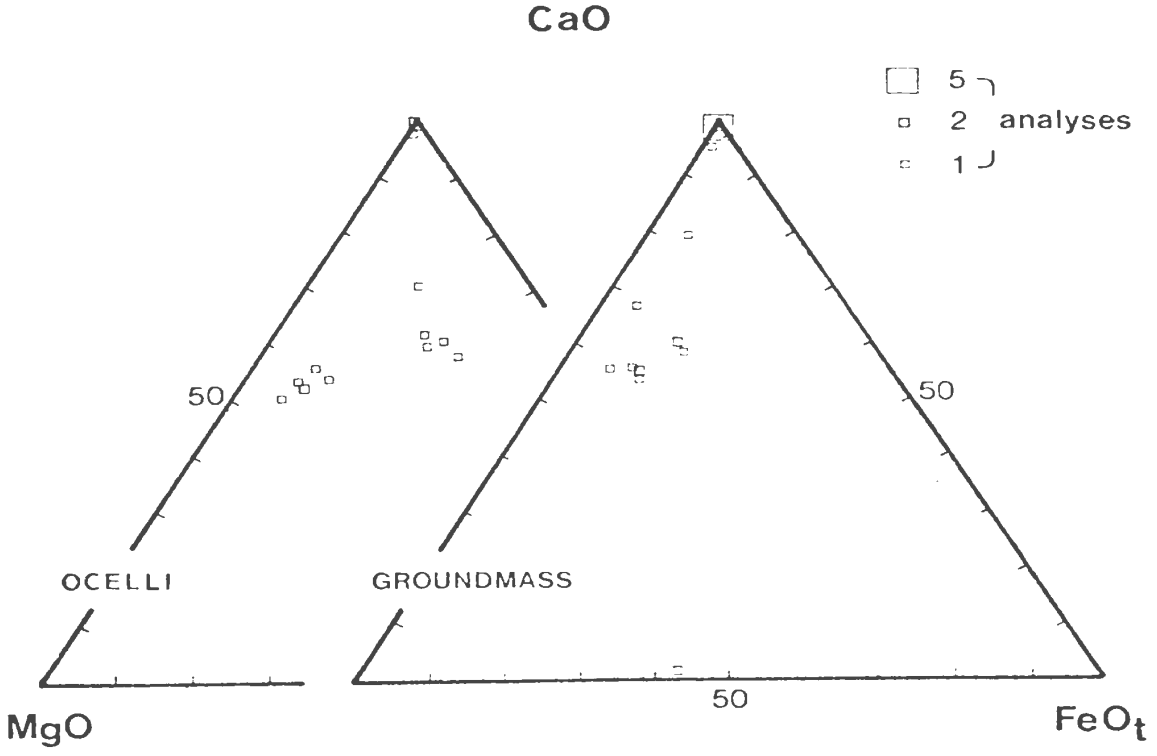
CaO
5
2 analyses
1
50
50
50
OCELLI
GROUNDMASS
MgO
FeOt

Figure 3-16: Compositional variation in carbonate minerals from the Aillik Bay Intrusive Suite. Different size symbols represent numbers of analyses. (A) rock type; (B) groundmass minerals from the suite compared to sannaite ocelli; (C) Ocelli vs. groundmass in sannaite. Squares = ocelli, circles = groundmass.

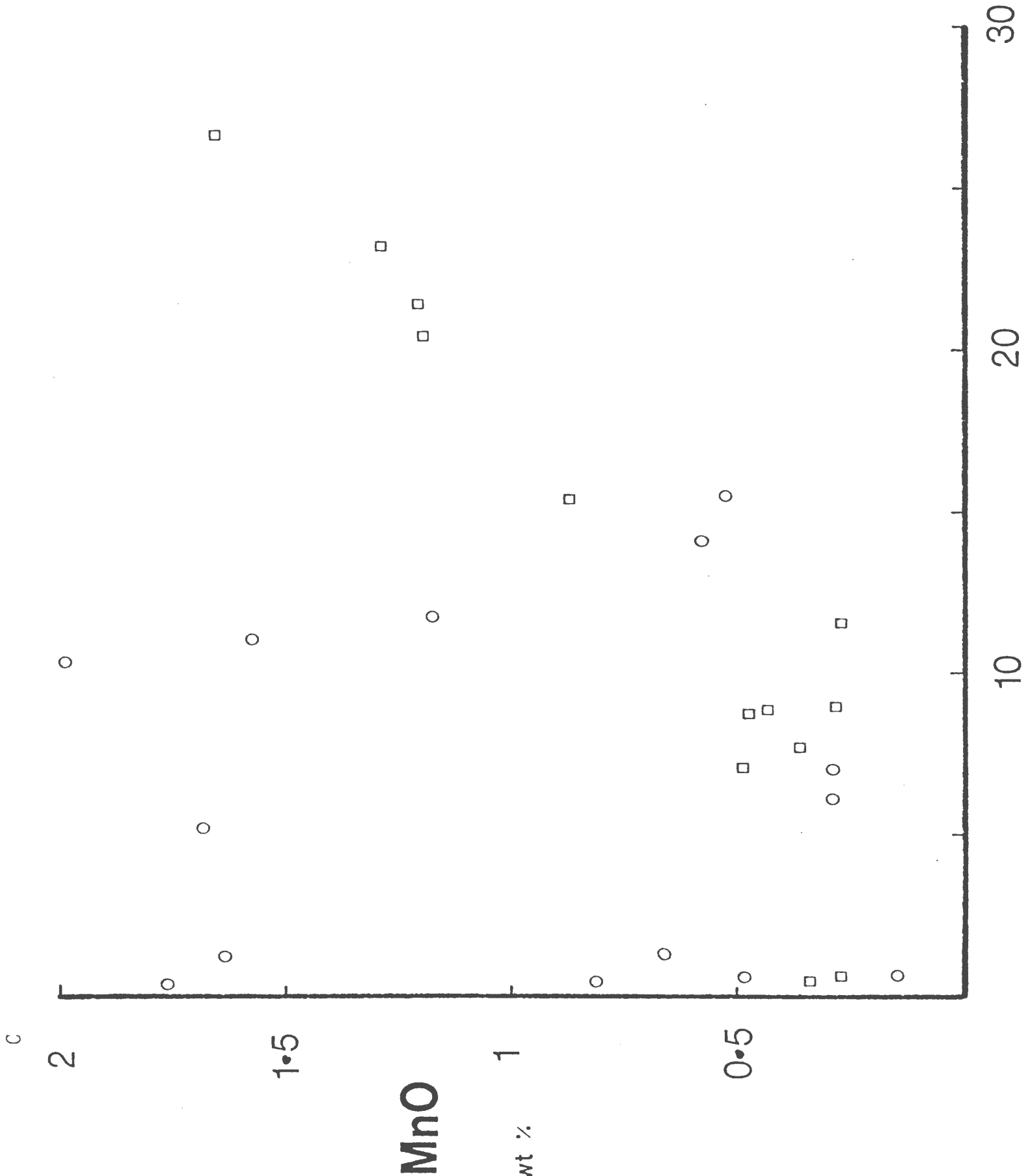

Figure 3-17: Phlogopite-clinopyroxene peridotite illustrating bundles of acicular to bladed olivine crystals.
Magnification x 40

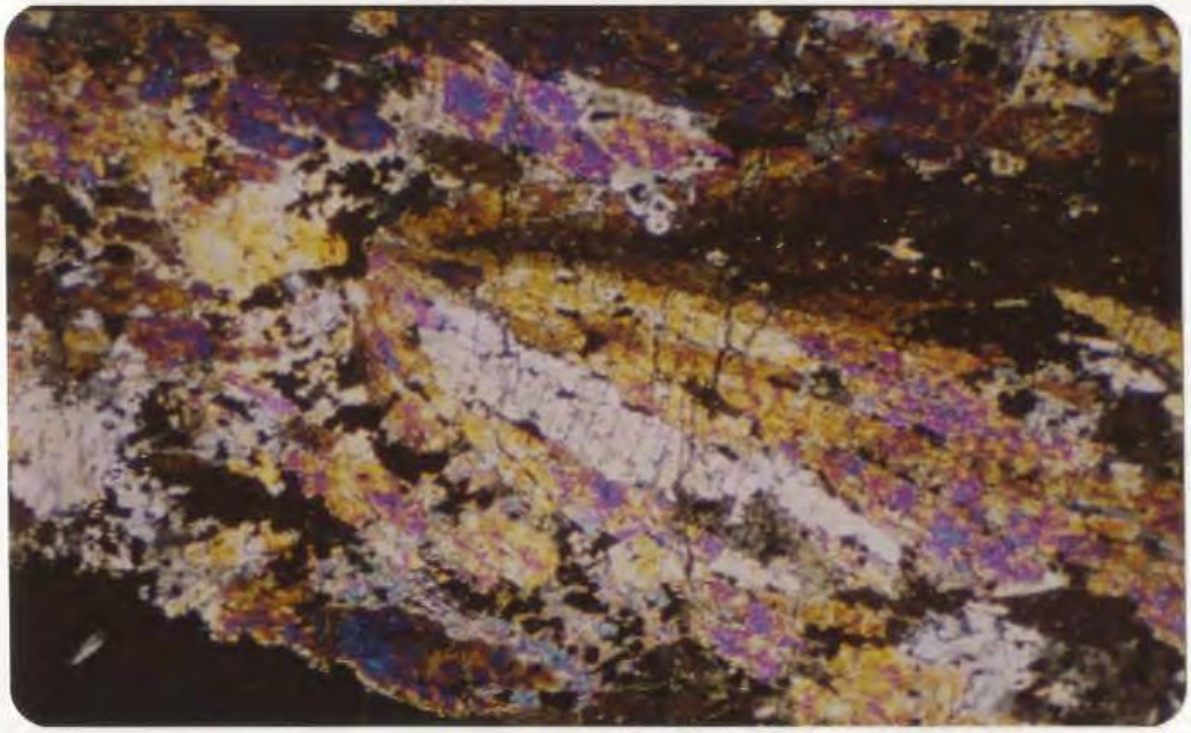

Figure 3-18: Acicular olivine in phlogopite-clinopyroxene-peridotite with large interstitial phlogopite crystals (bottom-mid grey). Oxide phases are concentrated at olivine-olivine boundaries, suggesting overgrowth by olivine.
Magnification x 60

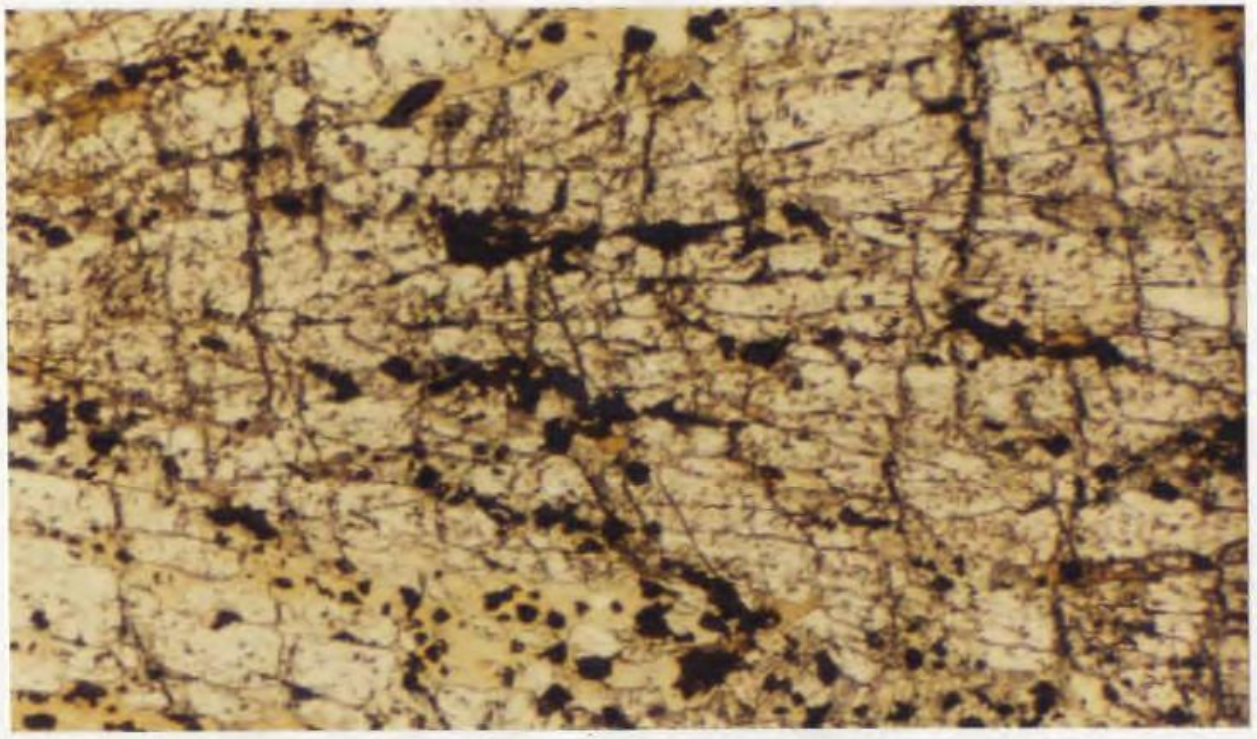

minerals occur along with randomly oriented apatite as inclusions in mica. Serpentine stringers cross olivine laths separated by interstitial phlogopite.

Mineral compositions are listed in table 3-14. Although the chief components in each phase are similar to those in the lamprophyres, there are several anomalies. Olivines can be divided into Ca-rich (1.1-1.5 wt%) and Ca-poor (0.3 wt%) types, of which only the latter occur in the lamprophyres. No textural distinction is apparent. Micas have extremely high Na/(Na+K), and titanomagnetites have high Mn.

This rock is possibly an earlier dyke type metasomatised by fluids from the alkaline complex.

The mica-pyroxene rock (fig.3-19) is 40% pyroxene laths, mostly 0.7 - 1mm x 0.2mm with no preferred orientation, and 35% larger (0.5-1.5mm) corroded grains of pale yellow-brown mildly pleochroic mica (α = pale yellow; γ = mid yellow-brown; $\beta = \gamma$ or slightly greener). Apatite needles up to 1mm x 0.1mm occur as inclusions in mica and pyroxene.

Yellow-brown to dark brown non-pleochroic amphibole (10-12%) occurs in patches poikilitically enclosing pyroxene, apatite, rutile and titanomagnetite. The amphibole is a subsilicic ferro-kaersutite by the classification of Leake (1978). Rutile (0.05-0.2mm) is commonly bordered by titanomagnetite, but occurs as discrete inclusions in mica. Other interstitial phases are carbonate, pyroxene and rare altered alkali-feldspar.

Representative analyses of mica, pyroxene and

TABLE 3-14: Mineral analyses from phl-cpx-peridotite

Sample no.	369-01	369-10	369-14	369-20	369-21	369-23
mineral	OL	OL	OL	CPX	CPX	CPX
SiO2	40.07	39.08	39.06	51.05	50.87	49.64
Al2O3	0.04	0.02	0.05	1.73	1.88	3.23
TiO2	0.00	0.04	0.04	1.14	1.18	1.89
FeOt	12.92	14.69	13.95	5.01	4.16	5.50
MgO	45.91	43.66	45.08	15.05	15.67	14.21
MnO	0.51	0.34	0.28	0.09	0.07	0.08
CaO	0.29	1.12	1.42	24.37	24.34	23.52
Na2O	0.00	0.04	0.01	0.37	0.37	0.60
K2O	0.02	0.01	0.00	0.03	0.03	0.02
Total	99.80	99.02	99.93	98.85	98.57	98.72
Fo	83.73	81.13	82.39			
Jadeite				2.27	2.75	4.37
Acmite				0.00	0.00	0.00
CaTiTsch.				3.14	3.23	5.22
CaTsch.				-1.58	-1.14	-0.84
Wollas.				46.70	46.17	43.83
Enstat.				41.14	42.54	38.86
Ferros.				7.83	6.44	8.56

Sample no.	369-80	369-81	369-84	369-02	369-03	369-04
mineral	MI	MI	MI	TM	TM	TM
SiO2	39.74	39.62	38.03	--	--	--
Al2O3	14.62	15.53	15.14	1.81	1.73	2.03
TiO2	1.80	2.13	3.22	10.79	10.61	10.35
FeOt	7.51	7.11	7.29	78.05	77.35	77.02
MgO	22.07	22.64	21.68	4.13	4.29	4.61
MnO	0.15	0.07	0.07	1.06	0.99	1.09
CaO	0.07	0.08	0.08	--	--	--
Na2O	1.35	1.81	1.09	--	--	--
K2O	7.51	7.01	7.81	--	--	--
Total	94.82	96.00	94.52	95.84	94.98	95.13

Structural formula on the basis of x oxygens;

x	22	22	22	4	4	4
Si	5.695	5.589	5.495	--	--	--
Al	2.470	2.582	2.578	0.093	0.090	0.105
Fe	0.900	0.839	0.881	2.845	2.845	2.820
Ti	0.194	0.226	0.350	0.354	0.351	0.341
Mn	0.018	0.008	0.009	0.039	0.037	0.040
Mg	4.715	4.761	4.669	0.268	0.281	0.301
K	1.373	1.262	1.440	--	--	--
Na	0.375	0.495	0.366	--	--	--
Ca	0.011	0.012	0.003	--	--	--

Figure 3-19: Mica-pyroxene rock: mica (yellow) and pyroxene (elongate, white) with minor apatite, rutile and titanomagnetite. This picture illustrates a kaersutite-rich part of the rock.

Magnification x 35

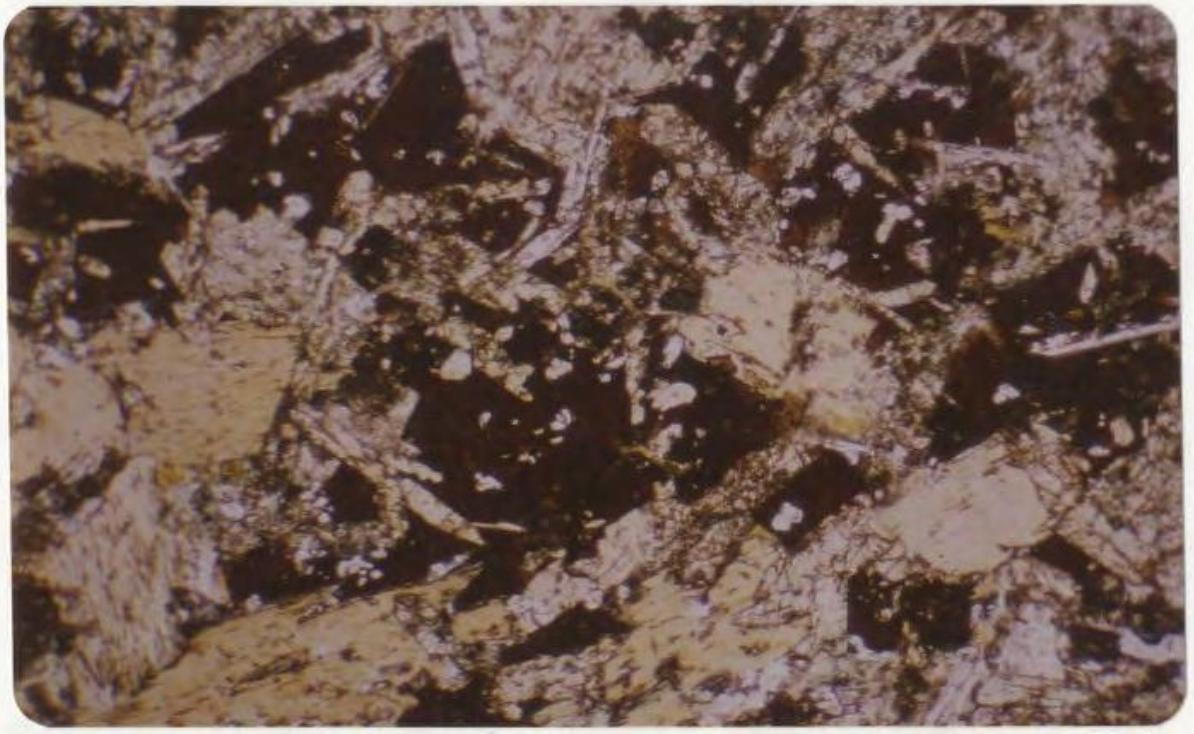

titanomagnetite are given in table 3-15. Micas are compositionally zoned toward lower Mg/(Mg+Fe) at grain margins. The cores are similar in composition to groundmass micas of the kimberlites, but are more sodic. As in the peridotite, titanomagnetites are manganoan.

Pyroxenes are more silicic and Al-Ti poor, but Ca,Mg,Fe relationships are not significantly different from those in the lamprophyres.

Pyroxene-biotite dominated rocks are also found in association with the Elchuru nepheline-syenite complex in India (Madhavan and Leelanandam,1977,1978), but no compositional data are available. Mica occuring in pyroxenites in carbonatite complexes (Heinrich,1966,p.42-3) is often thought to be due to fenitisation (Gittins et al.,1975b).

The pyroxene-carbonate-glimmerite is a seriate textured rock with pale to dark brown normal pleochroic mica ranging in size from 1.5 x 1mm to less than 0.1mm. 25% of the rock consists of 0.5-1mm pseudomorphs of yellow- green chlorite, presumably after olivine, and smaller euhedral to subhedral pyroxene grains. Small grains of titanomagnetite are abundant, and form rims around chloritised pseudomorphs. Unaltered carbonate forms a coarsely crystalline base with no ocellar structures.

THE NATURE AND ORIGIN OF LEUCOCRATIC OCELLI

As noted earlier in the section on sannaites, leucocratic patches occur in many rocks. Smaller ones are spherical or subspherical, and are normally filled with carbonate and

TABLE 3-15: Mineral analyses from cpx-mica rock.

Sample no.	386-55	386-56	386-02	386-07	386-01	386-03
mineral	CPX	CPX	MI-c	MI-r	TM	TM
SiO2	50.28	52.17	38.48	36.99	--	--
Al2O3	2.82	1.33	15.68	13.98	2.77	1.47
TiO2	1.44	0.62	3.03	2.33	10.14	6.91
FeOt	5.64	4.94	7.35	14.38	75.65	84.04
MgO	14.44	14.89	21.27	17.10	3.84	1.45
MnO	0.12	0.20	0.04	0.20	0.87	1.11
CaO	25.21	25.36	0.02	0.11	--	--
Na2O	0.43	0.49	0.56	0.41	--	--
K2O	0.01	0.01	8.31	8.38	--	--
Total	100.38	99.99	94.75	93.90	93.26	95.02

End members/structural formula on the basis of x oxygens;

x				22	22	4	4
Jadeite	3.00	3.42	Si	5.533	5.583	--	--
Acmite	0.00	0.00	Al	2.658	2.487	0.145	0.080
CaTiTsch.	3.83	1.68	Fe	0.884	1.815	2.816	3.252
CaTsch.	1.10	-1.14	Ti	0.328	0.265	0.339	0.240
Wollas.	45.59	48.35	Mn	0.005	0.026	0.033	0.044
Enstat.	38.08	39.95	Mg	4.559	3.848	0.255	0.100
Ferros.	8.39	7.74	K	1.525	1.614	--	--
			Na	0.156	0.120	--	--
			Ca	0.003	0.018	--	--

analcite which is coarser grained than the surrounding matrix phases. Larger ones are ellipsoidal or have irregular shapes, but their edges are always rounded. Large globules are commonly zoned, with an analcite-carbonate core and a K-felspar, nepheline, or analicitic outer zone including small pyroxene, biotite and opaque crystals. Alteration to sericite and zeolites, of which stilbite and natrolite have been positively identified, is frequently advanced.

Leucocratic patches are less common in olivine-rich sannaites, with the maximum development being numerous small carbonate- analcite globules.

Figures 3-20 to 3-23 demonstrate the variation in morphology and mineralogy of these leucocratic patches.

Leucocratic globules have been described from a variety of rock types, including basalt (Upton and Wadsworth,1971), spilite (Smith,1967), picrite (Drever,1960), basanite (Mackenzie and White,1970) and tholeiitic dolerite (Nakamura and Coombs, 1973), but are most commonly found in lamprophyres (eg.Ferguson and Currie,1971; Cooper,1979; Philpotts,1972,1976; Phillips,1968; Strong and Harris,1974).

The origin of such globules has been variously attributed to amygdales, liquid immiscibility and segregation vesicles. Origin as amygdales can be discounted for the zoned globules, since the outer zones contain mafic minerals nucleated within the globule, showing that they were crystallised from magmatic liquids. Inward growth from nuclei at the globule-groundmass boundary (drusy growth) would be expected in the case of a

vesicle (Phillips,1973). The inner zones probably originated as vesicles.

Fig.3-20 shows a globule which is interpreted to be due to silicate liquid immiscibilty. Acicular pyroxene crystals within the globule are bent to complement the embayed shape of the globule. This suggests that the pyroxenes existed in a melt before deformation of the globule, which in turn predated crystallisation of the groundmass pyroxenes outside the globule.

The globule is more felsic than the surrounding rock, containing abundant nepheline, analcite, plus minor alkali-felspar. This shows Na-enrichment reminiscent of that described by Strong and Harris(1974) from lamprophyres in which vesicles cleary postdate the globules.

The subspherical analcitic area at one end of the globule could be filling a bubble formed at a late stage due to contraction on crystallisation of the bulk of the globule's minerals. The near absence of apatite is noteworthy, since P and rare-earth elements (REE) should be strongly fractionated into the basic fraction when immiscible silicate liquids divide (Watson,1976).

Zoned ocelli are best explained by separation of a gas from the magma when much of the pyroxene and some of the biotite in the groundmass had already crystallised.

The subspherical shape of many of the inner zones of ocelli supports the idea of formation by a gas bubble. The frequently occurring tangential arrangement of pyroxene or biotite around a globule (eg.fig.3-21), is most likely to be caused by formation

Figure 3-20: Globule representing an immiscible liquid: acicular clinopyroxene (moderate relief) is bent to complement the edge of the deformed globule. Groundmass nepheline (light grey with cleavage) is not deformed. The clinopyroxene existed alone in a liquid and was deformed with the globule. Edge of globule is seen at the top of the picture only.

Magnification x 35

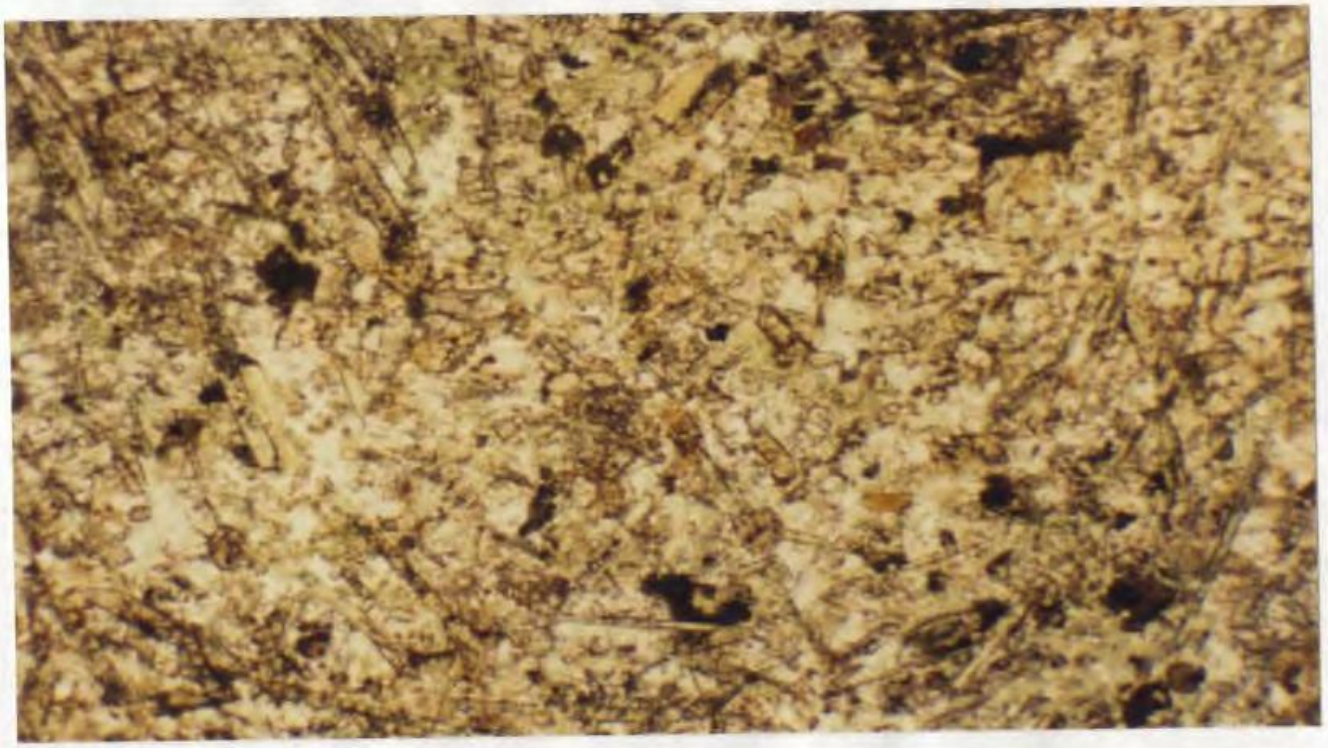

Figure 3-21: Zoned ocellus: carbonate-rich inner zone and nepheline-rich outer zone. Note tangential arrangement of pyroxene and mica- now mostly overgrown.

Magnification x 35

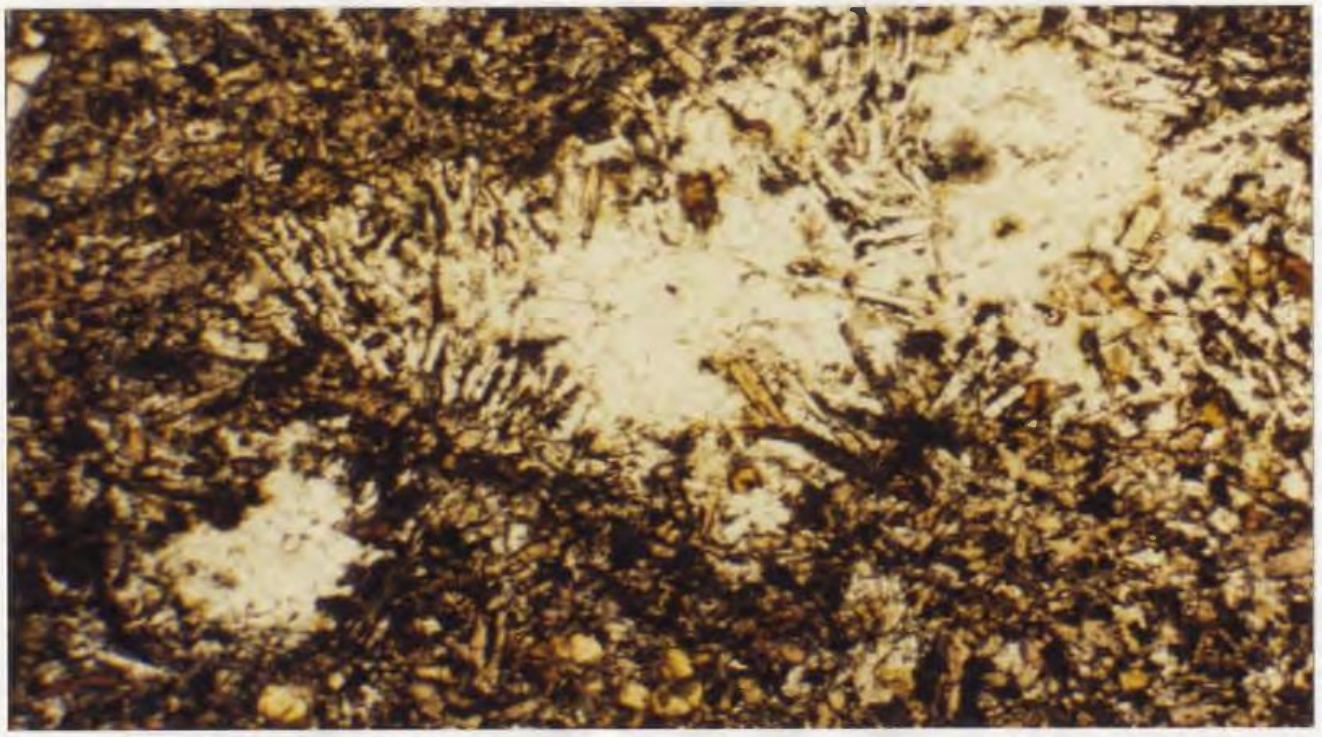

and expansion of gas bubbles in the partially crystallised magma. Late stage expansion of gas bubbles formed much earlier cannot be discounted.

Irregular shapes in large globules could be due to coalescence of gas bubbles in a semi-crystalline groundmass and may give the appearance of a single irregular ocellus. Small sub-spherical carbonate- analcite-globules are frequently connected by irregular feldspar- or nepheline-rich leucocratic veins containing mica and pyroxene. The veins originate as cracks in the crystalline mesh of pyroxene, which were later filled by residual fluids. The cracks could have been caused by expansion of gas bubbles now represented by the carbonate-analcite globules. Rafts of mica which originally defined individual ocelli are frequently found across the width of large leucocratic patches, attesting to their formation by coalescence.

The structure in fig.3-22 is clearly due to coalescence of two globules, now with differing mineralogies. The gases, now represented by the analcite- carbonate globule, have joined to form a single gas bubble with the liquid now filling one of the former vesicles.

The occurence of analcitic subspherical globules at the same end of adjacent ocelli (fig.3-23), further supports the idea that they represent a gas phase with a liquid lining. Similar structures are described by Upton and Wadsworth (1971), in which the liquid was chilled to a glass.

The liquids crystallising as the outer zones of ocelli are

Figure 3-22: 'Double globule' interpreted to be caused by coalescence of two globules. The gas phases combined into one globule, now represented by the carbonate-analcite inner zone (right). The cavity left was filled with typical outer zone material derived from late stage groundmass fluids, but the original shape of two globules was maintained due to a mostly crystalline groundmass (top and bottom centre).
Magnification x 35

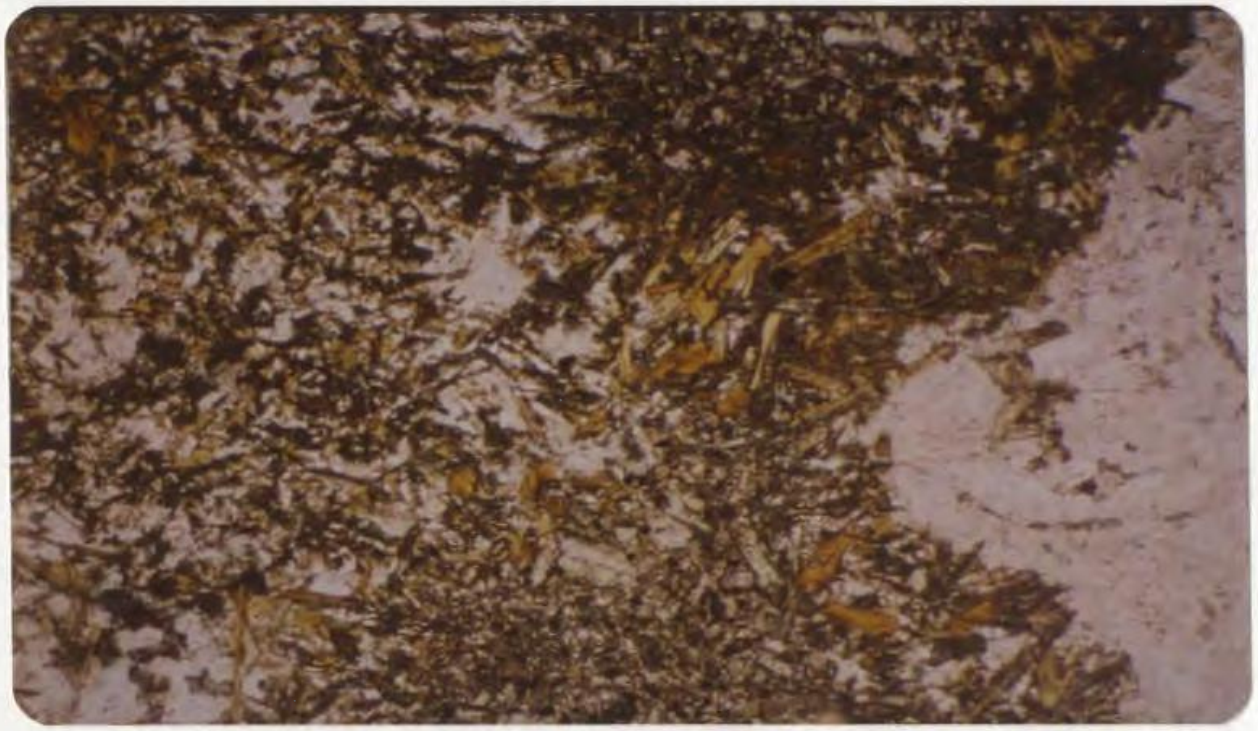

Figure 3-23: Zoned ocellus in sannaite. The inner zone is carbonate-analcite with a relatively sharp boundary between it and the outer zone. The outer zone is K-feldspar-nepheline-analcite with minor carbonate, mica, pyroxene and zeolites. Note that the other globule (top left corner) has its inner zone at the same end, probably indicating that the inner zones represent a gas.

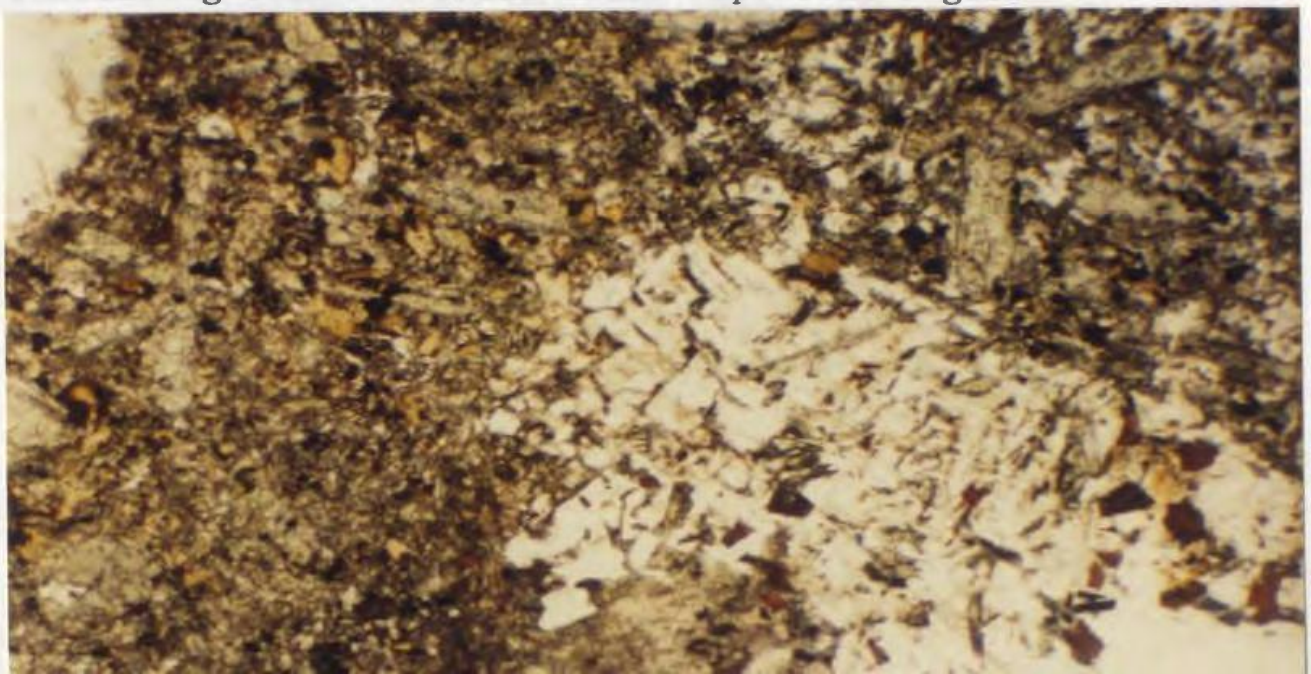

clearly fractionated and volatile enriched. Micas are frequently strongly iron enriched (table 3-16) and thin aegeritic rims occur on pyroxenes. Both these trends occur in the groundmass, as described earlier, but may be more marked in the ocelli, which is explained by the greater concentration of late stage fluids. Orthoclase, nepheline and analcite show no discernible difference between ocelli and groundmass.

The alternative view that the zoned ocelli represent volatile-rich immiscible liquids, from which a gas later separated to form the inner zones, fails to explain the following points: (i) Linings occur within globules with tangentially arranged minerals, (ii) Fractionation trends in ocelli linings are similar to groundmass trends. Distinct fractionation trends would be expected in the case of immiscible liquids (Roedder,1979). Nepheline occurs in ocelli only when it is also present in the groundmass.

The major problem with explaining segregation vesicles is the mechanism by which liquid is drawn into the vesicles. Any mechanism proposed should account for the variable ratio of core to lining, which can only partly be explained by differing levels of section through the ocelli. Smith (1967) considered escape of gas, re-solution of gas into the surrounding melt, cooling at constant pressure and an increase in external pressure, of which the latter two can not explain differing core to lining ratios.

Re-solution of gas into surrounding melt raises problems of melt availability at late stages of crystallisation, although

TABLE 3-16: Comparison of minerals in groundmass and ocelli

Sample no.	325-15	325-16	325-17	325-10	325-11	325-12
type	GD	GD	GD	nr OC	in OC	in OC
SiO2	34.41	33.27	34.68	34.57	33.75	33.54
Al2O3	16.12	16.57	16.58	16.42	15.63	16.11
TiO2	5.00	5.82	4.29	6.08	4.74	5.31
FeOt	12.77	13.18	13.15	15.39	21.27	18.81
MgO	14.98	14.45	15.43	13.21	9.46	10.96
MnO	0.14	0.15	0.12	0.19	0.29	0.25
CaO	0.01	0.14	0.02	0.06	0.05	0.05
Na2O	0.54	0.58	0.57	0.59	0.50	0.47
K2O	8.01	8.04	7.82	7.75	8.26	8.07
Total	91.97	92.19	92.65	94.25	93.96	93.56
Structural formula on the basis of 22 oxygens;						
Si	5.271	5.114	5.269	5.223	5.296	5.215
Al	2.911	3.002	2.970	2.924	2.891	2.953
Fe	1.636	1.694	1.671	1.945	2.791	2.446
Mn	0.018	0.020	0.015	0.024	0.039	0.033
Mg	3.421	3.311	3.495	2.975	2.213	2.540
K	1.565	1.577	1.516	1.494	1.654	1.601
Na	0.160	0.173	0.168	0.173	0.152	0.142
Ca	0.002	0.023	0.003	0.010	0.008	0.008

Sample no.	325-81	325-82	325-85	325-84
type	GD	GD	OC	OC
SiO2	44.35	45.13	43.39	38.81
Al2O3	7.93	6.65	9.99	12.38
TiO2	2.86	2.77	3.23	5.30
FeOt	7.13	7.62	6.89	8.20
MgO	13.38	12.53	11.08	9.80
MnO	0.13	0.11	0.08	0.11
CaO	23.10	23.39	22.25	22.68
Na2O	0.77	0.34	0.61	0.43
K2O	0.01	0.00	0.01	0.03
Total	97.83	98.55	97.88	97.74
End Members (by the method of Cawthorn and Collerson, 1974);				
Jadeite	4.92	2.26	4.15	2.89
Acmite	0.00	0.00	0.00	0.00
CaTiTsch.	7.02	7.17	8.15	13.24
CaTsch.	11.55	10.36	19.06	19.10
Wollas.	34.02	36.94	31.15	28.96
Enstat.	32.57	32.13	27.71	24.26
Ferros.	9.92	11.13	9.78	11.54

inhomgeneity in residual melt distribution could help to explain the differing thickness of ocelli linings. Escape of gas may be assisted by deformation during flow, but similar ocelli occur in rocks exhibiting no flow textures. Gas bubbles may well retain their subspherical shapes in a mushy groundmass when deformed (Philpotts,1977).

Perhaps contraction of the bulk of the groundmass on crystallisation may help to explain segregation. Minerals within the outer zones of ocelli are commonly boundary nucleated, which requires that they grew from a rigid margin.

In summary, carbonate-analcite dominated globules are formed by separation of a gas to form vesicles into which residual groundmass liquids were drawn. Tangential arrangement of minerals around the globules suggests expansion at a late stage when groundmass minerals were crystallising. Whether they were initiated at this stage or merely expanded by retrograde boiling is uncertain.

CHAPTER 4 : WHOLE-ROCK GEOCHEMISTRY

Members of the Aillik Bay dyke suite were analysed for major elements, trace elements and rare-earth elements (REE) in order to define the affinities and origin of the suite. Major and trace element results are presented in tables 4-1 to 4-4.

Major elements were analysed by atomic absorption spectroscopy, and trace and rare-earth elements by X-ray fluorescence. Details of analytical procedures are given in Appendix I. Low totals may be due to abundant minor elements, including halogens which were not analysed for.

Ferrous and ferric iron, CO2 and H2O were not analysed separately. Total iron as Fe2O3 is expressed as Fe2O3* in the following discussion. Despite some problems due to a different classification, the data of Hawkins (1977) can be used to suggest probable values (table 4-5). Sannaites and olivine sannaites are assumed to be equivalent to Hawkins' monchiquites. The increase in CO2/H2O from sannaites, through kimberlites to carbonatites corresponds to CaO, reflecting increasing modal carbonate.

MAJOR ELEMENTS

Major elements are represented graphically in figure 4-1. The salient features of major element chemistry of the suite as a whole are as follows:

(i) Extremely low SiO2, mostly less than 35 wt%. Silica abundance decreases from sannaites, through kimberlites to carbonatites.

Table 4-1 : Representative analyses of Sannaites from Allik Bay

+ Anal.#	313	325	329	332	333	355	356
SiO2	35.40	35.80	29.10	30.20	30.40	33.00	37.80
TiO2	6.36	2.40	5.50	4.86	4.89	4.80	5.75
Al2O3	7.40	11.80	5.70	7.40	7.33	6.21	8.78
Fe2O3*	14.60	11.47	15.50	14.13	14.35	14.80	15.28
MgO	7.13	8.93	9.78	5.95	5.93	11.15	8.35
MnO	0.23	0.20	0.21	0.30	0.29	0.19	0.18
CaO	13.50	12.53	18.33	17.00	16.60	10.83	12.13
Na2O	1.89	4.06	0.67	3.24	3.47	2.49	2.28
K2O	3.23	1.62	2.52	2.24	1.42	2.27	2.87
P2O5	2.45	1.00	2.50	2.16	2.08	0.95	0.95
LOI	4.98	9.20	7.78	9.79	10.69	11.38	4.31
Total	97.17	99.01	98.59	99.27	97.45	98.07	98.68
Ni	54	94	80	0	0	286	139
Cr	0	104	91	0	0	346	212
V	248	179	231	326	295	297	290
Rb	102	74	96	55	34	129	108
Sr	776	1812	1895	1784	2187	896	1131
Ba	880	1460	1175	1470	1087	961	1122
Zn	146	87	114	159	152	113	112
Zr	607	408	795	1200	723	335	482
Cu	123	10	143	19	5	66	64
Ga	20	15	15	18	23	16	23
U	3	3	4	16	0	0	0
Th	44	24	3	34	29	3	11
Nb	200	164	190	389	405	98	113
La	232	105	195	300	356	129	125
Ce	463	247	318	544	856	249	211
Y	99	49	68	109	104	41	44

+ Anal. # refers to rock specimen number, and corresponds to the first part (before the hyphen) of mineral analysis numbers given in preceding tables.

Table 4-1 (continued)

Anal.#	446	447	357	320	378	364	445
SiO2	35.80	34.40	33.50	32.50	32.60	33.00	37.50
TiO2	1.85	2.07	2.17	4.25	3.92	6.04	2.23
Al2O3	12.60	11.50	10.50	6.86	5.87	6.81	12.30
Fe2O3*	11.20	11.74	10.98	14.24	14.45	16.90	11.80
MgO	7.98	8.11	10.70	9.90	12.78	7.73	9.25
MnO	0.24	0.23	0.18	0.23	0.21	0.23	0.22
CaO	13.70	14.23	15.00	14.43	14.05	15.95	13.03
Na2O	4.13	3.36	2.82	2.30	0.97	2.21	4.03
K2O	1.33	1.24	1.91	2.06	2.53	2.26	1.67
P2O5	1.48	1.75	1.21	1.55	1.85	2.55	1.30
LOI	8.50	10.26	10.44	9.69	9.15	4.76	6.45
Total	98.81	98.89	99.41	98.01	98.38	98.44	99.78
Ni	72	66	122	188	382	67	123
Cr	70	56	181	210	353	0	129
V	157	161	213	305	225	333	191
Rb	46	53	51	70	236	88	53
Sr	2735	2191	1417	1755	1428	1391	1937
Ba	1774	1667	1134	1181	794	1052	1629
Zn	106	103	90	135	124	126	98
Zr	434	436	440	666	732	607	396
Cu	6	8	22	74	48	103	20
Ga	14	14	11	20	9	19	15
U	2	1	0	0	12	0	0
Th	7	44	5	11	35	17	11
Nb	208	200	140	181	115	166	190
La	201	220	133	170	201	189	179
Ce	283	309	183	258	348	347	257
Y	42	50	34	64	153	68	40

Table 4-1 (continued)

Anal.#	358	408	376	368	409
SiO2	33.90	33.20	30.20	34.40	33.20
TiO2	6.25	4.00	5.80	6.67	5.48
Al2O3	6.47	6.67	6.67	9.27	8.17
Fe2O3*	15.90	14.40	14.30	13.57	14.82
MgO	9.70	8.80	6.80	5.20	7.05
MnO	0.22	0.22	0.25	0.30	0.26
CaO	17.85	16.58	16.88	14.70	17.98
Na2O	1.71	1.89	2.45	4.64	2.53
K2O	2.20	1.74	1.16	1.19	2.79
P2O5	2.25	2.00	2.63	1.90	0.00
LOI	2.41	9.01	10.96	9.22	4.91
Total	99.13	98.51	98.10	98.78	97.49
Ni	119	141	13	--	21
Cr	54	218	0	0	0
V	289	295	305	279	381
Rb	101	49	60	54	104
Sr	2750	1761	1179	1791	2508
Ba	1148	886	2155	1125	1527
Zn	130	119	132	173	149
Zr	615	460	550	907	821
Cu	110	44	106	19	116
Ga	20	18	12	28	17
U	0	5	0	6	2
Th	7	4	58	22	0
Nb	193	145	228	372	247
La	195	196	259	327	168
Ce	334	329	442	528	258
Y	61	67	146	104	72

Table 4-2: Representative analyses of olivine sannaites from Aillik Bay

Anal.#	393	396	397	337o	337n	375	306
SiO2	25.80	28.80	32.10	28.30	29.60	31.10	34.80
TiO2	3.47	5.03	3.81	3.54	3.73	3.80	5.56
Al2O3	3.59	3.83	4.77	3.73	3.57	5.00	6.20
Fe2O3*	12.65	15.84	13.65	13.03	13.81	14.19	17.02
MgO	17.48	17.70	18.14	17.41	19.32	16.16	11.35
MnO	0.22	0.21	0.20	0.20	0.20	0.18	0.23
CaO	15.33	13.00	13.94	12.13	11.55	9.10	15.90
Na2O	0.25	0.80	0.35	0.68	0.63	1.84	2.22
K2O	1.98	1.54	1.60	1.41	1.63	2.27	1.95
P2O5	1.70	2.65	1.70	1.25	1.35	0.75	1.93
LOI	16.12	8.69	8.17	17.33	13.10	14.96	1.43
Total	98.59	98.09	98.43	99.01	98.49	99.35	98.59
Ni	547	583	616	578	758	582	278
Cr	527	393	736	604	695	648	191
V	228	192	227	215	210	255	323
Rb	68	56	72	76	62	134	95
Sr	1781	1565	1074	1581	1163	592	1725
Ba	1671	781	697	1171	863	658	1042
Zn	91	135	90	79	106	87	149
Zr	521	453	462	466	442	475	707
Cu	47	7	47	43	36	35	69
Ga	7	9	10	8	7	11	21
U	6	0	7	3	0	3	3
Th	14	23	14	4	7	21	6
Nb	169	142	110	98	109	67	147
La	265	235	172	187	181	115	114
Ce	380	430	419	302	328	177	277
Y	69	110	43	37	37	42	60

Table 4-3: Representative analyses of kimberlites from Aillik Bay

Anal.#	399	405	406	310	385	373	398
SiO2	22.30	24.00	18.70	24.30	24.00	26.50	20.20
TiO2	2.99	3.49	2.10	3.47	2.81	2.86	3.55
Al2O3	2.85	2.63	1.85	2.86	3.34	6.00	4.00
Fe2O3*	11.31	14.70	11.42	11.35	12.00	12.00	11.80
MgO	17.23	20.25	17.13	18.11	14.93	13.18	11.50
MnO	0.22	0.31	0.27	0.27	0.31	0.23	0.24
CaO	17.65	17.25	20.88	13.40	18.00	17.80	19.70
Na2O	0.41	0.12	0.28	0.39	0.61	1.22	0.85
K2O	2.05	1.48	1.74	2.28	2.38	2.89	2.05
P2O5	1.78	2.35	2.55	1.37	2.48	2.25	2.73
LOI	18.75	11.86	21.74	19.96	16.38	14.96	21.11
Total	97.54	98.79	98.47	97.76	97.54	98.77	97.71
Ni	449	516	452	582	373	161	238
Cr	529	628	448	561	480	331	251
V	209	168	161	159	201	177	188
Rb	59	46	64	125	68	85	56
Sr	2031	3640	3740	2208	1169	3905	1846
Ba	919	1435	1131	3723	1185	3104	902
Zn	103	116	92	94	105	88	131
Zr	495	321	360	511	672	688	420
Cu	8	16	0	7	51	19	18
Ga	6	6	3	7	9	9	8
U	7	14	23	3	21	15	25
Th	39	7	0	10	18	0	71
Nb	323	232	250	240	271	249	242
La	217	450	380	1801	234	609	244
Ce	518	722	554	3875	371	837	424
Y	256	68	53	38	68	46	191

Table 4-4: Representative analyses of Aillik Bay carbonatites

Anal.#	349	351	407	416	417
SiO2	18.50	20.80	20.00	10.90	5.95
TiO2	1.82	2.08	3.75	1.02	0.73
Al2O3	2.28	2.81	2.72	0.99	0.99
Fe2O3*	9.60	10.96	10.44	6.61	5.48
MgO	16.93	19.32	13.97	10.55	7.30
MnO	0.22	0.22	0.29	0.25	0.24
CaO	15.33	15.53	20.95	29.55	35.60
Na2O	0.80	0.45	0.82	0.89	0.29
K2O	2.38	2.58	1.79	1.13	0.84
P2O5	1.58	1.94	2.55	3.08	3.50
LOI	26.34	21.42	21.12	31.50	35.27
Total	95.78	98.11	98.40	96.47	97.33
Ni	459	552	296	0	124
Cr	435	628	365	355	190
V	155	138	241	139	177
Rb	178	146	54	51	5
Sr	3228	2468	2645	8260	5448
Ba	3173	2728	1928	982	363
Zn	83	85	96	73	85
Zr	651	633	743	1022	91
Cu	8	10	51	1	7
Ga	0	3	2	0	2
U	2	8	22	34	56
Th	21	11	26	0	82
Nb	214	201	252	273	183
La	364	491	290	421	413
Ce	435	976	625	541	523
Y	45	35	191	160	336

Table 4-5: Values of Fe2O3, FeO, Fe2O3/FeO, CO2, H2O, H2O/CO2 in Aillik Bay dykes (taken from Hawkins, 1977)

	Monchiquite	Kimberlite	Carbonatite
Fe2O3 range	3.53 - 7.57	2.22 - 13.42	0.03 - 5.54
FeO range	6.15 -11.49	4.52 - 9.54	1.13 - 9.85
Fe2O3/FeO range	0.31 - 1.06	0.23 - 2.06	0.006 - 1.58
avge. Fe2O3/FeO	0.56	0.74	0.38
CO2 range	3.15 - 13.02	7.71 - 27.11	18.36 - 39.14
H2O range	1.45 - 3.67	0.66 - 5.07	1.03 - 3.46
CO2/H2O range	1.35 - 8.98	2.32 - 34.70	5.31 - 31.91
avge. CO2/H2O	2.31	6.73	16.61

Figure 4-1: Oxide vs. MgO plots for major elements in sannaites (□), olivine sannaites (■), kimberlites (▽) and carbonatites (○) from Aillik Bay

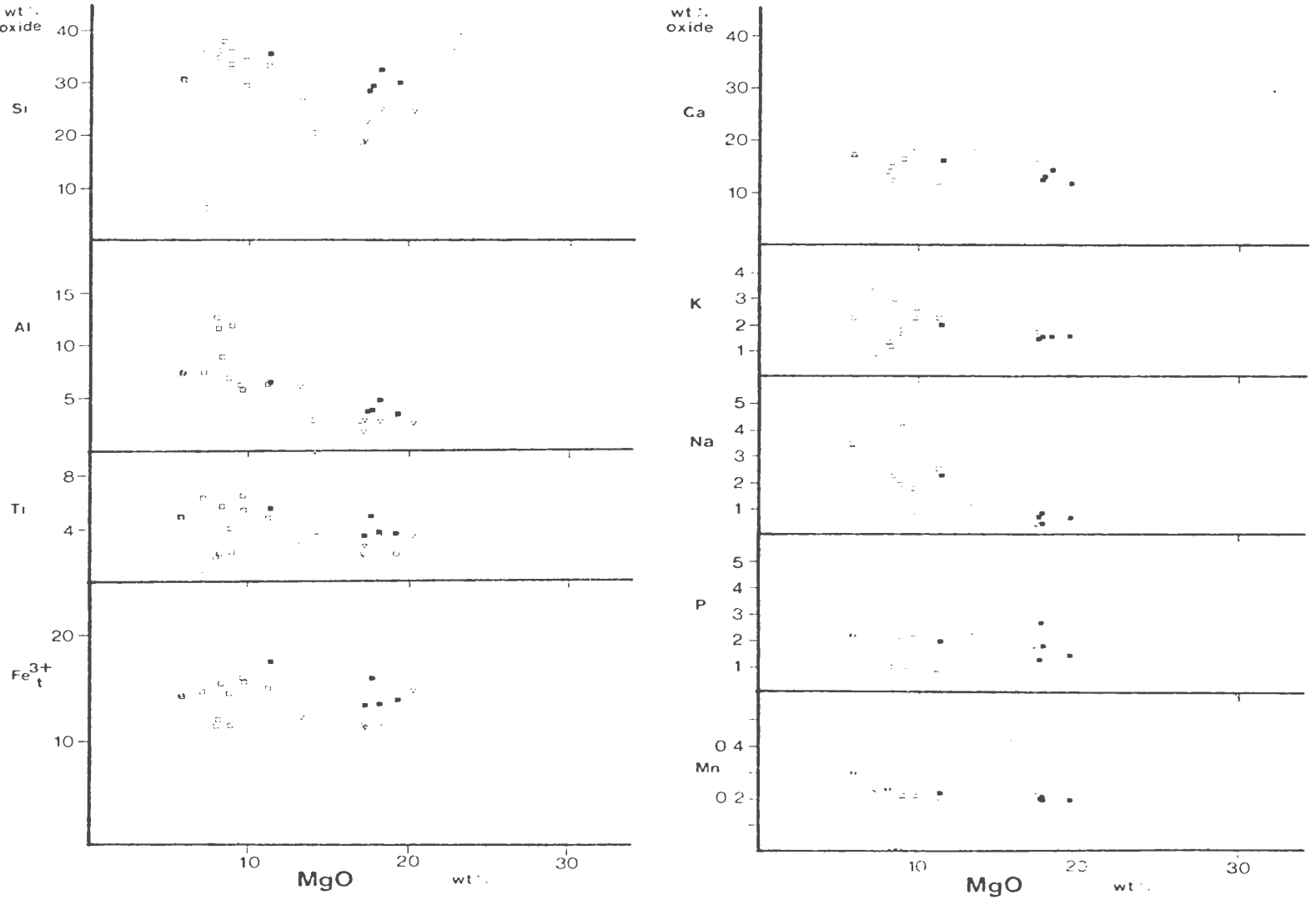

(ii) Enrichment in TiO_2, Al_2O_3, Na_2O, K_2O, P_2O_5 and CaO relative to average ultramafic rock (Wedepohl,1975).

(iii) Low MgO/Fe_2O_3* relative to average ultramafic rock.

(iv) Extreme volatile enrichment.

Silica contents of less than 40 wt% are common only in highly alkaline rocks or carbonate-rich rocks. Agpaitic ratios (Na_2O+K_2O/Al_2O_3) are 0.56 for average sannaite, 0.58 for average olivine sannaite, 0.74 for average kimberlite, and 1.22 for average carbonatite. All rock types are part of the nephelinite-carbonatite series of Currie (1975a).

SANNAITES

Aillik Bay sannaites and olivine sannaites are compared to other alkaline lamprophyres in table 4-6. Lamprophyres associated with nepheline syenites (anal.3-11) typically have SiO_2 contents below 40 wt%, but the 30-33 wt% of Aillik Bay lamprophyres is unusually low. The Aillik Bay rocks also differ in their lower Al_2O_3 and higher P_2O_5 and CO_2+H_2O, emphasizing the association with carbonatites. Analogous rocks occur at Oka, Quebec (anal.3) and Callander Bay, Ontario (anal.4,5), where rocks become carbonate-rich (Ferguson and Currie,1971). The New Zealand example (anal.7) is at the southern extremity of an extensive dyke swarm which contains carbonate-rich dykes in the north (Cooper,1979).

KIMBERLITES

The Aillik Bay kimberlites are chemically similar to

Table 4-6: Comparison of Aillik Bay sannaites with lamprophyres from nepheline syenite and carbonatite complexes.

Anal.#	1	2	3	4	5	6	7
SiO2	33.55	30.72	30.37	37.56	18.60	38.76	39.46
TiO2	4.45	4.33	2.39	3.75	1.03	3.79	3.89
Al2O3	8.35	4.42	9.20	10.40	4.10	15.42	13.43
Fe2O3	13.94*	14.67*	5.55	4.86	1.15	4.13	5.92
FeO	---	---	6.02	7.24	4.90	5.28	8.30
MgO	8.35	16.78	10.70	9.56	8.96	6.59	6.28
MnO	0.23	0.21	0.35	0.20	0.89	0.20	0.25
CaO	14.84	13.30	15.31	12.42	25.00	15.30	10.06
Na2O	2.65	0.94	1.54	1.64	0.47	4.90	3.97
K2O	2.06	1.63	3.79	3.64	3.49	2.25	2.13
P2O5	1.78	1.78	0.87	0.96	1.82	0.77	1.27
LOI	8.03	9.74	---	---	---	---	---
CO2	---	---	9.88	4.70	29.60	1.22	1.70
H2O	---	---	2.32	3.32	0.35	1.42	3.79
Total	98.23	98.52	98.31	100.25	100.36	99.86	100.45

Anal.#	8	9	10	11
SiO2	40.80	37.31	38.83	39.43
TiO2	2.94	2.96	0.60	2.73
Al2O3	11.76	11.87	10.83	10.76
Fe2O3	5.83	6.70	8.93	7.55
FeO	8.06	4.36	7.84	4.70
MgO	8.00	10.60	18.78	4.30
MnO	0.21	0.18	0.22	0.38
CaO	13.69	13.52	11.67	15.38
Na2O	3.69	3.22	0.96	7.60
K2O	1.38	3.42	0.97	4.00
P2O5	0.44	0.84	0.52	0.96
LOI	3.18	---		---
CO2	---	0.88	---	0.00
H2O	---	0.08	---	1.80
Total	99.98			99.59

EXPLANATION

1 Average sannaite - Aillik Bay
2 Average olivine sannaite - Aillik Bay
3 Lamprophyre ass. nepheline syenite (Gold,1970)
4,5 Lamprophyre ass. nepheline syenite (Ferguson and Currie,1971)
6 Lamprophyre, Ice River, B.C. (Currie,1975b)
7 Lamprophyre, Haast River, New Zealand (Cooper,1979)
8 Kotuite, Siberia (Egorov,1970)
9 Lamprophyre ass. melanephelinite, Siberia (Butakova and Egorov,1962)
10 Lamprophyre ass. ankaratrite, Siberia (Butakova and Egorov,1962)
11 Alnoitic lamprophyre ass. carbonatite, Kisingiri. (LeBas,1977,p.301)

'central complex kimberlites' (Dawson,1967,1968) which occur with carbonatites and ijolite series rocks, and not to cratonic, diamondiferous kimberlites. This is demonstrated in Table 4-7 where average Aillik Bay kimberlite is compared to examples of both kimberlite types. Cratonic kimberlite (anal.7-11) is typified by MgO > 22 wt%, stressing the importance of olivine to it's definition (Mitchell,1979; Skinner and Clement,1979). Lamprophyric kimberlites have MgO < 20 wt%, and generally have high contents of CaO, alkalies and P2O5. The least alkalic examples (Ile Bizard, anal.2, and Munjibbee, anal.6) do not occur within central complexes but are situated in areas with regional nephelinite-carbonatite magmatism.

The Nigerdlikasik and Saglek kimberlites (anal.12 and 13) appear to have cratonic affinities despite their association with the Labrador Sea rift.

CARBONATITES

Carbonatites frequently occur as the latest magmatic event in alkaline complexes. Carbonatite plugs are often more evolved than the Aillik Bay carbonatites, showing greater depletion in SiO2, TiO2, Al2O3, Na2O, K2O and MgO (table 4-8). Aillik Bay dykes are similar to carbonate-rich members of the Saguenay (anal.7) and Callander Bay (table 4-6, anal.5) dyke swarms. The high MgO values are partly due to vestigial silicate phases, and partly to the abundance of dolomitic carbonate. The Fen rauhaugite (dolomite carbonatite) is included for comparison. The more evolved carbonatite plugs have higher CaO, CO2 and MnO

Table 4-7: Aillik Bay kimberlites compared to diamondiferous and central complex kimberlites

Anal.#	1	2	3	4	5	6	7
SiO2	23.36	33.58	31.77	29.1	26.92	24.83	35.2
TiO2	3.02	2.27	1.98	3.7	4.71	2.33	2.32
Al2O3	3.40	6.93	7.99	4.1	4.47	2.13	4.4
Fe2O3	11.69*	13.20*	7.07	8.9	5.69	---	---
FeO	---	---	3.40	7.2	3.47	7.15*	9.8*
MgO	16.77	20.08	19.86	16.3	17.96	14.09	27.9
MnO	0.26	---	0.31	0.4	0.18	0.09	0.11
CaO	17.09	12.89	13.82	13.5	11.32	20.52	7.6
Na2O	0.50	0.18	1.62	1.6	0.11	0.09	0.32
K2O	2.02	0.77	2.28	1.3	2.92	0.59	0.98
P2O5	1.93	1.16	0.95	1.3	0.93	0.56	0.7
LOI	18.68	---	---	--	---	---	---
CO2	---	0.00	7.75	7.6	14.64	---	3.3
H2O	---	8.76	0.73	4.7	5.06	---	7.4
Total	98.72	99.82	99.63	99.7	98.38		100.03

Anal.#	8	9	10	11	12	13
SiO2	33.21	27.76	29.9	38.05	26.45	35.6
TiO2	1.97	1.90	4.0	1.32	1.88	3.06
Al2O3	4.45	3.18	4.0	4.14	2.02	3.46
Fe2O3	6.78	6.18	10.4	3.25	4.00	4.60
FeO	3.43	1.84	1.8	4.90	5.31	8.71
MgO	22.78	25.90	23.1	28.41	28.00	27.90
MnO	0.17	0.13	0.19	0.16	0.20	0.42
CaO	9.36	12.33	13.2	8.80	12.33	6.78
Na2O	0.19	0.11	0.07	0.31	0.23	0.82
K2O	0.79	0.41	1.8	1.07	1.60	2.00
P2O5	0.65	0.35	0.30	0.54	0.66	0.40
LOI	---	10.09$	9.9$	---	---	---
CO2	4.58	9.48	1.3	2.26	12.6	2.42
H2O	10.70	---	--	6.27	3.98	3.72
Total	99.06	99.64	99.96	99.48	99.67	99.67

EXPLANATION ($ = LOI - CO2)

1 Average kimberlite - Aillik Bay
2-6 Central complex type kimberlites:
2 Ile Bizard (Gold and Marchand, 1970)
3 Damkjernite, Fen (Griffin and Taylor, 1975)
4 Saguenay, Quebec (Gittins et al., 1975b)
5 Walloway, Australia (Ferguson and Sheraton, 1979)
6 Munjibbee, Australia (Colchester, 1972)
7-11 Diamondiferous ('true') kimberlites:
7 Average South African kimberlite (Dawson, 1967)
8 Average Lesotho kimberlite (Gurney and Ebrahim, 1973)
9 Daldyn, Siberia (Ilupin et al., 1974; average)
10 Colorado kimberlite (Smith, 1977)
11 Lattavaram, India (Paul et al., 1975)
12 Nigerdlikasik, Greenland (Emeleus and Andrews, 1975)
13 Saglek, Labrador (Collerson and Malpas, 1977)

Table 4-8 : Comparison of Aillik Bay carbonatites to carbonatites and carbonatised kimberlites/lamprophyres

Anal.#	1	2	3	4	5	6	7
SiO2	15.23	13.50	12.10	3.36	2.22	4.65	14.4
TiO2	1.88	1.30	0.80	0.30	0.15	0.59	2.5
Al2O3	1.96	3.67	3.55	1.69	2.01	1.42	2.3
Fe2O3	8.62*	2.68	3.12	6.13	1.99	17.10	8.0
FeO	---	4.65	3.78	2.99	6.23	1.90	5.4
MgO	13.61	10.07	5.64	3.10	9.40	0.50	12.9
MnO	0.24	0.50	0.61	0.31	0.90	0.68	0.4
CaO	23.39	26.59	35.12	44.35	30.24	40.06	26.6
Na2O	0.65	1.24	0.42	0.04	0.26	1.00	0.1
K2O	1.74	1.98	1.49	0.50	0.31	0.16	0.9
P2O5	2.53	2.96	2.06	3.26	1.00	1.60	4.8
LOI	27.13	---	---	---	---	---	--
CO2	---	27.98	28.73	32.80	35.96	28.43	17.2
H2O	---	1.87	1.39	0.30	0.26	0.16	2.9
Total	96.98	98.99	98.81	99.13	90.93+	99.00	98.9

EXPLANATION

1,Average carbonatite - Aillik Bay
2,Beforsite - Aillik Bay (Hawkins,1977)
3,Average carbonatite (Gold,1963)
4,Sovite, Fen (Barth and Ramberg,1966)
5,Rauhagite, Fen (Barth and Ramberg,1966) Low total due to high content of BaO and SO3
6,Aegerine-magnetite sovite, Malawi (Garson,1966)
7,Carbonate-rich kimberlite, Saguenay,Quebec (Gittins et al.,1975b)

contents manifested in carbonate and manganoan iron oxide development at the expense of most silicates.

In summary, the major element chemistry of the sannaites, kimberlites and carbonatites is characteristic of rocks associated with carbonatite-nephelinite series magmatism.

TRACE ELEMENTS

Trace element data for Aillik Bay dykes are given in tables 4-1 to 4-4, and are represented graphically in figure 4-2. Wedepohl and Muramatsu (1979) compiled average values for ultramafic rock, kimberlite, nephelinite, alkali olivine basalt and tholeiitic basalt. Most elements define either depletion (e.g.Ni,Cr,Rb,Zr, Nb,La,Ce,U,Th) or enrichment (e.g.Ga,V) trends from kimberlite to tholeiite in the order specified above.

In Aillik Bay dykes V,Rb,Sr,Ba,Zr,Nb,La,Ce and Y are enriched relative to average ultramafic rock (AUR), and either have values between those characteristic of kimberlite and nephelinite, or in excess of both. These elements generally lie in the upper part of the range for kimberlite given by Dawson (1980,p.57-58; after Muramatsu,1977). Ni and Cr are depleted relative to AUR and lie between kimberlite and nephelinite values except for olivine-poor sannaites, which are severely depleted in both Ni and Cr. Zn,Cu and Ga decrease in abundance from sannaite to carbonatite at Aillik Bay, but do not generally show much variation between the rock types studied by Wedepohl and Muramatsu (1979). U and Th are extremely enriched in kimberlites and carbonatites at Aillik Bay, but sannaites

Figure 4-2: Trace element vs. MgO plots for Aillik Bay dykes. Symbols as in figure 4-1.

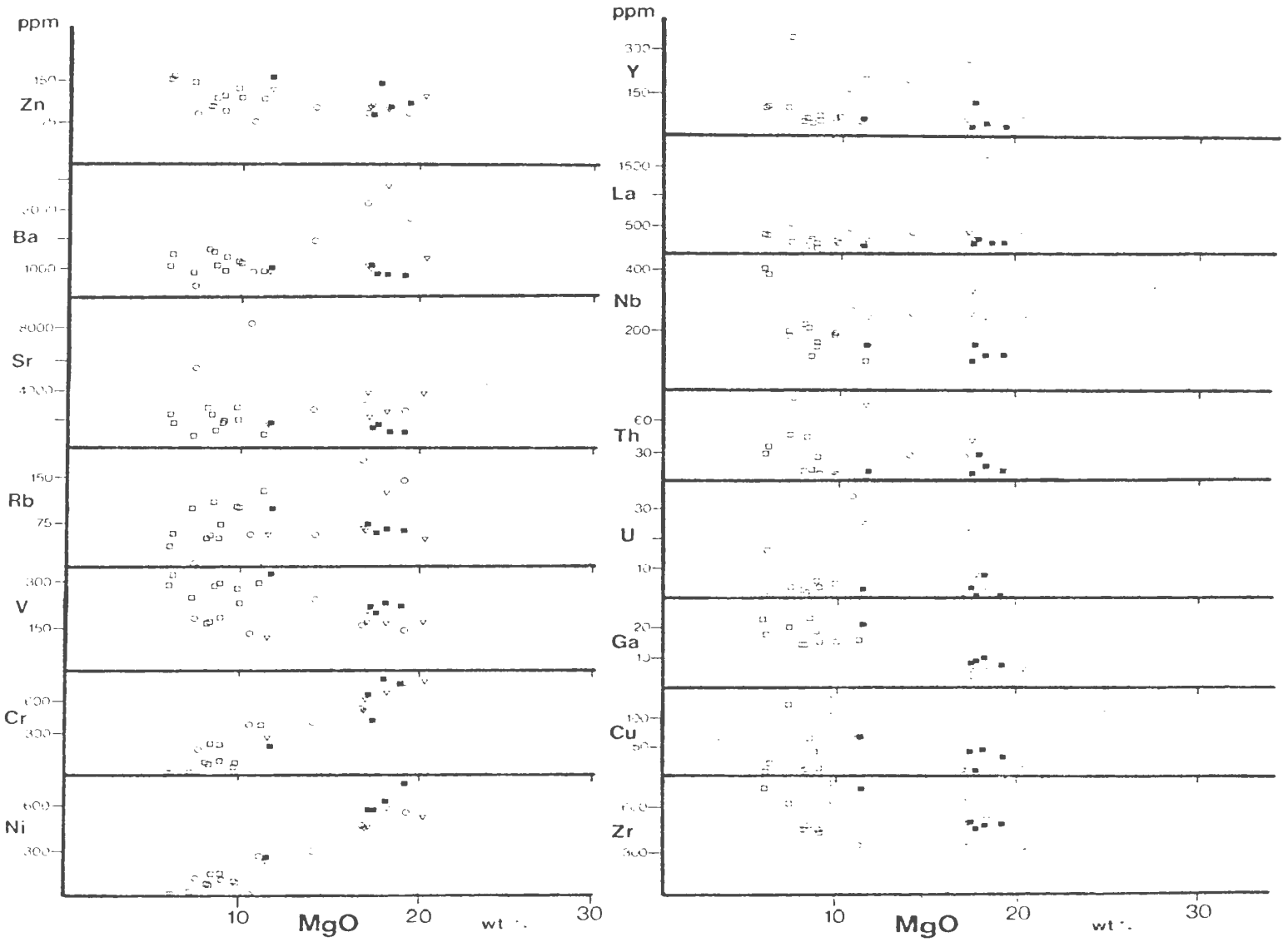

contain similar amounts to average kimberlite and nephelinite. Pb, As and Ag were not detected in any samples from Aillik Bay.

The abundances of trace elements in Aillik Bay dykes relative to kimberlite and nephelinite is explained by the influence of carbonatite. Although carbonatites were not studied by Wedepohl and Muramatsu (1979), they do note that Sr and Ba are more abundant in nephelinites than kimberlites despite showing a general decrease from kimberlite to tholeiite. Sr and Ba are the most characteristic marker trace elements for carbonatites, and the average trace element data reflect the association of nephelinites with carbonatites.

Within the Aillik Bay suite, Ni,Cr,Sr,Ba,U,Th,La,Ce,Y and to a small extent Nb are enriched in kimberlite relative to sannaite, whereas V,Zn,Cu,Ga,Zr and possibly Rb are depleted. Carbonatites show a definite reversal of Ni,Cr and Zr trends, whilst most other trends are maintained. Ni and Cr depletion is due to removal of silicate phases. Zr increase is characteristic of carbonatisation, but the Zr depletion in kimberlite can be considered anomalous. It is probably due to complex trace element movements in fluids associated with different episodes of carbonatisation. Samples 416 and 417 (table 4-4) represent different episodes within one dyke; initial increase in Zr is followed by severe depletion in a later carbonatite pulse. Depletions of Rb,Sr,Ba and Nb also occur, contrasting with the expected trends toward a more carbonate-rich rock. Y,U,Th, La and Ce are not lost, however, so complex relationships with carbonatite must exist.

Mica and titanomagnetite removal at a late stage can explain some of these observations. Apatite and perovskite fractionation cannot cause the observed trends, since these minerals would fail to discriminate between Nb, Zr and La,Y,Ce. Sr preferentially enters carbonates, and so its depletion in the most carbonate-rich rock appears anomalous, and must be due to reduced availability of Sr rather than removal of calcite. Pouliot (1970) described similar late Sr depletion in Oka carbonatites. Trace element studies of dolomitic carbonatites are lacking, and so the importance of carbonate type to trace element geochemistry cannot be assesed.

Apparent enrichment of La and Ce in kimberlites relative to carbonatites is misleading due to anomalously high REE content in one kimberlite sample.

RARE-EARTH ELEMENTS

Rare earth elements (REE) were analysed for several selected samples, and results are illustrated in figure 4-3 as a chondrite-normalised plot. High REE abundances and strong light REE (LREE) enrichment is seen in all cases, and is most pronounced in kimberlites and carbonatites. La and Ce values were obtained for all samples (tables 4-1 to 4-4), showing that the samples picked for complete REE analysis are representative in most cases. An exception is the REE-rich kimberlite sample, which shows depletion in HREE relative to other rocks in the suite.

The apparent holmium anomaly is considered to be due to

Figure 4-2: Chondrite-normalised plot of rare earth element abundances in selected dykes from Aillik Bay.

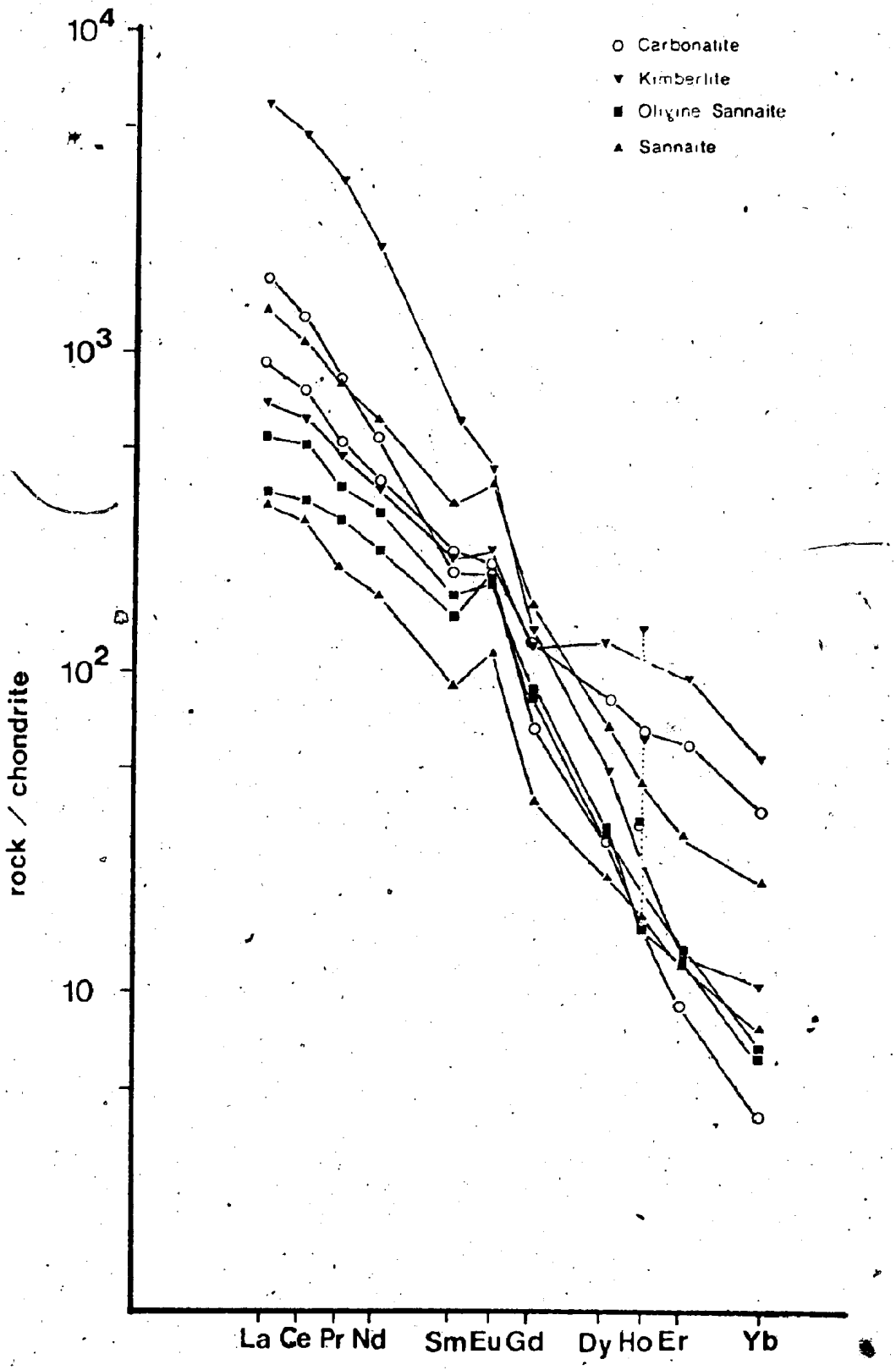

analytical error and so points in figure 4-3 are joined accordingly: holmium is much less abundant than dysprosium and erbium, and so errors are enhanced by the plot. The apparent anomaly is more marked in rocks with the strongest LREE/HREE fractionation and higher total REE. The analytical method (see appendix 2) uses less sample for REE-rich rocks, so that weighing errors are most significant in these samples. Europium anomalies are much less likely to be erroneous, and frequently exist due to variations in the relative abundances of the divalent and trivalent ions.

The strongly LREE enriched patterns are typical of alkaline rocks (Kapustin,1966; Balashov and Pozharitskaya,1968), and are seen in all alkaline lamprophyres, kimberlites and carbonatites. Abundances in the sannaites and olivine sannaites are similar to, or greater than other alkaline lamprophyres and associated rocks (Jahn et al.,1979; Kay and Gast,1973; Cullers and Medaris, 1977; Borodin and Pyatenko,1978; Roden et al.,1979). Cratonic kimberlites typically have chondrite-normalised values of 200-700 for La and less than 15 for Yb (Paul et al.,1975; Fesq et al.,1975; Mitchell and Brunfelt,1975a; Kaminskiy et al.,1978; Paul,1980). Aillik kimberlites have higher abundances similar to the carbonatites. Both kimberlites and carbonatites have patterns with variable slopes. Chondrite normalised values for ytterbium range from less than 5 to around 50, which is a similar range to carbonatites from other central complexes (Mitchell and Brunfelt,1975b; Eby,1971; Moller et al.,1980; Loubet et al.,1972). This reaffirms that the kimberlites are an integral part of the complex.

CHAPTER 5 : PETROGENESIS

Any petrogenetic model for the Aillik Bay dykes should take the following observations into account.

(a) There is a progression in time from abundant sannaites to rarer kimberlites and carbonatites.

(b) Structural relationships suggest that all the dykes are related to an intrusive centre.

(c) Sannaites and olivine sannaites are clearly spatially and genetically related, occurring together in banded dykes.

(d) Sannaite mineralogy shows chemical evolution typical of nepheline syenite associations.

(e) Some evidence for liquid immiscibility is found in the earliest sannaite dykes. Numerous ocelli may also represent immiscible fluids.

(f) Kimberlites are similar to rocks found in association with nephelinite- carbonatite rock series (Currie,1975a), and can be distinguished from cratonic kimberlites which do not have such associations.

(g) Most carbonatites display relict kimberlite textures.

(h) Carbonate is an essential part of all dyke-rock types.

The above points, which have been described or demonstrated in earlier sections, suggest that sannaites, olivine sannaites, kimberlites and carbonatites are related to an intrusive centre of nephelinite-carbonatite type. Some details of petrogenesis are here investigated further.

1. SANNAITE AND OLIVINE SANNAITE DERIVED FROM A COMMON PARENTAL MAGMA (SPM)

As noted earlier, the principal difference between sannaite and olivine- sannaite is the presence of abundant olivine phenocrysts in the latter, and well developed leucocratic ocelli in the former. The occurrence of banded dykes with olivine-rich and ocelli-rich bands supports the idea of a common origin for these rocks, and for the discrete sannaite and olivine sannaite dykes in which more distinct types occur.

An attempt is made here to define the sannaite parental magma (SPM) composition. Figure 5-1 shows major element oxide plots similar to figure 4-1 with solid symbols signifying average values for sannaite, olivine sannnaite, kimberlite and carbonatite. It should be possible to define the composition of SPM by using enrichment lines or polygons if crystal-liquid separation dominated the processes which produced the two types of sannaite. In figure 5-1, olivine (open circles) and clinopyroxene (open squares) are extracted from olivine sannaite in the average ratio of phenocryst occurrence (6:1). Enrichment lines for a mixture of nepheline (Ne), analcite (At) and K-feldspar (Kf) compositions, representing sannaite groundmass minerals and the outer zones of ocelli, are drawn for sannaites. Carbonate was not included in the extraction because carbonate-analcite globules similar to the inner zones of sannaite ocelli also occur in olivine sannaites. Only the outer zones are exclusive to the olivine-poor sannaites. The relative quantities of nepheline, analcite and K-feldspar in sannaite

Figure 5-1: Oxide vs. MgO plots for Aillik Bay dykes. Solid symbols signify average values for sannaite (■), olivine sannaite (◆), kimberlite (▼) and carbonatite (●). Open symbols signify mineral compositions. Olivine and clinopyroxene are extracted from olivine sannaite in the ratio 6:1, to suit phenocryst occurrence. Extraction lines from sannaite represent a mixture of analcite, K-feldspar and nepheline, with limiting cases (100% one mineral) marked by the initial. The intersection of the two extraction lines defines an approximate parental magma.

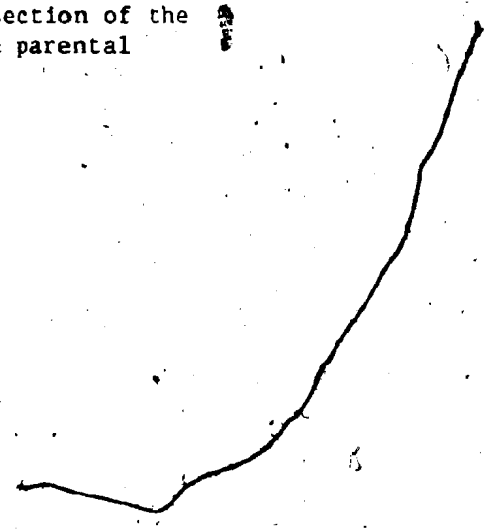

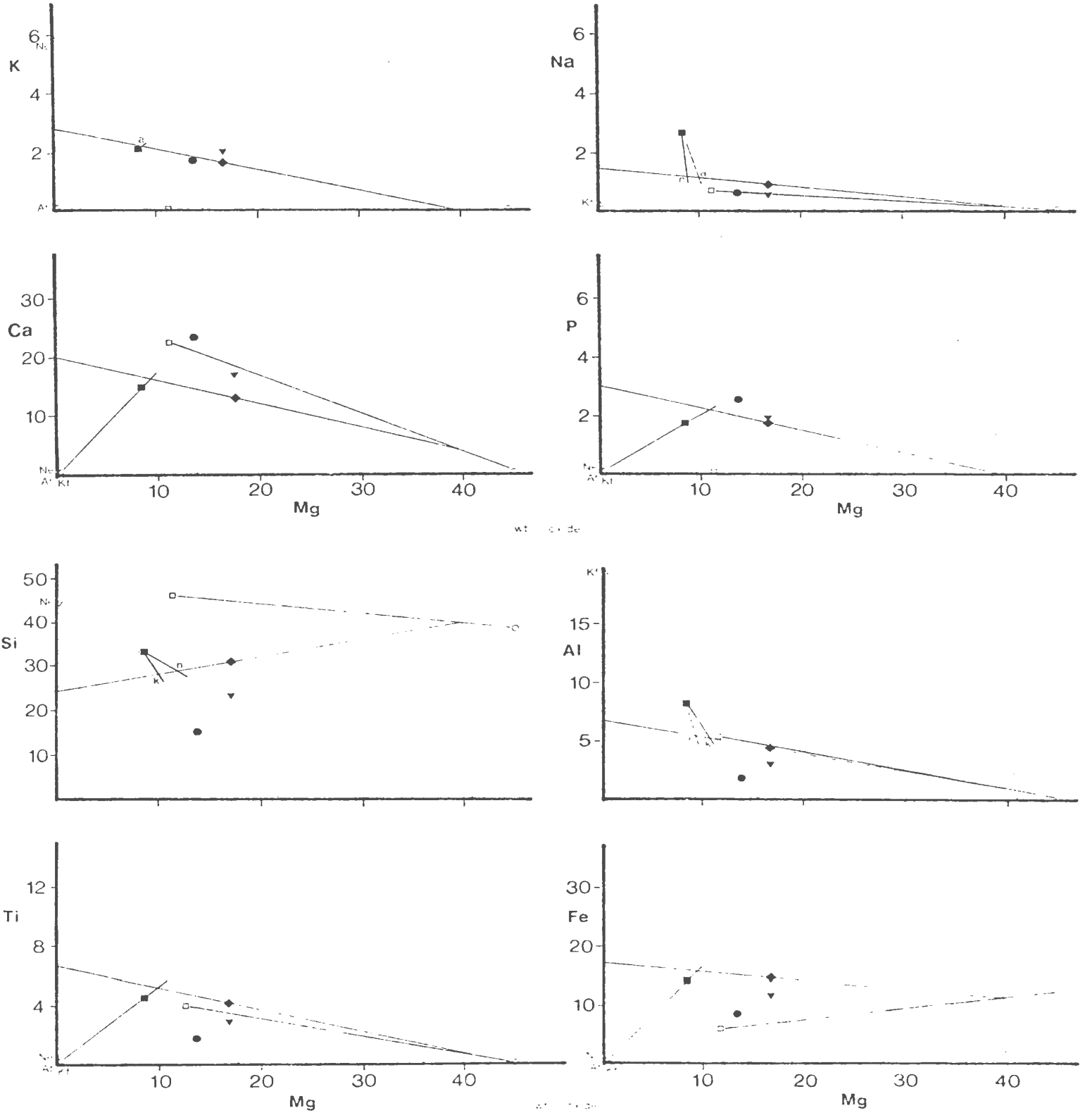
K
Na
Ca
P
Si
Al
Ti
Fe
Mg
Mg
Mg
Mg

groundmass is open to question because of alteration and variation between rocks. Multiple lines are shown in some diagrams in figure 5-1 to show the limiting cases for 100% nepheline (n), K-feldspar (k) or analcite (a). Mineral compositions plotted are average probe analyses from this study.

The intersection of enrichment lines from sannaites and olivine sannaites should define the SPM, which ideally will show identical MgO values for each diagram. The diagrams in figure 5-1 suggest that the proposed enrichments are possible and place the following limitations on the mineral phases involved: The Ca and Si plots confirm that carbonate did not play an important role in segregation of olivine sannaites from sannaites. Addition of carbonate to the sannaite extraction would result in an anomalously large MgO value for SPM. The Na and K plots show that the aluminosilicates involved in the enrichment for sannaites must have been dominantly sodic, suggesting a minor role for K-feldspar. The P plot shows a high MgO intersect, which can be rectified by adding apatite to the olivine sannaite enrichment. The same is possibly true for Ti; addition of a Ti bearing phase would produce a more horizontal enrichment line.

Computer subtraction calculations (Cawthorn,1974,program F) were performed using slight variations in mineral proportions subtracted. The calculated best fit with whole-rock chemical and petrographic modal analyses data is plotted in figure 5-2. The high MgO values are due to the computer program normalising data to 100% prior to calculation. CO2 values were not included since only loss on ignition data are available, and carbonate is not

Figure 5-2: Oxide vs. MgO plot for the best fit whole-rock extraction after computer modelling. Solid symbols represent average sannaite and olivine sannaite whole-rock compositions, and open symbols represent the 'residue' after the extraction calculation. The intersection of lines (circled) defines the SPM value for each element. P and K do not intersect, which could be overcome by slight modification of apatite and K-bearing felsic phases.

◆ Olivine Sannaite

■ Sannaite

○ Expected source comp.

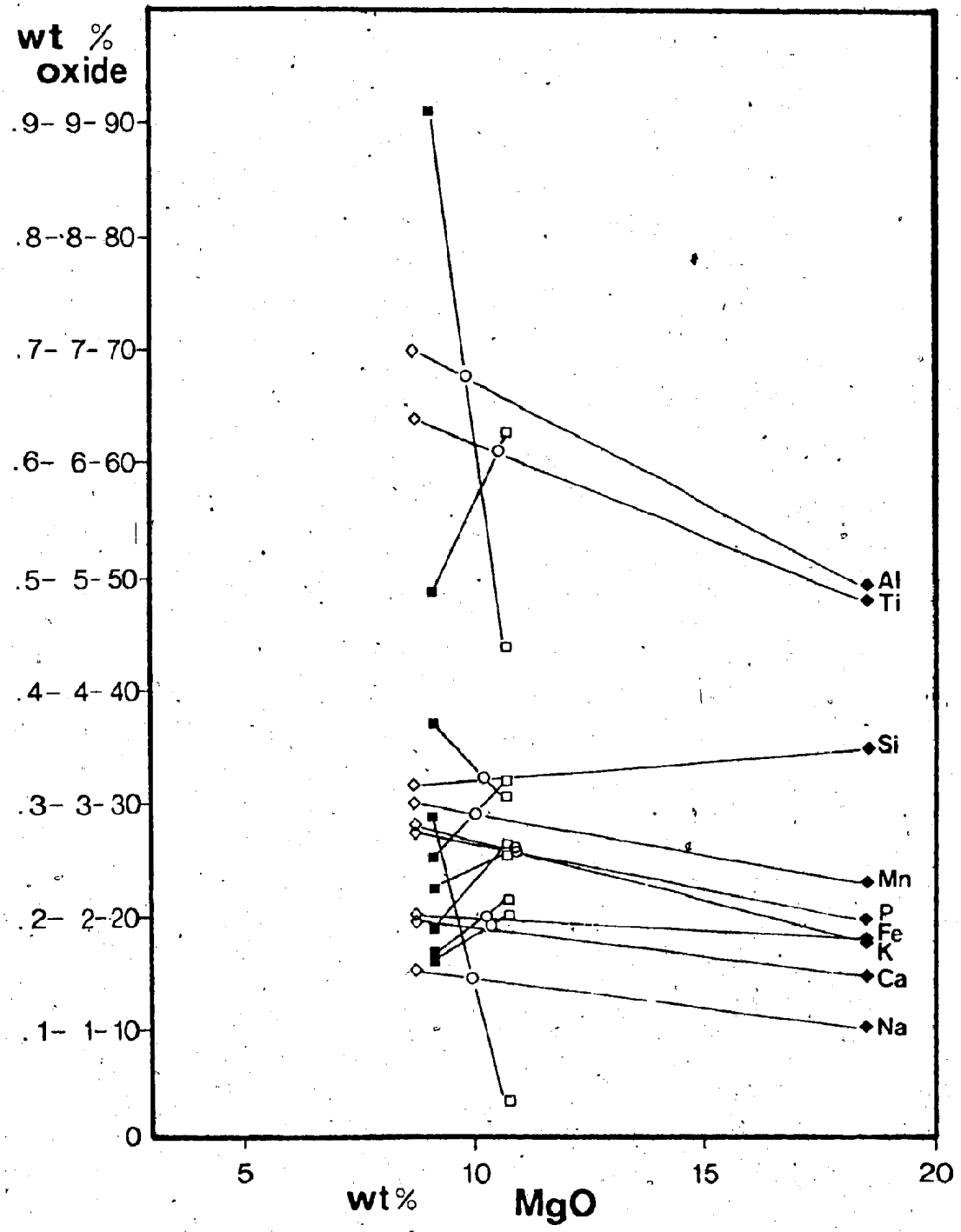

an important phase to this calculation. The subtractions calculated used 27.5% olivine, 5% clinopyroxene, 0.5% apatite and 0.4% rutile for olivine sannaite, and 15% analcite, 5% nepheline and no K-feldspar for sannaite. These achieve an intersection for all except potassium and phosphorus (figure 5-2), for which there was insufficient extraction. These could be allowed for by modification of apatite content and inclusion of some K-feldspar in the extraction, but further refinement of the model would be of dubious value since complete accuracy cannot be expected from this type of calculation (Cox et al.,1979,p.153-154).

In order to arrive at a composition for SPM, a value for the missing volatiles must be assumed. If the ten oxides treated in the program are assumed to form 94% of the total, then the SPM is deduced to have the following composition: 29.8% SiO_2, 5.6% TiO_2, 6.25% Al_2O_3, 18.6% Fe_2O_3(total Fe), 9.6% MgO, 17.9% CaO, 1.3% Na_2O, 2.4% K_2O, 2.2% P_2O_5 and 0.27% MnO (all wt%).

Roedder and Emslie (1970) describe how the composition of olivine is determined by the magnesium:ferrous iron ratio of the melt from which it crystallises, and is independent of temperature and probably pressure (Irving, 1971). The SPM defined by the extraction model has 13.6 mol% FeO (assumed total Fe as FeO) and 13.9 mol% MgO. According to figure 7 of Roedder and Emslie (1970) the SPM would crystallise olivines of Fo77-78 under equilibrium conditions. This is close to the average value of Fo79 for the olivine sannaites. Some trivalent iron must be present to explain higher observed values than calculated

values, because trivalent iron will not enter the olivine crystal structure. However, the small discrepancy between observed and calculated forsterite contents argues for a high FeO/Fe2O3 ratio, and thus low oxygen fugacity in the SPM. Low oxygen fugacity has previously been suggested as a condition of formation of alkaline ultrabasic rocks (Mitchell,1973,1975).

2. RELATIONSHIP OF KIMBERLITES AND CARBONATITES TO SANNAITES

It has been shown on the basis of mineralogy and structural associations that the kimberlites are related to other rocks of the Aillik Bay suite. Absolute ages are uncertain, and the presence of two distinct ages, one around 570 Ma (Leech *et al.*,1963) and one Mesozoic (King and McMillan,1975) cannot be discounted. Kimberlites and carbonatites on Cape Makkovik occur as a distinct set of dykes, with shallow dips, although kimberlites also occur as sub-vertical dykes. If two periods of intrusion occurred, it seems likely that the break came between the sannaites and the kimberlites.

Mass balance calculations (Cawthorn,1974,program E) were performed to see if kimberlite could be related to the SPM. This method defines the best balance of SPM and kimberlite mineral compositions that is equivalent to the bulk kimberlite composition. Once again, probe analyses from this study were used where possible. The following solutions were obtained:

Kimberlite = 50.17% SPM + 22.99% dolomite + 15.62% olivine +
7.66% mica (reverse pleochroic phenocrysts) +
2.29% apatite + 1.04% calcite (wt%)

The sum of squares of errors is 0.217, which defines a good fit. Repetition of the calculation using glimmerite micas did not produce such a good fit. The possibility was also considered that kimberlite is a hybrid rock formed by carbonatisation of olivine sannaites, since carbonate-mica metasomatism often occurs around carbonatites (Heinrich,1966). This gave the solution:

Kimberlite = 68.08% olivine sannaite + 22.9% dolomite +
6.93% mica + 1.87% apatite + 0.23% calcite
(sum of squares of errors = 0.25) (wt%).

The apparent vindication of two different hypotheses for the origin of the kimberlites emphasises that computer models should fit the geological constraints (Wright and Doherty,1970). In fact, neither solution is ideal: if carbonate-mica alteration of olivine sannaite gives rise to kimberlite there should be more abundant rocks derived from the carbonatisation of olivine-poor sannaites. If kimberlites are derived from the SPM, the occurrence of nodules and phenocrysts of widely differing compositions is difficult to explain.

The range in Fo values (71-87) of kimberlitic olivines suggests that either one or more generations of olivine is exotic, or that the Mg:Fe ratio in the parental magma was extremely variable. A continuous range of olivine compositions is difficult to explain in terms of exotic crystals; a large number of grains with a small compositional range would be expected. Roedder and Emslie (1970) note that their correlation

of olivine composition with melt composition may be open to question if (i) there is insufficient Mg and Fe to form olivine (ii) there are complexes in the melt tying up Mg or Fe (iii) temperature and composition vary greatly from the experimental conditions. Caution should therefore be applied when considering the Fo contents of olivine from the kimberlites in view of their low SiO2 contents and the presence of dolomite as a Mg-bearing phase.

Despite a lack of proof of the relative ages of olivine phenocrysts in kimberlites, it is probably valid to propose that the Fe-rich olivines formed before the Mg-rich olivines. The Fe-rich olivines are Ca-poor, which signifies a deep-seated origin (Simkin and Smith,1970 ; Finnerty and Boyd,1978). Moore and Erlank (1977) suggested that high iron, low nickel olivines in South African olivine melilitites indicate crystallisation under low oxygen fugacity, and not necessarily from a Mg- and Ni-poor melt. The olivines in the Aillik Bay kimberlites could therefore describe a trend of increasing Ca,Ni and Mg starting with those crystallised at depth under low fO2. Reduction in pressure during magma ascent would be expected to lead to increased oxygen activities (Moore and Erlank,1977). Pressure drop could also be caused by a loss of volatiles. Low Ca content in later olivines can be attributed to coexistence with carbonate phases.

Micas may describe a similar chemical trend if the green pleochroic micas crystallised first. Green phenocryst cores are frequently more rounded than red reverse pleochroic cores,

possibly indicating earlier formation. The green micas are more iron-rich, but probably crystallised under lower fO2 than the red micas, since the reverse pleochroism is due to tetrahedral ferric iron (Faye and Hogarth,1968).

In summary, the mineralogy of the kimberlites describes a greater range in conditions of crystallisation than would be expected if it crystallised from the SPM. Kimberlites become increasingly carbonate-rich with time, such that carbonatite must be an integral part of kimberlite genesis.

3. GENESIS OF THE AILLIK BAY SUITE BY PARTIAL MELTING

Of the three main hypotheses proposed to explain the genesis of kimberlitic liquids (Gurney,1974;Dawson,1971,1980 p.212-215), partial melting of mantle material appears to best explain the currently available data. Other explanations include zone refining and fractional crystallisation from a picritic melt.

The zone refining process proposed by Harris and Middlemost (1970) requires a low geothermal gradient typical of cratonic areas, and is thus inappropriate for a rift environment.

O'Hara and Yoder (1967) suggested that kimberlite may be produced by fractional crystallisation of eclogite from a picritic melt, which was itself produced by partial melting of the diopside-garnet fraction of garnet lherzolite at 80-110 km depth. Kimberlite would be the last remaining fraction of melt, and would be emplaced after basaltic lavas which would be essentially co-magmatic. This hypothesis has been criticised on

the grounds that kimberlite does not necessarily occur along with more voluminous rocks of less extreme composition (Dawson,1971). The eclogite xenoliths once presumed to be cognate have been shown to have lower 87Sr/86Sr than garnet lherzolite xenoliths, and to be considerably older than the host kimberlite (Allsopp et al.,1969). Mitchell and Brunfelt (1975a) estimated that 96% crystallisation would be required to produce a kimberlitic liquid.

Thus the partial melting hypothesis has become increasingly popular, especially with the consideration of hydrous and carbonated peridotite starting materials. The attraction of this hypothesis is that most continuous elemental depletions and enrichments between alkali basalts, nephelinites and kimberlites (Wedepohl and Muramatsu,1979; see chapter 4, this work) can be explained as being due to variations in either the fraction of melting or the depth at which melting occurs (Wyllie, 1979,1980; Eggler and Wendlandt,1979).

H2O is stable under mantle conditions in hydrous phases; amphibole at depths up to 80–90 km, and phlogopite to 150 km or more, depending on temperature (Kushiro,1969;Carswell,1975). The presence of H2O causes a substantial drop in the peridotite solidus temperature (fig.5-3), but melting experiments generally fail to produce silica-undersaturated melts (Mysen and Boettcher,1975; Kushiro,1972; Bravo and O'Hara,1975).

Dolomite is the most stable carbonate phase under mantle geotherm conditions (Eggler et al.,1976), giving way to magnesite at pressures above about 40kb (Eggler and

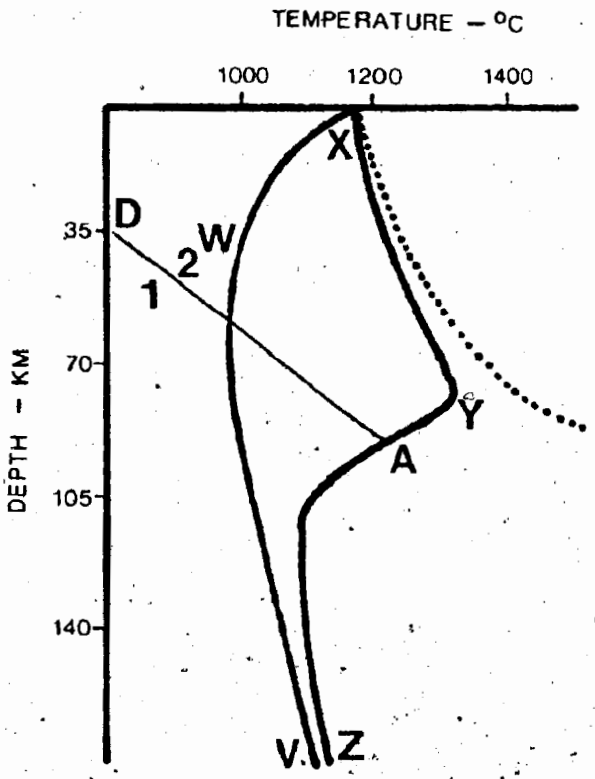

Figure 5-3: The effect of H2O and CO2 on the solidus of peridotite

--- = Volatile-free peridotite solidus
XYZ = Peridotite-CO2 solidus
XWV = Peridotite-H2O solidus
A-D = Carbonation surface for the reaction:
(1) Opx + Ca-Dol = (2) Ol + Cpx + CO2
(after Wyllie, 1979)
A-Z = Buffered solidus

Wendlandt,1979). Evidence for the presence of CO2 in the mantle includes CO2-rich fluid inclusions in xenoliths and olivine phenocrysts (Roedder, 1965; Green and Radcliffe,1975), and rare carbonate inclusions (McGetchin and Besancon,1973; Smith,1979). The addition of CO2 to peridotite compositions causes a slight drop in solidus temperature at low pressures, but a much greater drop at pressures above about 25kb (fig 5-3; Wyllie and Huang, 1975; Eggler, 1978). Melts produced from carbonated peridotite compositions are silica undersaturated and carbonate-rich (Eggler, 1974; Wyllie and Huang, 1975).

Peridotite compositions including both H2O and CO2 could thus form a variety of liquids depending on the relative amounts of H2O and CO2. In order to produce silica-undersaturated melts, a CO2-rich composition is required. Figure 5-4, taken from Wyllie (1980), summarises probable phase relations in peridotite with 100*CO2/(CO2+H2O) = 80. The continental and oceanic geotherms of Ringwood (1966) are superimposed on figure 5-4. Which of these is more applicable in the case of Aillik Bay depends on the precise time of magma generation relative to rift formation. Nephelinite-carbonatite magmatism is typical of a very early stage of rifting, and so the relevant geotherm may be closer to the continental than the oceanic geotherm. Royden and Keen (1980) have shown that most rifting of the Labrador Sea in the Makkovik area occurred in the late Cretaceous, which is after the proposed date for Aillik Bay magmatism. In either case, melting should occur at depths of 90-120 km (fig.5-4).

It takes 5 % CO2 to form the maximum possible amount of

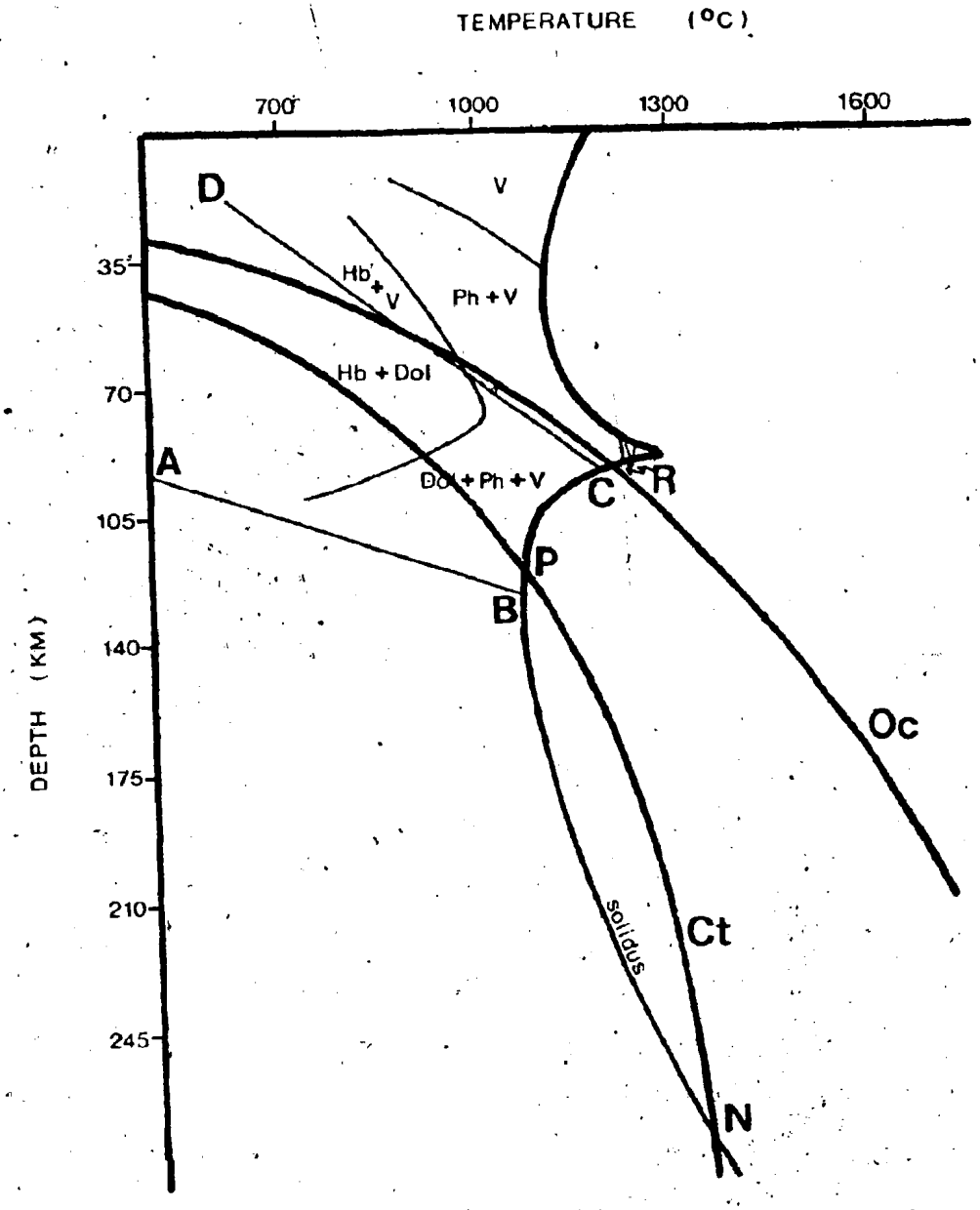

Figure 5-4: Phase relationships for peridotite + H20 + CO2 with 100*CO2/(CO2+H2O)=80 (after Wyllie, 1980). Ct and Oc are continental and oceanic geotherms. Partial melt will exist on the continental geotherm between N and P. Magmas moving along N-P will solidify at P releasing vapors which could cause mantle metasomatism. Small melt fractions along the solidus P-R will be CO2-rich and silica-poor. Melt type depends on geotherm type and fraction of partial melting. Rising volatiles from below c.260 km may cause melting at N to give rise to kimberlites.

dolomite from mantle compositions, but only 0.02% H2O to form the maximum amount of phlogopite allowed by the low K concentrations (Eggler, 1977; Ringwood, 1975 p.225). Unless there has been considerable metasomatic enrichment of the mantle in K in the magma source region, H2O will be present in amounts much greater than required to form the maximum amount of phlogopite. Under these conditions, melting at depths in the range 90-130 km will be controlled by dolomite in a buffered reaction (Eggler, 1977; Wyllie, 1977a p.197-198). Near-solidus melts are extremely enriched in CO2, probably carbonatitic (Wyllie and Huang, 1975; Eggler, 1976) and become more silicic, possibly kimberlitic or melilititic, at higher pressures (Wyllie, 1977b, 1979).

It has been shown from trace element studies that increasing the fraction of partial melting leads to progressive depletion of the melt in incompatible elements (Gast, 1968; Sun and Hanson, 1975). The elemental trends from nephelinite through alkali basalts to tholeiitic basalts described by Wedepohl and Muramatsu (1979) may be simply an expression of melt fraction. Extrapolation to lower melt fractions is complicated by accessory phases. Peridotite-CO2-H2O experimental work outlined above suggests that carbonatitic melts should characterise the lowest melt fractions. The common association of alkaline lamprophyres with carbonatites and nephelinitic rocks can therefore be explained by a small variation in melt fraction.

The Aillik Bay lamprophyres have trace element abundances between those characteristic for nephelinite and kimberlite,

with some clearly influenced by carbonatite (see chapter 4). Therefore, if derived by partial melting, the Aillik Bay lamprophyres must have been produced by a melt fraction less than the 3% suggested for nephelinites (Gast,1968). The influence of carbonatite implies that the melt fraction was much lower than 3%, or that later mixing occurred. Complications of solidus relationships will be caused by the presence of incompatible elements such a P,Ti and S, which are not considered in most peridotite melting experiments. Ti,P and S all cause polymerisation of the melt, and may cause a further drop in solidus temperature, although phase relationships are not yet clear in complex systems (Kushiro, 1975; Arculus, 1975; Ryerson and Hess, 1980; Mysen and Popp, 1978).

If it is assumed that the kimberlites and carbonatites represent a smaller melt fraction of similar materials to the sannaites (or SPM), then examination of their chemistry may provide clues as to the accessory phases important in their genesis.

The commonest REE-rich phases in kimberlites and carbonatites are carbonates, apatite and perovskite. Carbonatitic calcites typically have LREE-enriched patterns with roughly similar slope to sannaite whole-rock analyses (fig.4-3), but their abundances are similar or slightly less (Eby, 1971). The higher modal carbonate in kimberlites and carbonatites can therefore explain parallelism of most patterns, but not the overall abundances. Apatite and perovskite are both extremely enriched in REE. Perovskite has a strongly fractionated

REE-enriched pattern, whereas apatite has a less fractionated pattern (Eby, 1971; Nagasawa et al.,1980).Both apatite and perovskite typically have negative europium anomalies, but the whole-rock patterns do not reflect this due to the strong positive europium anomaly in mica, which is caused by the larger Eu2+ ion entering interlayer sites (Philpotts, 1970). The variation in HREE can be explained as variations in carbonate and apatite, assuming that dolomite has similar REE patterns to calcite. The anomalously high REE content in one kimberlite sample is almost certainly due to higher modal perovskite.

Generation of LREE-enriched patterns such as those of the Aillik Bay dykes by partial melting requires either a LREE-enriched source (Sun and Hanson, 1975; Hanson,1980) or disequilibrium melting of one or more LREE-enriched phases (Campbell and Gorton, 1980); eg. fluorapatite is stable in the mantle at depths proposed here for partial melting, and is unlikely to remain in the solid residuum after even very small fractions of melting (Watson, 1979, 1980).

Nd isotopic data indicate that LREE-enriched mantle sources would be the exception rather than the rule (DePaulo and Wasserburg, 1976; DePaulo, 1979 p.204). However, Lloyd and Bailey (1975) have shown that metasomatic fluids are likely to cause enrichment of incompatible elements in cratonic regions, as evidenced by metasomatised xenoliths in alkaline mafic and ultramafic rocks (Lloyd and Bailey, 1975; Harte et al., 1975; Boettcher et al., 1979; Wass and Rogers, 1980; Ehrenberg, 1978). High LREE/HREE values will result from this metasomatic

enrichment due to higher ionic radii, and thus greater incompatibility in the LREE (Hanson, 1980 p.373).

A cooling diapir, possibly kimberlitic in nature, on reaching the solidus at around 100 km depth will exsolve vapor if the phase relations shown in fig.5-2 are applicable (Wyllie, 1980; Mysen, 1975). These vapors may then assist metasomatism of the mantle at this level, so that later partial melts will lead to carbonatitic and lamprophyric liquids. Wendlandt and Harrison (1979) showed that LREE will preferentially partition into a CO2-rich vapor, so that LREE- enrichment of the mantle is explained by this process. This model may be particularly applicable to the Labrador Sea rift, since true kimberlites occur together with lamprophyres in Greenland (Scott,1979). Collerson and Malpas (1977) envisaged two stages of evolution for kimberlites at Saglek, Labrador, to explain the presence of groundmass melilite and glimmerite nodules. Kimberlite magmatism may therefore be an indirect cause of central complexes such as Aillik Bay.

The ultimate source of the metasomatising fluid remains a mystery: Wyllie (1980) requires an input of volatiles from below about 260 km. The earth's apparent depletion in potassium relative to chondrites has caused some authors to propose enrichment in K at depth, possibly in the core (Goettel,1976; Somerville and Ahrens, 1980). Kushiro (1980) has shown that melts produced in the system Mg_2SiO_4-$KAlSiO_4$-SiO_2 have higher K_2O contents with increasing pressure.

Experimental work investigating the effect of very low

oxygen fugacities is in very early stages (Pasteris, 1981). In view of the common association of reduced carbon as diamonds and graphite with the deepest derived kimberlites, CO and hydrocarbons may be more relevant volatile species (Eggler et al.,1979; Eggler,1980). Freund et al. (1980) have shown that carbon may be stored in forsterite solid-solution. Carbon supersaturation may occur at shallower depths under reducing conditions, explaining the observed depth limit of diamonds (Freund et al.,1980 p.1331), and also explaining release of carbon to form metasomatising fluids.

4.THE ROLE OF FLUID IMMISCIBILITY

Textural evidence for coexisting immiscible liquids is found only in one sannaite (sample 447). The leucocratic ocelli in the sannaites are believed to have been formed by segregation of residual melt into vesicles. The time of formation of the vesicles is uncertain, since later expansion will destroy all preceding textures. It is therefore pertinent to consider evidence for immiscibility in lamprophyres.

Many studies of lamprophyres associated with carbonatite and nepheline syenites have called upon large scale immiscibility to explain the origin of carbonatite and syenite rock types. Examples are the Monteregian Hills of Quebec, where there is a compositional break between silica-poor and silica-rich alkalic rocks (Philpotts,1976); Callander Bay, Ontario, where carbonatite, melteigite, nepheline syenite and camptonite are thought to have been derived by successive

episodes of immiscibility from an olivine nephelinite liquid (Ferguson and Currie,1971); and Fen, Norway, where a carbonated nephelinite parental magma was proposed by Mitchell and Brunfelt (1975b).

Leucocratic ocelli, which are frequently said to be a manifestation of the proposed immiscibilty, are more common in alkaline lamprophyres than in any other rock type (Philpotts, 1972; Rock, 1977), and so lamprophyres are often considered to be starting points for explanations of different rock types by immiscibility (eg.Currie, 1975b; Philpotts, 1976).

Koster van Groos and Wyllie (1968, 1973) showed that immiscibility of silicate and carbonate magmas is promoted by the presence of alkalies. Experimental studies of liquid immiscibility have recently been extended to high pressures, where it has been shown that immiscibility could be a relevant process to lamprophyres due to their enrichment in Ti,P,S,H2O,CO2 etc.. Visser and Koster van Groos (1979) have shown that P2O5 can stabilize immiscibility to higher pressures than in P-free systems. Thus, immiscibility would become more widespread at lower pressures, since melts progressively poorer in P2O5 would become involved. CO2 and S are more soluble in silicate melts at high pressures similar to conditions at which partial melting occurs (Eggler, 1974; Mysen and Popp,1978), and so will be inclined to separate from a rising magma. Crystallisation, causing enrichment of incompatible elements in residual melt, and increasing fO2 (Freestone,1978a; Naslund,1976) will promote fluid immiscibility as a late-stage

process.

Freestone (1978b) discovered that Ti and P expand the immiscibility field in the system fayalite-leucite-silica towards more silica-undersaturated compositions, but suggested that alkaline lamprophyres are outside the immiscibility field. In compositions most applicable to lamprophyres, Freestone (1978b) defined a metastable sub-liquidus immiscibility field which causes an isothermal step in the liquidus (fig.5-5). This can be taken to support an origin as segregation vesicles (Smith, 1967) for the abundant zoned ocelli; a small drop in temperature will cause a large amount of crystallisation, and yet the residual melt will persist for a relatively large temperature interval. The uprise of the sannaite magma was accompanied by falling temperature. When the temperature of the isothermal step in the liquidus was reached, rapid crystallisation resulted in the formation of a crystalline mesh dominated by acicular pyroxene. This supports the assertation of Donaldson (1976) that acicular crystals are not necessarily indicative of rapid temperature drop, but merely rapid crystallisation. Exsolution of volatiles from the residual melt as the magma continued its upward journey caused the nucleation and growth of gas bubbles, which in turn caused fracturing of the crystalline mesh (mechanism originally proposed by Bailey, 1928, quoted by Carman et al., 1975). This is evidenced by long irregularly shaped 'ocelli' which have sub-spherical carbonate-analcite globules occurring at intervals along their length. The fractures between the carbonate-analcite globules

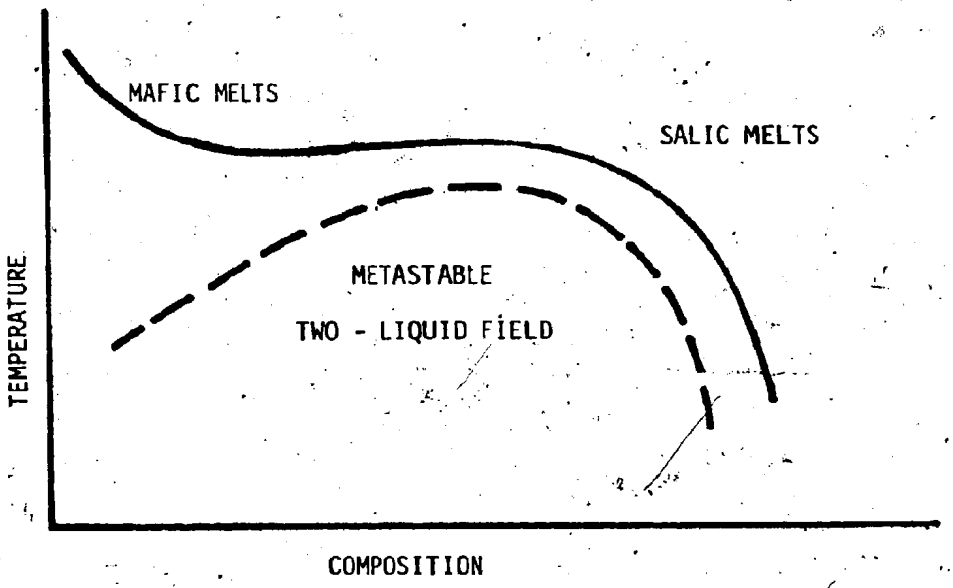

Figure 5-5: Freestone's (1978b) temperature-composition profile of an alkaline mafic magma. A large amount of crystallisation, notably pyroxene, occurs over a small temerature interval. The residual melt can persist for a relatively large temperature interval, resulting in crystallisation of strongly differentiated late-stage mineralogy after acicular pyroxenes.

are filled by K-feldspar, nepheline or analcite with Fe-mica and pyroxene, representing residual melt drawn int the fracture.

If the immiscible globule in sample 447 represents a widespread process, then its Na-rich chemistry suggests it may be the origin of nepheline syenite- type rocks which probably make up the central part of the unexposed complex. There is considerable experimental and chemical evidence to suggest that immiscibility is likely in the alkaline lamprophyres. However, the late-stage formation of segregation vesicles is likely to eliminate any textural evidence in support of liquid immiscibility.

5. STRUCTURAL ASPECTS OF MELT SEGREGATION AND EMPLACEMENT

The invocation of partial melting hypotheses for kimberlite has been unpopular in the past because of the difficulty in explaining the following points: (i) Where kimberlites occur with other alkaline rocks, they are the youngest, with the possible exception of carbonatites. (ii) Extremely low fractions of melt must be physically separated from their source-rocks in order to amalgamate into magmas.

Kimberlites and carbonatites are the youngest rocks observed at Aillik Bay. It is suggested from the discussion of partial melts that they may also represent lower fractions of melt than the lamprophyres. It has been suggested (Eggler and Wendlandt, 1978) that the rarity of kimberlitic rocks is due to the rarity of tectonic settings conducive to their ascent. Emplacement of low fractions of melt from considerable depths

will be assisted by structural pathways formed by earlier magmatism. Such structural inheritance also explains why lamprophyres are frequently the latest magmatic episode in an area (Rock,1977), and yet their compositions are apparently parental to the rocks they postdate (eg.Currie, 1975b; Philpotts, 1972): easier passage to near surface conditions leaves less time for evolution of the later lamprophyres into 'daughter rocks'. The attitudes of dykes described in chapter 2 shows that the magmas giving rise to all dyke-rock types are related to the intrusive centre, and thus used the structural weakness created or used by the earlier central complex rocks. Progressively deeper-derived rocks representing progressively smaller melt fractions can be explained by this process (Wyllie,1980).

The problem of separation of very small melt fractions may be partly overcome by usage of pre-existing structures in the mantle. Silica-undersaturated melts enriched in incompatible elements could be generated at higher melt fractions from an enriched mantle due to the buffered reactions described by Eggler (1977, 1978) and Wyllie (1979).

The presence of carbonate selvages to some Aillik Bay dykes demonstrates the existence of a CO2-rich fluid moving ahead of the magma. Anderson (1979) described how the low viscosity of a CO2-rich fluid can assist stress-corrosion cracking. The rapid crack growth facilitated by the low viscosity fluid is preceded by a period of slow stable crack growth due to surface chemical effects (Rudnicki, 1980). Seepage of small amounts of magma into

cracks immediately after their formation, but before a large pressure buildup initiates rapid crack growth, must be considered as a possible mechanism for melt separation. Another possibility is linked to dilation in incipient shear zones. At 50–75% of the effective shear strength of a rock, an increase in rock volume occurs (Frank, 1965; Brace et al., 1966), causing a local drop in pore-fluid pressure. This could draw in small fractions of melt which in turn cause shear failure due to lowering of the rocks' effective shear strength (Nur,1972). The melt could therefore create its own escape channel despite low initial shear stresses. It is not possible to ascertain whether this process could occur in the mantle; dilatancy may occur in dunite to at least 10kb and 600°C (Brace,1978), but is likely to be limited at higher pressures by increased plasticity. Within the plastic region, escape of melt would most likely occur through a succession of vertically oriented ductile faults (Yoder,1978). Ductile faulting is a slow process, and so melts existing in such conditions are likely to be more equilibrated with their host rocks than melts within the elastic region. Dilatancy may occur well into the ductile field in the case of low porosity rocks (Gowd and Rummel,1980), and may be enhanced by repeated stressing (Brace,1978). Byerlee (1978) suggested that hydrous minerals could be the locus of sliding planes, which may be applicable to areas of mantle metasomatism. Mechanical extraction of low melt fractions could therefore be more effective in areas of mantle metasomatism, and buffered melt compositions may not require such small amounts of melt as previously thought.

CHAPTER 6: SUMMARY

The Aillik Bay intrusive suite comprises dykes of sannaite, olivine sannaite, kimberlite and carbonatite. Sannaites are alkaline lamprophyres with phenocrysts of Ca-Ti-salitic clinopyroxene and rarer olivine, which is characteristically altered to carbonate and serpentine. The phenocrysts are set in a two-stage groundmass: the first is a crystalline mesh dominated by acicular clinopyroxene, whereas the second is a true groundmass comprising K-feldspar, Ti-biotite, titanomagnetite, apatite, clinopyroxene, nepheline, carbonate and analcite. Sannaites are characterised by leucocratic ocelli, which are commonly zoned with a carbonate-analcite core, occasionally including sulphides and sulphates, giving way to an outer zone comprising biotite and clinopyroxene set in K-feldspar, analcite and nepheline. Alteration of ocellar minerals to zeolites is frequently advanced.

Olivine sannaites are distinguished from sannaites by higher modal olivine (up to 35%) and rarer clinopyroxene phenocrysts. Ocelli are small and restricted to carbonate-analcite mineralogy similar to the cores of zoned ocelli in the sannaites. Sannaites and olivine sannaites occur as bands within the same dyke, or as discrete dykes with more distinctive mineralogy. The margins of bands within banded dykes frequently exhibit well-defined flow texture.

Kimberlites are yellow-weathering dykes comprising olivine and mica phenocrysts set in a groundmass dominated by mica,

carbonate, titanomagnetite, and apatite. The mineralogy of kimberlites, notably olivine(Fo<87), Mg-poor titanomagnetite and lack of high pressure marker minerals such as magnesian ilmenite, pyrope and Cr-diopside is characteristic of kimberlites from central complexes and not cratonic kimberlites. Diamond potential is therefore low. Olivines and micas are zoned, indicating variable conditions of crystallisation, starting with a deep-seated low oxygen fugacity environment.

Kimberlites contain abundant xenoliths which, in addition to country rock, include small (2cm max.) ultramafic nodules which are dominantly members of the MARID suite (mica-amphibole- rutile- ilmenite- diopside).

Discrete carbonatite dykes are rare, but both calcitic (sovite) and dolomitic (beforsite) types are present. Metasomatic carbonatites, displaying relict textures of kimberlites are much more common, occurring as bands within kimberlite dykes.

All the major rock types are characteristic of nephelinite-carbonatite series magmatism which typically occurs as central complexes including ijolite or nepheline syenite. The attitudes of dykes suggest that they form incomplete concentric and radial sets defining an intrusive centre sited 8-10km to the northeast of Turnavik Island. Structural considerations require a rising magma chamber, producing sannaites followed by kimberlites and carbonatites. Two episodes of concentric dyke emplacement are separated by a period of radial dykes. Dykes segmented during intrusion in response to flow instabilities; a separate

volatile-rich low viscosity fluid, which is evidenced by carbonate- rich dyke selvages, enhanced segmentation of the dykes. This low viscosity fluid probably assisted in the formation of parallel fracture zones which are concentrated within 4 to 5 metres of the most volatile-rich dykes.

The proposed location of the central complex is apparently controlled partly by the Archean-Aphebian boundary, which runs between Turnavik Island and Cape Aillik in a northeasterly direction, and partly by deep-seated structures beneath the Labrador Sea, which include one defined by an east-west gravity anomaly to the east of the Aillik Bay area.

It is proposed that all rock types are generated by partial melting of a peridotitic mantle previously enriched in incompatible elements by metasomatism. Recent experimental studies in the system peridotite-H_2O-CO_2 show that partial melting will occur at 90-120km depth even with a continental geothermal gradient. The presence of H_2O and CO_2 causes a buffered solidus reaction which will maintain high CO_2 and low SiO_2 in derived melts. Carbonatite will be characteristic of low melt fractions, giving way to lamprophyre or kimberlite at higher melt fractions, depending on depth. The observed evolution from lamprophyre through kimberlite to carbonatite is explained by a process of structural inheritance: pathways opened by the emplacement of lamprophyre will enable deeper derived melts and /or lower melt fractions to reach the surface, giving rise to kimberlite and carbonatite.

Low fractions of melt in such conditions explain the

concentration of incompatible elements, including rare earths, in the Aillik Bay dykes. The concentration of Ti, P and S has recently been shown to expand the silicate immiscibility field. The emplacement of lamprophyre caused unmixing, seen as immiscible globules in one sannaite sample. The sodic mineralogy of the immiscible globule suggests that such a process may have given rise to a nepheline syenite magma, which probably makes up the central intrusion. Sannaites contain nepheline, and pyroxenes with sodic rims are characteristic of nepheline syenite associations. The experiments of Freestone (1978b) suggest that liquids rich in Ti, P and S, analogous to the lamprophyres, may have a metastable sub-liquidus miscibility gap, causing an isothermal step in the liquidus surface. If this is applied to the sannaites it can explain the rapid crystallisation of pyroxene followed by later development of zoned micas and ocelli. Pyroxene crystallisation may trigger volatile exsolution, resulting in formation of gas bubbles, and yet the residual melt will persist for a relatively large temperature interval, resulting in Fe-rich biotite and the growth of sodic rims on pyroxene. This process is likely to destroy any evidence for earlier liquid immiscibility. It is proposed that emplacement of the initial magma was too slow to preserve lamprophyre, which unmixed, leading to the development of a nepheline syenite (or similar) plug. The structural pathway thus created enabled a later magma pulse to emplace lamprophyre bearing evidence of the unmixing process. Later pulses carried progressively deeper-derived and smaller melt fractions to the

surface, culminating in kimberlites and carbonatites. The presence of immiscible globules or segregation vesicles may be governed by either the depth or the speed at which unmixing occurs, or more detailed factors controlled by these.

REFERENCES

AGARD,J.(1960) Les carbonatites et les roches a silicates et carbonates associes du massif de roches alcalines du Tamazert (haut Atlas de Midelt, Maroc) et les problemes de leur genese. Int.Geol.Cong. 21st session, 13/293-303

AKASAKA,M.,ONUMA,K.(1980) The join $CaMgSi_2O_6$ - $CaFeAlSiO_6$ - $CaTiAl_2O_6$ and its bearing on the Ti-rich fassaitic pyroxenes. Contrib. Miner. Petrol. 71/ 301-312

ALLSOPP,H.L.,NICHOLAYSEN,L.O.,HAHN-WEINHEIMER,P.(1969) Rb/K ratios and Sr isotopic composition of minerals in eclogite and peridotitic rocks. Earth. Planet. Sci. Lett. 5/231-244

ANDERSON,E.M.(1951) 'The Dynamics of faulting'. 2nd ed., Oliver and Boyd,Edinburgh

ANDERSON,O.L.(1979) The role of fracture dynamics in kimberlite pipe formation. Proc. 2nd. Int. Kim. Conf. 1/344-353

ANDREWS,J.R.(1969) A kimberlite dyke in the Nigerdlikasik area, Frederikshab district. Geol. Gronds. Unders. Rapp., 19/35-37

ANDREWS,J.R.,EMELEUS,C.H.(1971) Preliminary account of kimberlite intrusions from the Frederikshab district, Southwest Greenland. Geol. Gronds. Unders. Rapp.,31 26pp.

ANDREWS,J.R.,EMELEUS,C.H.(1975) Structural aspects of kimberlite dyke and sheet intrusion in Southwest Greenland. Phys. Chem. Earth 9/43-50

ANDREWS,J.R.,EMELEUS,C.H.(1976) Kimberlites of West Greenland. In: "Geology of Greenland" ed.A.Escher and W.S.Watt. p.575-581.

ARCULUS,R.J.(1975) Melting behaviour of two basanites in the range 10-35 kbar and the effect of TiO_2 on the olivine-diopside reactions at high pressures. Carn. Inst. Wash. Yb. 74/512-515

ARSENYEV,A.A.(1963) The laws of the distribution of kimberlites in the eastern part of the Siberian platform. Dokl. Akad. Nauk., Earth Sci. Sec, 137/355-357

BAHAT,D.(1979) Interpretation on the basis of Hertzian theory of a spiral carbonatite structure at Homa Mountain, Kenya. Tectonophysics 60/235-246

BAHAT,D.(1980) Hertzian fracture, a principal mechanism in the emplacement of the British Tertiary intrusive centres. Geol. Mag. 117/463-470

BAILEY,D.G.(1978) The geology of the Walker Lake-MacLean Lake area (13K/9, 13J/ 12), Central Mineral Belt, Labrador. Nfld.

Mines. En. Min. Devt. Div. Rept 78-1/1-8

BAILEY,D.G.,FLANAGAN,M.J.,LALONDE,A.(1979) Geology of Eastern Central Mineral Belt (13J/10-15,130/2,3) Labrador. Nfld. Mines. En. Min. Devt. Div. Rept. 79-1/103-108

BAILEY,D.G.,FLANAGAN,M.J.,LALONDE,A.,DOHERTY,R.A.(1981) Kaipokok Bay - Big River map area; Nfld. Mines. En. Min. Devt. Div. Map 81-18.

BALASHOV,Y.A.,POZHARITSKAYA,L.K.(1968) Factors governing the behaviour of rare earth elements in the carbonatite process. Geochem. Int. 5/271-288

BARRIERE,M.(1976a) Flowage differentiation: limitation of the "Bagnold effect" to the narrow intrusions. Contrib. Mineral. Petrol. 55/139-145

BARRIERE,M.(1976b) Architecture et dynamisme du complexe eruptif centre de Ploumanac'h (Bretagne). Bull. Bur. Res. Min. Geol., Sec 1, Num 3/247-295

BARTH,T.F.W.,RAMBERG,I.B.(1966) The Fen circular complex. In: 'Carbonatites' ed.O.F.Tuttle and J.Gittins. p.225-257

BARUA,M.C.(1969) Geology of the U-Mo bearing rocks of the Aillik-Makkovik Bay area, Labrador. M.Sc.Thesis, Queens University, 76pp.

BHATTACHARJI,S.(1967) Mechanics of flow differentiation in ultramafic and mafic sills. J.Geol. 75/101-112

BLACK,R.,MORTON,W.H.,REX,D.C.(1976) Block tilting and volcanism within the Afar in the light of recent K/Ar age data. In: "Afar between Continental and Oceanic Rifting" ed.A.Pilger and A.Rossler

BOCTOR,N.Z.,SVISERO,D.P.(1978) Iron-titanium oxide and sulfide minerals in carbonatite from Jacupiranga, Brazil. Carn. Inst. Wash. Yb 78/876-880

BOETTCHER,A.L.,O'NEIL,J.R.,WINDOM,K.E.,STEWART,D.C.,WILSHIRE,H.G. (1979) Metasomatism of the upper mantle and the genesis of kimberlites and alkali basalts. Proc. 2nd. Int. Kim. Conf. 2/173-182.

BORODIN,L.S.,PYATENKO,I.K.(1978) General petrological aspects of Paleozoic alkali magmatism in the Kola peninsula and the rare earth distributions in alkali-ultrabasic lamprophyre dykes. Geochem. Int. 15/124-135

BRACE,W.F.(1978) Volume changes during fracture and frictional sliding: A review. Pure App. Geophys. 116/603-614

BRACE,W.F.,PAULDING,B.W.,SCHOLTZ,C.(1966) Dilatancy in the

fracture of crystalline rocks. J. Geophys. Res. 71/3939-3953

BRAVO,M.S.,O'HARA,M.J.(1975) Partial melting of phlogopite-bearing synthetic spinel- and garnet-lherzolites. Phys. Chem. Earth 9/845-854

BRIDGWATER,D.(1970) A compilation of K/Ar age determinations on rocks from Greenland carried out in 1969. Geol. Gronds. Unders. Rapp. 28/47-55

BRIDGWATER,D.(1971) Routine K/Ar age determinations on rocks from Greenland carried out for GGU in 1970. Geol. Gronds. Unders. Rapp. 35/52-60

BRIDGWATER,D.,ESCHER,A.,NASH,D.F.,WATTERSON,J.(1973) Investigations on the Nagssugtoqidian boundary between Holsteinsborg and Kangamiut, Central West Greenland. Geol. Gronds. Unders. Rapp. 55/22-25

BROGGER,W.C.(1921) Die Eruptivgesteine des Kristianiagebietes IV. Das Fengebiet in Telemark,Norwegen. Skr.Norske.Vidensk.i OsloMat-Natury.Kl. 9.

BROOKS,C.K.,NOE-NYGAARD,A.,REX,D.C.,RONSBO,J.G.(1978) An occurrence of ultrapotassic dykes in the neighbourhood of Holsteinsborg, West Greenland. Bull. Geol. Soc. Denmark 27/1-8

BUTAKOVA,E.L.,EGOROV,L.S.(1962) The Maimecha-Kotui complex of alkaline and ultrabasic rocks. In: 'Petrology of Eastern Siberia.' Acad.Sci. Moscow. p.419-589

BYERLEE,J.(1978) Friction of rocks. Pure App. Geophys. 116/615-626

CAMERON,M.,PAPIKE,J.J.(1981) Structural and chemical variations in pyroxenes. Am.Miner.66/1-51

CAMPBELL,I.H.,GORTON,M.P.(1980) Accessory phases and the generation of LREE- enriched basalts - a test for disequilibrium melting. Contrib. Miner. Petrol. 72/157-173

CARMAN,M.F.,CAMERON,M.,GUNN,B.,CAMERON,K.L.,BUTLER,J.C.(1975) Petrology of Rattlesnake Mountain sill, Big Bend national park, Texas. Bull. Geol. Soc. Am. 86/177-193

CARSWELL,D.A. (1975) Primary and secondary phlogopites and clinopyroxenes in garnet lherzolite xenoliths. Phys. Chem. Earth 9/417-429

CAWTHORN,R.G.(1974) Computer programs available for geological calculations. Memorial University unpubl.

CAWTHORN,R.G.,COLLERSON,K.D.(1974) The recalculation of pyroxene end-member parameters and the estimation of ferrous and

ferric iron content from electron microprobe analyses. Am.Mineral. 59/1203-1208

CHATTERJEE,S.K.(1974) 'Petrography of the igneous and metamorphic rocks of India'. 559pp.MacMillan,Madras

CHRISTIE,A.M.,ROSCOE,F.M.,FAHRIG,W.L.(1953) Preliminary map, central Labrador coast, Newfoundland (Descriptive notes). Geol. Surv. Can. Paper 53-14

CLARK,A.M.S.(1971) A structural reinterpretation of the Aillik Series, Labrador. M.Sc.thesis, Memorial University. 79pp.

CLARK,A.M.S.(1974) A reinterpretation of the stratigraphy and deformation of the Aillik Group, Makkovik, Labrador. Ph.D.thesis, Memorial University, 345pp.

CLARK,A.M.S.(1979) Proterozoic deformation and igneous intrusion in part of the Makkovik Sub-province, Labrador. Precamb.Res. 10/95-114

CLARKE,D.B.,PEDERSEN,A.K.(1975) Tertiary volcanic province of West Greenland. In:"Geology of Greenland" ed.A.Escher and W.S.Watt,.p.364-385

CLARKE,D.B.,UPTON,B.G.J.(1971) Tertiary basalts of Baffin Island: Field relations and tectonic setting. Can. J. Earth. Sci. 8/248-258

COLCHESTER,D.M.(1972) A preliminary note on kimberlite occurrences in South Australia. J. Geol. Soc. Austr. 19/383-386

COLLERSON,K.D.,MALPAS,J.(1977) Partial melts in upper mantle nodules from Labrador kimberlites. 2nd. Int. Kim. Conf. Ext. Abs.(unpaged).

COOPER,A.F.(1971) Carbonatites and fenitisation associated with a lamprophyric dyke swarm intrusive into schists of the New Zealand Geosyncline. Bull. Geol. Soc. Am. 82/1327-1340

COOPER,A.F.(1979) Petrology of ocellar lamprophyres from Western Otago, New Zealand. J.Petrol. 20/139-163

COOPER,G.E.(1951) The petrology of some syenites and granites in Labrador. M.Sc.thesis, McGill University

COX,K.G.,BELL,J.D.,PANKHURST,R.J.(1979) The interpretation of igneous rocks 450pp. George Allen and Unwin. London

CULLERS,R.L.,MEDARIS,G.(1977) Rare earth elements in carbonatite and cogenetic alkaline rocks: examples from Seabrook Lake and Callander Bay, Ontario. Contib. Miner. Petrol. 65/143-153

CURRIE,K.L.(1970) An hypothesis on the origin of alkaline rocks suggested by the tectonic setting of the Monteregian Hills. Can. Miner. 10/411-420

CURRIE,K.L.(1975a) 'The Alkaline Rocks of Canada' Bull. Geol. Surv. Can. 239, 228pp.

CURRIE,K.L.(1975b) The geology and petrology of the Ice River alkaline complex, British Columbia. Geol. Surv. Can. Bull. 245/65pp.

CURRIE,K.L.,FERGUSON,J.(1970) The mechanism of intrusion of lamprophyre dykes indicated by offsetting of dykes. Tectonophysics 9/525-535

CURTIS,L.W.,GITTINS,J.(1979) Aluminous and titaniferous clinopyroxenes from regionally metamorphosed agpaitic rocks in central Labrador. J.Petrol. 20/165-186

DALY,R.A.(1902) The geology of the northeast coast of Labrador. Bull. Museum. Comparative Zool. Harvard,38: Geol Sci 5, No.5/205-269

DAVIDSON,L.M.,PARK,R.G.(1978) Late Nagssugtoquidian stress orientation derived from deformed granodiorite dykes north of Holsteinsborg, West Greenland. J. Geol. Soc. Lond. 135/283-289

DAWSON,J.B.(1967) A review of the geology of kimberlite. In:'Ultramafic and Related Rocks' ed.P.J.Wyllie p.241-251

DAWSON,J.B.(1968) Recent researches on kimberlite and diamond geology. Econ. Geol. 63/504-511

DAWSON,J.B.(1971) Advances in kimberlite geology. Earth. Sci. Rev. 7/187-214

DAWSON,J.B.(1980) "Kimberlites and Their Xenoliths" Springer-Verlag,New York,250pp.

DAWSON,J.B.,SMITH,J.V.(1975) Chemistry and origin of phlogopite megacrysts in kimberlite. Nature 253/336-338

DAWSON,J.B.,SMITH,J.V.(1977) The MARID (mica-amphibole-rutile-ilmenite-diposide) suite of xenoliths in kimberlite. Geochim. Cosmochim. Acta 41/309-323

DELANEY,J.S.,SMITH,J.V.,CARSWELL,D.A.,DAWSON,J.B.(1980) Chemistry of micas from kimberlites and xenoliths II. Primary- and secondary-textured micas from peridotite xenoliths. Geochim. Cosmochim. Acta 44/857-872

DEPAULO,D.J.(1979) Implications of correlated Nd and Sr isotopic variations for the chemical evolution of the crust and mantle. Earth. Planet. Sci. Lett. 43/201-211

DEPAULO,D.J.,WASSERBURG,G.J.(1976) Nd isotopic variations and petrogenetic models. Geophys. Res. Lett. 3/249-252

DOHERTY,R.A.(1980) The geology of the Adlavik Islands. Nfld. Mines. En. Min. Devt. Div. Rept 80-1/161-165

DOIG,R.(1970) An alkaline province linking Europe and North America. Can. J. Earth. Sci. 7/22-28

DONALDSON,C.H.(1976) An experimental investigation of olivine morphology. Contrib. Miner. Petrol. 57/187-213.

DOUGLAS,G.V.(1953) Notes on localities visited on the Labrador coast in 1946 and 1947. Geol. Surv. Can. Paper 53-1

DREVER,H.I.(1960) Immiscibility in the picritic intrusion at Igdlorssuit, West Greenland. 21st Int. Geol. Congr. 13/47-58

DUNHAM,A.C.,EMELEUS,C.H.(1967) The Tertiary geology of Rhum, Inner Hebrides. Proc. Geol. Assn. 78/391

EBY,G.N.(1971) Rare earth, yttrium and scandium geochemistry of the Oka carbonatite complex, Oka, Quebec. Ph.D. thesis Boston Univ.

EGGLER,D.H.(1974) Effect of CO2 on the melting of peridotite. Carn. Inst. Wash. Yb. 73/215-224

EGGLER,D.H.(1976) Does CO2 cause partial melting in the low velocity layer of the mantle. Geology 4/69-72

EGGLER,D.H.(1977) The principal of the zone of invariant vapor composition: an example in the system CaO-MgO-SiO2-CO2-H2O and implications for the mantle solidus. Carn. Inst. Wash. Yb. 76/428-435

EGGLER,D.H.(1978) The effect of CO2 upon partial melting of peridotite in the system Na2O - CaO - Al2O3 - MgO - SiO2 - CO2 to 35 kb, with an analysis of melting in a peridotite - H2O - CO2 system. Am. J. Sci. 278/305-343

EGGLER,D.H.,WENDLANDT,R.F.(1978) Phase relations of a kimberlite composition. Carn. Inst. Wash. Yb. 77/751-756

EGGLER,D.H.,WENDLANDT,R.F.(1979) Experimental studies on the relationship between kimberlite magmas and partial melting of peridotite. Proc. 2nd. Int. Kim. Conf. 1/330-338

EGGLER,D.H.,KUSHIRO,I.,HOLLOWAY,J.R.(1976) Stability of carbonate minerals in a hydrous mantle. Carn. Inst. Wash. Yb. 75/631-636

EGGLER,D.H.,MYSEN,B.O.,HOERING,T.C.,HOLLOWAY,J.R.(1979) The solubility of carbon monoxide in silicate melts at high

pressures and its effect on silicate phase relations. Earth. Planet. Sci. Lett. 43/321-330

EGGLER,D.H.,BAKER,D.R.,WENDLANDT,R.F.(1980) fO2 of the assemblage graphite- enstatite-forsterite-magnesite: experiment and application to mantle fO2 and diamond formation. Geol. Soc. Am. Abs. Prog. 12/420.

EGOROV,L.S.(1970) Carbonatites and ultrabasic-alkaline rocks of the Maimecha- Kotui region, N.Siberia. Lithos 3/341-359

EHRENBERG,S.N.(1978) Petrology of potassic volcanic rocks and ultramafic xenoliths from the Navajo volcanic field, New Mexico and Arizona. Ph.D.thesis. U.C.L.A. 259pp.

ELDERS,W.H.,RUCKLIDGE,J.C.(1969) Layering and net veining in hornblende lamprophyre intrusions from the coast of Labrador. J.Geol. 77/721-729

EMELEUS,C.H.,ANDREWS,J.R.(1975) Mineralogy and petrology of kimberlite dyke and sheet intrusions and included peridotite xenoliths from Southwest Greenland. Phys. Chem. Earth 9/179-197

EMELEUS,C.H.,UPTON,B.G.J.(1976) The Gardar period in southern Greenland. In: "Geology of Greenland" ed.A.Escher and W.S.Watt. p.152-181

ESCHER,A.,WATTERSON,J.(1973) Kimberlites and associated rocks in the Holsteinsborg - Sondre Stromfjord region, Central West Greenland. Geol. Gronds. Unders. Rapp. 55/26-27

EVANS,C.R.,TARNEY,J.(1964) Isotopic ages of Assynt dykes. Nature 204/638-641

FAHRIG,W.L.,FREDA,G.,(1975) Paleomagnetism of the Mesozoic coast parallel dolerite dikes of West Greenland. Can. J. Earth. Sci. 12/1244-1248

FAHRIG,W.L.,LAROCHELLE,A.(1972) Paleomagnetism of the Michael Gabbro and possible evidence of the rotation of Makkovik Subprovince. Can. J. Earth. Sci. 9/1287-1296

FAHRIG,W.L.,IRVING,E.,JACKSON,G.D.(1971) Paleomagnetism of the Franklin diabases. Can. J. Earth. Sci. 8/455-467

FALLER,A.M.,SOPER,N.J.(1979) Palaeomagnetic evidence for the origin of the coastal flexure and dyke swarm in central E.Greenland. J. Geol. Soc. Lond. 136/737-744.

FAYE,C.H.,HOGARTH,D.D.(1968) On the origin of reverse pleochroism of a phlogopite. Can.Miner. 8/25-34

FERGUSON,J.(1973) The Pilanesberg alkaline province, Southern Africa. Trans. Geol. Soc. South Africa 76/249-270

FERGUSON,J.(1980) Tectonic setting and paleogeotherms of kimberlites with particular emphasis on Southeastern Australia. In: "Kimberlites and Diamonds" ed.J.E.Glover and D.I.Groves. Univ. Wn. Aus. Sp. Pub. 8,1-14

FERGUSON,J.,CURRIE,K.L.(1971) Evidence of liquid immiscibility in alkaline ultrabasic dykes at Callander Bay, Ontario. J.Petrol. 12/561-585

FERGUSON,J.,SHERATON,J.W.(1979) Petrogenesis of kimberlitic rocks and associated xenoliths of Southeastern Australia. Proc. 2nd. Int. Kim. Conf. 1/340-360

FESQ,H.W.,KABLE,E.J.D.,GURNEY,J.J.(1975) Aspects of the geochemistry of kimberlites from the Premier mine, and other selected South African occurrences with particular references to the rare earth elements. Phys. Chem. Earth 9/687-707

FINNERTY,A.A.,BOYD,F.R.(1978) Pressure depenedent solubility of calcium in forsterite coexisting with diposide and enstatite. Carn. Inst. Wash. Yb. 77/ 713-717.

FRANTSESSON,E.V.(1970) The Petrology of Kimberlite. trans.D.A.Brown. Austr. Nat. Univ. Publ. 150/195pp.

FRANK,F.C.(1965) On dilatancy in relation to seismic sources. Rev. Geophys. 3/484-503

FREESTONE,I.C.(1978a) Compositional dependence of liquid immiscibility. Prog. Exptl. Petrol. (NERC) 4/7-10

FREESTONE,I.C.(1978b) Liquid immiscibility in alkali-rich magmas. Chem. Geol. 23/115-123

FREUND,F.,KATHREIN,H.,WENGELER,H.,KNOBEL,R.,HEINEN,H.J.(1980) Carbon in solid solution in forsterite - a key to the untractable nature of reduced carbon in terrestrial and cosmogenic rocks. Geochim. Cosmochim. Acta 44/1319-1333

FRYER,B.J.(1977) Rare earth evidence in iron formation for changing oxidation states. Geochim. Cosmohcim. Acta. 41/361-367

GALLAGHER,M.J.(1963) Lamprophyre dykes from Argyll. Min. Mag. 33/415-430

GANDHI,S.S.(1976) Geology and isotopic ages of uranium occurences of Kaipokok Bay-Big River area,Labrador. unpubl.BRINEX rept.

GANDHI,S.S.,GRASTY,R.L.,GRIEVE,R.A.F.(1969) The geology and geochronology of the Makkovik Bay area, Labrador. Can. J. Earth. Sci. 6/1019-1035

GARSON,M.S.(1966) Carbonatites in Malawi. In: "Carbonatites" ed.O.F.Tuttle and J.Gittins. p.33-71

GAST,P.W.(1968) Trace element fractionation and the origin of tholeiitic and alkaline magma types. Geochim. Cosmochim. Acta 32/1057-1086

GILL,F.D.(1966) Petrography of molybdenite-bearing gneisses, Makkovik area, Labrador. M.Sc.thesis, Toronto University.

GITTINS,J.(1966) Summaries and bibliographies of carbonatite complexes. In: "Carbonatites" ed.O.F.Tuttle and J.Gittins. p.417-541

GITTINS,J.,ALLEN,C.R.,COOPER,A.F.(1975a) Phlogopitisation of pyroxenite; its bearing on the composition of carbonatite magmas. Geol. Mag. 112/503-507

GITTINS,J.,HEWINS,R.H.,LAURIN,A.F.(1975b) Kimberlitic-carbonatitic dykes of the Saguenay River Valley, Quebec, Canada. Phys. Chem. Earth 9/137-148

GOETTEL,K.A.(1976) Potassium in the earth's core: evidence and implications. p.479-489 In "The physics and chemistry of minerals and rocks" ed.R.G.J. Strens. Wiley. London.

GOLD,D.P.(1963) Average chemical composition of carbonatites. Econ. Geol. 58/ 988-991

GOLD,D.P.(1970) The Oka carbonatite and alkaline complex. In: "Geology of the Monteregian Hills" ed.G.Pouliot. p.43-62

GOLD,D.P.,MARCHAND,M.(1970) Alnoites, kimberlite and diatreme breccia pipes and dykes. In: 'Geology of the Monteregian Hills' ed.G.Pouliot. p.5-19

GOMES,C.B.,MORO,S.L.,DUTRA,C.V.(1970) Pyroxenes from the alkaline rocks of Itapirapua, Sao Paulo, Brazil. Am. Miner. 55/224-230

GOWD,T.N.,RUMMEL,F.(1980) Effect of confining pressure on the fracture behaviour of a porous rock. Int. J. Rock. Mech. Min. Sci. Geomech. Abs. 17/225-229

GOWER,C.F.(1980) Geology of the Benedict Mountains and surrounding areas (13J east and 13I). Nfld. Mines. En. Min. Devt. Div. Rept. 80-1/182-191

GOWER,C.F.(1981) "The Geology of the Benedict Mountains,Labrador" Nfld. Mines. En. Min. Devt. Div. Rept.81-3

GOWER,C.F.,RYAN,A.B.,BAILEY,D.G.,THOMAS,A.(1980) The position of the Grenville Front in eastern and central Labrador. Can. J. Earth. Sci. 17/784-787

GRASTY,R.L.,RUCKLIDGE,J.C.,ELDERS,W.H.(1969) New K-Ar age determinations on rocks from the east coast of Labrador. Can. J. Earth. Sci. 6/340-344

GREEN,H.W.,RADCLIFFE,S.V.(1975) Fluid precipitates in rocks from the earth's mantle. Bull. Geol. Soc. Am. 86/846-852

GRIFFIN,W.L.,TAYLOR,P.N.(1975) The Fen Damkjernite: Petrology of a "Central-Complex kimberlite". Phys. Chem. Earth 9/163-177

GURNEY,J.J.(1974) The origin of kimberlite - modern concepts. Trans. Geol. Soc. South Africa 77/353-361

GURNEY,J.J.,EBRAHIM,S.(1973) Chemical composition of Lesotho kimberlites. In: 'Lesotho Kimberlites' ed.P.H.Nixon. p.280-284

HAGGERTY,S.E.(1973) Spinels of unique composition associated with ilmenite reactions in the Liqhobong kimberlite pipe, Lesotho. In: "Lesotho Kimberlites" ed.P.H.Nixon. p.149-158

HAGGERTY,S.E.(1975) The chemistry and genesis of opaque minerals in kimberlite. Phys. Chem. Earth 9/295-307

HANSEN,K.(1980) Lamprophyres and carbonatitic lamprophyres related to rifting in the Labrador Sea. Lithos 13/145-152

HANSON,G.N.(1980) Rare earth elements in petrogenetic studies of igneous systems. Ann. Rev. Earth. Planet. Sci. 8/371-406

HARRIS,P.G.,MIDDLEMOST,E.A.K.(1970) The evolution of kimberlites. Lithos 3/ 77-88

HARTE,B.,COX,K.G.,GURNEY,J.J.(1975) Petrography and geological history of upper mantle xenoliths from the Matsoku kimberlite pipe. Phys. Chem. Earth 9/477-506

HARTMAN,P.(1969) Can Ti4+ replace Si4+ in silicates? Mineral. Mag. 37/366-369

HATCH,F.H.,WELLS,A.K.,WELLS,M.K.(1972) Petrology of the Igneous rocks. 551pp. Murby,London

HAWKINS,D.W.(1977) Emplacement, petrology and geochemistry of ultrabasic to basic intrusives at Aillik Bay, Labrador. M.Sc.thesis, Memorial University 236pp.

HEINRICH,E.W.(1966) Geology of Carbonatites. Rand and McNally, New York. 555pp.

HEINRICH,E.W.,MOORE,D.G.(1970) Metasomatic potash feldspar rocks associated with igneous alkalic complexes. Can. Miner. 10/571-584

HILL,D.P.(1977) A model for earthquake swarms. J. Geophys. Res.

82/1347-1352

HUANG,W.T.(1962) Petrology. 480pp. McGraw-Hill.

HUGGINS,F.E.,VIRGO,D.,HUCKENHOLTZ,H.G.(1977) Titanium-containing silicate garnets. I.The distribution of Al, Fe3+, and Ti4+ between octahedral and tetrahedral sites. Amer. Mineral. 62/475-490.

HURLBUT,C.S.,GRIGGS,D.T.(1939) Igneous rocks of the Highwood Mountains, Montana. Bull. Geol. Soc. Am. 50/1032-1112

ILUPIN,I.P.,SOBOLEV,S.F.,ZOLOTAREV,B.P.,LEBEDEV-ZINOVYEV,A.A. (1974) Geochemical specialisation of kimberlites from various parts of Yakutia. Geochem. Int. 11/357-370

IRVING,A.J.(1971) Geochemical and high pressure experimental studies of xenoliths, megacrysts and basalts from sotheastern Australia. Ph.D.thesis Australian Nat. Univ.

JAHN,B-M.,SUN,S-S.,NESBITT,R.W.(1979) REE distribution and petrogenesis of the Spanish Peaks Igneous Complex, Colorado. Contrib. Miner. Petrol. 70/281-298

JANSE,A.J.A.(1969) Gross Brukkaros, a probable carbonatite volcano in the Nama plateau of southwest Africa. Bull. Geol. Soc. Am. 80/573-586

JOHNSON,A.M.(1970) Dyke patterns at Spanish Peaks, Colorado. In: "Physical Processes in Geology"(Johnson) p.400-428

JOHNSON,R.L.(1966) The Shawa and Dorowa carbonatite complexes, Rhodesia. In: "Carbonatites" ed.O.F.Tuttle and J.Gittins p.205-244

KAITARO,S.(1952) On some offset structures in dilation dykes. Bull. Comm. Geol. Finl. 157/67-74

KAITARO,S.(1953) Geologic structure of the Late Precambrian intrusives in the Ava area, Aland Island. Bull. Comm. Geol. Finl. 162/71pp.

KAMINSKIY,F.W.,SAZONOVA,O.F,FRANTSESSON,Y.V.(1978) Rare-earth levels in kimberlites and ultrabasic xenoliths. Geochem. Int. 15, 4/68-74

KAPUSTIN,Y.L.(1966) Geochemistry of rare-earth elements in carbonatites. Geochem. Int. 3/1054-1064

KAY,R.W.,GAST,P.W.(1973) The rare earth content and origin of alkali-rich basalts. J.Geol. 81/653-682

KING,A.F.(1963) Geology of the Cape Makkovik Peninsula, Aillik, Labrador. M.Sc.thesis, Memorial University

KING,A.F.,MCMILLAN,N.J.(1975) A Mid-Mesozoic breccia from the coast of Labrador. Can. J. Earth. Sci. 12/44-51

KOMAR,P.D.(1976) Phenocryst interactions and the velocity profile of magma flowing through dykes or sills. Bull. Geol. Soc. Am. 87/1336-1342

KOSTER VAN GROOS,A.F.,WYLLIE,P.J.(1968) Liquid immiscibility in the join NaAlSi3O8-Na2O3-H2O and its bearing on the genesis of carbonatites. Am. J. Sci. 266/932-967

KOSTER VAN GROOS,A.F.,WYLLIE,P.J.(1973) Liquid immiscibility in the join NaAlSi3O8-Na2CO3-H2O. Am. J. Sci. 273/465-487

KRANCK,E.H.(1939) Bedrock geology of the seaboard region of Newfoundland- Labrador. Nfld. Geol. Surv. Bull. 19, 44pp.

KRANCK,E.H.(1947) Indications of movement of the earth-crust along the coast of Newfoundland-Labrador. Bull. Comm. Geol. Finl. 140/89-96

KRANCK,E.H.(1953) Bedrock geology of the seaboard of Labrador between Domino Run and Hopedale, Newfoundland. Geol. Surv. Can. Bull. 26/45pp.

KRANCK,E.H.(1961) An unusual type of deformation in a basic sill. Bull. Geol. Inst. Univ. Uppsala 40/163-168

KRESTEN,P.(1980) The Alno-Complex: tectonics of dyke emplacement. Lithos 13/ 153-158

KUMARAPELI,P.S.(1978) The St.Lawrence paleorift system: A comparative study. In: "Tectonics and Geophysics of Continental Rifts" ed.I.B.Ramberg and E.R. Neumann, D.Riedel. p.367-384.

KUSHIRO,I.(1969) Stability of amphibole and phlogopite in the upper mantle. Carn. Inst. Wash. Yb. 68/245-247

KUSHIRO,I.(1972) Effect of water on the composition of magmas formed at high pressures. J.Petrol. 13/311-344

KUSHIRO,I.(1975) On the nature of silicate melt and its significance in magma genesis: regularities in the shift of the liquidus boundaries involving olivine, pyroxene and silica minerals. Am. J. Sci. 275/411-431

KUSHIRO,I.(1980) Changes with pressure of degree of melting and K2O contents of liquids in the system Mg2SiO4-KAlSiO4-SiO2. Carn. Inst. Wash. Yb. 79/267-271

KUZNETSOVA,I.G.,POROSHIN,Y.Y.,ORLOV,D.M.(1980) Titanium in the structure of clinopyroxenes and its petrogenetic significance. Int. Geol. Review 22/1061-1066

LANGMHYR,F.J.,PAUS,P.E.(1968) The analysis of inorganic siliceous materials by atomic absorption spectrophotometry and the hydrofluoric acid decomposition technique. Pt.I. The analysis of silicate rocks. Anal. Chimica Acta 43/397-408

LARSEN,L.M.(1980) Lamprophyric and kimberlitic dykes associated with the Sarfartoq carbonatite complex, southern West Greenland. Geol. Gronds. Unders. Rapp. 100/65-69

LARSEN,O.(1966) K-Ar age determinations from Western Greenland. Geol. Gronds. Unders. Rapp.11/57-67

LARSEN,O.,MOLLER,J.(1968a) Potassium-Argon age studies in Western Greenland. Can. J. Earth. Sci. 5/683-691

LARSEN,O.,MOLLER,J.(1968b) K-Ar age determinations from West Greenland I. Reconnaissance program. Geol. Gronds. Unders. Rapp. 15/82-86

LEAKE,B.E.(1978) Nomenclature of amphiboles. Am. Miner. 64/1023-1062

LEBAS,M.J.(1977) Carbonatite-Nephelinite volcanism. Wiley.London. 347 pp.

LEBAS,M.J.(1980) Alkaline magmatism and uplift of continental crust. Proc. Geol. Assn. 91/33-38

LEBEDEV,A.P.(1964) Kimberlites of Northeastern U.S.S.R. and allied problems. Liv. Manch. Geol. J. 4/87-104

LEECH,G.B.,LOWDEN,J.A.,STOCKWELL,C.H.,WANLESS,R.K.(1963) Age determinations and geological studies. Geol. Surv. Can. Paper 63-17/114-117

LLOYD,F.E.,BAILEY,D.K.(1975) Light element metasomatism of the continental mantle: the evidence and the consequences. Phys. Chem. Earth 9/389-416

LOUBET,M.,BERNAT,M.,JAVOY,M.,ALLEGRE,C.J.(1972) Rare earth contents in carbonatites. Earth. Planet. Sci. Lett. 14/226-232

MACDONALD,R.(1966) Petrological studies of some alkalic and peralkalic dyke rocks from the Tugtutoq-Narssaq area. Geol. Gronds. Unders. Rapp. 11/44-47

MACKENZIE,D.E.,WHITE,A.J.R.(1970) Phonolite globules in basanite from Kiandra, Australia. Lithos 3/309-317

MADHAVAN,V.,LEELANANDAM,C.(1977) A study of the relative proportions of mafic and felsic rocks in the Elchuru alkaline massif, Andhra Pradesh. Chayanica Geologica 3/122-132

MADHAVAN,V.,LEELANANDAM,C.(1978) Some observations on the rocks of the Elchuru alkaline pluton, Prakasam district, Andhra Pradesh. J. Geol. Soc. India 19/523-526.

MARTEN,B.E.(1977) The relationship between the Aillik Group and the Hopedale Complex, Kaipokok Bay, Labrador. Ph.D.thesis, Memorial University 389pp.

MARTIN,H.,MATHIAS,M.,SIMPSON,E.S.W.(1960) The Damaraland sub-volcanic ring complexes in South West Africa. Int. Geol. Congr. 21st session, 13/156-174

MARTIN,R.J.(1980) Pore-pressure stabilization of failure in Westerly Granite. Geophys. Res. Lett. 7/404-406

MARTIN,R.J.,DURHAM,W.B.(1975) Mechanisms of crack growth in quartz. J. Geophys. Res. 80/4837-4844

MATHIAS,M.(1974) Alkaline rocks in southern Africa. In: "The Alkaline Rocks" ed.H.Sorensen. p.189-202. Wiley.

MCGETCHIN,T.R.,BESANCON,J.R.(1973) Carbonate inclusions in mantle-derived pyropes. Earth. Planet. Sci. Lett. 18/408-410

MCHONE,J.G.(1978) Distribution, orientations and ages of mafic dykes in central New England. Bull. Geol. Soc. Am. 89/1645-1655

MCLENNAN,S.M.,TAYLOR,S.R.(1980) Geochemical standards for sedimentary rocks: trace element data for USGS standards SCo-1,MAG-1 and SGR-1. Chem Geol. 29/333-343

MCMAHON,B.M.,HAGGERTY,S.E.(1979) The Oka carbonatite complex: magnetite compositions and the related role of titanium in pyrochlore. Proc. 2nd. Int. Kim. Conf. 1/382-392

MELCHER,G.L.(1966) The carbonatites of Jacupiranga, Sao Paulo, Brazil. In: "Carbonatites" ed.O.F.Tuttle and J.Gittins p.169-181

MINATIDIS,D.G.(1976) A comparative study of trace element geochemistry and mineralogy of some uranium deposits of Labrador, and evaluation of some uranium exploration techniques in a glacial terrain. M.Sc.thesis, Memorial University.

MITCHELL,R.H.(1973) Composition of olivine, silica activity and oxygen fugacity in kimberlite. Lithos 6/65-81

MITCHELL,R.H.(1975) Theoretical aspects of gaseous and isotopic equilibria in the system C-H-O-S with application to kimberlite. Phys. Chem. Earth 9/903-915

MITCHELL,R.H.(1978a) Composition of spinels in micaceous kimberlite from the Upper Canada Mine, Kirkland Lake,

Ontario. Can. Miner. 16/591-595

MITCHELL,R.H.(1978b) Manganoan magnesian ilmenite and titanian clinohumite from the Jacupiranga carbonatite, Sao Paulo, Brazil. Am. Miner. 63/544-547

MITCHELL,R.H.(1979a) The alleged kimberlite-carbonatite relationship: additional contrary mineralogical evidence. Am. J. Sci. 279/570-589

MITCHELL,R.H.(1979b) Mineralogy of the Tunraq kimberlite, Somerset Island, N.W.T., Canada. Proc. 2nd. Int. Kim. Conf. 1/171-179

MITCHELL,R.H.(1980) Pyroxenes of the Fen alkaline complex, Norway. Am. Miner. 65/45-54

MITCHELL,R.H.,BRUNFELT,A.O.(1975a) Rare-earth element geochemistry of kimberlite. Phys. Chem. Earth 9/671-686

MITCHELL,R.H.,BRUNFELT,A.O.(1975b) Rare earth element geochemistry of the Fen alkaline complex, Norway. Contrib. Miner. Petrol. 52/247-259

MOHR,P.A.,POTTER,E.C.(1976) The Sagatu Ridge dyke swarm, Ethiopian rift margin. J. Volc. Geotherm. Res. 1/55

MOLLER,P.,MORTEANI,G.,SCHLEY,F.(1980) Discussion of REE distribution patterns of carbonatites and alkalic rocks. Lithos 13/171-179

MOORE,A.E.,ERLANK,A.J.(1977) Olivine compositional complexity in olivine melilitites from Namaqualand, South Africa, and its bearing on kimberlite genesis. Ext. Abs. 2nd. Int. Kim. Conf. (unpaged)

MOORE,J.M.(1975) A mechanical interpretation of the vein and dyke systems of the S.W.England orefield. Min. Dep. 10/374-388

MOORE,T.H.(1951) Igneous dyke-rocks of the Aillik - Makkovik area, Labrador. M.Sc.thesis, McGill University

MOORHOUSE,W.W.(1959) The study of rocks in thin section. Harper and Row, New York. 514pp.

MURAMATSU,Y.(1977) Geochemische untersuchungen an kimberliten, einem Granat- peridotit und einem Eklogit-Einschlu ssaus-Kimberley, Südafrika. Ph.D. thesis. Gottingen.

MYSEN,B.O.(1975) Solubility of volatiles in silicate melts at high pressure and temperature: the role of carbon dioxide and water in feldspar, pyroxene and feldspathoid melts. Carn. Inst. Wash. Yb. 74/454-468

MYSEN,B.O.,BOETTCHER,A.L.(1975) Melting of a hydrous mantle II.

Geochemistry of crystals and liquids formed by anatexis of mantle peridotite at high pressures and high temperatures as a function of controlled activities of water, hydrogen and carbon dioxide. J. Petrol. 16/549-590

MYSEN,B.O.,POPP,R.K.(1978) Solubility of sulfur in silicate melts as a function of fS2 and silicate bulk composition at high pressures. Carn. Inst. Wash. Yb. 77/709-713

NAGASAWA,H.,SCHREIBER,H.D.,MORRIS,R.V.(1980) Experimental mineral/liquid partition coefficients of the rare earth elements (REE), Sc and Sr for perovskite, spinel and melilite. Earth. Planet. Sci. Lett. 46/431-437

NAKAMURA,R.,COOMBS,D.S.(1973) Clinopyroxene in the Tawhiroko tholeiitic dolerite at Moeraki, northeastern Otago, New Zealand. Contrib. Miner. Petrol. 42/213-228

NASLUND,H.R.(1976) Liquid immiscibility in the system KAlSi3O8-NaAlSi3O8-FeO- Fe2O3-SiO2 and its application to natural magmas. Carn. Inst. Wash. Yb. 75/ 592-597

NEUMANN,E.R.,RAMBERG,I.B.(1978) Paleorifts - concluding remarks. p.409-424 In: "Tectonics and Geophysics of Continental Rifts" ed. I.B.Ramberg and E.R. Neumann. D.Riedel

NIXON,P.H.,MITCHELL,R.H.,ROGERS,N.W.(1980) Petrogenesis of alnoitic rocks from Malaita, Solomon Islands, Melanesia. Min. Mag. 43/587-596

NUR,A.(1972) Dilatancy, pore fluids, and premonitory variations of ts/tp travel times. Bull. Seismol. Soc. Am. 62/1217-1222

ODE,H.(1957) Mechanical analysis of the dyke pattern of the Spanish Peaks area, Colorado. Bull. Geol. Soc. Am. 68/567-576

O'HARA,M.J.,YODER,H.S.(1967) Formation and fractionation of basaltic magmas at high pressures. Scot. J. Geol. 3/67-117

PASTERIS,J.D.(1981) Kimberlites: Strange bodies? EOS (Trans. Am. Geophys. Union) 62/ 713-716

PATERSON,M.S.(1978) Experimental rock deformation - The brittle field. Springer-Verlag,New York. 254pp.

PAUL,D.K,(1980) Indian diamonds and kimberlites. In: 'Kimberlites and Diamonds' ed.J.E.Glover and D.I.Groves. Univ. Wn. Austr. Sp. Pub. 5/48-63

PAUL,D.K.,POTTS,P.J.,GIBSON,I.L.,HARRIS,P.G.(1975) Rare-earth abundances in Indian kimberlites. Earth. Planet. Sci. Lett. 25/151-158

PHILLIPS,W.J.(1968) The crystallisation of the teschenite from

the Lugar Sill, Ayrshire. Geol. Mag. 105/23-34

PHILLIPS,W.J.(1973) Interpretation of crystalline spheroidal structures in igneous rocks. Lithos 6/235-244

PHILLIPS,W.J.(1974) The dynamic emplacement of cone sheets. Tectonophysics 24/69-84

PHILPOTTS,A.R.(1972) Density, surface tension and viscosity of the immiscible phase in a basic alkaline magma. Lithos 5/1-18

PHILPOTTS,A.R.(1976) Silicate liquid immiscibility: its probable extent and petrogenetic significance. Am. J. Sci. 276/1147-1177

PHILPOTTS,A.R.(1977) Archean variolites - quenched immiscible liquids: discussion. Can. J. Earth. Sci. 14/139-144

PHILPOTTS,J.A.(1970) Redox estimation from a calculation of Eu2+ and Eu3+ concentrations in natural phases. Earth. Planet. Sci. Lett. 9/257-268

PIPER,J.D.A.,GIBSON,I.L.(1972) Stress control of processes at extensional plate margins. Nature Phys. Sci. 238/83-86

PLATT,R.G.,MITCHELL,R.H.(1979) The Marathon Dikes: I.Zirconium rich titanian garnets and manganoan magnesian ulvospinel-magnetite spinels. Am.Min. 64/546-550

POLLARD,D.D.(1973) Derivation and evolution of a mechanical model for sheet intrusion. Tectonophysics 19/233-269

POLLARD,D.D.,JOHNSON,A.M.(1973) Mechanics of growth of some laccolithic intrusions in the Henry Mountains, Utah II; Bending and failure of overburden layers and sill formation. Tectonophysics 18/311-354

POLLARD,D.D.,MULLER,O.H.,DOCKSTADER,D.R.(1975) The form and growth of fingered sheet intrusions. Bull. Geol. Soc. Am. 86/351-363

POULIOT,G.(1970) Study of carbonatitic calcites from Oka, Que. Can. Mineral.10/ 511-540

RAMSAY,D.M.,STURT,J.A.(1970) The emplacement and metamorphism of a synorogenic dyke swarm from Stjernoy, northwest Norway. Am. J. Sci. 268/264-286

RILEY,G.C.(1951) The bedrock geology of the Makkovik area and its relation to the Aillik and Kaipokok Series. M.Sc.thesis, McGill University

RIMSAITE,J.(1971) Distribution of major and minor constituents between mica and host ultrabasic rocks and between zoned

mica and zoned spinel. Contrib. Miner. Petrol. 33/259-272

RINGWOOD,A.E.(1966) Mineralogy of the mantle. In:'Advances in Earth Sciences' ed.P.M.Hurley p.357-399. M.I.T.Press

RINGWOOD,A.E.(1975) Composition and petrology of the Earth's mantle. McGraw- Hill. New York

ROBERT,J-L.(1976) Titanium solubility in synthetic phlogopite solid solutions. Chem. Geol. 17/213-227

ROCK,N.M.S.(1977) The nature and origin of lamprophyres: some definitions, distinctions and derivations. Earth. Sci. Rev. 13/123-169

RODEN,M.F. (1981) Origin of coexisting minette and ultramafic breccia, Navajo volcanic field. Contrib. Miner. Petrol. 77/195-206

RODEN,M.F.,SMITH.D.(1979) Field geology, chemistry and petrology of Buell Park minette diatreme, Apache County, Arizona. Proc. 2nd. Int. Kim. Conf. 1/364-381

RODEN,M.F.,SMITH,D.,MCDOWELL,F.W.(1979) Age and extent of potassic volcanism on the Colorado plateau. Earth. Planet. Sci. Lett. 43/279-284

RODRIGUES,B.(1970) Major tectonic alignments of alkaline complexes in Angola. Proc.Conf.Afr.Geol.Ibadan. ed.T.F.J.Dessauvagie and A.J.Whiteman. p.149-153

ROEDDER,E.(1965) Liquid CO2 inclusions in olivine-bearing nodules and phenocrysts in basalts. Am. Mineral. 50/1746-1782

ROEDDER,E.(1979) Silicate liquid immiscibility. In:'The evolution of the igneous rocks, fiftieth aniversary perspectives. ed.H.S.Yoder. Priceton Univ. Press. p.15-57

ROEDER,P.L.,EMSLIE,R.F.(1970) Olivine-liquid equilibrium. Contrib. Miner. Petrol. 29/275-289

ROYDEN,L.,KEEN,C.E.(1980) Rifting process and thermal evolution of the continental margin of Eastern Canada determined from subsidence curves. Earth. Planet. Sci. Lett. 51/343-361

RUDNICKI,J.W.(1980) Fracture mechanics applied to the earth's crust. Ann.Rev. Earth. Planet. Sci. 8/489-525

RYAN,A.B.(1979) Regional geological mapping in the central mineral belt, 1978 (13K/east), Labrador. Nfld. Mines. En. Min. Devt. Div. Rept. 79-1/90-94

RYAN,A.B.,KAY,E.A.(in press) Basement-cover relationships and plutonic rocks in the Makkovik Subprovince, north of Postville, coastal Labrador (13J/3, 13O/4). Nfld. Dept.

Mines. En. Min. Devt. Div. Rept.

RYERSON,F.J.,HESS,P.C.(1980) The role of P2O5 in silicate melts. Geochim. Cosmochim. Acta.44/611-624

SAFFMAN,P.G.,TAYLOR,G.(1958) The penetration of a fluid into a porous medium or Hele-Shaw cell containing a more viscous fluid. Proc. Roy. Soc. Lond. Ser. A. 245/312-329

SCOTT,B.H.(1979) Petrogenesis of kimberlites and associated potassic lamprophyres from central west Greenland. Proc. 2nd. Int. Kim. Conf. 1/190-205

SECHER,K.,LARSEN,L.M.(1978) A new Phanerozoic carbonatite complex in South West Greenland. Geol. Gronds. Unders. Rapp. 90/46-50

SECHER,K.,LARSEN,L.M.(1980) Geology and mineralogy of the Sarfartoq carbonatite complex, southern West Greenland. Lithos 13/199-212

SIMKIN,T.,SMITH,J.V.(1970) Minor element distribution in olivine. J.Geol. 78/304-325

SMITH,C.B.(1977) Kimberlite and mantle derived xenoliths at Iron Mountain, Wyoming. M.Sc. thesis. Colorado State University. 164pp.

SMITH,D.(1979) Hydrous minerals and carbonates in peridotite inclusions from the Green knobs and Buell Park kimberlitic diatremes on the Colorado Plateau. Proc. 2nd. Int. Kim. Conf. 2/345-356

SMITH,R.E.(1967) Segregaton vesicles in basaltic lava. Am. J. Sci. 265/696-713

SMITH,J.V.,BRENNESHOLTZ,R.,DAWSON,J.B.(1978) Chemistry of micas from kimberlites and xenoliths: I.Micaceous kimberlites. Geochim. Cosmochim. Acta 42/959-971

SMYTH,W.R.,MARTEN,B.E.,RYAN,A.B.(1975) Geological mapping in the Central Mineral Belt, Labrador: redefinition of the Croteau Group. Nfld. Mines. En. Min. Devt. Div. Rept. 75-1/51-74

SNYMAN,P.C.(1974) Possible classification parameters of South African kimberlites. Trans. Geol. Soc. South Africa 77/85-91

SOMERVILLE,M.,AHRENS,T.J.(1980) Shock compression of KFeS2 and the question of potassium in the core. J. Geophys. Res. 85/7016-7024

SORENSEN,H.(1974) "The Alkaline Rocks" Wiley. 622pp.

SPRY,A.(1969) Metamorphic Textures. Pergamon, Oxford. 350pp.

STEVENSON,I.M.(1970) Rigolet and Groswater map areas, Newfoundland (Labrador). Geol. Surv. Can. Paper 69-48

STOCKWELL,C.H.(1964) Fourth Report on structural provinces,orogenesis, and time-classification of rocks of the Canadian Precambrian Shield. Geol. Surv. Can. Paper 64-17

STRACKE,K.J.,FERGUSON,J.,BLACK,L.P.(1979) Structural setting of kimberlites in southeastern Australia. Proc. 2nd. Int. Kim. Conf. 1/71-91

STRECKEISEN,A.(1979) Classification and nomenclature of volcanic rocks, lamprophyres, carbonatites and melilitic rocks. Neues. Jb. Min. Abh. 134/1-14

STRONG,D.F.,HARRIS,A.(1974) The petrology of Mesozoic alkaline intrusives of Central Newfoundland. Can. J. Earth Sci. 11/1208-1219

SUBRAMANIAM,V.,VILADKAR,S.G.,UPENDRAN,R.(1978) Carbonatite-alkali complex of Samalpatti, Dharmapuri district, Tamil Nadu. J. Geol. Soc. India 19/206-216

SUN,S-S.,HANSON,G.N.(1975) Origin of Ross Island basanitoids and limitations upon the heterogeneity of mantle sources for alkali basalts and nephelinites. Contrib. Miner. Petrol. 52/77-106

SUTTON,J.S.(1972) The Precambrian gneisses and supracrustal rocks of the western shore of Kaipokok Bay, Labrador, Newfoundland. Can. J. Earth. Sci. 9/1677-1692

TAYLOR,F.C.(1971) A revision of the Precambrian structural provinces in Northeastern Quebec and Northern Canada. Can. J. Earth. Sci. 8/579-584

TAYLOR,F.C.(1972) The Nain Province. In: Variation in Tectonic styles in Canada. (ed.R.A.Price and R.J.W.Douglas) Geol. Surv. Can. Sp. Paper 11/436-452

UKHANOV,A.V.(1965) Olivine melilitite from the diamond-bearing diatremes on Anabar. Dokl. Akad. Nauk, Earth Sci. Sec. 153/176-178

UPTON,B.G.J.(1970) Basic rocks of the Gardar igneous province. Geol.Gronds. Unders. Rapp. 28/26-29

UPTON,B.G.J.(1974) The alkaline province of southwest Greenland. In: "The Alkaline Rocks" ed.H.Sorensen. p.221-238

UPTON,B.G.J.,WADSWORTH,W.J.(1971) Rhyodacite glass in Reunion basalt. Min.Mag. 38/152-159

VAN DER LINDEN,W.J.M.(1975) Crustal attenuation and sea-floor

spreading in the Labrador Sea. Earth. Planet. Sci. Lett. 27/409-423

VAN DER LINDEN,W.J.M.(1977) How much continent under the ocean. Marine Geophys. Res. 3/209-224

VAN DER LINDEN,W.J.M.,SRIVASTAVA,S.P.(1975) The crustal structure of the continental margin off central Labrador. Geol. Surv. Can. Paper 74-30/233-245

VARTIAINEN,H.,KRESTEN,P.,KAFKAS,K. (1978) Alkaline lamprophyres from the Sokli complex, northern Finland. Bull.Geol.Surv.Finl.50/59-68

VELDE,D.(1975) Armalcolite - Ti-phlogopite - diopside - analcite bearing lamproites from Smoky Butte, Garfield County, Montana. Am. Miner. 60/566-573

VISSER,W.,KOSTER VAN GROOS,A.F.(1979) Effect of pressure on liquid immiscibility in the system K20 - FeO - Al203 - SiO2 - P205. Am. J. Sci. 279/1160-1175

VON ECKERMANN,H.(1948) The alkaline district of Alno Island. Sveriges Geol. Unders. ser. Ca. No.36

VON ECKERMANN,H.(1966) Progress of research on the Alno carbonatite. In: "Carbonatites" ed.O.F.Tuttle and J.Gittins. p.3-31

WALKER,G.P.L.(1975) A new concept of the evolution of the British Tertiary intrusive centres. J. Geol. Soc. Lond. 131/121-141

WALTON,B.(1966) Carbonatite-lamprophyre dykes of Mesozoic age. Geol. Gronds. Unders. Rapp. 11/37-39

WANLESS,R.K.,STEVENS,R.D.,LACHANCE,G.R.,DELABIO,R.N.(1970) Age determinations and geological studies. K-Ar isotopic ages, report 9. Geol. Surv. Can Paper 69-2A/73-74

WANLESS,R.K.,STEVENS,R.D.,LACHANCE,G.R.,DELABIO,R.N.(1972) Age determinations and geological studies. K-Ar isotopic ages, report 10. Geol. Surv. Can. Paper 71-2/88-89

WANLESS,R.K.,STEVENS,R.D.,LACHANCE,G.R.,DELABIO,R.N.(1974) Age determinations and geological studies. K-Ar isotopic ages, report 11. Geol. Surv. Can. Paper 73-2/101-104

WASS,S.Y.,ROGERS,N.W.(1980) Mantle metasomatism - precursor to continental alkaline volcanism. Geochim. Cosmochim. Acta 44/1811-1823

WATSON,E.B.(1976) Two-liquid partition coefficients: experimental data and geochemical implications. Contrib. Miner. Petrol. 56/119-134

WATSON,E.B.(1979) Apatite saturation in basic to intermediate magmas. Geophys. Res. Lett. 6/937-940

WATSON,E.B.(1980) Apatite and phosphorus in mantle source regions: an experimental study of apatite/melt equilibria at pressures to 25 kbar. Earth. Planet. Sci. Lett. 51/322-335

WATT,W.S.(1969) The coast-parallel dyke swarm of Southwest Greenland in relation to the opening of the Labrador Sea. Can. J. Earth Sci. 6/1320-1321

WEDEPOHL,K.H.(1975) The contribution of chemical data to assumptions about the origin of magmas from the mantle. Fortschr. Mineral. 52/141-172

WEDEPOHL,K.H.,MURAMATSU,Y.(1979) The chemical composition of kimberlites compared with the average composition of three basaltic magma types. Proc. 2nd. Int. Kim. Conf. 1/300-312

WENDLANDT,R.F.,HARRISON,W.J.(1979) Rare earth partitioning between immiscible carbonate and silicate lquids and CO2 vapour: results and implications for the formation of light rare earth-enriched rocks. Contrib. Miner. Petrol. 69/409-419

WHEELER,E.P.(1933) Diabase dykes on the Labrador coast. J. Geol. 41/418-431

WHITE,M.V.W.(1976) A Petrological study of acid volcanic rocks in a part of the Aillik Series, Labrador. M.Sc.thesis, McGill University 92pp.

WILLIAMS,H.,TURNER,F.J.,GILBERT,C.M.(1955) Petrography. W.H.Freeman, San Francisco, 406pp.

WRIGHT,T.L.,DOHERTY,P.C.(1970) A linear programming and least squares computer method for solving petrological mixing problems. Bull. Geol. Soc. Am. 81/ 1995-2008

WYLLIE,P.J.(1977a) Mantle fluid compositions buffered by carbonates in peridotite - CO2 - H2O. J. Geol. 85/187-207

WYLLIE,P.J.(1977b) Peridotite - CO2 - H2O, and carbonatitic liquids in the upper asthenosphere. Nature 266/45-47

WYLLIE,P.J.(1979) Kimberlite magmas from the system peridotite-CO2-H2O. Proc. 2nd. Int. Kim. Conf. 1/319-329

WYLLIE,P.J.(1980) The origin of kimberlite. J. Geophys. Res. 85/6902-6910

WYLLIE,P.J.,HUANG,W.L.(1975) Peridotite, kimberlite and carbonatite explained in the system CaO-MgO-SiO2-CO2. Geology 3/621-624

YODER,H.S.(1978) Basic magma generation and aggregation. Bull. Volcanol. 41/ 301-316.

ZUSSMAN,J.(1979) The crystal chemistry of the micas. Bull. Mineral. 102/5-13

* SKINNER,E.M.W.,CLEMENT,C.R.(1979) Mineralogical classification of Southern African kimberlites.Proc. 2nd. Int. Kim. Conf. 1/129-139

APPENDIX I: ANALYTICAL TECHNIQUES USED IN THIS STUDY

A.MAJOR AND TRACE ELEMENT WHOLE ROCK ANALYSES

Rock powders were prepared by (a) removing weathered edges with a trim saw, and splitting the rock with a hammer beneath plastic to minimise metal contamination from the hammer head, (b) powdering rock chips in a tungsten carbide ball mill for 3. minutes. The ball mill and rings were cleaned thoroughly between samples by washing with distilled water, and then drying with compressed air. The powders were stored in a glass jar until use.

MAJOR ELEMENTS: Major elements were determined by atomic absorption spectroscopy by Mrs C.Andrews on a Perkin Elmer 370 atomic absorption spectrometer using a method modified after that of Langmhyr and Paus (1968). Synthetic standards were used. Loss on ignition was determined by weighing an amount of sample in a porcelain crucible, heating to 1050 C for two hours, cooling in a dessicator, and weighing to determine the percent loss of volatiles.

TRACE ELEMENTS: Pressed pellets were prepared by weighing out 10g rock powder and mechanically mixing with 1 - 1.5g phenyl formaldehyde thermal binding agent. After pressing into a pellet, the discs were fused by baking in an oven at 200 C for 10 minutes. Trace elements were determined with a Philips 1450 x-ray fluorescence spectrometer with teletype input/output and automatic sample change. Analytical calibration programs were prepared by D.Press. USGS PCC-1 was used as a monitoring standard. Analyses are considered accurate to within 10ppm for

most elements, and 10-25 ppm for Ba, Sr and V. Precision is within 10 ppm.

B.RARE EARTH ELEMENTS

Rare earth elements were determined for selected samples by a modified thin-film x-ray fluorescence method similar to that described by Fryer (1977) after Eby (1971,p.45-85). Samples were weighed out accurately to contain 20 mg yttrium, using determinations from pressed pellets. This involved weights of 0.06 to 1.4 g for the samples in this study. 2 ml of 25 mg Tm solution and 10ml 6N HCl were added to the powders and centrifuged for 4 minutes. Excess solution was then decanted, and the remaining material evaporated to dryness on a hot plate in a 100 ml teflon beaker. After this initial step, the method of Fryer (1977) was followed.

C. ELECTRON MICROPROBE ANALYSES

Mineral analyses were obtained using a fully automated JEOL JXA-50A electron probe microanalyser with Kriesel control through a PDP-11 computer. Analyses were performed with a beam current of 0.21 - 0.23 microamps, a beam diameter of approximately 1 micron (larger for feldspars) and an accelerating voltage of 15KV. Counts were made for 30 seconds or to a maximum of 30,000 counts, and corrected by the MAGIC correction program.

Calibrations against known standards were used as outlined below:

Olivine and clinopyoxene: Si,Al,Mg,Ca = pyroxene; Fe,Mn

hedenbergite; Na = jadeitic pyroxene; K = orthoclase; Ti = titanpyroxene; Cr = chromian spinel; Ni = nickel olivine.

Mica: Si,Al,Mg,Ca,Fe = Pyrope garnet; Na,K,Ti,Mn as for clinopyroxene.

Carbonate: Fe,K,Na = hornblende; Al,Mn = hedenbergite; Mg,Ca = dolomite; Si,Ba = barium glass; P = apatite; Sr = aragonite.

Feldspar: Si,Al,Na,Sr = anorthoclase; K = orthoclase; Ca = plagioclase; Fe = hedenbergite.

Oxides: Mg,Al,Ti,Fe = synthetic glass; Cr = chromian spinel; Mn = hedenbergite.

APPENDIX II:

Analyses of coarse-grained ultramafic rocks associated with the Alkaline Complex

Anal.	369	370	386	429
SiO2	31.50	33.40	32.80	30.00
TiO2	5.29	3.63	4.90	4.29
Al2O3	4.50	2.03	6.24	4.94
Fe2O3	12.78	14.45	13.97	13.85
MgO	21.32	30.00	9.45	16.93
MnO	0.25	0.35	0.22	0.27
CaO	13.38	10.05	21.60	14.60
Na2O	0.62	0.39	0.43	0.32
K2O	1.97	0.91	1.82	3.04
P2O5	2.50	1.85	3.10	1.36
LOI	4.29	2.84	3.75	8.93
Total	98.40	99.90	98.28	98.19
Ni	159	259	38	412
Cr	0	0	0	640
V	148	121	208	200
Rb	57	20	47	80
Sr	1084	973	1243	1460
Ba	1034	<491	1137	4569
Zn	89	104	101	107
Zr	408	298	823	437
Cu	68	14	96	7
Ga	7	3	11	10
U	5	3	0	11
Th	15	13	0	25
Nb	279	239	320	253
La	283	250	208	651
Ce	438	411	249	893
Y	75	69	100	50

EXPLANATION:

369, 370 : Peridotite, Turnavik Island
386 : Mica-clinopyroxene rock, Cape Makkovik
429 : Pyroxene glimmerite, Cape Makkovik

Analyses of intrusives predating the alkaline complex

Anal.	389	403	302	343	434	391	352
SiO2	45.40	43.80	52.90	45.60	41.90	44.20	44.60
TiO2	0.20	1.95	0.72	2.31	2.40	3.77	3.01
Al2O3	4.32	15.50	15.10	15.40	7.74	16.48	12.70
Fe2O3*	12.52	14.85	8.44	14.51	12.69	16.48	12.70
MgO	28.80	6.68	6.50	5.98	17.35	4.48	3.03
MnO	0.16	0.33	0.15	0.20	0.16	0.22	0.10
CaO	2.10	6.73	9.15	8.15	8.03	7.15	7.43
Na2O	0.42	2.61	3.09	2.98	1.61	3.54	3.75
K2O	2.00	4.77	1.76	0.78	3.71	2.26	2.49
P2O5	0.00	0.18	0.05	0.28	0.65	1.30	1.86
LOI	2.70	1.82	1.47	2.84	2.44	1.16	3.52
Total	98.62	100.22	99.33	99.03	98.68	98.76	98.37
Ni	640	47	24	64	517	0	3
Cr	1171	37	165	58	378	0	0
V	46	244	205	191	137	79	155
Rb	57	229	39	35	107	39	73
Sr	30	222	497	418	1461	460	702
Ba	443	694	522	504	2294	1379	1524
Zn	99	535	69	109	118	103	72
Zr	44	107	91	181	268	233	182
Cu	235	0	0	13	4	0	7
Ga	3	21	17	21	14	18	18
U	0	0	0	2	0	0	0
Th	0	0	4	2	0	0	0
Nb	5	4	6	13	79	19	37
La	31	35	41	60	107	88	98
Ce	22	39	40	96	108	119	132
Y	14	35	46	39	23	57	43

EXPLANATION:

389 : Hornblende peridotite
403 : H1 amphibolite dyke
302,343,434 : H2 diorite dyke
391,352 : H3 diabase

Figure 1-4b

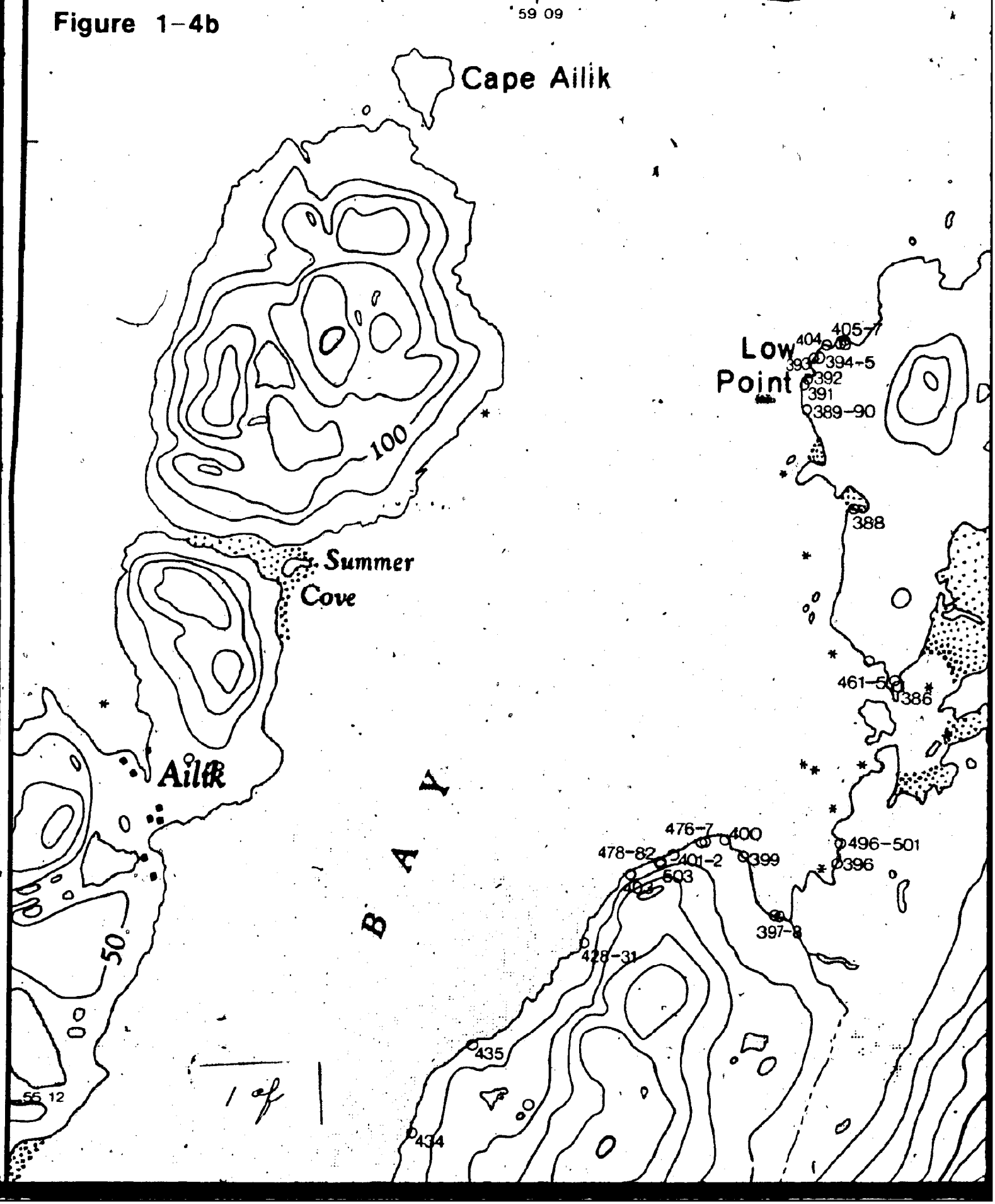
59 09
Cape Ailik
Low Point
Summer Cove
Ailik
B A Y
100
50
404
405-7
394-5
392
391
389-90
388
386
476-7
400
478-82
401-2
399
503
496-501
396
397-8
428-31
435
434
56 12

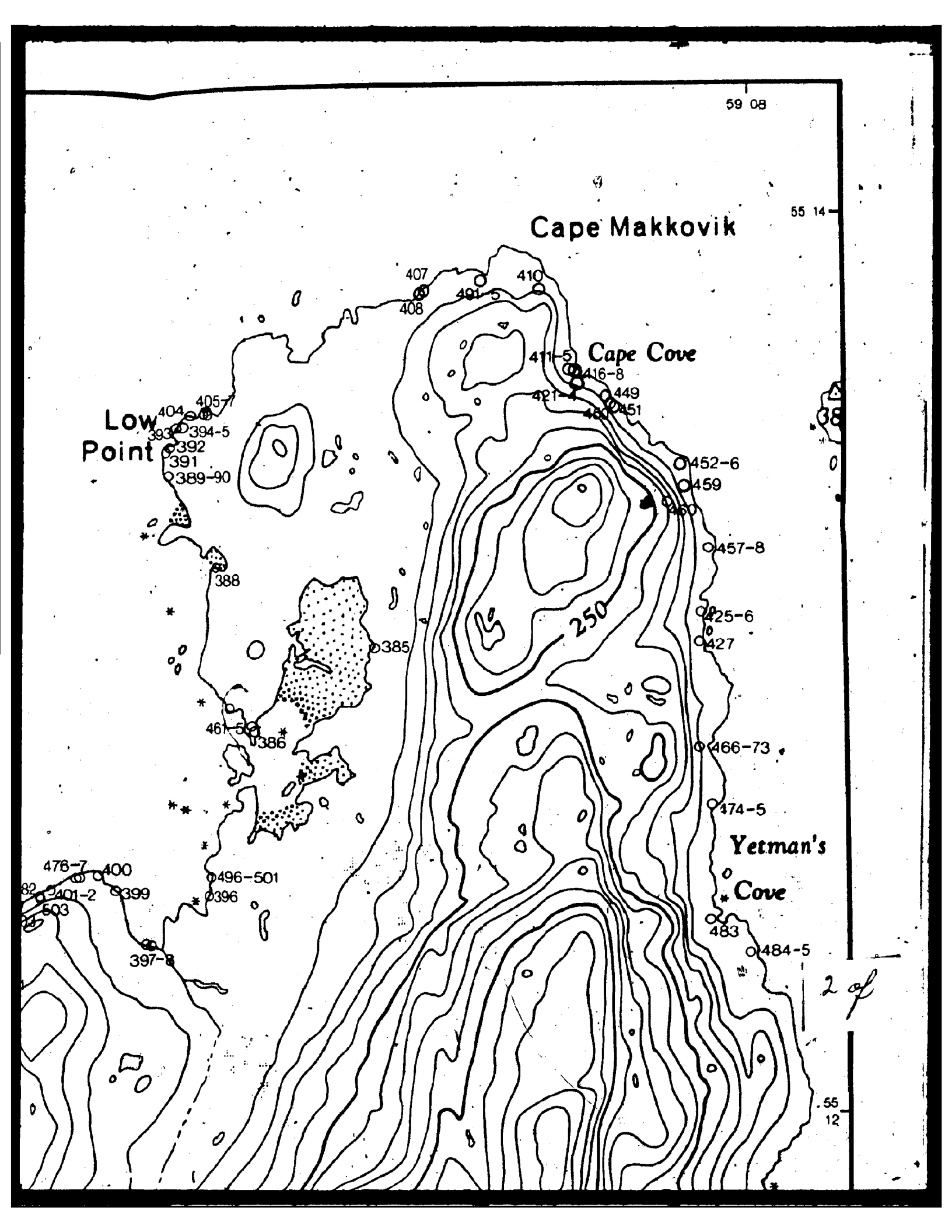
59 08
55 14
Cape Makkovik
Cape Cove
Low Point
Yetman's Cove
250
407
408
410
491-5
411-5
416-8
449
451
421-4
480
405-7
404
393
394-5
392
391
389-90
452-6
459
460
457-8
388
425-6
427
385
461-5
386
466-73
474-5
476-7
400
401-2
399
503
496-501
396
397-8
483
484-5
2 of
55
12

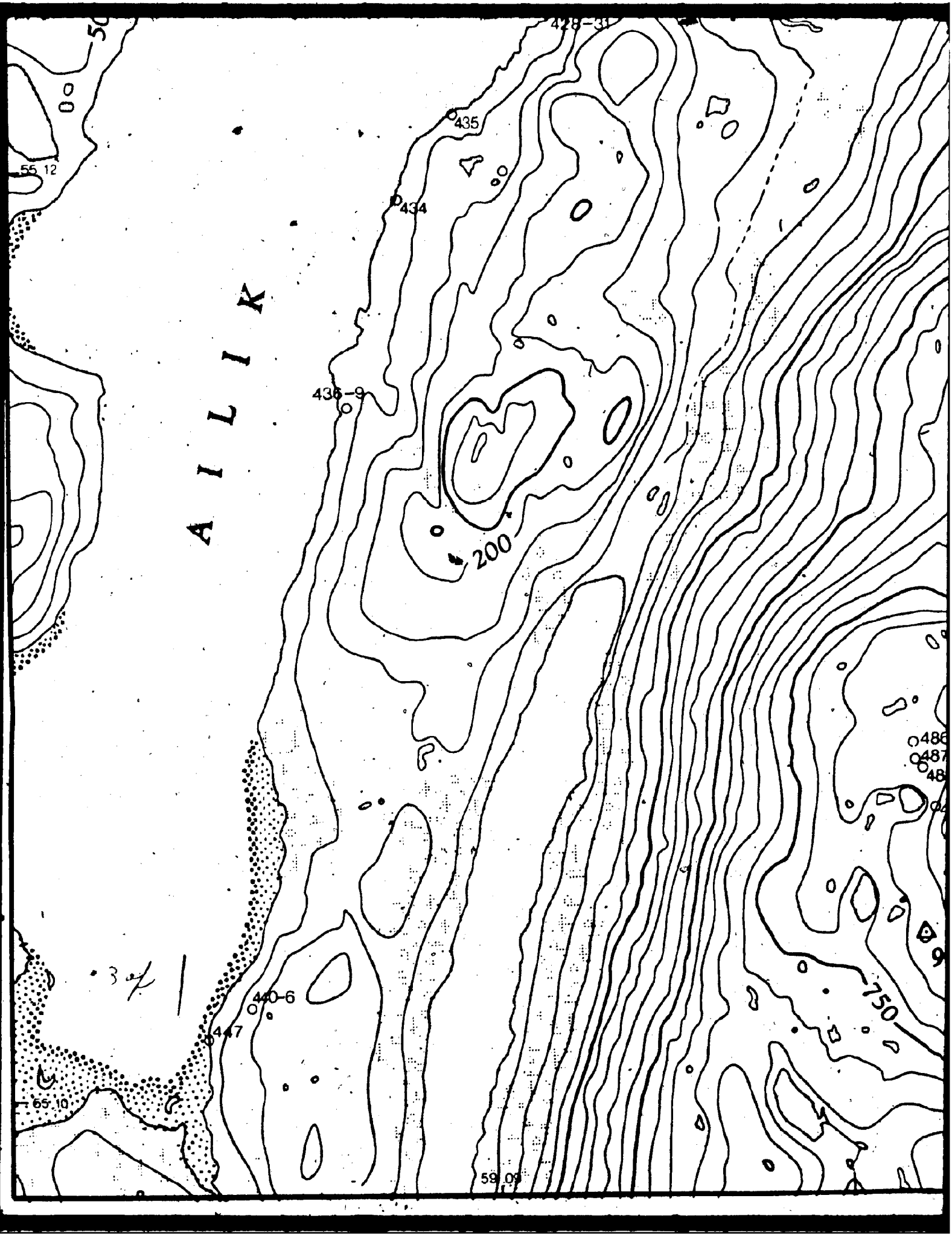
AILIK
435
434
436-9
200
750
440-6
447
55 12
65 10
59 09

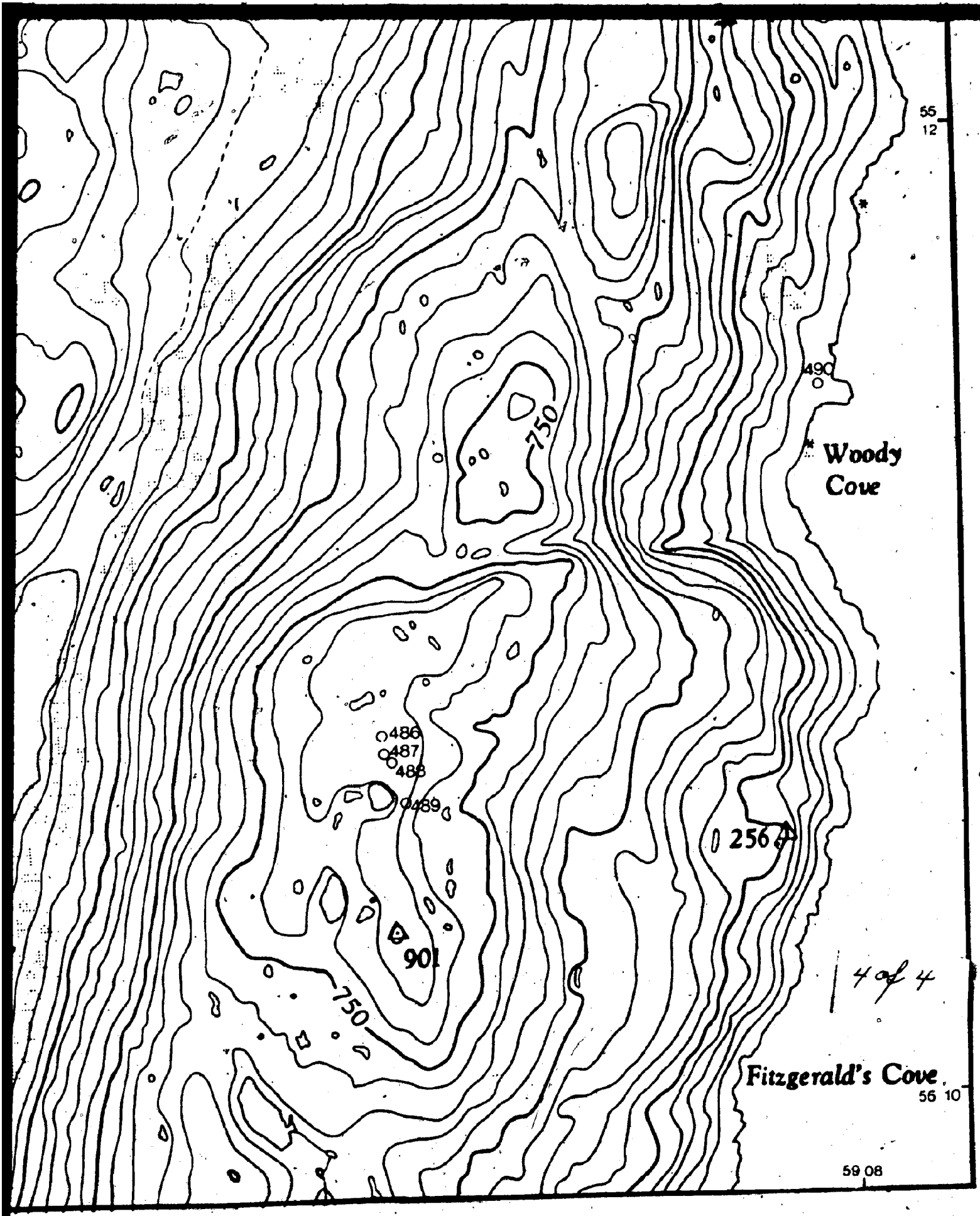
55
12
490
Woody
Cove
750
486
487
488
489
256
901
750
1 of 4
Fitzgerald's Cove
56 10
59 08

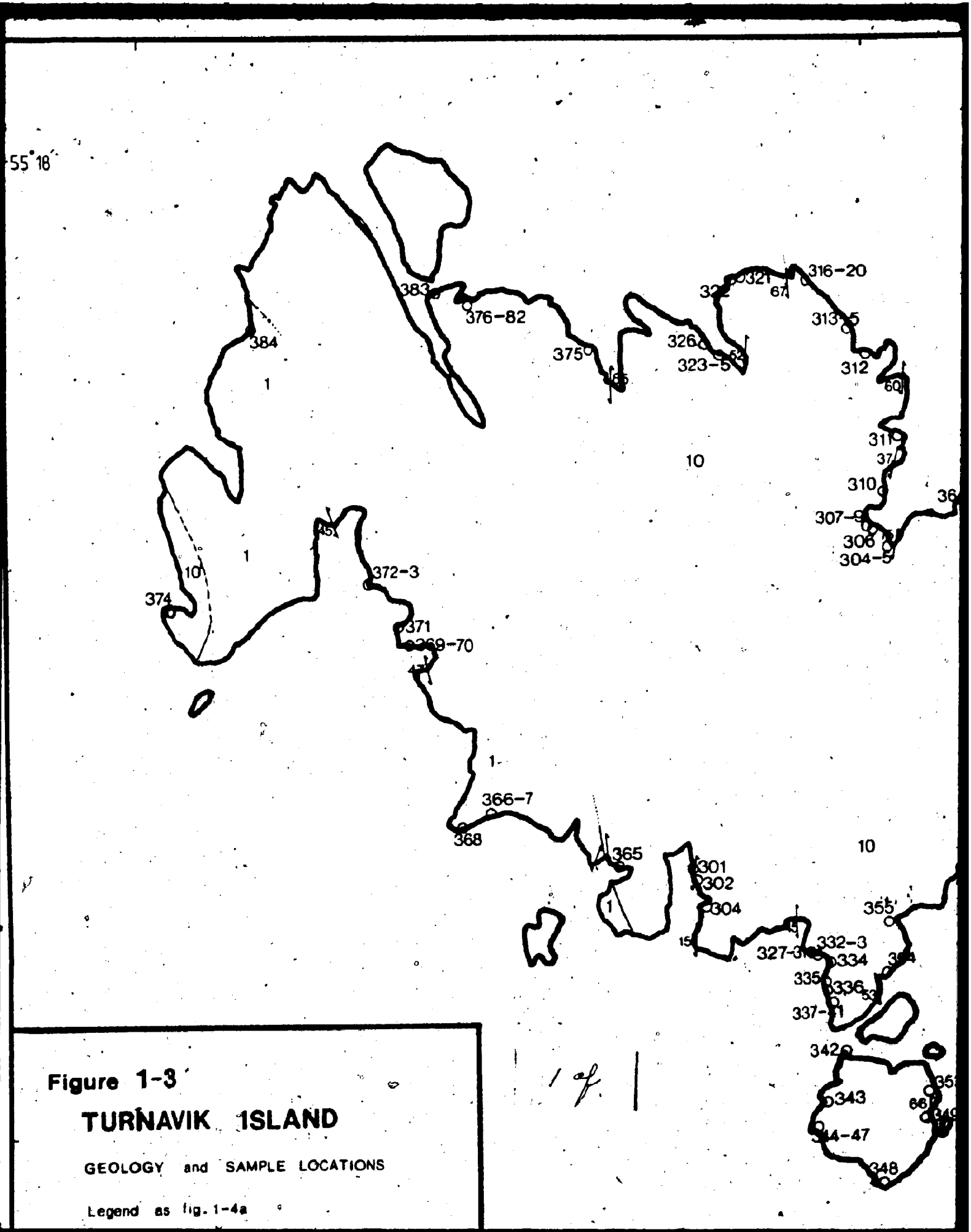

Figure 1-3

TURNAVIK ISLAND

GEOLOGY and SAMPLE LOCATIONS

Legend as fig. 1-4a

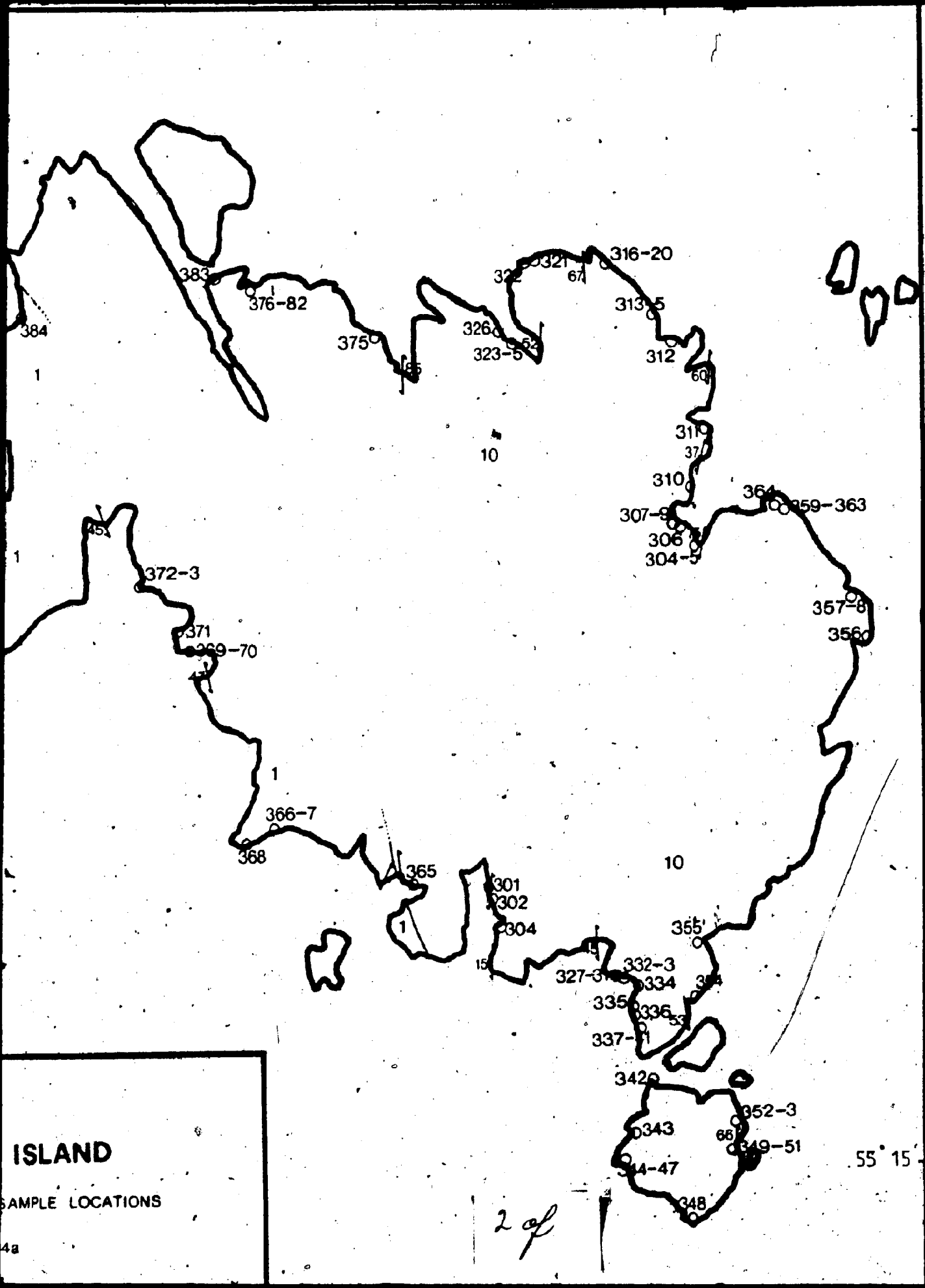
316-20
321
67
383
376-82
313-5
384
375
326
323-5
312
1
10
310
364
359-363
307-9
306
304-5
372-3
357-8
356
371
369-70
1
366-7
368
365
10
301
302
304
355
332-3
327-3
334
335
336
337-1
342
352-3
343
68
349-51
344-47
348
55° 15'
ISLAND
SAMPLE LOCATIONS
4a
2 of

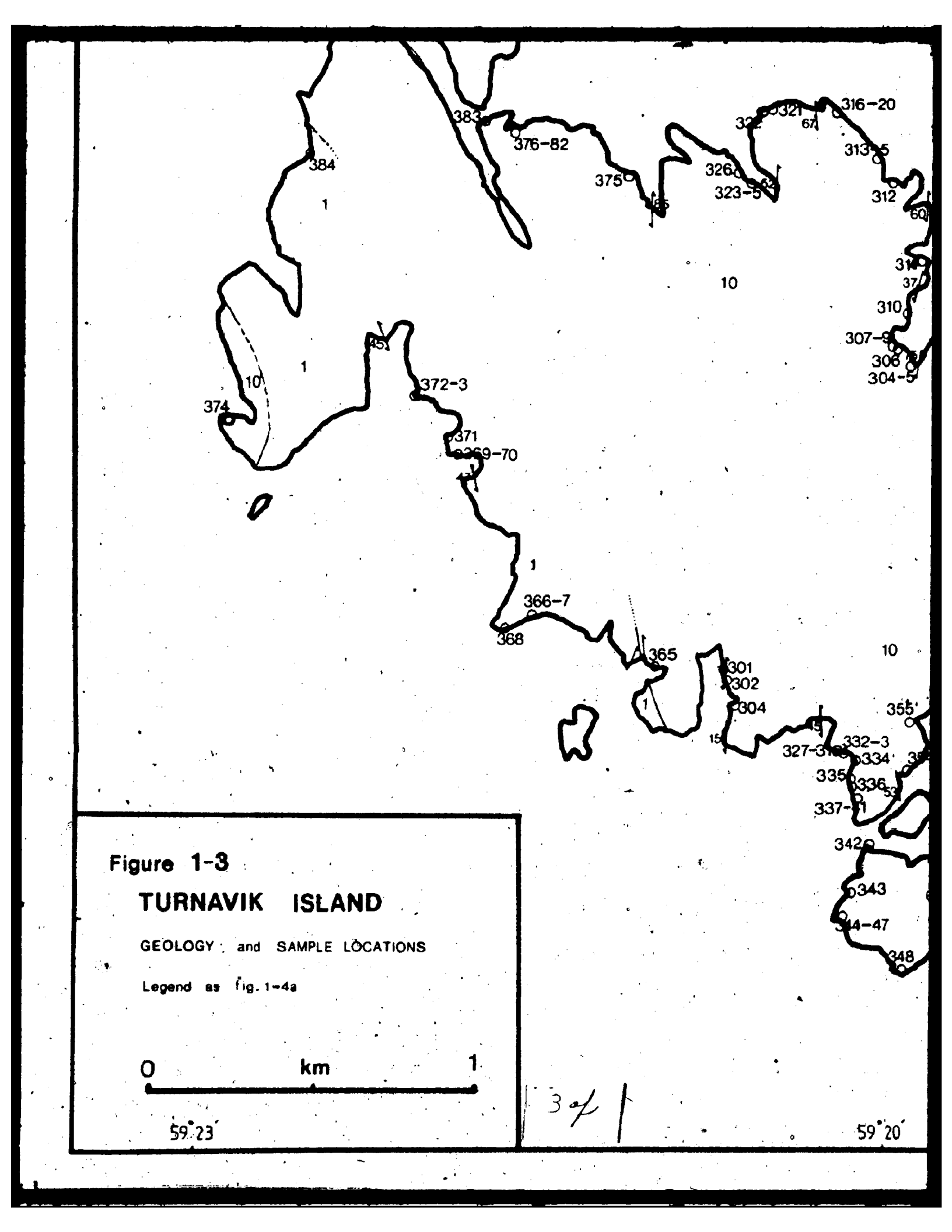

Figure 1-3

TURNAVIK ISLAND

GEOLOGY and SAMPLE LOCATIONS

Legend as fig. 1-4a

3 of 1

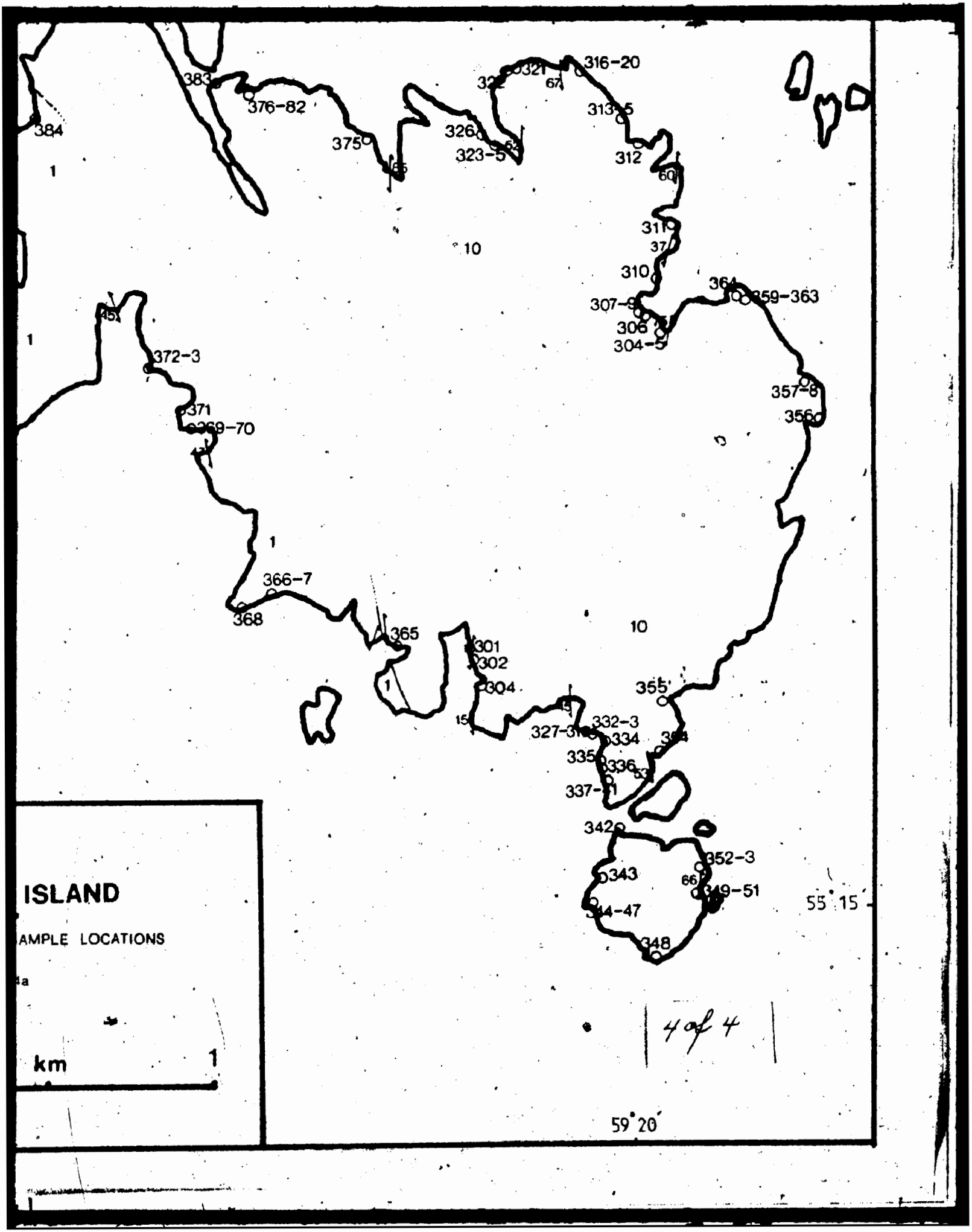
316-20
321
383
376-82
384
375
326
323-5
312
313-5
1
10
311
310
364
359-363
307-9
306
304-5
372-3
357-8
356
371
369-70
366-7
368
365
301
302
304
355
332-3
327-31
334
335
336
337-41
342
352-3
343
349-51
344-47
348
55° 15'
59° 20'
ISLAND
AMPLE LOCATIONS
km
1
4 of 4

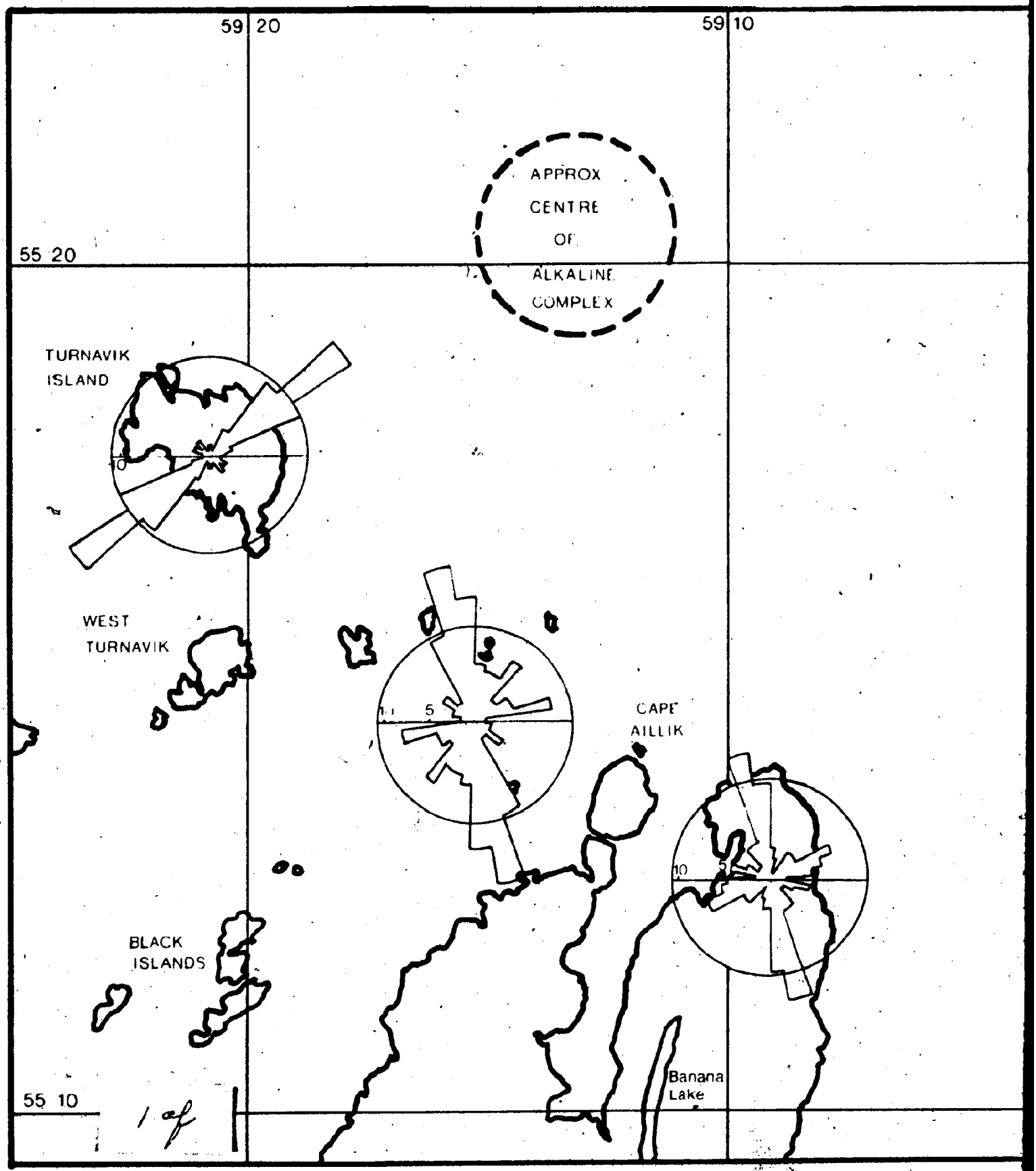
59 20
59 10
APPROX
CENTRE
OF
ALKALINE
COMPLEX
55 20
TURNAVIK
ISLAND
10
WEST
TURNAVIK
5
CAPE
AILLIK
10
BLACK
ISLANDS
Banana
Lake
55 10
1 of

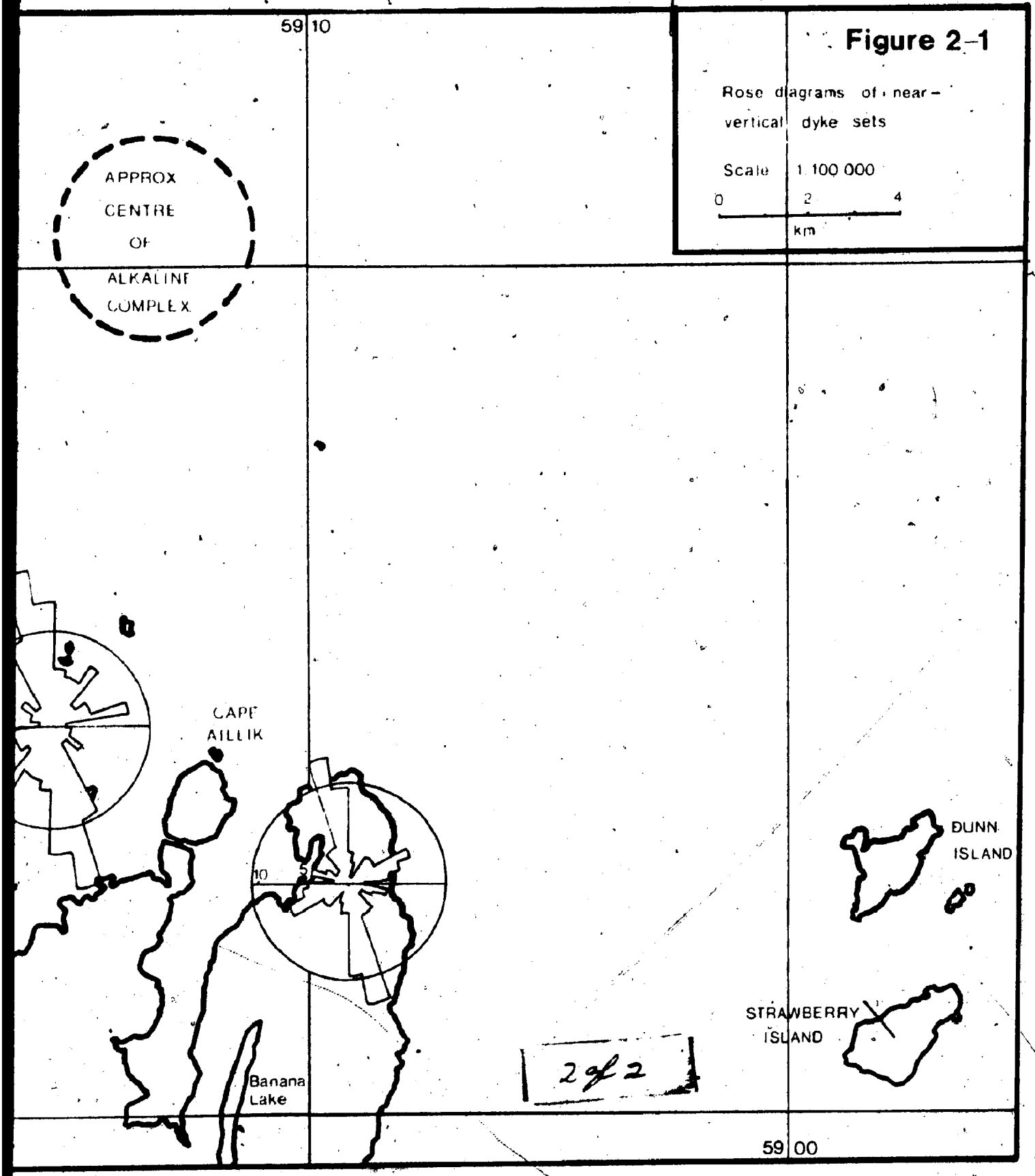

Figure 2–1

Rose diagrams of near–vertical dyke sets

Scale 1:100 000

0 2 4

km

2g2

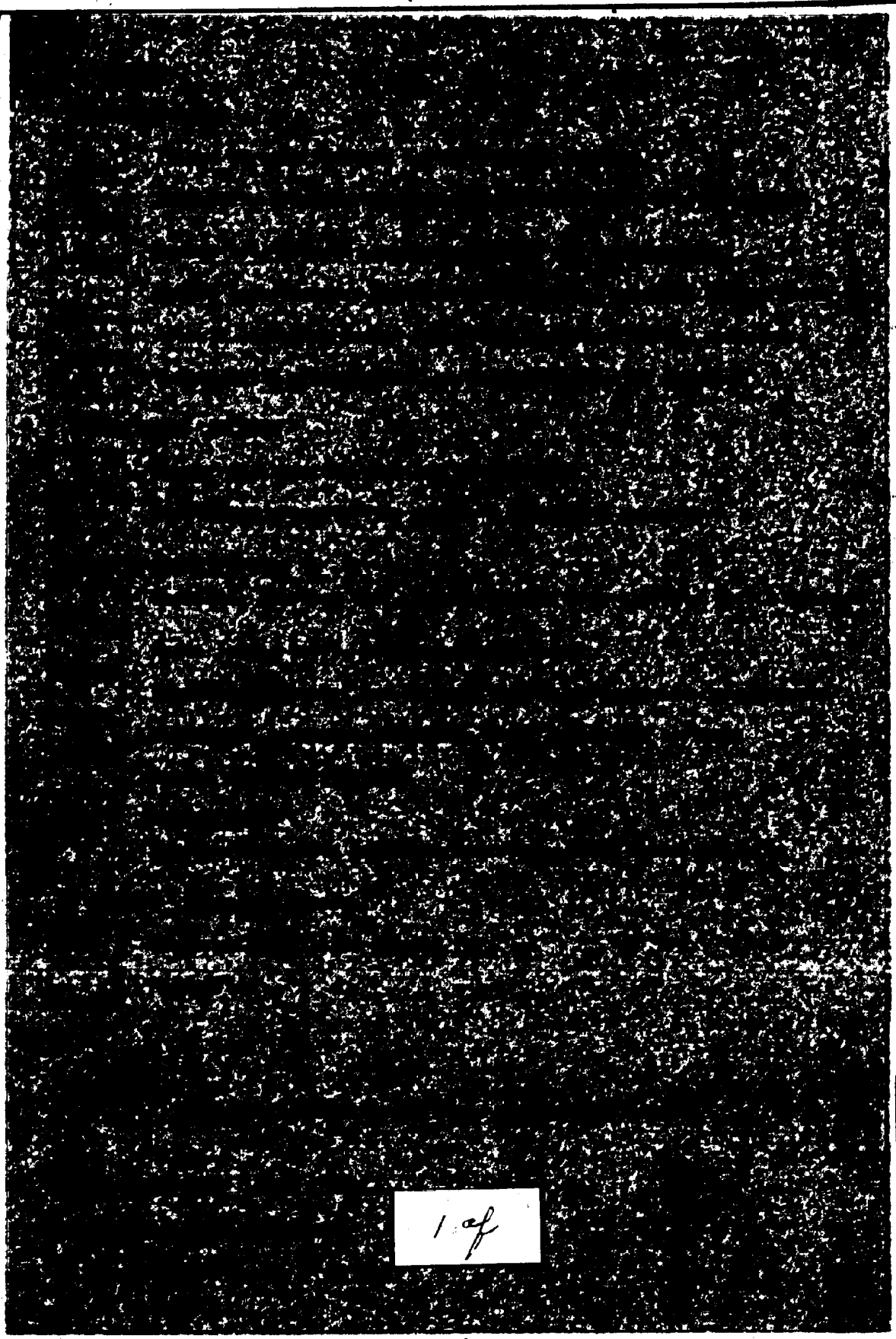

1 of

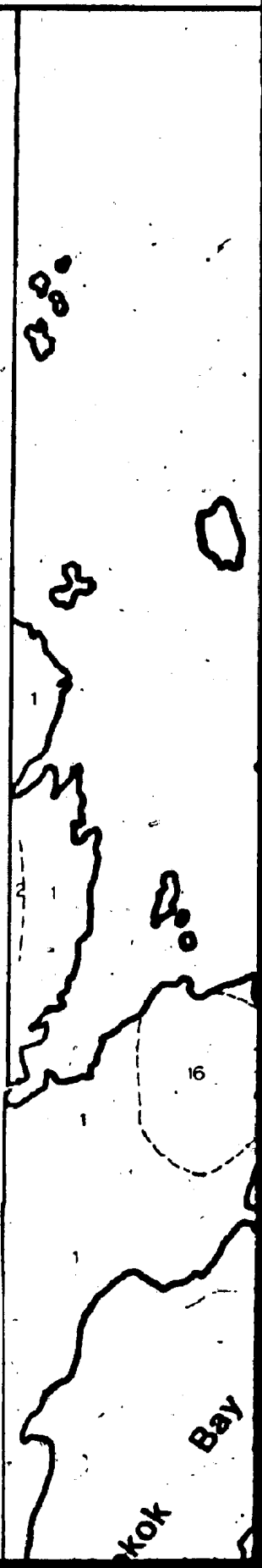

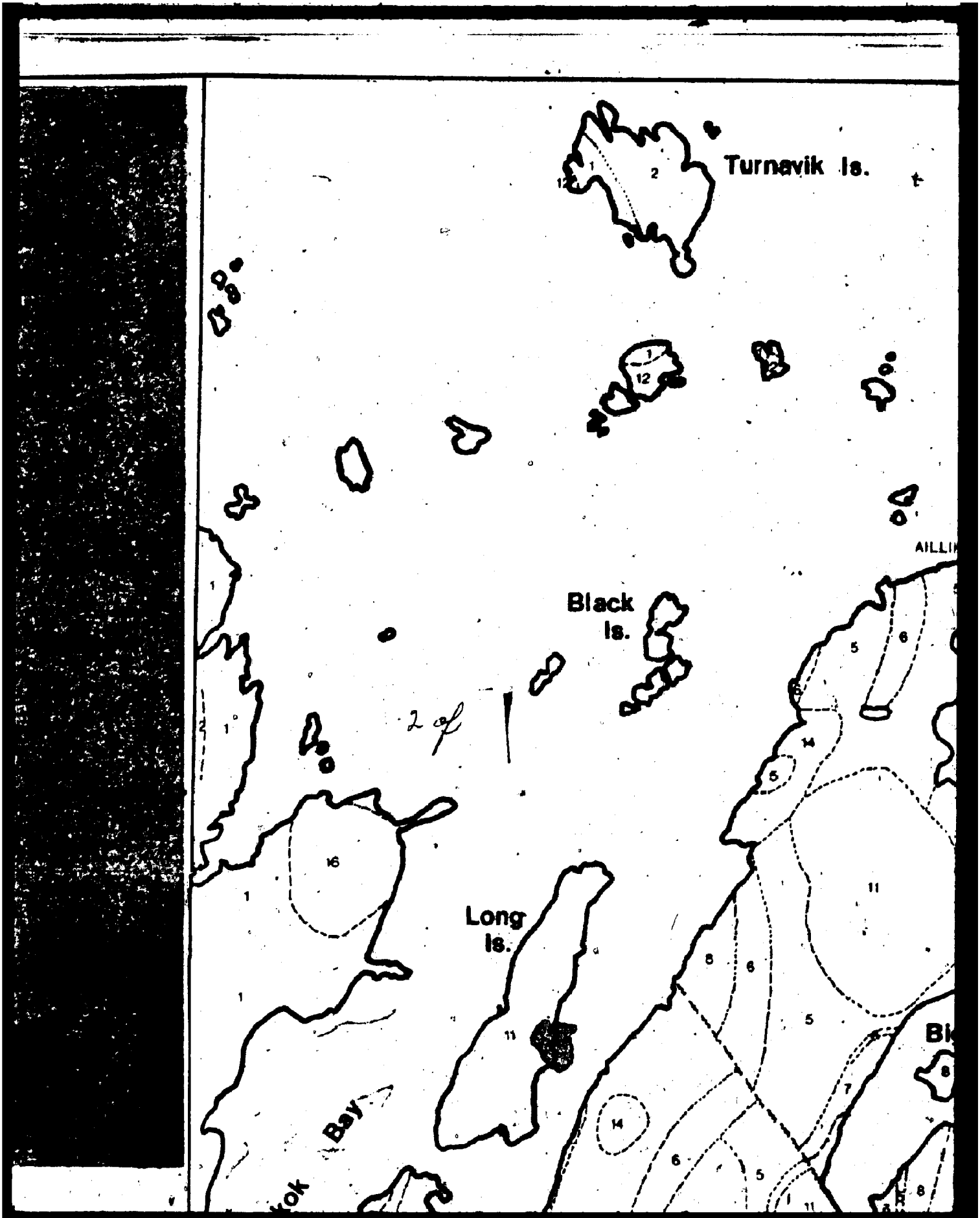
Turnavik Is.
Black Is.
Long Is.
AILLI
Bay

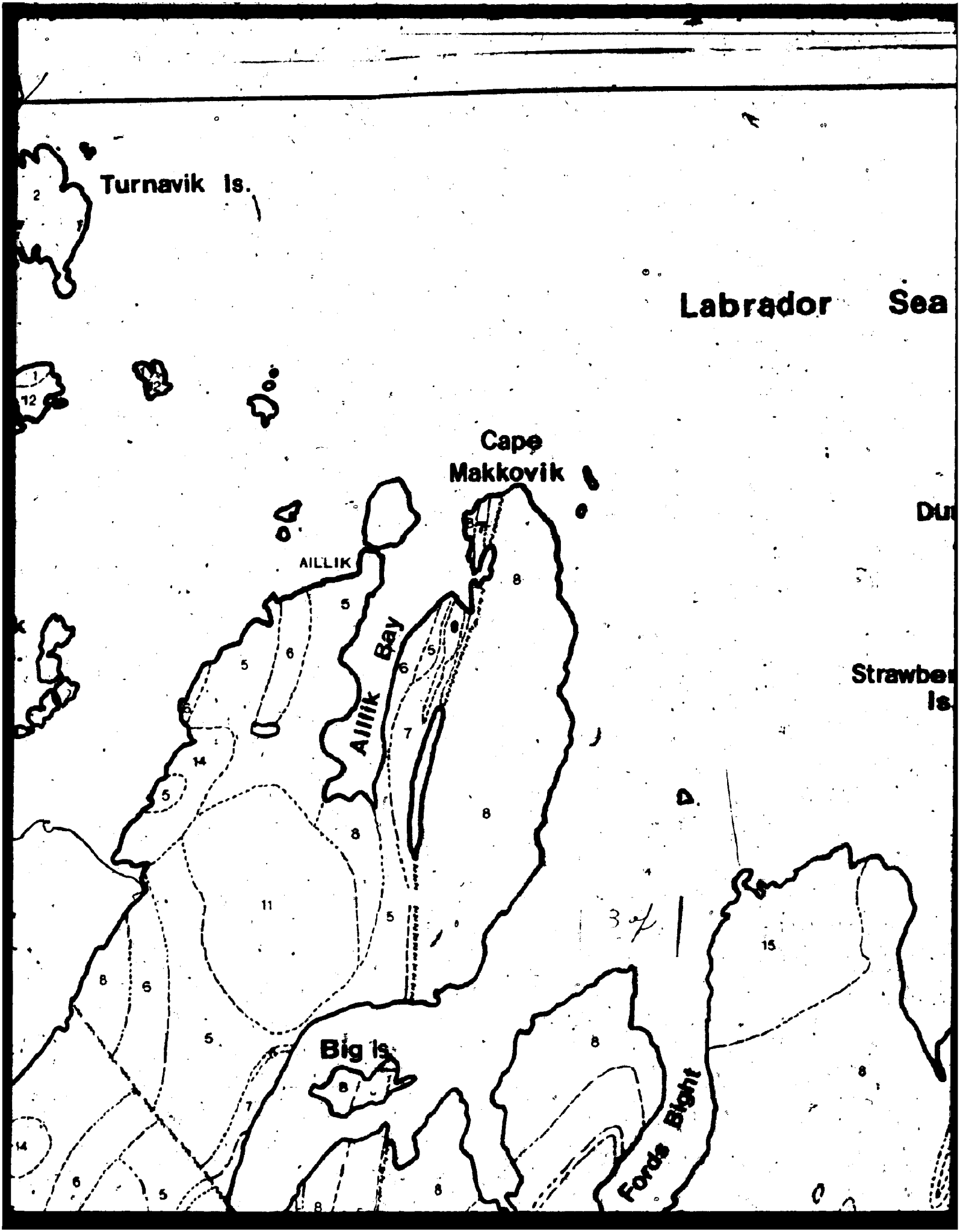
Turnavik Is.
Labrador Sea
Cape Makkovik
AILLIK
Aillik Bay
Big Is.
Fords Bight
Strawber Is.

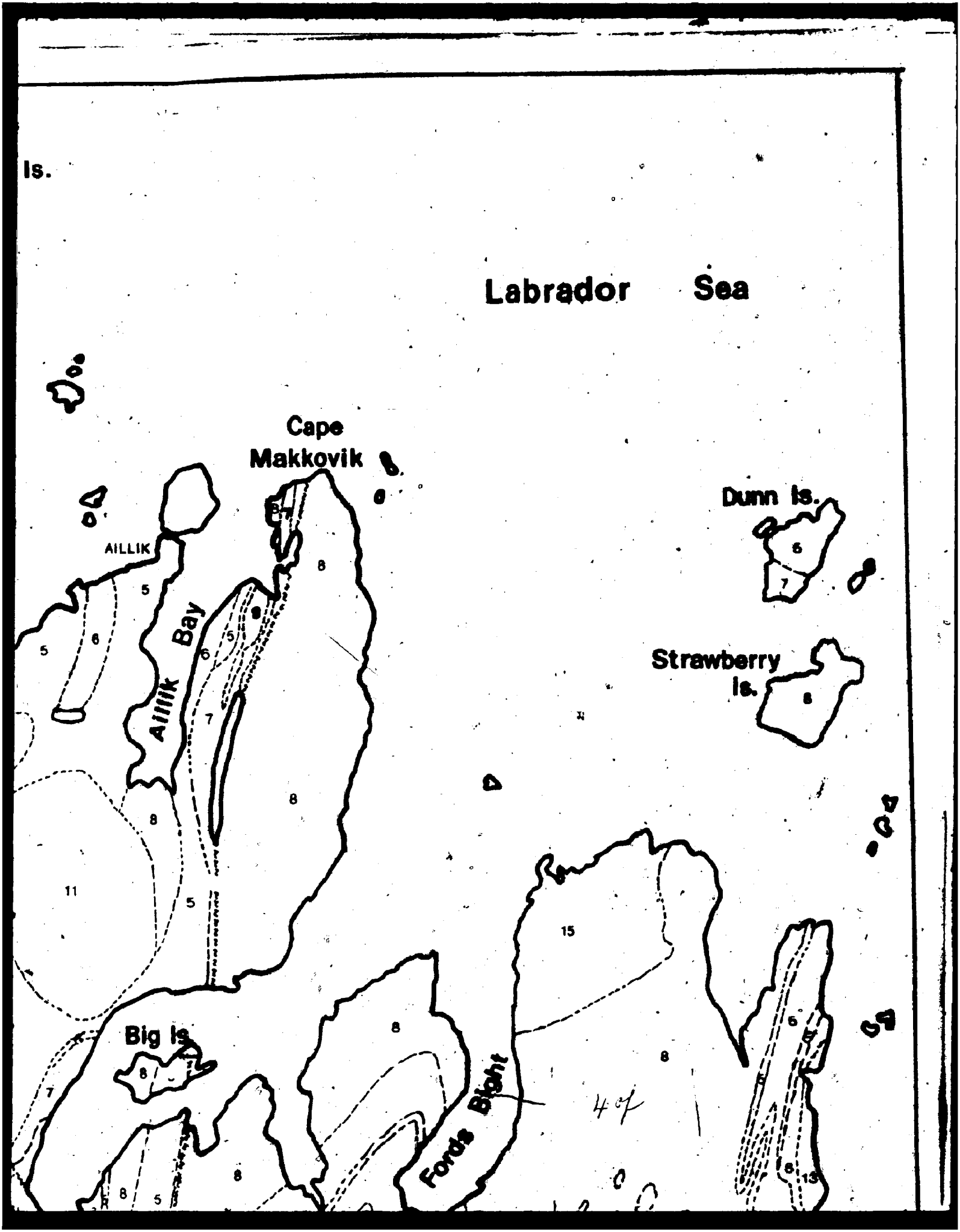
Is.
Labrador Sea
Cape Makkovik
AILLIK
Aillik Bay
Dunn Is.
Strawberry Is.
Big Is.
Fords Bight
4 of

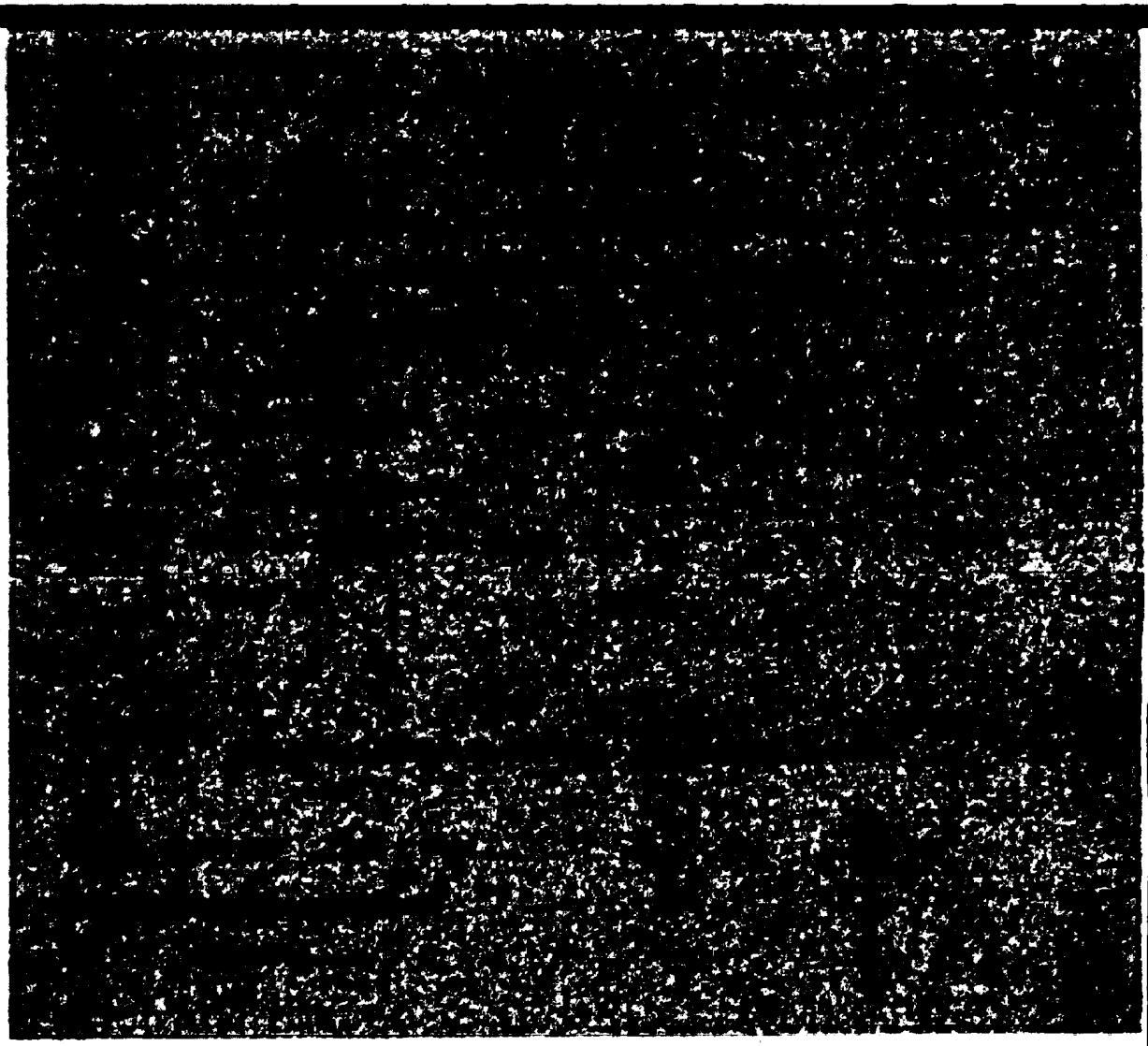

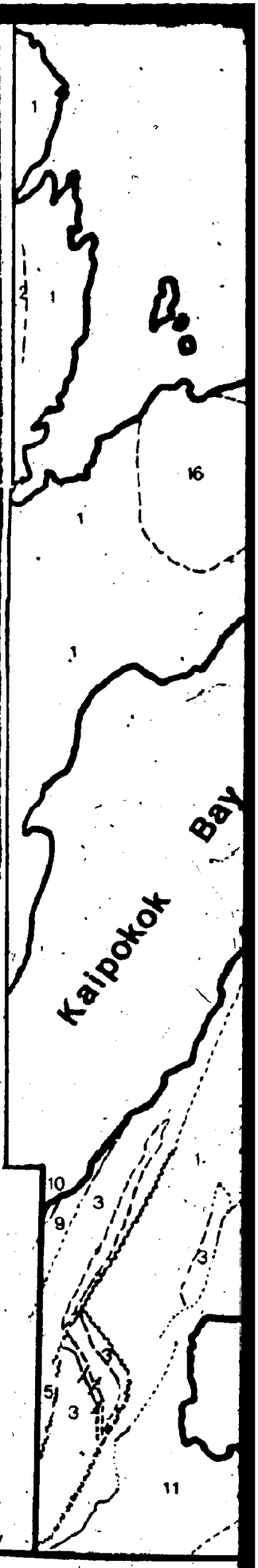

Figure 1-2

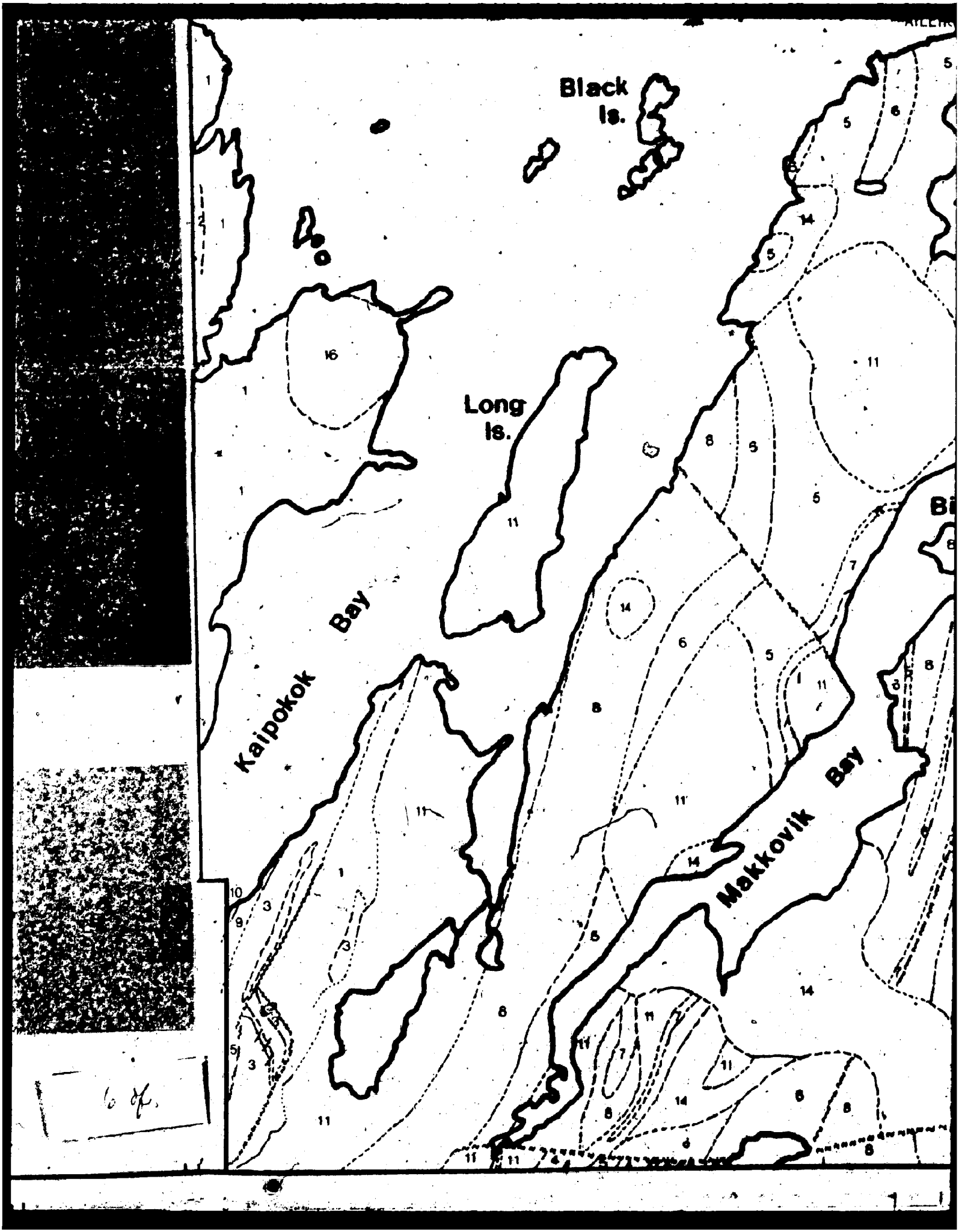
Black Is.
Long Is.
Kaipokok Bay
Makkovik Bay

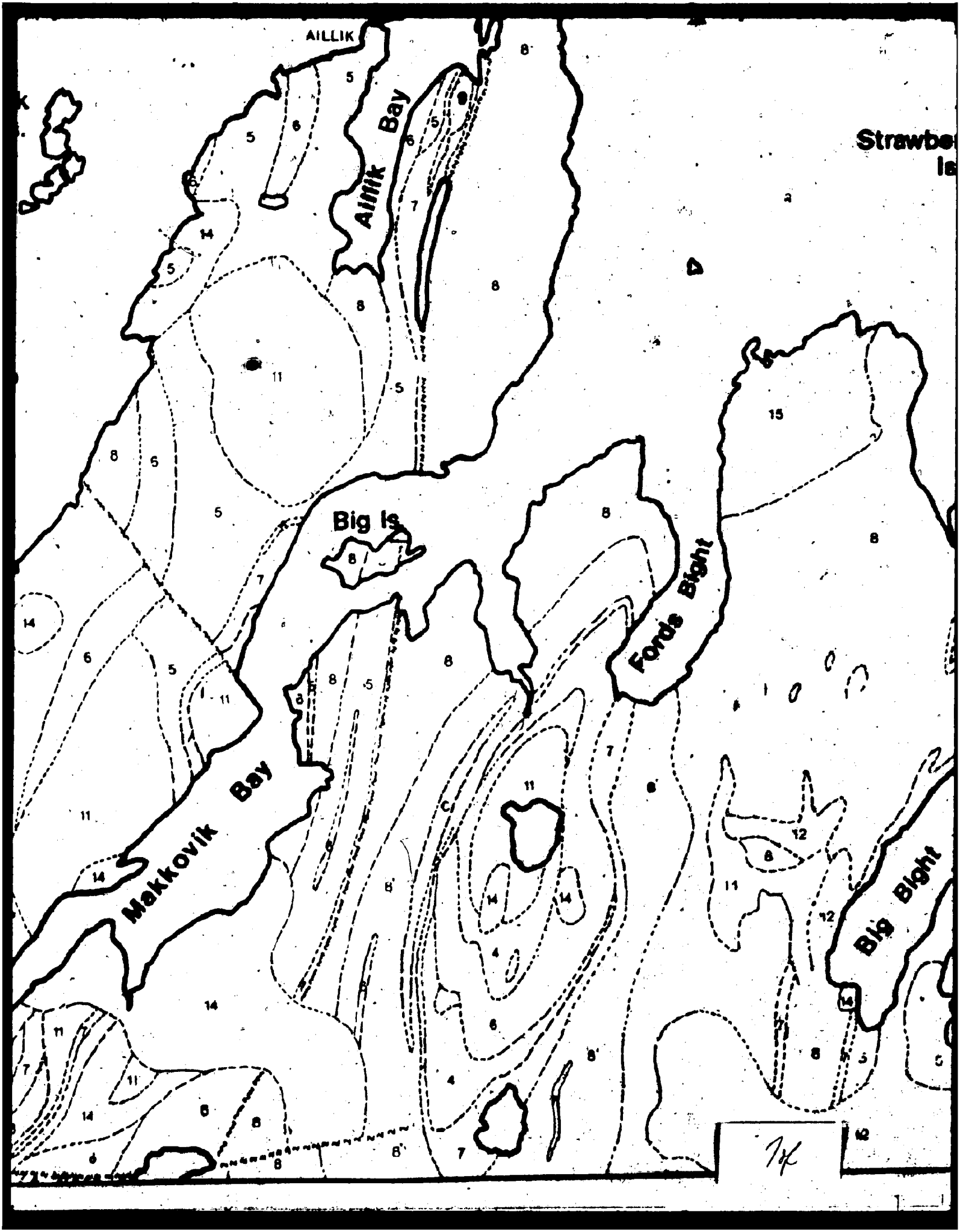
AILLIK
Aillik Bay
Big Is.
Fords Bight
Makkovik Bay
Big Bight
Strawbe
Is
14

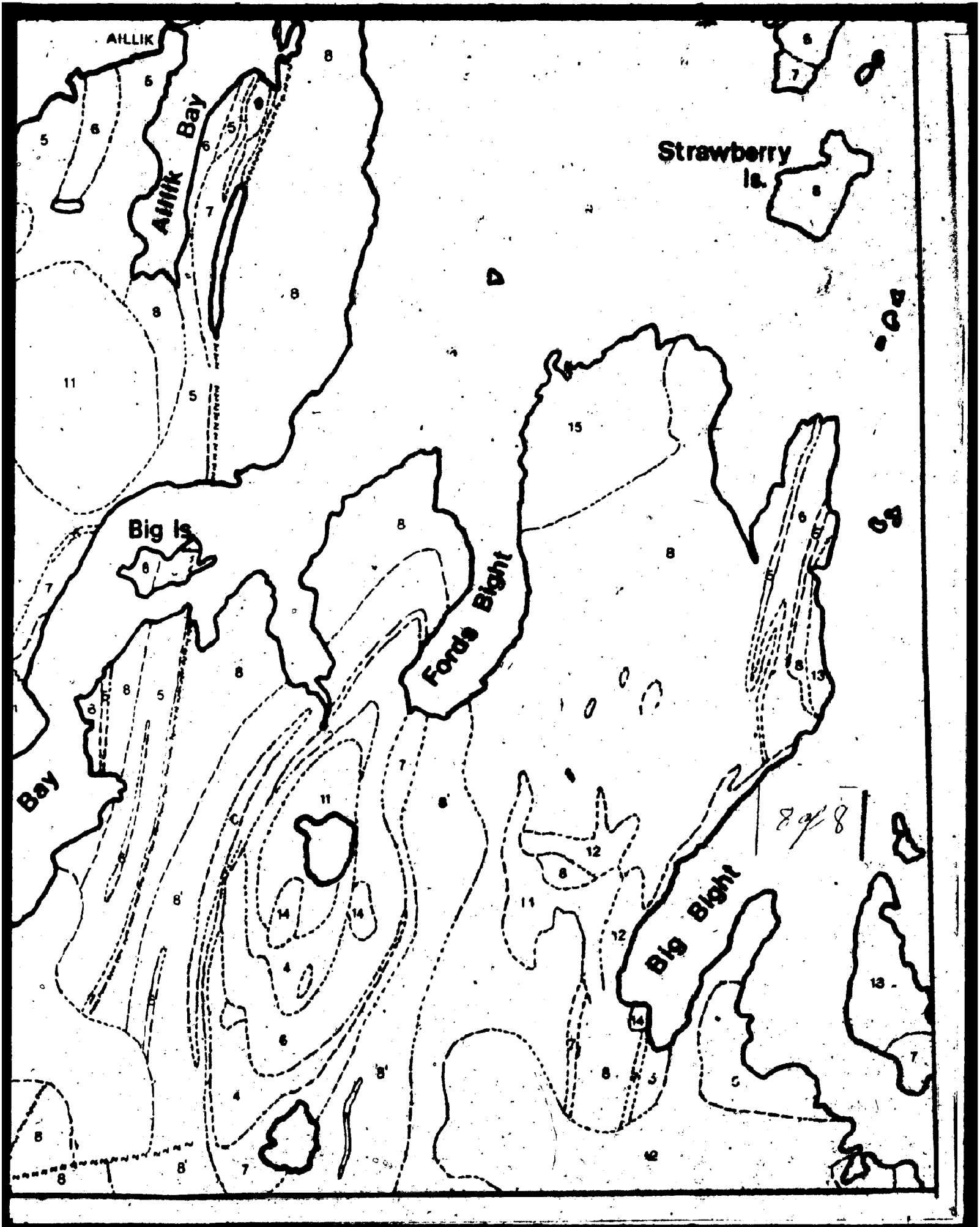
AILLIK
Aillik Bay
Strawberry Is.
Big Is
Fords Bight
Bay
Big Bight

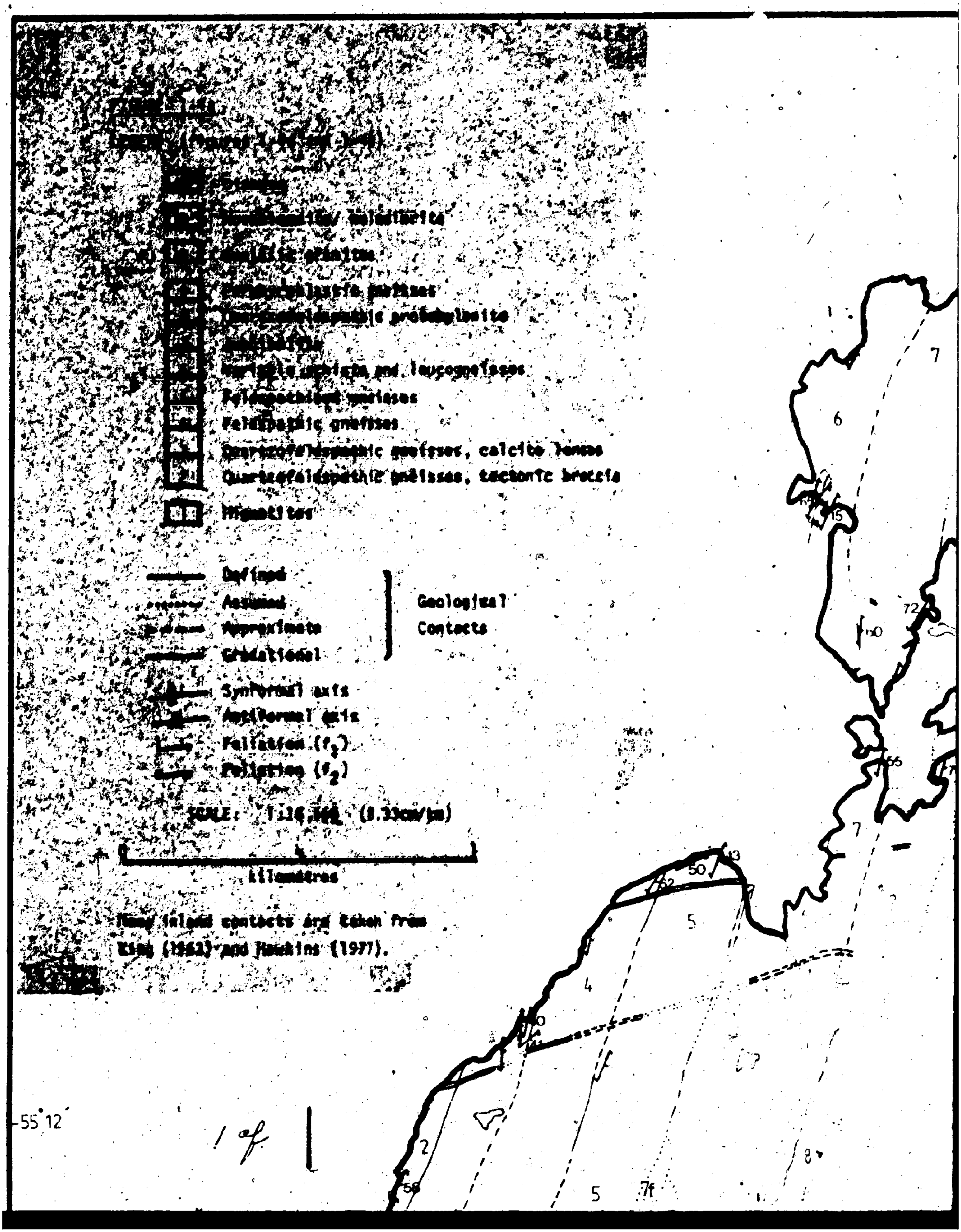

Quartzofeldspathic gneisses, tectonic breccia
Migmatites
Defined
Assumed
Approximate
Geological
Contacts
Synformal axis
Antiformal axis
kilometres
and Hawkins (1977).
55°12'

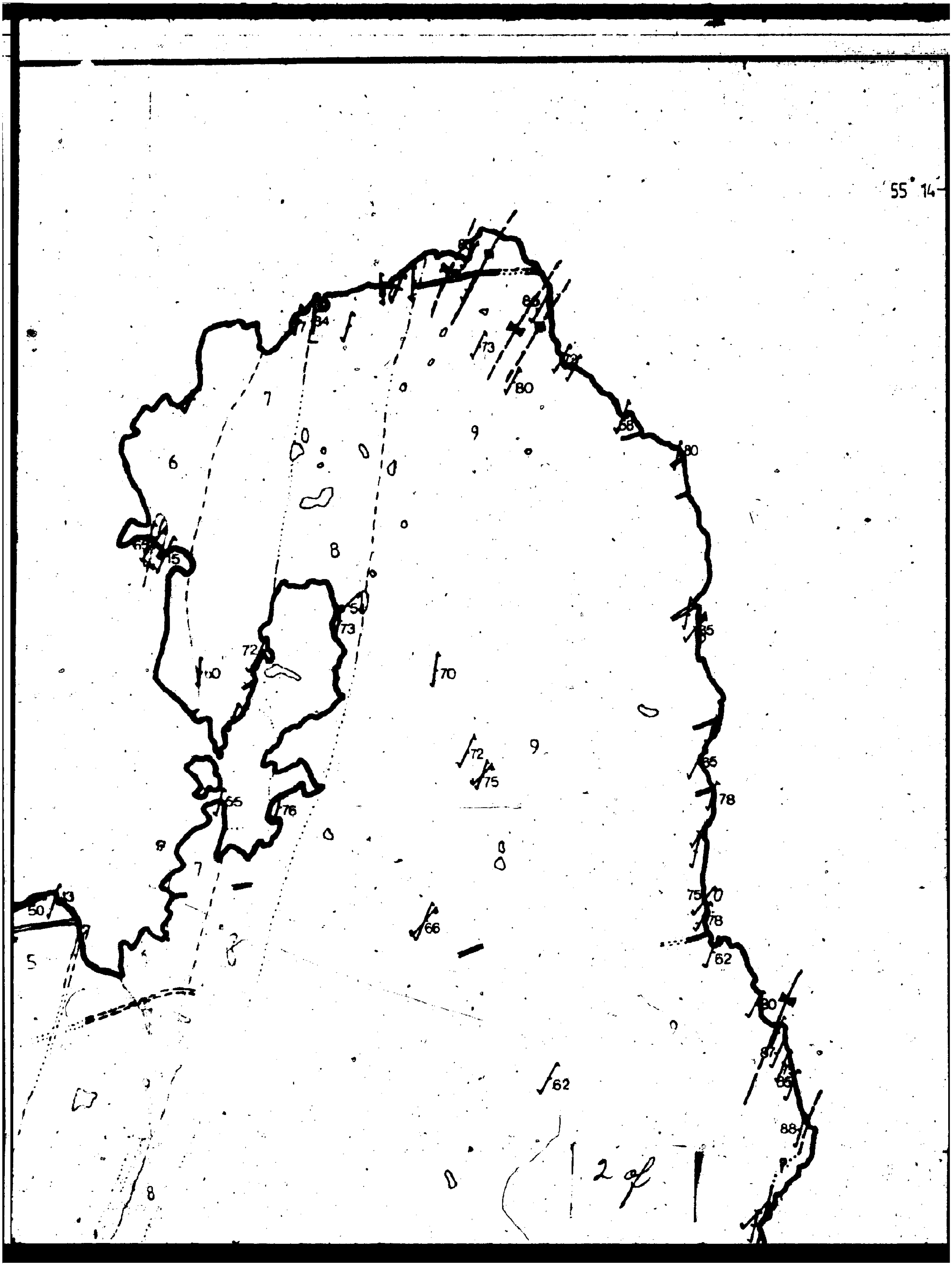
55° 14'
2 of

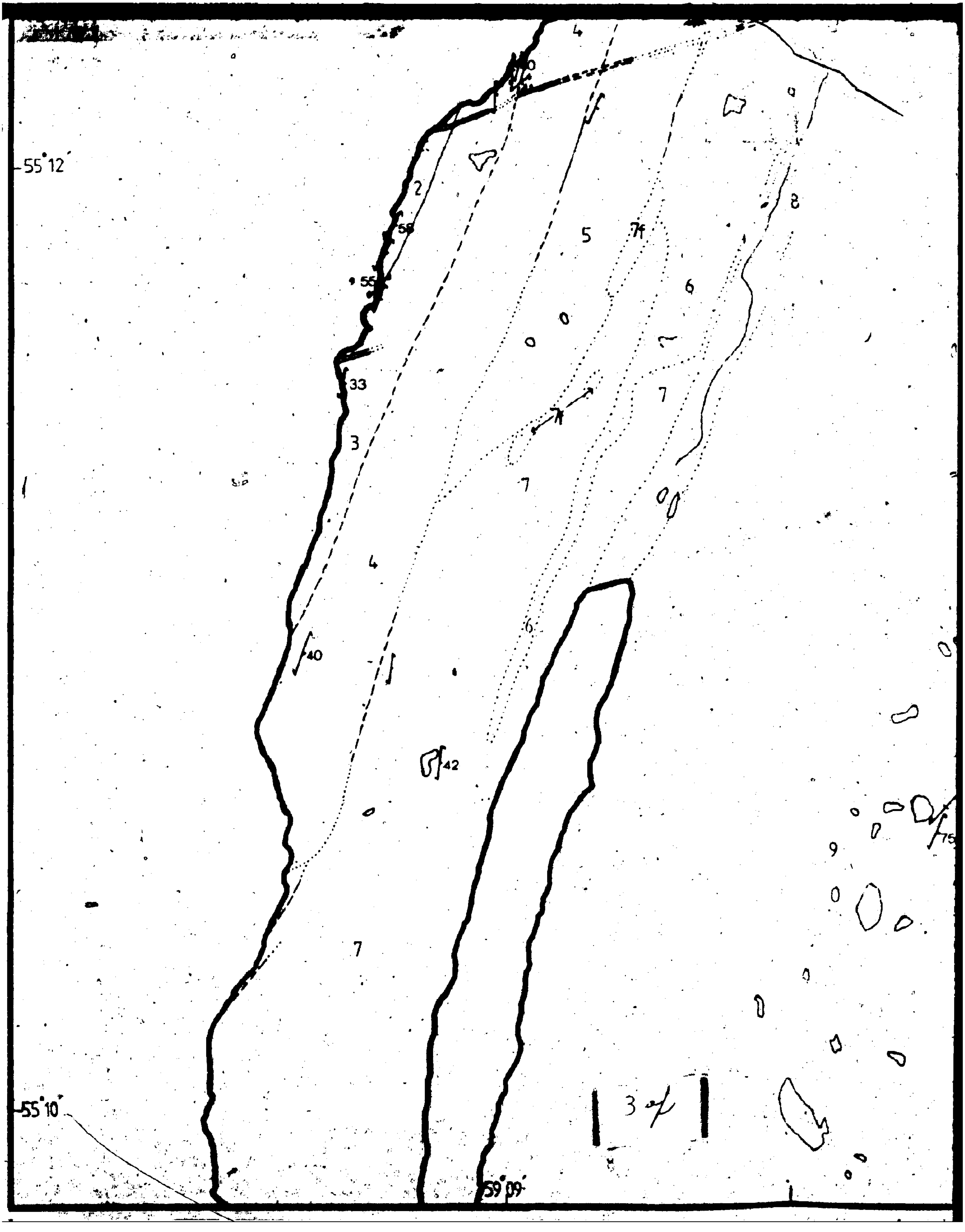
55°12'
55°10'
59°09'
58
55
33
40
42
3 of

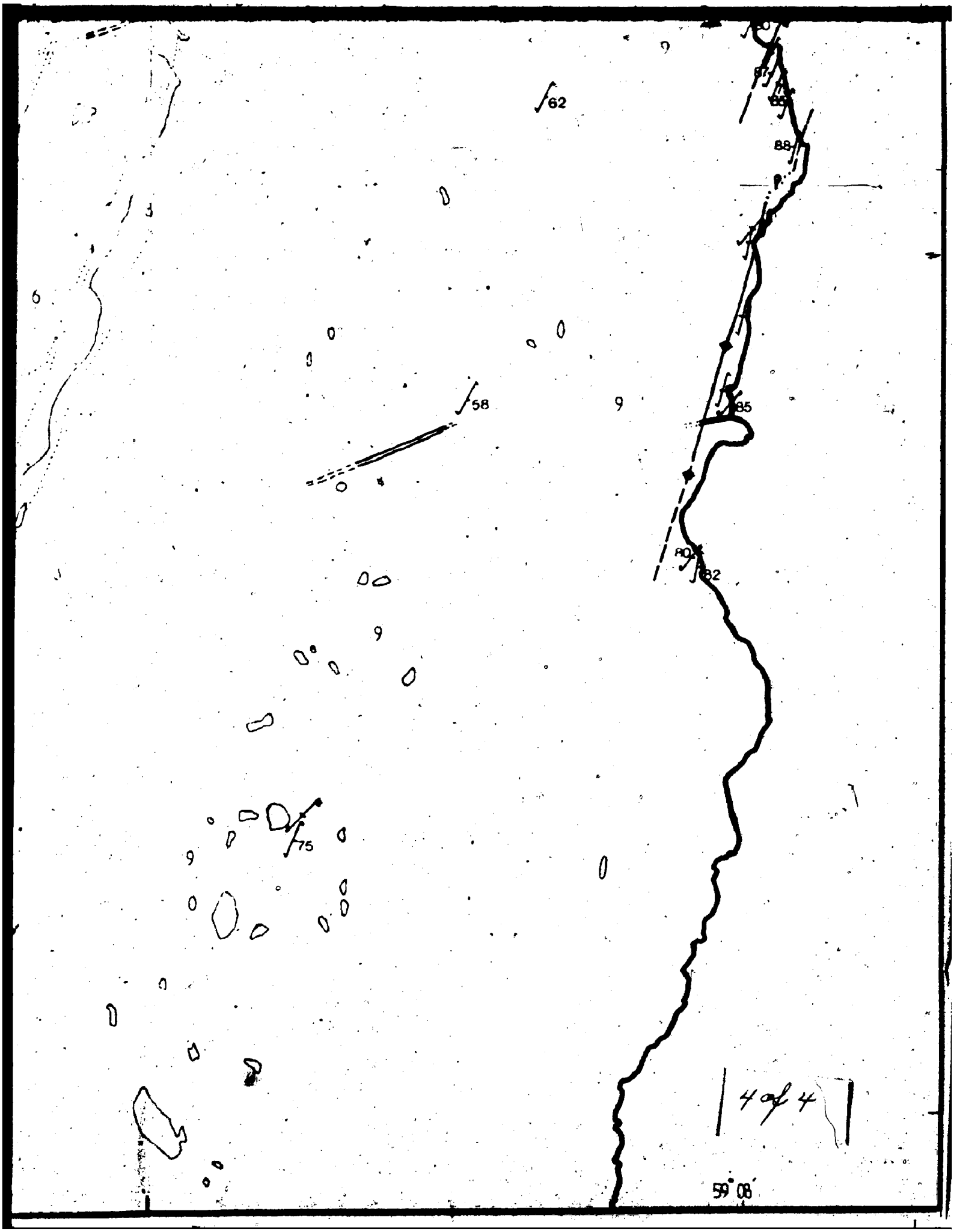
62
58
85
82
75
4 of 4
59° 08'